# Long-term testing near Tucson, Arizona for concentrate management using halophyte irrigation; with associated slowsand filtration (SSF) and reverse osmosis (RO) treatment

USBR Cooperative Agreement No: R09SF32010, UA FRS #321010

Through

**Desert Southwest Cooperative Ecosystem Study Unit**

**US Bureau of Reclamation, Tucson Office**

**University of Arizona,**

Environmental Research Laboratory

Chemical and Environmental Engineering

**Final Report**

**July 22, 2011**

# Table of Contents

# Executive Summary

There are many challenges facing water utility managers in the Southwest. One, in particular, the salinity problem, has long-term implications on all aspects of the region's water resource situation. Through our partnership we have assembled a research and development infrastructure that includes a cadre of highly qualified professional and supporting facilities that is focused on addressing the salinity challenge. The R&D program has been developed under the council and assistance of the partnering organizations.1 While the methods that have been adopted or are being considered to mitigate/reduce the salinity of Central Arizona Project water2 are: recharge and recovery, blending with groundwater, and reverse osmosis our focus has been on the latter for two related reasons. First, both recharge and recovery and blending have been effective in providing a safe, palatable water supply under a normal planning horizon but only reverse osmosis holds the promise for a long-term solution. Second, the Northwest Water Partners and the US Bureau of Reclamation have been collaborating on the feasibility of a major reverse osmosis facility in Northwest Tucson for which additional research is needed.

## Research Program

The desalination R&D program described here addresses all parts of the reverse osmosis treatment train including concentrate management. The overarching objective is to optimize desalination performance in RO treatment systems consisting of pretreatment (microfiltration versus slow sand filtration, reverse osmosis itself and brine management (minimization and disposal). We aggressively investigated each of these areas through field site operations, data acquisition and monitoring, performance evaluation, technology assessment, and systems analysis. It is emphasized that these are not completely independent areas of study. That is, brine minimization and disposal objectives may well depend on upstream water softening and water recovery during reverse osmosis, so that a systems approach is best suited to establish optimal performance criteria and minimize overall costs.

The research program described was designed to (i) compare slow sand filtration (SSF) and microfiltration (MF) as pretreatment technologies for desalination by reverse osmosis (RO); (ii) monitor the long-term RO performance over a period that would support comparison of inter-seasonal effects and establish limits to membrane life and (iii) compare the costs and benefits of the following four brine management alternatives:

- Enhanced evaporation, or conventional brine disposal;
- Vibratory shear enhanced processing of brine to increase water recovery during desalination;
- Ion exchange softening ahead of RO treatment, to enhanced over all recovery; and
- Farming of Halophyte (salt-tolerant vegetation) for animal feed to make use of RO concentrate.

[1] The water utility and agency partners include: the Northwest Water Partners (Metro Water District, Oro Valley Water, Marana Water, and Flowing Wells Irrigation District), Tucson Water, the US Bureau of Reclamation, the Central Arizona Project, and the University of Arizona (Environmental Research Laboratory, Chemical and Environmental Engineering, Water Quality Center, and Water Sustainability Program)

[2] The level salinity of Central Arizona Project water upon delivery in Tucson, measured as Total Dissolved Solids (TDS), above the EPA's maximum recommended level (MRCL) and varies by season.

These objectives were pursued via a combination of laboratory/field-scale experiments and systems approaches developed over the four-year study.

This report contains the details of our project activities over the past two years. It is structured to report on task deliverables for the 2009-2011 contract scope. In order to maintain a continuous record of project-related activities, reports, manuscripts and research summaries that are provided in the appendices include results from previous efforts at the project field site funded under USBR's Science and Technology program from 2006-2009. A very brief overview of the primary experimental results is presented here. For a more detailed presentation and discussion of previous results, please refer to Appendix 4.

## Results – Economic Comparison

From the research program to date we have compiled performance data and associated cost analyses that are sufficient to prepare a preliminary cost comparison for various treatment train options (Table 1). Pretreatment options consist of slow sand filtration and microfiltration. Brine management options include IX softening ahead of reverse osmosis, VSEP treatment after reverse osmosis and irrigation of halophytes in addition to advanced evaporation (baseline case).

We continue to refine the numbers based on ongoing performance evaluations as data from research components continue to be generated. For example, the IX cost data is based on theoretical performance and will be updated as soon as data from a scaled application are available. The data analysis representing a comparison of SSF and MF is complete, as is an economic analysis of several methods available for brine minimization and disposal including halophyte farming (HF). However, additional research on the economic potential of products including, halophytes for animal feed, aquaculture and purified mineral salts is needed.

**Table 1: Alternative treatment trains and associated unit costs in $/Ccf (2010 dollars)**

| Options[1] | SSF | MF | IX | RO | $RO_3$ | VSEP | EEVAP | HF | Total Cost[2] |
|---|---|---|---|---|---|---|---|---|---|
| ***1*** | 0.335 | - | - | 0.497 | - | - | 1.605 | - | 2.437 |
| ***2*** | 0.335 | - | 0.109 | 0.669 | | - | 0.369 | - | 1.482 |
| ***3*** | 0.335 | - | - | 0.497 | - | 0.599 | 0.305 | - | 1.736 |
| ***4*** | 0.335 | - | - | 0.497 | - | - | - | 0.898 | 1.730 |
| ***5*** | - | 0.467 | - | 0.497 | - | - | 1.605 | - | 2.569 |
| ***6*** | - | 0.467 | 0.109 | 0.669 | | - | 0.369 | - | 1.614 |
| ***7*** | - | 0.467 | - | 0.497 | - | 0.599 | 0.305 | - | 1.868 |
| ***8*** | - | 0.467 | - | 0.497 | - | - | - | 0.898 | 1.862 |

[1]The alternative treatment trains are discernable from the table headings. That is, option #1 consists of slow sand filtration followed by reverse osmosis treatment and enhanced evaporation for brine disposal.

[2]All the costs are for 15 MGD treatment plant operating for 30 years with the discount operator of 6%. See Appendix 1 for additional notes and assumptions.

## Academic and Research Outcomes

2009-2011 proved very productive for the students using the salinity research field site in Marana. Student participation was high with a number of Chemical Engineering students contributing to and learning about Reverse Osmosis (RO) operations and monitoring. Andrea Corral completed her Masters in Chemical and Environmental Engineering (CHEE) with her work on the SSF/MF performance comparison (see Appendix 3). She will continue in the CHEE PhD Program. Justin Nixon completed his CHEE Masters degree with his work on the IX (see results in Appendix 10). Under Dr. Robert Arnold and Dr.Wendell Ela's guidance Umur Yenal competed his PhD based on the research he conducted at the Marana Field site. Many of his findings are summarized in Appendix 4.

On the concentrate management side (CM) Bob Seaman continues as a half time Research Technician to look after field site operation and CM data collection. Students contributions from Soil, Water and Environment Science (SWES) include Matt Kluvo who contributed to the literature review of the animal feed value of halophytes and Deserie Soliz, a SWES PhD candidate who took over the work of Dr. Fiona Jordan. Contributing SWES/ERL faculty include Dr. Ed Glenn, Dr Steve Nelson, Martin Yoklic and Dr. Jim Riley.

## Sponsor Support

Our water utility partners under the supervision and coordination of Chris Hill were essential to what we accomplished in 2009-2011. During the past two years their technical support and expertise enabled the construction and the installation of the infrastructure for the Microfiltration system and the ongoing maintenance and repairs required to keep the research site operational. We acknowledge and thank the staff of Metro Water, Flowing Wells Water, Marana Water and Oro Valley Water, our NWWP partners. In addition to this critical in-kind support they provide funding for students, researcher and consultants. Tucson Water has had a slightly different role but also of critical import through their ongoing water quality analysis for the project and their purchase of the VSEP equipment. Together, this support has been essential to the matching requirement for the research grants we have received from the Bureau and our institutional sponsors. Appendix 2 provides a summary of in-kind support and complementary research funding associated with this research program.

The ongoing support of the US Bureau of Reclamation through their S&T program, coordinated of Eric Holler, with technical support from Chuck Moody and other USBR staff, remains the foundation for this salinity research program. Our other sponsors including: from the University of Arizona the Water Sustainability Program (TRIF), the Water Quality Center (WQC) and the Salt River Project.

Through this research we remain mindful of both the broader importance of this work to the region and to the more immediate needs of our water utility partners. We have focused on research that will aid their decision process that will to bring CAP water to their users as efficiently and effectively as possible. At the same time we have developed and tested a number of more sustainable approaches to desalination. We thank all for their support.

## *Related project and program activities for this period include:*

- Construction and commissioning of the MF facilities was completed in late Summer 2009
- A second peer review article on halophytes for concentrate management titled "Water Consumption, Irrigation Efficiency and Nutritional Value of *Atriplex lentiformis* Grown on Reverse Osmosis Brine in a Desert Irrigation" was published in Agriculture , Ecosystems and Envrionment Journal, 140 (2011) 473–483. See USBR Report, Appendix B
- Three project related posters were presented at MultiState Salinity Coalition meeting; two in February 2010 and one in February 2011.
- All corrective actions to items on the 2009 Safety Audit Recommendations have been completed.
- A storm damaged the chemical injection shed in mid January 2010. Safety protocols were undertaken and an incident report was submitted to CAP and other. Shed was replaced and systems reassembled.
- Dr. Wendell Ela et. al. submitted a proposal to NSF on Solar Membrane Desalination, no award.
- Dr. Nelson et. al. submitted a proposal to the Water Reuse Foundation on Aquaculture using RO Concentrate, no award.
- Chris Hill, Metro Water, and the project team submitted a proposal response to USBR FOA R11SF80351 to expand the project to demonstration scale and address "Water Supply Expansion in Northwest Pima County Arizona, awaiting a response.
- A third manuscript on the halophyte research titled "Sustainable Irrigation Strategies for the Forage Halophyte, *Atriplex lentiformis"* has been submitted to the journal Agricultural Water Management.

**Martin Yoklic, Principal Investigator**

# Introduction

This project addresses both the aquifer salt degradation issue and the corollary need for a concentrate disposal capability among non-coastal desalting facilities. Salt management through a combination of RO for treatment of Colorado River Water (CRW) and irrigation of salt tolerant crops for concentrate disposal will allow reuse of CRW RO concentrate for productive use such as agriculture and landscape irrigation.

This report summarizes activities and outcomes related to the Steps summarized in the current USBR/DECESU contract and other tasks associated with the long-term research agenda.

### *Contract Steps*

2009

Step 1, O&M of SSF/RO pilot - performance and cleaning

Step 2, Halophyte Test Plot O&M - productivity and salinity

Step 3, Neutron Probe Monitoring - moisture in test plots

Step 4, Productivity/potential of Halophytes for animal feed

2010

Step 1, Ion Exchange as RO pretreatment

Step 2, Co-precipitation and purity of mineral precipitates

Step 3, O&M of SSF/RO pilot - concentrate production

Step 4, Salt Balance and feasibility of Halophytes for CM

Step 5, Aquaculture w/concentrate - viability and economics

Other

Slowsand compared to Microfiltration pretreatment

Treatment Train option economic evaluation

Project Management

# Contract Step Reports

***2009 Step 1 - O&M of SSF/RO pilot - performance and cleaning***

The Bureau's Mobile Treatement Facility (MTF) has been in operation at the CMID/CAWCD turnout in Marana AZ since 2007. The pilot desalinations research site includes the MTF, plus slow sand filtration (SSF) and microfiltration (MF) on the front end to evaluate pretreatment options. The MF is also on loan from the Bureau. On the concentrate management side the halophyte field site has been continuously operated since concentrate production began in 2007. In 2008 the City of Tucson purchased a pilot scale Vibratory Shear Enhancement Process (VSEP) unit to add to concentrate management option evaluation. More recently, additional work on Ion Exchange (IX) at the bench scale has been added to test this option for the front end of the treatment train. See Research Summary, Appendix 4.

Data has been recorded continuously during the operation of the MTF including recording of the water transport coefficient across the vessels of the MTF reverse osmosis (RO) system. During the period of operation the membranes have been changed twice and the system cleaned twice. For the protocols on the membranes and cleaning see reporting under the previous S&T contract.

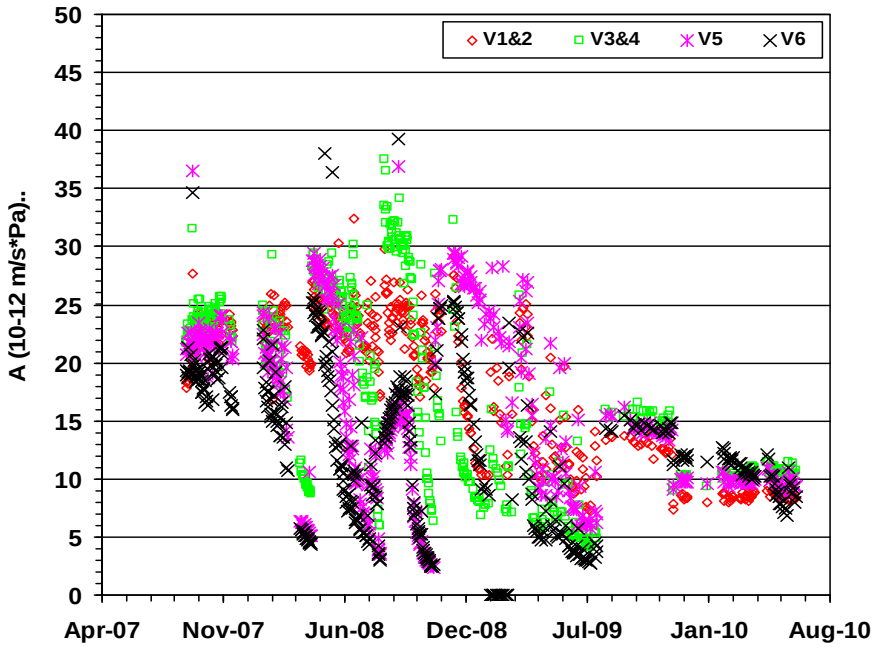


Figure 1, MTF vessel performance 7/07 – 7/09

See Figures 1 & 2 for the performance record of the MTF RO including water transport coefficient (A) and the membrane changes and cleanings. The first membrane cleaning occurred in April 2008 following an increase in product TDS for all vessels. The membranes were replaced in August 2008. The membranes were changed again and the vessels were cleaned in October 2008 corresponding to a change in the pretreatment protocol; the commissioning of the MF system.

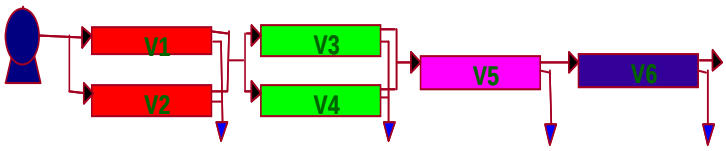


Figure 2, RO vessel arrangement

The MTF RO system has been operating with SSF feed water since since it was commissioned at the research site. In the Fall of 2009 a MF system was installed to compare performance of SSF with MF. Since that time, RO performance has been monitored using MF for feed water supply. A report comparing SSF to MF for RO pretreatment is included, see Appendix 3.

***2009 Step 2 - Halophyte Test Plot O&M - productivity and salinity***

*A. lentiformis* had a maximum yield of 24.4 t $ha^{-1}$ when irrigated with brine from a reverse osmosis plant (3 g $L^{-1}$ TDS) at an irrigation rate of 1.0 $ET_o$ (approximately 2 m $yr^{-1}$) in an irrigation district in Marana, Arizona.. Results of this research are presented in Appendix 5.

The halophyte test plots were planted with *Atriplex lentiformis*, a native species, in late Spring of 2007. Their irrigation using RO concentrate of CAP water began with the fullcommissioning of the MTF in the summer of 2007. The field test plots have been continuously monitored since that time for: soil moisture at depth, EC of the concentrate water, EC of drainage from the lined test plots and for changes in soil salinity (see 2010 Step 4) and field productivity.

Randomly selected plant samples collected in the summer of 2009 showed little variation between plant productivity and irrigation regime (irrigation rates are based on daily evapotranspiration measures for the 1.0 ET and 1.5 ET 1.5 trials with the ET constant irrigation delivered daily based on the average annual ET/365). Both the total biomass and leaf only biomass of the sampled plants for the various irrigation rates are show in Figure 3. This data reflects a single cutting or randomly selected plant after 3 years of growth. The annual average leaf productivity exceeds 5 t $ha^{-1}$ (dry weight). However, in an agronomic setting the annual productivity of *Atriplex lentiformis* may be increased to 10 t $ha^{-1}$ or more with biannual harvest (Watson et.al. 1993). See 2009 Step 4 for findings to date on productivity and potential of halophytes for animal feed.

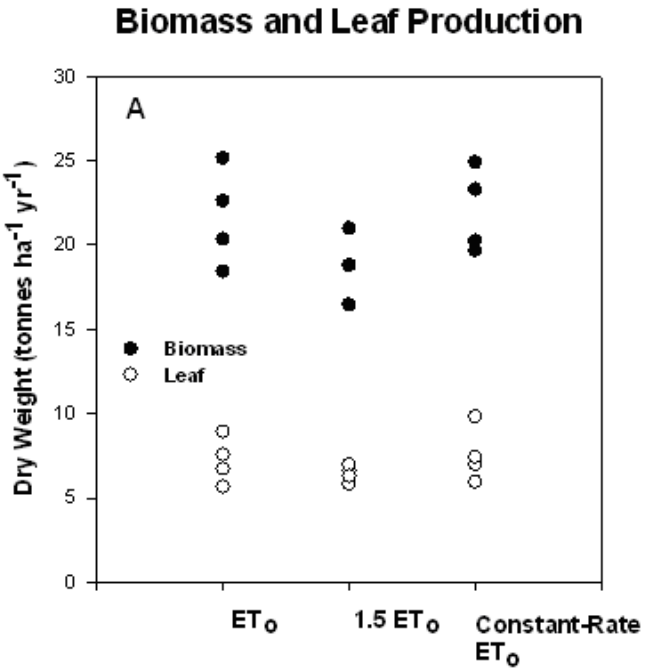


Figure 3, Biomass and Productivity, lined plots

The EC (salinity) of the concentrate from MTF RO of CAP water is plotted in Figure 4. Drainage salinity measures are for the lined plots trials (drainage lysimeters). Each of the three trials have four replicates receiving irrigation at rate based on the Et for a reference crop in this region. The three field trials are 1.5 ET (drainage = 14.5%), ET constant (drainage = 8%). and 1.0 ET rate (no measurable drainage). The salinity of the drainage for 1.5 ET and Et C are also show in Figure 4.

The EC of the concentrate irrigation water ranged between 2.5 and 4.5 while the EC of the drainage from the trials ranged from 5.0 to 8.0. The drainage EC from the 1.5 ET plots ran slightly higher that the EC from the ET constant plots. The individual plot drainage was highly variable drainage. These results are from the combined drainage within a trial. The variability of drainage from plots within a trial indicate preferential pathway may have formed in some plots. The actual drainage below the root zone may be less in the field.

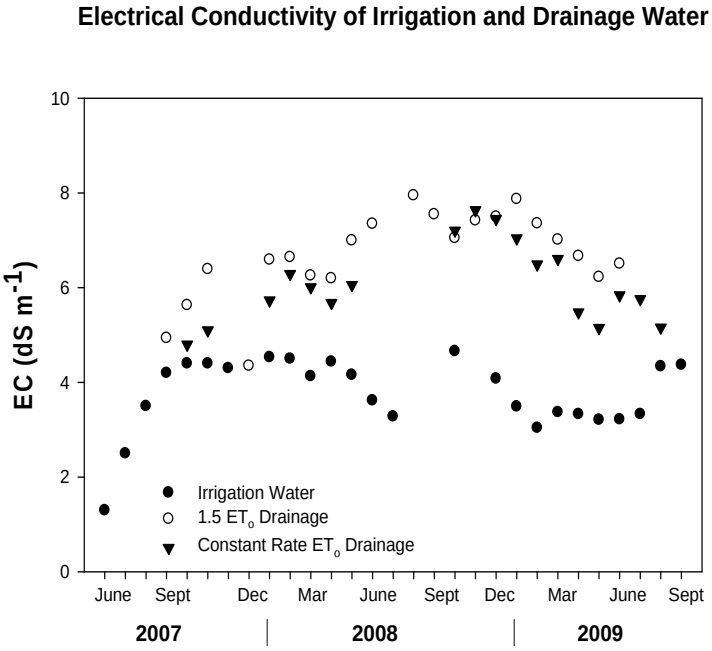


***2009 Step 3 - Neutron Probe Monitoring - moisture in test plots***

Evidence of water use within rooting depth is provided by a short study conducted in the spring of 2009 during a period when concentrate availability was limited due to repairs to the MTF RO. In this study, the scheduled soil moisture measurements were taken with the neutron probe then the irrigation turned off for one month. At the end of the "dry down" period the moisture was again recorded (Figure 5).

Our hypothesis that the halophyte *Atriplex lentiformis* can be irrigated with RO concentrate from CAP water in Tucson at rates equal to or slightly greater than reference crop ET is supported by both the drainage analysis and the dry down experiment. This hypothesis is further substantiated by comparing the soil water storage with drainage values and the water applied at three ET rates plus recorded rainfall for the lined trials (see figure 6).

These graphs indicate that through best management practices, i.e. deficit irrigation bases on irrigation control using reference crop ET, drainage below the root zone can be managed to

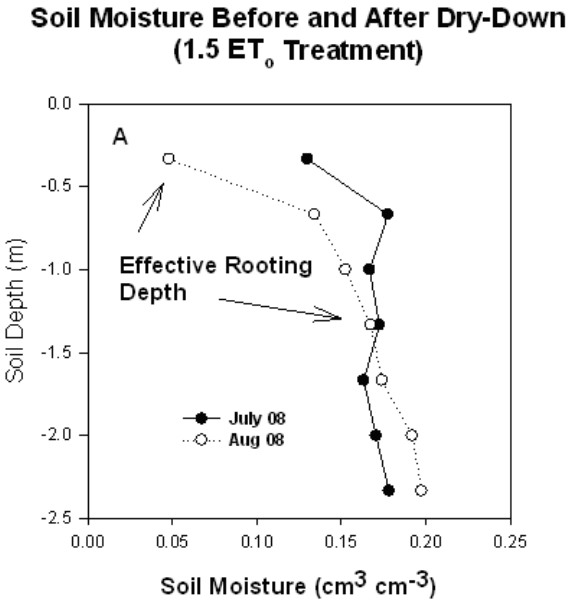


Figure 5, Soil Moisture from Dry-Down, ET 1.5

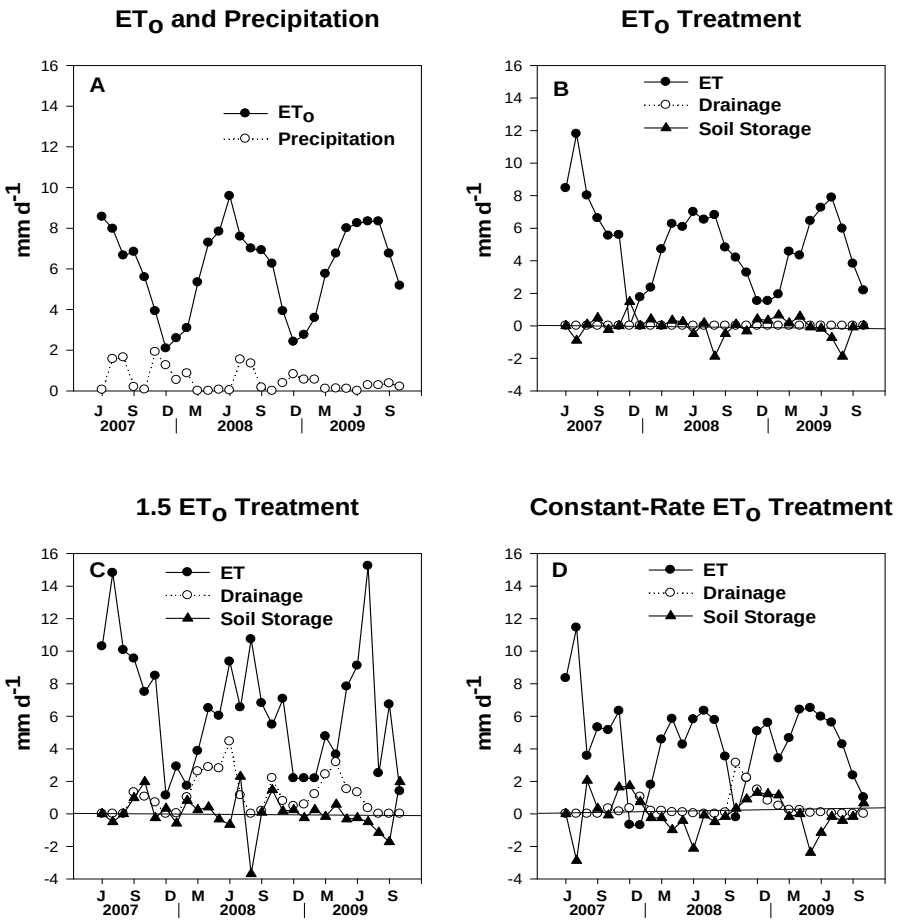


Figure 6, Soil Moisture from Dry-Down, ET 1.5

provide for aquifer protection. Drainage from individual plots within the 1.5 ET and Et constant trials were highly variable and in total were 14.5% and 8% respectively. This variability is likely due to anomalies including rainfall events, irrigation valve failure, and the development of preferential pathways or a combination of these. The lack of drainage in the Et 1.0 trial demonstrates that the salts from the concentrate irrigation can be held within or near the root zone.

Soil moisture monitoring using neutron probe continues. See Fig. 7 for year one record.

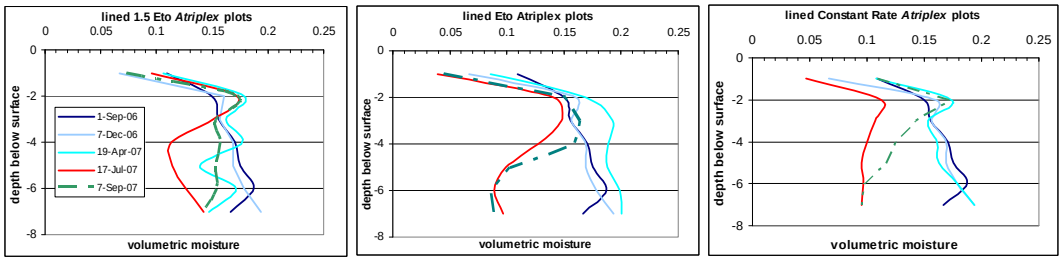

***2009 Step 4 - Productivity/potential of Halophytes for animal feed***

Field productivity and the nutrient value of *Atriplex lentiformis* was monitored to assess the potential of the halophyte for forage or commodity additive in livestock feed. In addition, a review of the literature on halophyte use for animal feed is underway. Preliminary results from this review are presented in Appendix 6.

In the late summer of 2009-2010 total biomass from the 3 years growth was measured and averaged (24.0 tonnes $ha^{-1}$ $yr^{-1}$ ) The trials showed no significant difference in biomass productivity between the three irrigation rates. Assuming leaf production is annual the leaf and small stem portion of the biomass for this year was 0.7 kg $m^{-2}$ or 7.0 tonnes $ha^{-1}$ $yr^{-1}$. See Figure 8.

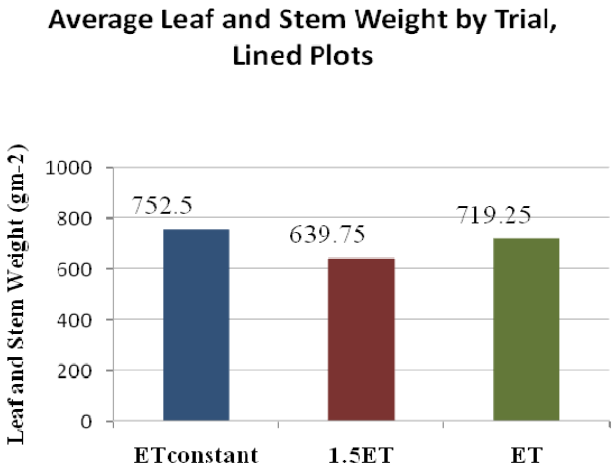


Fig 8 – Average Productivity per Hectare

Table 1 compares nutrient values for *Atriplex lentiformis* and *A. nummularia* with other traditional forage crops grown in the region. Only leaves and small stems were used for the proximate analysis of the *Atriplex spp*.

The proximate analyses show *Atriplex* to be comparable to conventional forage in protein and other digestables but higher in salt. Productivity is similar to conventional crops in tonnes per hectare. This past year the trial plots were thinned from four to two rows each. This will provide access to assess productivity from multiple annual clippings and to spacing associated with an agronomic setting to facilitate field management and mechanical harvesting. Methods for plant material processing that will facilitate integration of the plants as a commodity to the feed lot and dairy industry require further study.

Table 1, Proximate analysis Atriplex spp. compared to other forage crops (% dry matter)

| Item | CP | Ash | ADF | Na | K | ADL |
|---|---|---|---|---|---|---|
| ***Cynodon* hay**[a] | 12.3 | 8.8 | 26.1 | 0.10 | 1.5 | 6.4 |
| ***Atriplex lentiformis***[b] | 12.2 | 20.7 | 27.6 | 4.20 | 1.6 | -- |
| ***Atriplex nummularia***[b] | 19.8 | 26.3 | 11.4 | 5.47 | 4.5 | -- |
| ***Medicago sativa* L. (alfalfa)**[c] | 17.5 | 11.5 | 28.4 | 0.009[d] | 2.9[d] | 7.9 |
| ***Hibiscus cannabinus* L. (kenaf)** [c] | 11.0 | 11.8 | 41.2 | -- | -- | 10.5 |
| ***Sorghum spp.* (Sudan grass)**[d] | 10.8 | 7.64 | 41.6 | 0.010 | 1.9 | 4.6 |

a. Swingle, R.S. et al. 1996. Growth performace of lambs fed mixed diets containing halophyte ingredients.
b. Proximate analysis of plants. 2010.
c. Swingle, R.S. et al. 1978. Chemical composition of kenaf forage and its digestibility by lambs and in vitro.
d. Dann, H.M. et al. 2008. Comparison of brown midrib sorghum-sudangrass with corn silage on lactational performance and nutrient digestibility in Holstein dairy cows.

***2010 Step 1 Ion Exchange as RO pretreatment***

Bench scale investigations of Ion Exchange as a pretreatment for RO were conducted in early 2009 by the Chemical and Environmental Engineering Department as a proof of concept. . IX softening ahead of RO treatment was investigated to estimate reduction in membrane scaling and to evaluate recovery increases using a combination of pre-softening and reverse osmosis (see Appendix 9. Pre-softening extends recovery during reverse osmosis by removing the most prominent cations in scaling reactions—free barium and calcium ions. IX as an RO pretreatment in combination with VSEP, post RO (Appendix 11) suggest that very high recoveries, on the order of 99%, are feasible when reverse osmosis is carried out using a pre-softened water in combination with the deployment of VSEP Theoretical analyses were carried out to determine probable process limitations, which are now felt to result from development of very high osmotic pressures on the feed side of RO membranes, with consequences for pressure requirements in downstream RO vessels (Appendix 10).

***2010 Step 2 - Co-precipitation and purity of mineral precipitates***

No activity due to funding limitations.

***2010 Step 3 - O&M of SSF/RO pilot - concentrate production***

The indicators used to evaluate the status of the pilot-scale reverse osmosis unit and time-dependent trends in performance were the membrane permeation coefficient and salt transport coefficient, defined previously. Both indicators reflected a gradual deterioration of performance over periods on the order of months (Appendix 4). Periodic cleaning and/or membrane replacement temporarily restored membrane performance, but was quickly followed by loss of membrane permeability when the unit was returned to operation. In general, deterioration of performance was most rapid in the downstream RO vessels, suggesting that scaling was the primary cause of changes in membrane permeability. In all cases, however, the performance characteristics of upstream membranes followed the same trends after a modest lag on the order of weeks to months. The combination of SSF pretreatment and RO was capable of adequate performance for desalination of Central Arizona Project water, with periodic cleaning, for a period on the order of one or two years.

*Membrane autopsies.*After a period of months to years of semi-continuous operation, select membranes were removed from the field-scale RO unit and autopsied to determine the probable cause of diminished performance. Deposited materials were scraped from the membrane surfaces, inventoried and analyzed for evidence of mineral scaling and bacterial fouling. Although experimental evidence was in the end inconclusive, it seems that material was deposited from a combination of sources that included primarily (i) a mixture of alumino-silicate clays; (ii) mineral precipitation—barium sulfate, calcium carbonate and gypsum; and (iii) colloidal organics. Heterotrophic plate counts were invariably low and could not account for even a modest fraction of membrane surface coverage. Additional work is warranted in this area if membrane useful life is to be extended (see Section 1.3 in Appendix 4). The complete results of this work are presented in Appendix A2. A similar set of membrane autopsies will be used to determine the nature of deposited material on RO membranes following an extended period of MF pretreatment and RO desalination under otherwise identical conditions. Results will be used to further examine the relative advantages of SSF versus MF pretreatment.

***2010 Step 4 - Salt Balance and feasibility of Halophytes for CM***

Higher application rates reduced water use efficiency (WUE) and yield, while WUE increased on lower rates. On concentrate salinities from RO of CRW, *A. lentiformis* will maintain productivity with minimal discharge of drainage on 0.8 $ET_o$ irrigation. On higher salinities, yield can be maintained only at higher water application rates and the discharge of drainage increases. A mass balance determined for the field plots showed that lysimeter basins had not yet reached equilibrium conditions after three years, and most of the salt applied in the irrigation water was still stored in the root zone. See Appendix 7.

***2010 Step 5 - Aquaculture w/concentrate - viability and economics***

A number of bench top bio-assays have been conducted or are underway to determine viability of aquaculture species (shrimp and Tilapia) on concentrate. Survivability and growth rate on both RO and VSEP concentrate are being evaluated. In addition bench top studies to examine the viability of *A. lentiformis* on VSEP concentrate have been conducted. A brief on each of these experiments is presented in Appendix 8. The economic analysis was not performed because of funding limitations.

## Slowsand compared to Microfiltration pretreatment

Pretreatment of raw water for RO separation of soluble components is an absolute necessity for preservation of RO membrane integrity, prevention of fouling and extension of membrane life. There are, however, several ways to provide pretreatment, including SSF and MF. These two pretreatment alternatives were studied previously, leading to a conclusion that both methods performed adequately but that, land permitting, SSF was much less expensive. Because RO membrane post mortems indicated that clay particles on the RO membranes may have been derived from SSF, however, MF pretreatment was revisited.

After MF pretreatment was initiated in April 2009, the record of time-dependent water permeation coefficients for RO treatment grew much steadier (Figure 1). Results suggest that the quality of MF-treated water may be superior to that SSF effluent for downstream RO separation of water-soluble components. See Appendix 3.

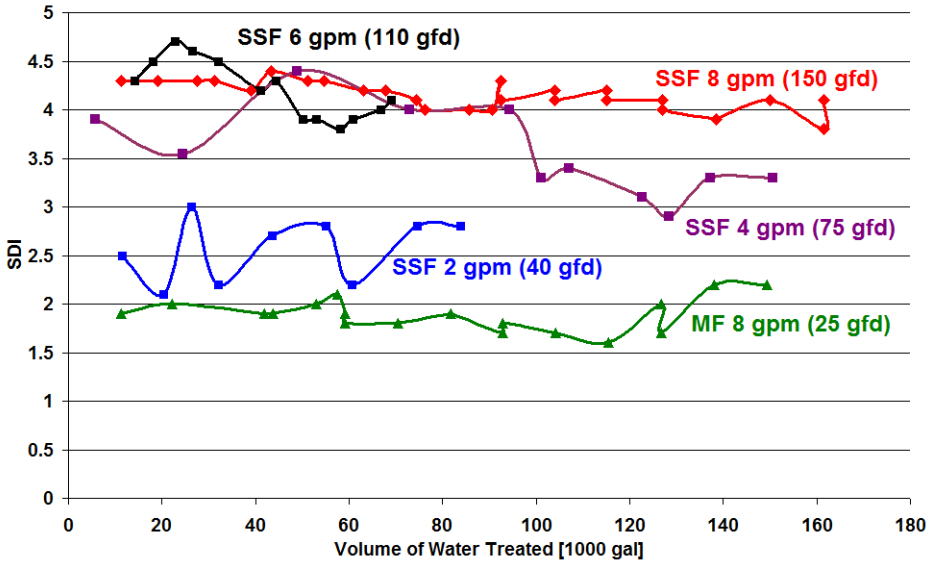


Figure 9 - Comparison of SSF and MF of silt density index (SDI)

Comparison of SSF and MF effluent SDI values (Figure 9) indicates that (i) SSF effluent quality is sensitive to the water application rate and (ii) SSF SDI values can approach those of the MF effluent if CAP water application rates are maintained at $\leq 0.027$ gpm/ft$^2$.

A detailed presentation of results is provided on Appendix 3. Side-by-side comparison of the pretreatment options suggests that microfiltration is capable of out-performing slow sand filtration based on silt density index values in reactor effluents. However, there were extended periods in which SDI values were continuously very low—on the order of MF SDIs. There was no readily apparent explanation for the periods of improved performance. Both the SSF and MF processes were capable of satisfying criteria for extended operation for RO treatment (SDI < 5) and, frequently, manufacturer's requirements for RO membrane warranty (SDI < 3). MF performance was in this range on all but a very few occasions. Neither SSF or MF treatment was expected to remove dissolved carbon and did not. Particulate organic carbon was normally a very small fraction of total organic carbon in Central Arizona Project water, so that there was little removal of organic carbon via either pretreatment process. Results to follow as an addendum to this report include numbers of heterotrophic bacteria in the SSF and MF effluents and the findings of membrane autopsies following an extended period of reverse osmosis treatment using water pretreated via MF. The latter results will be compared with results of membrane autopsies following an extended period of SSF pretreatment.

## Treatment Train Options Economic Evaluation

From the research program to date we have compiled performance data and associated cost analyses that are sufficient to prepare a preliminary cost comparison for various treatment train options (Table 1. Pretreatment options consist of slow sand filtration and microfiltration. Brine management options include IX softening ahead of reverse osmosis, VSEP treatment after reverse osmosis and irrigation of halophytes in addition to advanced evaporation (baseline case).

The economic comparison including the assumptions are presented in Appendix 1

## Project Management

This Cooperative Agreement, dated September 24. 2009, included a scope and budget based on a two year effort. It was partially funded for FY 2009-2010 but was not extended for the second year FY 2010-2011. While the scope of the agreement was broken into Steps (Tasks) for each "Calendar Year" 2009 and 2010 for contractual efficiency, the actual research program is organized using UA fiscal year (July 1- June 30) and includes Steps and Tasks that overlap (due to graduate student research continuity and program requirement from supporting partners).

Because the USBR funding for 2010 was not available, research continued with only partner support, supplemental grants and student/faculty commitment. As a result the scope and outcomes for the second year steps were not fully realized. Our proposal for a new USBR S&T program was not awarded but the review comments suggest that we apply to the WATERSmart program for pilot demonstration scale research. We await a response to this proposal.

## List of Appendices

**1: Treatment Train Options: Cost Analysis and Assumptions**

**2: In Kind Support, Contributions, and Complementary Program Grants**

**3: Comparison of Microfiltration and Slow Sand Filtration as a Pretreatment of Desalination of Central Arizona Project (CAP) Water**

**4: Reverse Osmosis Treatment of Central Arizona Project Water: Research Program Summary 2007-2010**

**5: Water consumption, irrigation efficiency and nutritional value of *Atriplex lentiformis* grown on reverse osmosis brine in a desert irrigation district**

**6: Ruminant Digestion and the Nutritive Potential of Halophytes (*Atriplex* spp.) for use in the Feed Lots and Dairy Industry: A Literature Review**

**7: Sustainable Irrigation Strategies for the Forage Halophyte, *Atriplex lentiformis***

**8: Bio-Assays of Aquaculture Species using Reverse Osmosis Concentrates: Preliminary Findings and Growth/Survivability of two Halophyte Species using RO and VSEP Concentrates**

**9: Ion Exchange Pre-Treatment of Reverse Osmosis Feed Water Using Regenerant Recycle**

**10: Use of Ion Exchange Softening with Regenerant Recycle as Pretreatment for Reverse Osmosis Desalination of Central Arizona Project Water**

**11: Ion Exchange vs. Vibratory Shear Enhanced Processing (VSEP®) for Optimized Salt Management in Lower Colorado River Water**

# Appendix 1:

Treatment Train Options: Cost Analysis and Assumptions

# Treatment Train Options: Cost Analysis and Assumptions

From the research program to date we have compiled performance data and associated cost analyses that are sufficient to prepare a preliminary cost comparison for various treatment train options (Table 3). Pretreatment options consist of slow sand filtration and microfiltration. Brine management options include IX softening ahead of reverse osmosis, VSEP treatment after reverse osmosis and irrigation of halophytes in addition to advanced evaporation (baseline case).

We continue to refine the numbers based on ongoing performance evaluations as data from research components continue to be generated. For example, the IX cost data is based on theoretical performance and will be updated as soon as data from a scaled application are available. The data analysis representing a comparison of SSF and MF is complete, as is an economic analysis of several methods available for brine minimization and disposal (see above).

**Table 3.** Alternative treatment trains and associated unit costs in $/Ccf (2010 dollars)

| Options[1] | SSF | MF | IX | RO | $RO_3$ | VSEP | EEVAP | HF | Total Cost[2] |
|---|---|---|---|---|---|---|---|---|---|
| ***1*** | 0.335 | - | - | 0.497 | - | - | 1.605 | - | 2.437 |
| ***2*** | 0.335 | - | 0.109 | 0.669 | | - | 0.369 | - | 1.482 |
| ***3*** | 0.335 | - | - | 0.497 | - | 0.599 | 0.305 | - | 1.736 |
| ***4*** | 0.335 | - | - | 0.497 | - | - | - | 0.898 | 1.730 |
| ***5*** | - | 0.467 | - | 0.497 | - | - | 1.605 | - | 2.569 |
| ***6*** | - | 0.467 | 0.109 | 0.669 | | - | 0.369 | - | 1.614 |
| ***7*** | - | 0.467 | - | 0.497 | - | 0.599 | 0.305 | - | 1.868 |
| ***8*** | - | 0.467 | - | 0.497 | - | - | - | 0.898 | 1.862 |

[1]The alternative treatment trains are discernable from the table headings. That is, option #1 consists of slow sand filtration followed by reverse osmosis treatment and enhanced evaporation for brine disposal.
[2]All the costs are for 15 MGD treatment plant operating for 30 years with the discount operator of 6%.
[3]The unit value of the water cost is assumed as $1,000/AF.
[4]The personnel cost is assumed as $100,000 per personnel per year.
[5]Reverse Osmosis (two-stage) is running at 80% recovery in all the options. And the third-stage RO is running at 95% following the two-stage RO after MF pretreatment and IX softening, bringing the overall recovery to 99%.
[6]The personnel cost is included in each unit operation cost separately and the number of personnel required for SSF, MF, IX, RO, VSEP, EEVAP and HF is seven, two, one, four, two, two and one, respectively. $RO_3$ (third-stage RO) personnel is included in the RO.
[7]The cost for water not treated by the RO and/or VSEP is included in the EEVAP or HF.
[8]The cost for water used for IX regeneration and its disposal is included in the EEVAP cost for Options 2 and 6.
[9]The cost for water to clean VSEP is included in the VSEP cost.

***Assumptions and references for SSF:***

1. The approach velocity is chosen as 0.107 gpm/$ft^2$ (8 gpm/75 $ft^2$). The range is 0.1-0.4 m3/h/m2 specified for Slow Sand Filtration by WHO (Geneva, 1974) and the Arizona Department of Environmental Quality (Arizona Department of Environmental Quality, 1978) specifies a range of 0.032 to 0.16 gal/min/ft2 [0.08 to 0.4 m/h, 2.0 to 10.0 MGD/acre].
2. Construction cost is from the "Costing Summaries for Slow Sand Filtration and Ceramic Media Filtration"; New England Water Treatment Assistance Center.
3. The cost of land is chosen as $20,000. The range is $3,000-30,000 in Arizona Valley.
4. The thickness of the sand layer is chosen as 3 ft. The range is specified as 2-4 ft (0.6-1.2 m) by WHO.
5. The porosity of the sand is assumed as 0.4 (reference by Wikipedia).
6. The density of the sand is assumed as 1602 kg/$m^3$ (reference by simetric.co.uk).
7. The cost of sand is assumed as $273.75 (reference by Oglebay Norton Industrial Sands, Inc. 2006; from Martin Yoklic; Silica Sand Filter Media ES 0.27-0.33 mm, UC 1.7 in 1.5 ton supersacks, with delivery).
8. The thickness of gravel layer is assumed as 1.5 ft composed of 0.5 ft of 1-in, 0.5 ft of 3/4-in, and 0.5 ft of 3/8-in gravel (reference by BOR Report #90).
9. The porosity of the gravel is assumed as 0.2 (reference by Wikipedia).
10. The density of the gravel is assumed as 1682 kg/$m^3$ (reference by simetric.co.uk).
11. The cost of gravel is assumed as: (reference by www.areamulchandsoils.com/price%20list%20gravels.html)

| Size of Gravel | Cost ($/ton) |
|---|---|
| 3/4-1 1/2 inches | 26.5 |
| 1/4-3/4 inches | 24.5 |
| 1/4 inches | 24.75 |

12. The height of the freeboard is assumed as 1 m (the range is specified as 1-1.5 m by WHO.)
13. The thickness of Schmudzdecke layer removed is assumed as 1.5 cm (The range is specified as 1-2 cm by Letterman, 1991; reference by Gary S. Logsdon).
14. The frequency of the cleaning is assumed via the formula presented below that is calculated with the operation data collected during the Marana Study.

$$y = -0.1771X^3 + 4.375X^2 - 35.292X + 101.5$$

where, X is the flow rate of the SSF in gpm.

15. Working hours spent for each cleaning per 100 $m^2$ of SSF is assumed as 2.5 hours (reference by Letterman, 1991).
16. It is assumed that the resanding is performed by using the same sand removed during the cleaning of the SSFs after it is being cleaned.
17. After the depth of sand in a slow sand filter reaches about one half of the original depth due to repeated sand scrapings, clean sand is added to the filter to restore the bed depth. Good practice involves removing sand to the bottom of the filter bed, placing new or cleaned sand in the trench created by the sand (reference by SSFs for Small Water Systems by Gary S. Logsdon).
18. The SSFs will be in operation for 30 years without any new construction.

***Assumptions and references for MF:***

1. The unit price, raw water pumping and yard piping for MF is included in the construction cost. The construction cost is supplied by Malcom Pirnie, Inc., Tucson Office to Justin. We need to check the reference from Justin's thesis.
2. The O&M cost for MF is obtained from the cost manual page 99 (need to get the full reference from Dr. Ela).
3. Mf will be in operation for 30 years without any new additions to the existing facility.

***Assumptions and references for IX:***

1. Manufactured equipment, excavation and site work, concrete, steel, labor for construction, pipe and valves, electrical and instrumentation, housing, miscellaneous and contingency costs are included in the construction and miscellaneous costs of IX facility.
2. The depth of resin and the contractor diameter are assumed as 8 and 12 ft for each IX contractor, respectively.
3. Twelve IX contractors are used for treating 15 MGD influent water.
4. The bed volume spent per regeneration is assumed as 10.
5. The resin price is \$4,240/$m^3$ (Ion Exchange Chemistry and Operation; Ion Exchange Systems and Equipment. REMCO Engineering Water Systems and Controls. 8 May 2009 http://www.remco.com/ix.htm)
6. Resin lifetime is assumed as 5 years.
7. It is assumed that all divalent cations (i.e. $Ca^{+2}$, $Mg^{+2}$, $Ba^{+2}$ and $Sr^{+2}$) are removed via IX and replaced with $Na^{+}$ ions instead, which increases the power requirement for the two-stage RO as a results of the increase in the ion concentration. However, it solves the probability of precipitation of divalent cations at the same time.

***Assumptions and references for RO and $RO_3$:***

1. The two-stage RO is assumed to be running at 80% recovery for all the options listed.
2. Third-stage RO ($RO_3$) is assumed to be running at 95% recovery with the assumption of no precipitation of divalent cations since they are all removed via IX theoretically. In plate-and-frame and jar-test precipitation studies, this theory is tested in the lab and concluded that it is possible to do so. However, there is no pilot-scale study to back this theory up, yet.
3. The construction cost for both RO and $RO_3$ is assumed by using the formula presented below: (Reference Table 16:32; Product and Process Design Principles; Warren D. Seider; 2004; Second Edition)

$$\text{Cost [\$]} = 2.1\ [\$/\text{gal/d}] \times Q_{\text{product}}\ [\text{gal/d}]$$

4. For the pumping cost, the energy cost is assumed to be 0.12\$/kWh.
5. The gas constant is 0.08206 L.atm/mol/K and the operating temperature is assumed to be 21 $^{o}$C (294.15 $^{o}$K).
6. The energy required for pumping is calculated by using the formula presented below:

$$\Sigma\Pi_i = R \times T \times \Sigma C_i/MW_i$$

where, $\Pi_i$ is the osmotic pressure of ion i
R is the gas constant (0.08206 L.atm/mol/K)
T is the water temperature (294.15 $^oK$)
$C_i$ is the concentration of ion i (g/L)
$MW_i$ is the molecular weight of ion i (g/mol)

The total pressure required for a sustainable water production is supposed to be greater than the sum of minimum amount of osmotic pressure in the reject stream of each RO and the $\Delta P$ calculated by:

$$\Delta P \text{ [psi]} = F \text{ [gfd]} / A \text{ [gfd/psi]}$$

where, $\Delta P$ is the pressure required to produce water with a flux of F via the selected membrane type
F is the water flux
A is the water transport coefficient specific to the selected membrane type

Therefore, the total pressure required (pumping pressure) is calculated via $P_{total} = \Sigma\Pi_I + \Delta P$ with the assumption of hydraulic headloss (including the minor headloss due to the valves, elbows, etc.) through the RO unit is negligible.

7. The water flux is assumed as 15 gfd for Hydranautics ESPA4 membranes to be on the safe side. Manufacturer claims that the water flux for this membrane type is 30 gfd.
8. The water transport coefficient (A) for the first set of ESPA membranes tested during Marana study was around $20\times10^{-12}$ m/s.Pa when they were clean and for the the second set Koch membranes was around $15\times10^{-12}$ m/s.Pa. Therefore, an average value of $17\times10^{-12}$ m/s.Pa (0.248 gfd/psi) for this economic analyses study.
9. The total membrane area required to produce $Q_{product}$ (calculated by $Q_{total} \times R_{RO}$) is calculated via:

$$A_{total} \text{ [ft}^2\text{]} = Q_{product} \text{ [gal/d]} / F \text{ [gfd]}$$

10. The active membrane area for each ESPA4 is assumed as 400 $ft^2$ per manufacturer's spec sheet (reference hydranautics.com).
11. The cost for each ESPA4 8040 is assumed as 594.99 $. (Reference http://www.thepurchaseadvantage.com/page/TPA/PROD/hydranautics_brackish_water_ro_membranes.html/CDHYESPA4; The Siemens Water Technologies)
12. The lifetime of each membrane is assumed as 3 years.

***Assumptions and references for VSEP:***

1. VSEP is assumed to be running at 82.4% recovery for Options 3 and 7. This is defined as the optimum recovery via economic analysis depending on the experimental runs performed in the Marana study.
2. Total run time between each cleaning is assumed to be 37 hours.
3. Automated cleaning time for large-scale (i84) VSEP units is assumed to be 2 hours (reference New Logic, Inc.).

4. Average permeate flux for VSEP with ESPA2 membranes is assumed to be 47.28 gfd via experimental study performed at Marana with the pilot-scale VSEP unit.
5. The membrane area for a single i84 VSEP unit is assumed to be 1500 $ft^2$ (reference New Logic, Inc.; http://www.vsep.com/products/i84.html)
6. The cost for a single i84 VSEP unit is assumed as $250,000 (reference New Logic, Inc., personal communication with Larry Stowell).
7. The service life of VSEP units is assumed to be 10 years (reference New Logic, Inc., personal communication with Larry Stowell).
8. The lifetime of a single set of membranes for VSEP units is assumed as 2 years and the cost of each set is $70,000 (reference New Logic, Inc., personal communication with Larry Stowell).
9. The amount of water spent for each cleaning, including the water used for flushing the unit following the cleaning, of a single i84 VSEP unit is assumed as 1200 gal and the cost of chemicals for each cleaning is $104 (reference New Logic, Inc., personal communication with Larry Stowell).

***Assumptions and references for EEVAP:***

1. The construction and O&M costs for enhanced evaporation ponds are taken from the Malcom Pirnie Inc. and Separation Processes Inc. report (2008) “Evaluation for Water Treatment Options for TDS Control”.
2. All the disposed water from the treatment plant, i.e. the untreated brine, IX regenerant, etc., assumed to end up in enhanced evaporation ponds.

# Appendix 2:

In Kind Support, Contributions, and Complementary Program Grants

# In Kind Support, Contributions, and Complementary Program Grants

### In Kind Support and Contribution Summary (2007-2008)

| | 2007 | | 2007 | | 2007 | | 2008 | |
|---|---|---|---|---|---|---|---|---|
| | Cash | IKS | Cash | IKS | Cash | IKS | Cash | IKS |
| NW Water Partners | $45,000 | | $45,000 | | $60,000 | | $60,000 | |
| All Water Partners | | $49,481 | | $84,544 | | $69,016 | | $59,737 |
| UA Faculty | | $38,000 | | $38,000 | | $38,000 | | $38,000 |
| Waived Indirects | | $0 | | $46,350 | | $15,066 | | $35,999 |
| | $45,000 | $87,481 | $45,000 | $168,894 | $60,000 | $122,082 | $60,000 | $133,736 |

### In Kind Support and Contribution Summary (2009-2010)

| | 2009 | | 2010 | | Total Project | | |
|---|---|---|---|---|---|---|---|
| | Cash | IKS | Cash | IKS | Cash | IKS | Total |
| NW Water Partners | $60,000 | | $60,000 | | $330,000 | | |
| All Water Partners | | $60,000 | | $60,000 | | $382,778 | |
| UA Faculty | | $38,000 | | $38,000 | | $228,000 | |
| Waived Indirects | | $3,790 | | $0 | | $101,205 | |
| | $60,000 | $101,790 | $60,000 | $98,000 | $330,000 | $711,983 | $1,041,983 |

### Bureau of Reclamation - Research Program Funding

Long-term testing near Tucson, Arizona for concentrate management using halophyte irrigation; with associated slowsand filtration (SSF) and reverse osmosis (RO) treatment.

| Funding Agency | | Status | Year | Amount |
|---|---|---|---|---|
| USBR | S&T | Funded | 06-07 | $90,000 |
| USBR | S&T | Funded | 07-08 | $29,225 |
| USBR | S&T | Funded | 08-09 | $69,996 |
| USBR | | Funded | 09-10 | $65,000 |
| USBR | | Unfunded | 10-11 | $0 |
| | | | | $254,221 |

| Complimentary Research Grants | Funding Agency | Status | Year | Amount |
|---|---|---|---|---|
| Maximizing water recovery during R O treatment - 2year | WSP | Funded | 06-08 | $90,049 |
| Brine Minimization/Salt Management Using VSEP Technology | WSP | Funded | 07-08 | $49,945 |
| Underground Storage and Recovery of CAP Water | WSP | Funded | 08-09 | $41,438 |
| VSEP Equipment (City of Tucson) | COT | Funded | 07-08 | $58,000 |
| Project Internship | AWI | Funded | 07-08 | $5,000 |
| RO Pretreatment Using Ion Exchange | AWI | Funded | 07-08 | $48,625 |
| Recovery and Residual Mgmt. for RO Treatment of CAP Water | AWI | Funded | 07-08 | $44,932 |
| Student Internship for project to UA Chem Eng. | Oro Valley | Funded | 08-09 | $10,000 |
| Salt River Project through UA Chemical Eng. | SRP | Funded | 08-09 | $50,000 |
| Salt River Project through UA Chemical Eng. | SRP | Funded | 09-10 | $50,000 |
| Salt River Project through UA Chemical Eng. | SRP | Funded | 10-11 | $50,000 |
| | | | | $497,989 |

| Total Program | Amount | % of Total | |
|---|---|---|---|
| Total USBR Program Support | $254,221 | 13.2% | |
| Total USBR Internal Support | $130,000 | 6.8% | *Estimated* |
| Total NWWP and TW In-Kind | $382,778 | 19.9% | |
| Total NWWP Funding Support | $330,000 | 17.2% | |
| Total Complementary Research Grants | $497,989 | 25.9% | |
| Total UA Faculty and Waived F&A | $329,205 | 17.1% | |
| | $1,923,472 | | |

# Appendix 3:

Comparison of Microfiltration and
Slow Sand Filtration as a Pretreatment of
Desalination of Central Arizona Project (CAP) Water

# Comparison of Microfiltration and Slow Sand Filtration as a Pretreatment of Desalination of Central Arizona Project (CAP) Water


## Abstract

Sustainable water supply in semiarid southwestern United States depends on the utilization of waters of impaired initial quality, including brackish and reclaimed water, or on exploiting new water resources that are geographically distant. The Colorado River is both geographically distant from major population centers in Arizona and, from the perspective of salt content, modestly impaired (total dissolved solids content ~800 mg/L south of Lake Mead). Arizona is entitled to withdraw up to 2.8 MAF of water from the Colorado River each year, of which 1.6 MAF is transported to the state's interior via the Central Arizona Project (CAP) canal. Each year, the CAP transports ~200,000 metric tons of salt to Tucson alone, and without salt management steps, accessible ground water and regional soils may accumulate salt at a rate that presents sustainability problems. A pilot study was conducted to establish the long-term feasibility of using reverse osmosis (RO) treatment to manage salt levels in CAP water. Microfiltration (MF) and slow sand filter (SSF) were compared as RO pretreatment options. The study generated a record of side-by-side performance of SSF and MF over a one-year period. SSF and MF are compared on the basis of performance characteristics including effluent silt density index and cost.


**Keywords:** desalination; microfiltration; reverse osmosis; slow sand filtration


## Introduction

Southwestern cities are among the fastest growing in the United States, a condition that stresses limited water supplies. Satisfaction of projected water demand in Las Vegas and Phoenix for the year 2020 will depend on: conservation, use of impaired quality waters such as wastewater effluent or brackish groundwater, importation of water, and groundwater overdraft. Arizona law mandates a rough balance between groundwater withdrawal and replenishment rates by year 2025 in the "Active Management Areas" (areas around major population centers) [1]. In the Tucson Active Management Area (TAMA; Figure 1), projected compliance is based on full utilization of regional allocation of Central Arizona Project (CAP) water, and reclamation of municipal wastewater effluent. Uncertainty regarding the long-term availability of Colorado River water delivered to the CAP presents a major impediment to water resource planning [2]; improvement of water treatment processes are essential for sustainability.

Reverse osmosis (RO) is a reliable, efficient method to separate water from soluble components; however, pretreatment of feed water is required to maintain RO efficiency. Adequate pretreatment will: preserve membrane integrity, reduce fouling, and extend membrane life. Of the several methods of RO pretreatment available, slow sand filtration (SSF) and microfiltration (MF) were chosen for this comparison. These two pretreatment alternatives were previously studied, leading to a conclusion that both methods performed adequately and that, land permitting, SSF was much less expensive. However, RO membrane post mortems indicated that clay particles on the membranes may have been derived from SSF; therefore MF pretreatment was revisited in the latter phase of this investigation.

## Literature Review

*Slow Sand Filtration*

The method of slow sand filtration dates back to the Roman Empire and is one of the first water treatment techniques used in the development of municipal water treatment facilities. In 1804, Sir Robert Thom designed the first municipal water treatment facility, which used slow sand filtration to supply drinking water to every household of Paisley, Scotland. Since then, slow sand filtration has mainly been replaced with rapid sand filtration due to the demand increases of municipalities and the flow limitations of slow sand filters. However, in low water demand instances, such as in small towns and developing countries, it is very practical and widely used due to the absence of a need for electrical power, and the low complexity of process operation.

In slow sand filtration, water is passed through a porous bed of filter medium that physically removes suspended particles [4]; however, there is also biological removal of particles as well [5]. Slow sand filters differ from other media filters in the following aspects: rate of filtration and presence of a biological layer on top of the sand called the schmutzdecke, a German term for dirt cover. A typical slow sand filter is comprised of: a layer of raw water above the filter medium, the medium itself (sand), the schmutzdecke, and an under drain system to collect the filtered water (Figure A1-1).

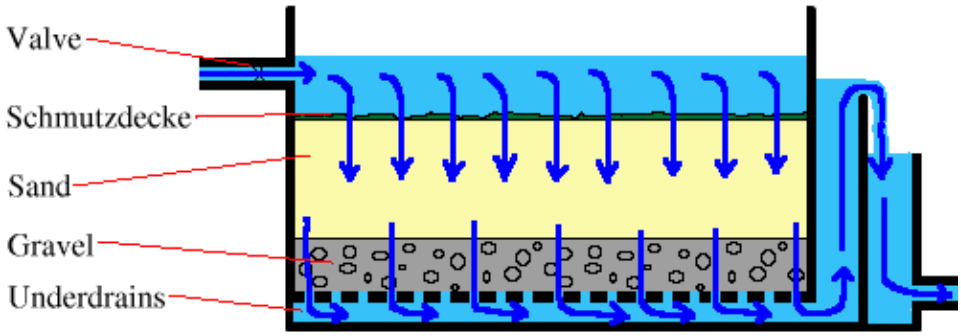


**Figure A1-1.** Typical Slow Sand Filter Design (Figure is taken http://www.thewatertreatments.com/wp-content/uploads/2010/09/filter-slow-sand-filter.gif)

The supernatant layer of raw water above the sand provides the hydraulic head that drives the filtration process, and is typically 1 to 1.5 meters in depth. The sand serves as a filter media removing suspended particles via adsorption and straining, and as a physical support for the biological layer or schmutzdecke [6]. Most under drain systems are comprised of a perforated pipe surrounded by gravel that supports the sand above it. The schmutzdecke plays a vital role in the filtration process in that it acts as a physical net-like barrier to trap suspended particles. Microbes within the layer biodegrade trapped particles.

The mechanism of slow sand filtration was originally thought to be strictly physical removal of suspended particles in the water; however, after scientific examination and study of the schmutzdecke, it is now known that much removal comes from biological activity at the top of the sand layer [5]. The factors influencing the schmutzdecke performance are: sand filter maturity, and contact time with the water. It is necessary to let a filter mature to build up

resident micoflora that actively participates in the degradation process, while simultaneously controlling the flow rate to prevent washout and allow ample contact time for biodegradation.

SSF is a feasible option for RO pretreatment because it requires less capital investment than MF and is simple to operate [7]. Due to the absence of high pressure processes, little mechanical operation is required for SSF; the head above the water is ample force to drive low flow needed for contact time. Furthermore, the process of SSF doesn't require special materials and hardware such as membranes, compressed air, valves, etc which drive up the capital cost of MF substantially.

However, in large municipal systems, SSF requires a large land footprint [8], several acres in most cases. The low overflow rates in SSF increase the surface area required for large volumes of water to be treated. Another disadvantage of SSF is the labor intensive cleaning that decreases the water delivery efficiency and increases operational cost. The time required for a filter cleaning and subsequent re-maturation is typically in the order of days to weeks. Lower times can be achieved using wet harrowing, but times required for MF cleanings are much shorter. This decreases the delivery of water and presents a design limitation. Labor required for cleaning increases the operational cost of SSF.

This experiment utilized two slow sand filters that were constructed similarly but used slightly different sands. The surface area of each SSF was 7 $m^2$ and the supernatant head of water above the sand was approximately 1.5 m (constant head operation). The maximum flow rate attainable for each SSF without sand wash out was 0.0722 $L/m^2/s$. The sand bed depth fluctuated from 0.64 m when sand fully cleaned, to 0.4 m after multiple scrapings of the schmutzdecke. The two sand filters were always operated in parallel at the same flow rate to gain replicate data treating the same water.

*Microfiltration*

The process of microfiltration (MF) uses micro porous membranes to sieve suspended particles from a fluid. This is a completely mechanical process in that no chemical or biological activity takes place. It is effective in removing relatively high molecular weight particles in the 100,000 to 5,000,000 range such as: algae, bacteria, some dyes and pigments, proteins, cryptosporidium, giardia, and if below 0.2 microns, virus, and colloidal silica. A pilot plant operated for 6 months in Wisconsin completely removed coliforms from a 1-2 log feed stream concentration [9].

Pressure membranes listed in order of decreasing pore size and increasing operating pressure include: microfiltration, ultra filtration, nano filtration, and reverse osmosis membranes. Since MF utilizes the largest pore size of the pressure membrane family, from 0.1μm-10μm, it operates at the lowest operating pressure (10-100psi).
Microfiltration is in the class of pressure membranes in which water is passed through a membrane in either dead-end or cross flow configuration. Dead-end systems force raw water through the membrane as the only outlet in the system. The flux declines at a rate that depends on water quality. Backwash is needed to regain the original integrity. Backwash water is usually sent back to the facility headworks or to waste. On cross flow systems permeate passes through the membrane normal to the primary direction of the flow, which is parallel to the membrane

surface. The feed water is concentrated along the membrane in the direction of flow before it is sent to another stage or to waste. The cross flow velocity decreases fouling but increases concentrate or waste. The type of system utilized depends on feed water constituents and desired filtrate quality.

The membranes used for MF greatly vary in geometric configuration and include: flat sheet, pleated sheet, tubular, spiral wound, track etched, and hollow fiber. Each of these has advantages and disadvantages that are carefully considered when choosing an MF system to use. Membranes can also vary in composition (natural and synthetic) and range from simple fibrous material to various polymers. These materials include but are not limited to: cellulose acetate or nitrate, polyvinylidene difluoride, polyamides, polysulfones, polycarbonates, etc.

Disadvantages of MF include electrical power consumption, chemical storage and disposal, and capital investment. Since the system uses pressure, the process requires pumps that consume energy and therefore add to the operational cost. Another disadvantage is the requirement of chemicals for periodic cleaning of the membranes. These chemicals are hazardous and need to be stored, handled, and disposed of accordingly, thus increasing the cost of operation. Finally, the capital investment required to use microfiltration is high and will be the largest factor when considering design.

Many advantages are associated with MF including: smaller land footprint, low operational maintenance cost and minimal operator input. The land requirement for an MF system is much less than the traditional SSF system. The MF system can run for long periods (3-12 weeks) without chemical cleaning of the membranes, thereby, reducing the cost of operation. Because the MF can be programmed to backwash at specific intervals, it requires no daily operator input or adjustment, thus decreasing cost and increasing reliability. Researchers in Korea were able to show that MF consistently produces water with SDI values less than 3 when treating water contaminated by red-tide algal blooms [10].

## Material and Methods

The project was conducted at a pilot-scale facility, located about 20 miles north of Tucson on I-10. The facility was built by the U.S. Bureau of Reclamation (USBR) in cooperation with the City of Tucson and a consortium of utilities in northwest Pima County –the Northwest Water Providers (NWWP). NWWP consisting of the Metro Water District, Town of Marana, Oro Valley and the Flowing Wells Irrigation District. The pilot-scale desalination plant treats CAP water. Unit operations consist in slow sand filtration (SSF) or microfiltration (MF), chemical addition to prevent membrane scaling and fouling, reverse osmosis and Vibratory Shear Enhance Processing (VSEP®) treatment of RO brine or salt tolerant plants (halophytes) irrigation. A process schematic is also provided (Figure A1-2).

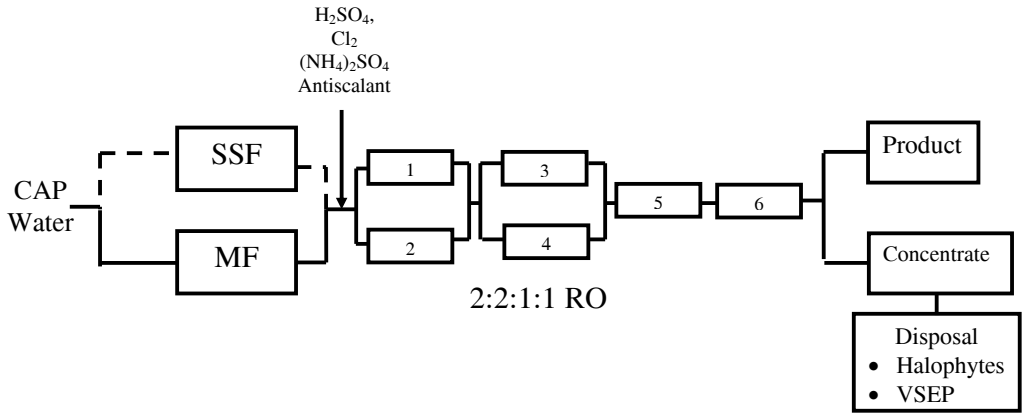


**Figure A1-2.** Schematic of the Pilot-Scale Desalination of CAP Water in Marana, AZ, USA

In the Tucson Active Management Area (TAMA, Figure A1-3) projected compliance with state requirements is based on full utilization of regional rights to Central Arizona Project (CAP) water and a degree of reclamation/reuse of municipal wastewater effluent. Uncertainty regarding the long-term availability of Colorado River water to the CAP, however, is a major impediment to water resources planning [2]. For illustration of water resources planning and dependence on new water resources, we focus momentarily on the TAMA. Native ground water in accessible aquifers of the TAMA contains 200-300 mg/L total dissolved solids (TDS) (Table 1). Traditionally, these waters have been directly served to the public following disinfection. When CAP water reaches Tucson, it contains ~750 mg/L TDS (Table A1-1), a figure that will rise with water demand in the upper Colorado River Basin states. Full use of its CAP allocation in the TAMA will bring at least 200,000 metric tons of salt to the Tucson area annually [3]. Since Tucson is the southern terminus of the CAP canal, without salt management steps, essentially none of that salt will leave the region, and the average salinity of accessible TAMA ground waters will double over a 50-year period.

**Table A1-1.** CAP water quality – comparison to Tucson well data

| Water Quality Constituent [mg/L] | Tucson Water Production Wells | CAP Water |
|---|---|---|
| **Total Dissolved Solids** | 259 | ~750 |
| **Hardness (as $CaCO_3$)** | 119 | 270 |
| **Sodium** | 40 | 112 |
| **Chloride** | 17 | 104 |
| **Calcium** | 29 | 56 |
| **Magnesium** | 5 | 31 |
| **Sulfate** | 45 | 280 |
| **Alkalinity (as $CaCO_3$)** | 126 | 98 |
| **TOC** | <1 | 3.5 |

The addition of CAP water to the TAMA water resource portfolio (Figure A1-3) has already increased TDS levels in delivered water, and membrane treatment necessary to maintain average TDS levels near 450 mg/L is being considered. While essential to salt management, however, reverse osmosis (RO) will consume energy and produce brine. It has been estimated that recovery during RO treatment of CAP water will be limited to 75-80% to avoid membrane scaling [11]. If even a third of the regional CAP allotment is treated in this manner, the value of water lost as brine will be on the order of $\$20M \cdot yr^{-1}$, based on a unit water value of $1000 per acre foot. Further, inland communities like Tucson have no ready sink for RO brines, so that disposal costs will add significantly to the cost of RO treatment [11].

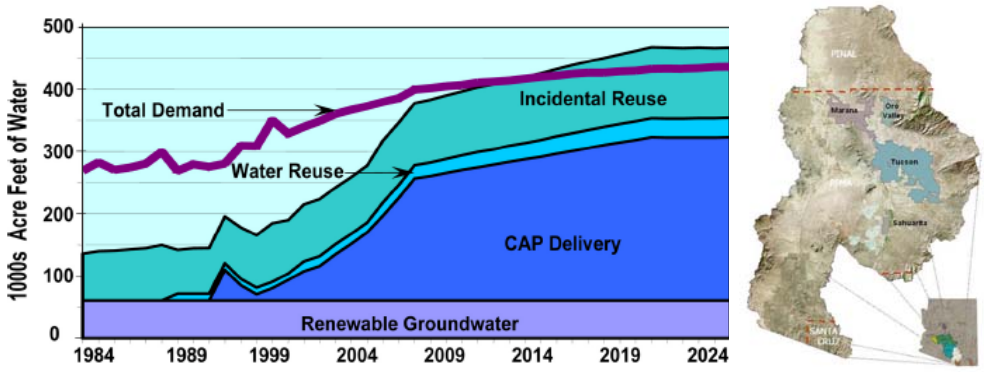


**Figure A1-3.** The water supply/demand projections for the TAMA. The geographic boundaries of the TAMA are shown in the map at right.

*Slow Sand Filters*

The SSF design parameters investigated in this study are summarized in Table A1-2. The SSFs are designed to operate at a filtration rate of 6.3 $m^3/m^2.d$. The range specified by The Arizona Department of Environmental Quality is 1.9 to 9.4 $m^3/m^2.d$ [7]. Filtering area for each SSF used here was about 7 $m^2$. Hydraulic control points were at filter outlet valves. The operational strategy was designed to minimize excess SSF filtrate production and associated chemical demand. That is, the objective was to produce only as much water as necessary for RO operation.

*Cleaning*

A traditional cleaning method was chosen for this experiment for simplicity and reliability. This method involved draining the water on top of the sand and scraping the schmutzdecke off. The influent water supply was stopped, and the filter was drained to below the sand bed surface. The schmutzdecke was then manually removed and discarded to waste. The filter was then refilled and run for 2-7 days to rebuild a schmutzdecke before the effluent was again used as RO influent.

**Table A1-2.** Slow sand filters design parameters

| Slow Sand Filters | |
|---|---|
| Product flow per filter [$m^3$/d] | 43.6 |
| Filtration rate [$m^3/m^2$.d] | 6.3 |
| Total filter area per filter [$m^2$] | 7 |
| Number of filters [ - ] | 2 |
| Initial height of filter sand bed [m] | 0.91 |
| Minimum height of filter sand bed [m] | 0.46 |
| Sand uniformity coefficient, $d_{60}/d_{10}$ | 1.5 |
| Height of the under drains, including gravel layer [m] | 0.91 |
| Height of the supernatant water [m] | 1.52 |
| Free board [m] | 0.31 |
| Total filter basing height [m] | 3.81 |

*Microfiltration*

The microfiltration system used here was a MEMCOR 3M10C Continuous Microfiltration (CMF) Unit. This unit has three hollow fiber filtration modules. The membranes have a nominal pore size of 0.2 microns. Water flows through the membranes along an outside-in path, meaning that pressurized feed water is introduced to the outside surface of the fiber (shell side), and filtrate is collected on the inside of the fiber (lumen). The specifications of the unit are summarized in Table A1-3 [12].

The Memcor 3M10C has two modes of operation: filtration and backwash. During the filtration mode, product water is generated, and suspended materials collect on the outside of the membrane fiber. This unit only operates in a dead end mode, meaning that there is no feed water recirculation.

*Cleaning*

As the suspended solids collect on the membrane surface, the pressure difference between the outside of the fiber and the inside increases. When the transmembrane pressure difference reaches a specified level, the system backwashed to remove suspended solids from the membrane surface, pushing water from the fibers lumen to the shell side. Here backwash was automatic at 50 minutes intervals and dumped to waste. When the transmembrane pressure (TMP) reached 15 psi membranes were thoroughly cleaned in place (CIP). This is chemical cleaning in which a caustic commercial solution, Memclean, was used. CIP was performed for a 24-hour extended soak followed by a through rinse, brought the TMP back down to original level.

**Table A1-3.** Microfiltration Unit Specifications

| MEMCOR CMF Unit | |
|---|---|
| Unit model | 3M10C |
| Number of filtration modules [ - ] | 3 |
| Membrane area of each filtration module [$m^2$] | 15 |
| Total membrane area [$m^2$ ] | 45 |
| Membrane material [ - ] | Polypropylene |
| Nominal membrane pore size [μm] | 0.2 |
| Maximum filtration rate [$m^3/m^2.d$] | 1.8 |
| Operation filtration rate [$m^3/m^2.d$] | 0.97 |
| Maximum Transmembrane Pressure [psi] | 15 |

*Sampling Protocol*

The sampling frequency depended of the approach velocity of the slow sand filters and the time of the year. Higher approach velocities during summer resulted in daily sampling. At lower approach velocities, the sampling was performed every other day. Routine sampling included measurement of conductivity, temperature, pH, SDI, turbidity and flow rates for each SSF and for the MF unit.

*Analytical*
*Silt Density Index (SDI)*

Samples for SDI measurements are passed at a constant pressure (30 psi) through a 0.45-□m membrane filter at constant temperature (± 1°C). Particle accumulation reduces the filtration rate over the 15-minute standard test period. Flow data yield a plugging factor, defined as the percentage decrease in the flow passing through the filter compared to the original rate. SDI values are then calculated as follows:

$$SDI = \frac{PF}{t}$$

Where, **SDI** is the silt density index [-]
**PF** is the plugging factor [%]; the time-dependent percentage decrease in flow rate
**t** is the time [minutes]

To protect RO membranes from influent particle accumulation and fouling, SDI values below 5.0 are adequate. However, to comply with membrane warranties, manufacturers require maintenance of SDI < 3.0 in RO influent. The SDI instrument used to perform the test was a Chemetec Model FPA-3300 and the filters used were MILLIPORE Millex® -HA MF-Millipore Membrane (mixed cellulose esters) syringe driven filter unit for clarification of aqueous solutions.

*Turbidity*

A turbidity meter was used to measure the turbidity of the SSFs and MF. Turbidity was measured on the day water samples were collected.

## Results and Discussion

Two variables were used to compare SSF and MF. The variables chosen were seasonal variation and approach velocities. To determine the influence of these variables several experiments were conducted running CAP water as influent for the SSF and MF. The MF unit had a constant approach velocity of 0.97 $m^3/d.m^2$ and the approach velocities of the SSFs varied as 1.6 $m^3/d.m^2$, 3.1 $m^3/d.m^2$, 4.7 $m^3/d.m^2$ and 6.3 $m^3/d.m^2$ during constant head operation.

*SSF and MF Comparison*

In an earlier long-term study of SSF as a pre-treatment for RO treatment of CAP water, the loss of RO permeate flux after approximately 18 months was 68%. That study suggested that the operation of SSF was sensitive to flow rate. The flow rate increased, the quality of the water from SSF decreased [3]. However, the study did not include a controlled parametric study of flow rate or compare SSF performance directly with microfiltration as an alternative pre-treatment technology.

The results of this study show that both SSFs produced higher SDI values at the beginning of the runs performance improved during a 2-3 days ripening period for the filter to build up a schmutzdecke. SDI values improved after several days. Values for the North and South SSFs and MF unit at different approach velocities during winter season are compared in Figure 1. When the SSFs ran at 25% of the design approach velocity (1.6 $m^3/d.m^2$), the SDI of the effluent was better than that of the MF producing 0.97 $m^3/d$.

Results obtained for the North and South SSFs during summer are shown in Figure 2. Compared to the winter run the north SSF at the design approach velocity (6.3 $m^3/m^2d$) showed a 58% reduction of the SDI values. Also a significant difference compared to the south SSF was noticed. At 75% of the design flow rate (4.7 $m^3/m^2d$), the North SSF produced an average SDI value of 2.2 while the South SSF average SDI was 3.4. Due to maintenance of the CAP canal the experiment at 50% of design flow rate (3.1 $m^3/d.m^2$) was truncated before maximum head loss was achieved. The South SSF SDI values were high at the beginning but improved as the filter ripened (Figure 2). North SSF values were steadier and lower. For the run at 25% of the design approach velocity, SDI values in the two reactors did not differ significantly. The average SDI values for the North and South SSF were 2.9 and 3.4, respectively.

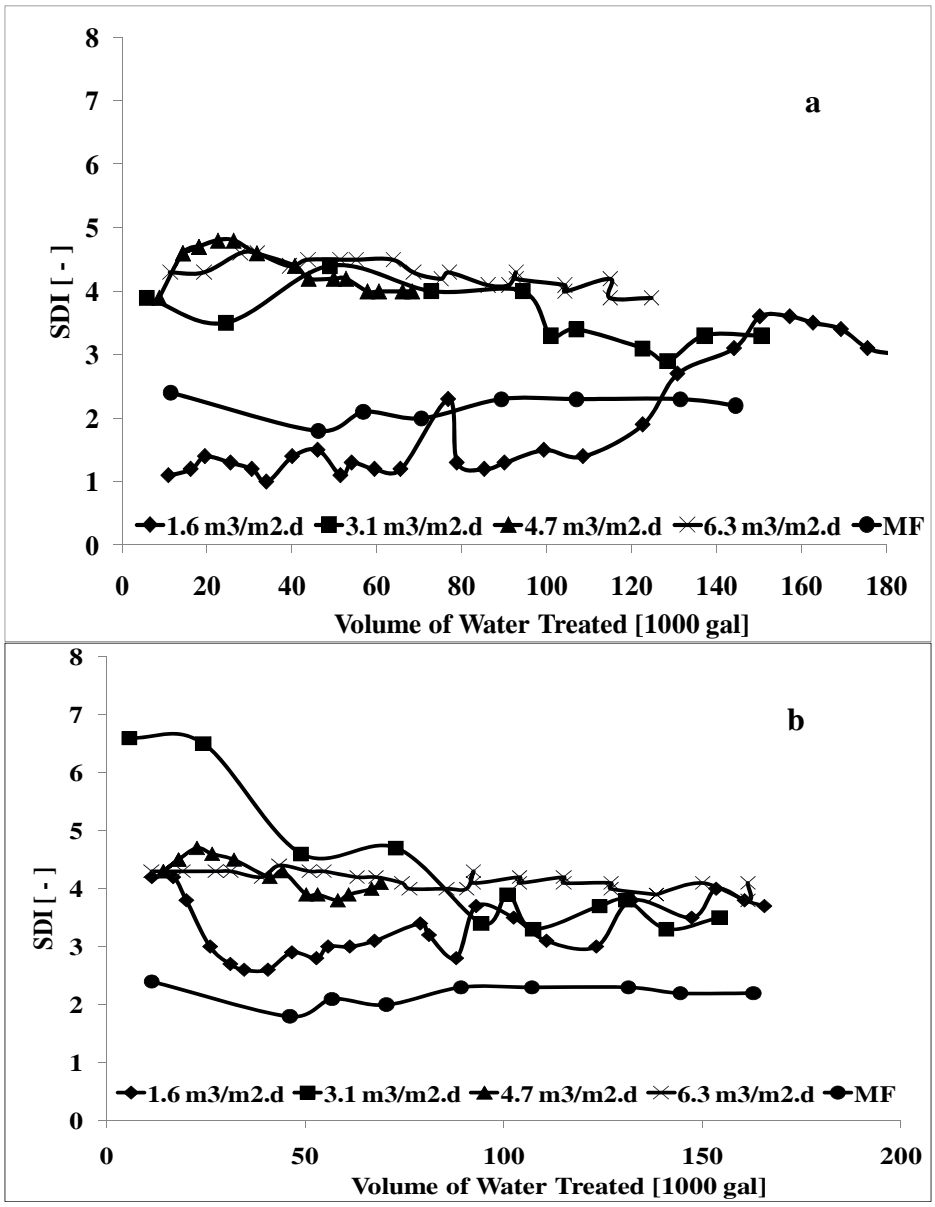


**Figure A1-4.** a. North and b. South SSF SDI values vs. the Volume of Water Treated during winter 2010

The performance of the North SSF improved significantly during the last 6 months of the study (Figure A1-4). Before this improvement in the performance new clean sand was added to the North SSF as shown in Figure A1-4. A new experiment was started at the design approach velocity (6.3 $m^3/d.m^2$). The SDIs test for this experiment showed average values of 2.2. These SDI values are 58% of the average value obtained during the previous run at the design approach velocity during winter. The average SDI value during the winter was 4.5.

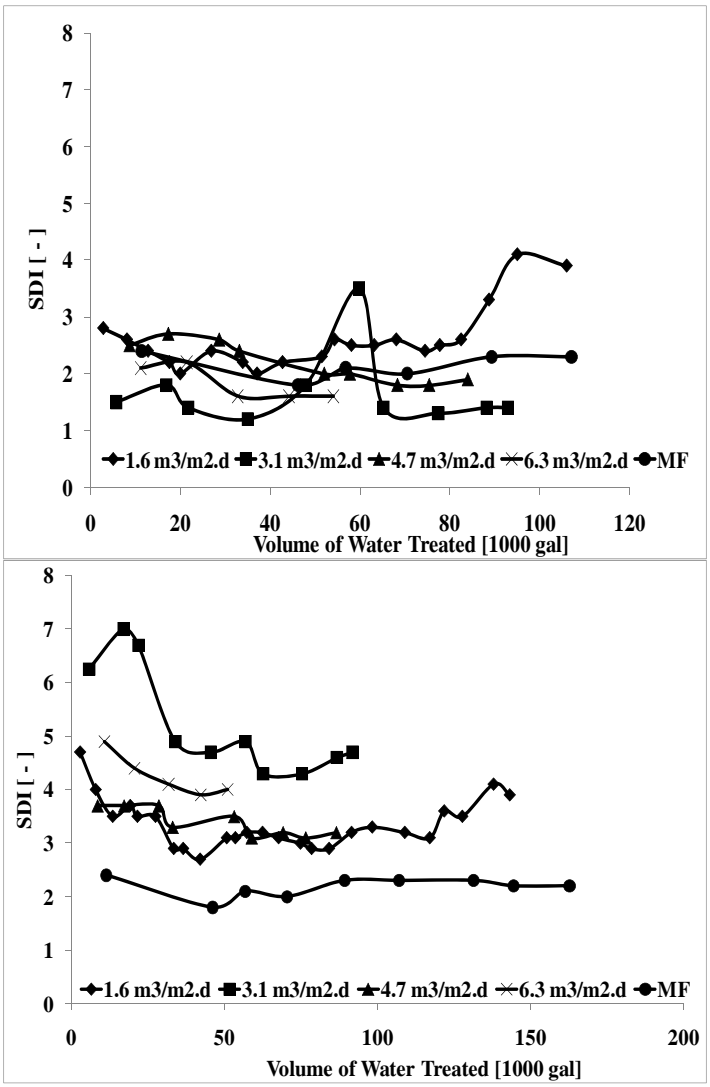


**Figure A1-5.** a. North and b. South SSF SDI values vs. the Volume of Water Treated during summer

Differences in contemporary performance of the north and south SSFs may have been due to differences in type and distribution of filter media. The North SSF's bed had a finer grain size distribution compared with the south SSF, and different type of sand. A finer grain size distribution would provide the North SSF with a larger surface area per unit volume perhaps increasing the filter efficiency. The North SSF contained native sand from Yuma while the South held commercial silica sand media [13]. Figure A1-7 shows the effluent turbidity both SSFs during summer and winter. The north and south SSF were capable to reduce the turbidity of the influent in an 84% and 79% respectively (Table 4). It is important to notice that even though the influent turbidity during the summer is as high as 3 NTU, the effluent turbidity was reduced to the same levels as the ones obtained during the winter. The difference in the filter media could explain the difference in the turbidity of the effluent of the two SSFs.

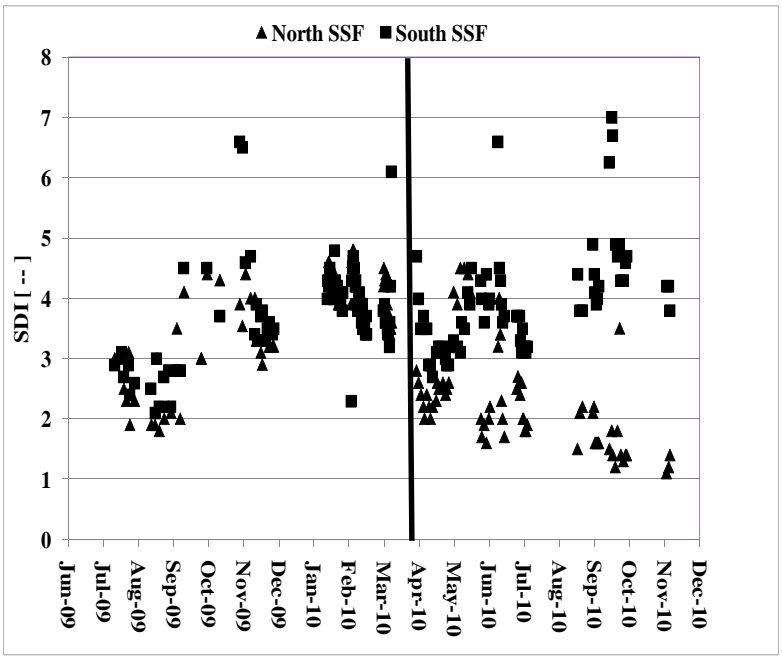


**Figure A1-6.** SDI values for the north and south SSF during the duration of the study. The vertical line shows when clean sand was added to the North Slow Sand Filter.

The MF unit also successfully removed turbidity from the CAP water. The raw CAP water presented turbidity values as high as 24 NTU (not shown). The average removal of turbidity from the raw CAP water by the MF unit was 85% (Table A1-4).

### a. North SSF Summer

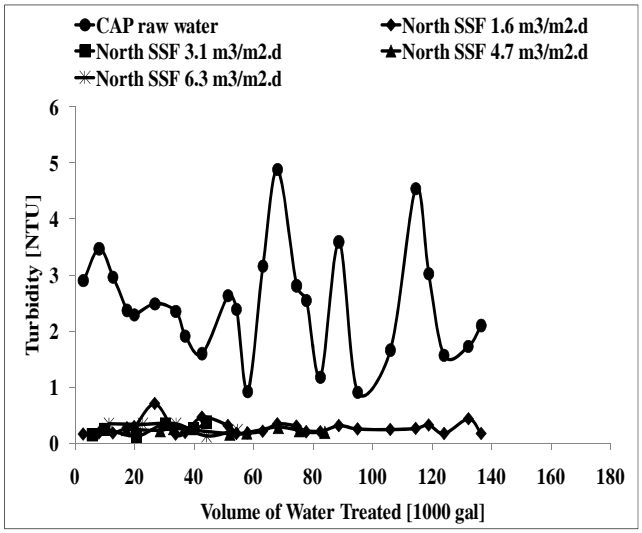

**b. South SSF Summer**

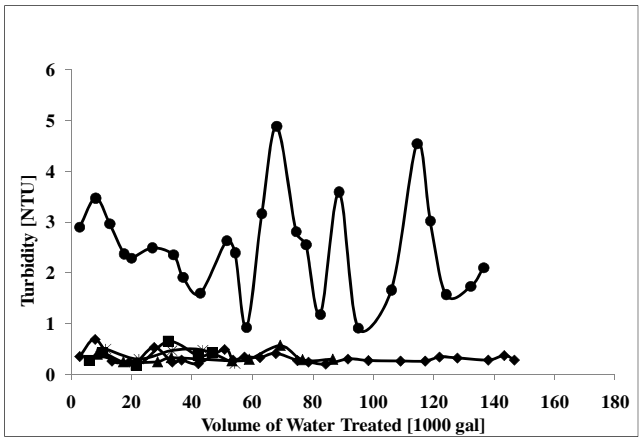


**c. North SSF Winter**

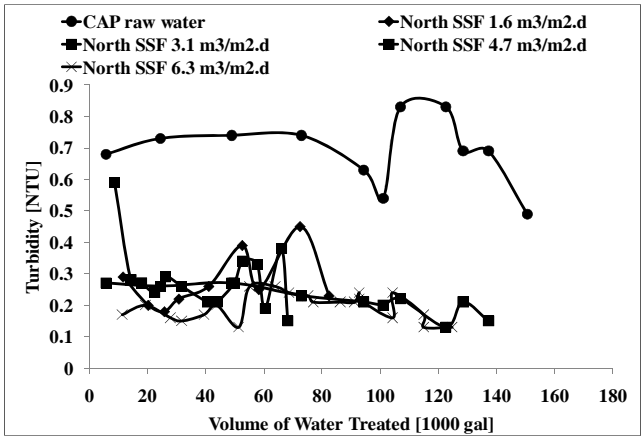


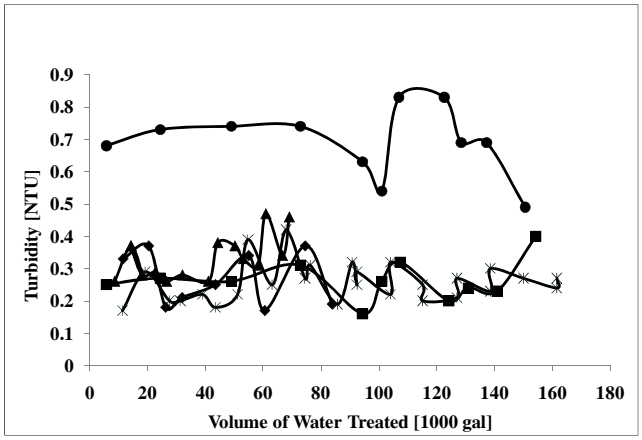


**d. South SSF Winter**

**Figure A1-7.** Effluent turbidity of the north and south SSF for a) & b) summer and c) & d) winter

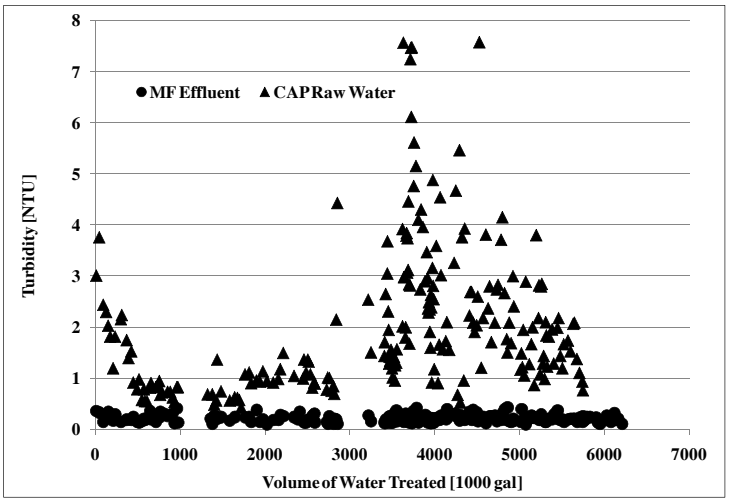


**Figure A1-8.** CAP Raw Water and MF Effluent Turbidity

**Table A1-4.** Summary of the major parameters measured for SSFs and MF over a 1-year period

| Parameter | Raw CAP Average | North SSF Effluent Average | Removal % | South SSF Effluent Average | Removal % | MF Average | Removal % |
|---|---|---|---|---|---|---|---|
| **TDS [mg/L]** | 989.00 | 852.61 | 1.38 | 865.15 | 1.25 | 569.56 | 4.24 |
| **Turbidity [NTU]** | 2.41 | 0.25 | 84.0 | 0.32 | 79.4 | 0.23 | 85.3 |
| **SDI [ - ]** | NA* | 3.10 | -- | 3.85 | -- | 1.97 | -- |
| **HPC [CFU/ mL]** | 1242.00 | 1115.65 | 10.17 | 1098.52 | 11.55 | NA | -- |

* The SDI tests for the CAP raw water failed due to high content of particulate matter which results in high turbidity.

The optimal operation of the SSFs is that one in which we produce good quality water and the frequency of the cleaning is low. The minimum length of filter run should be at least 14 days under the most unfavourable conditions [6].The length of the runs was affected, in this study, by the approach velocity and the season. Running the filters at low approach velocity will result in longer filter runs and better water quality (Figure A1-9). During summer months the water temperatures reached 32°C; higher temperatures result in faster growth of algae in the influent water.

*Increasing operation head losses and the frequency of cleaning.* Factors in finding an optimal SSF design properly minimize the total cost of the filter construction predominantly the total filter surface area and the operational cost, which is a function of the cleaning frequency. There

is an obvious trade off between overflow rate and length of filter runs and, perhaps the volume of water treated per unit filter area between cleanings. If the required rate of water production ($Q_T$) is known, then the average overflow rate must be $Q_T/A_T = V_T$. Since filters experience periodic cleaning, during which no water is produced, the average overflow rate must include cleanings periods.

That is:

$$V_T = V_O(1 - f)$$

where $v_O$ is the overflow rate when filters are actually in operation and *f* is the fraction of time during which filters are retired for cleaning. *f* is a function of cleaning frequency and the time required for cleaning such that:

$$f = \frac{Vt_c}{24}$$

where,

*v* is the frequency of filter cleaning ($day^{-1}$) and $t_c$ is the required cleaning time (hours).

The *f* is dimensionless. Based on the experimental results provided, it seems that *f* is itself a function of Vo, so that $f = g(V_O)$, which can be determined from operational data, and

$$V_T = \frac{Q_T}{V_T} = \frac{Q_T}{V_O[1 - g(V_O)]}$$

The capital cost of filter construction should be proportional to area, so that

$$CapitalCost = \frac{k_1 Q_T}{Vo[1 - g(V_O)]}$$

The operating cost requires much more thought, but if operating cost is proportional to the product of total surface area ($A_T$) times cleaning frequency, (V), then

$$Cost\ O\ \&\ M = k_2 V\left\{\frac{1}{r}\left[1 - \left(\frac{1}{1+r}\right)^n\right]\right\}$$

Where

r is the discount rate and
n is the filter design life in years

The operation and maintenance cost is the present worth of operational costs over the design life. Thus, the total present value cost is a function of a single independent variable, $V_O$ such that

$$Present\ Value\ Cost = \frac{k_1 Q_T}{V_O}[1 - g(V_O)] + k_2 \frac{24 A_T}{t} g(V_O)\left\{\frac{1}{r}\left[1 - \left(\frac{1}{1+r}\right)^n\right]\right\}$$

And when $g(V_O)$ is known it should be possible to find an analytical solution for present worth minimum by setting the first derivative of this expression equal to zero and solving for $V_O$, the operational overflow rate.

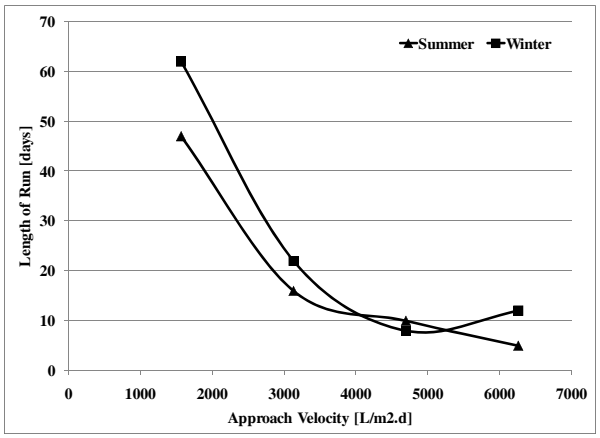


**Figure A1-9.** Approach Velocity vs. Length of the Run of the SSFs during Winter and Summer

Figure A1-10 illustrates the effectiveness of the cleaning in place (CIP) performed on the MF unit during this study. The marker types indicate the different cycles before each cleaning. Cleaning was restored TMP values as low as 5 psi. There was no indication of permanent fouling of the membranes. Is important to notice that the initial value of TMP is higher - ~ 9 psi. This suggests that new membranes take several weeks to wet-out all their pores. A factor that influences the unit's time between cleanings is the quality of the influent. This is apparent during the months of summer when water is pumped from the CAP to the farms for irrigation and a worsening of quality of the water is noticeable.

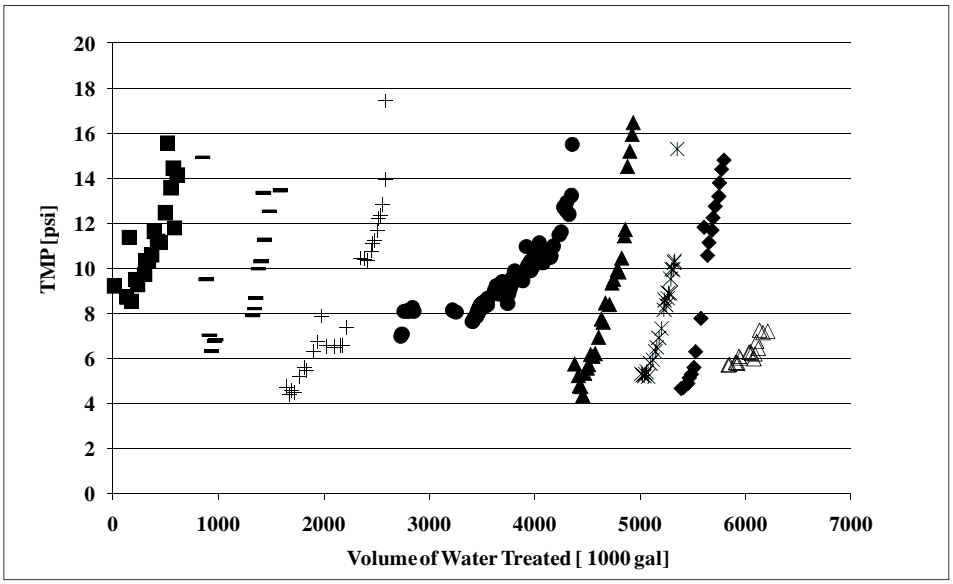


**Figure A1-10.** Volume of Water Treated by Microfiltration vs. Transmembrane Pressure (TMP)

**Economic Analysis**

The economic analysis for the MF and the SSFs was developed for a 15MGD water treatment plant. A total cost for each approach velocity and area of SSFs was found this with the information of the time between cleaning gathered from the experiments. Table 5 summarizes the economic analysis for the SSFs and MF. The MF has a high operation and maintenance cost. This could be explained since a more qualified personal should be hired to operate the unit and the cost of chemicals to clean the membrane increase the cost.

The SSFs total cost ranges from 6.5 M$/yr at the lowest approach velocity to 2.2 M$/yr at the highest approach velocity. The total cost for the SSFs does not include the cost of land and pump and piping. The cost of land would affect significantly the total cost. The cost of land highly depends on the location and the availability of vast areas of land.

**Table A1-5.** Summary of the Economic Analysis for the SSF at different Approach Velocities and MF

| Unit | Land [$m^2$] | Capital Cost M$/yr | Operation & Maintenance Cost M$/yr | Total Cost M$/yr |
|---|---|---|---|---|
| SSF @ 1564.52 L/d.$m^2$ | 36290.25 | 5.5 | 1* | 6.5** |
| SSF @ 3129.04 L/d.$m^2$ | 18145.13 | 2.8 | 0.8* | 3.6** |
| SSF @ 4693.56 L/d.$m^2$ | 12096.75 | 1.9 | 0.8* | 2.7** |
| SSF @ 6258.08 L/d.$m^2$ | 9072.56 | 1.5 | 0.7* | 2.2** |
| MF | | 2.3 | 0.9 | 3.2 |

*The sand scrapped from the SSFs will be sieve and use to re-sand the filters when needed.
** The total cost does not include the cost of piping & pumping and the land cost for the SSF.

The cost of operation and maintenance for the SSFs at 3129.04 and 4693.56L/d.$m^2$ (Table A1-5) is the same because as the approach velocity decreases the frequency of cleaning also increases so at this approach velocity this stabilizes. However, as the approach velocity goes down the area needed to satisfy the water treatment plant capacity increases significantly as shown in Figure A1-11.

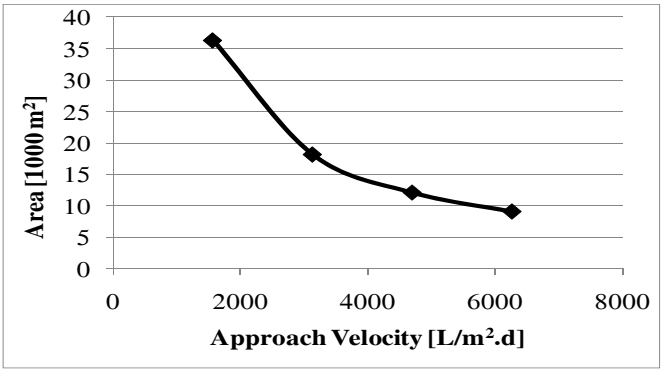

**Figure A1-11.** SSFs Area Needed for a 15 MGD Water Treatment Plant

The total cost for the MF would be 3.2 M$/yr this value does not include the cost of land but the footprint of the MF technology is significantly smaller than the one for the SSFs.

**Impact of the Pre-treatment on RO Performance**

The process of reverse osmosis (RO) is a reliable, efficient method to separate water from soluble components; however, pre-treatment of feed water is required to maintain RO efficiency. Adequate pre-treatment will: preserve membrane integrity, reduce fouling, and subsequently extend membrane life. RO hydraulic performance is defined in terms of a temperature corrected water transport coefficient (A), which is a measure of membrane permeability to clean water.

$$A_{1\&2} = \frac{F_{1\&2}}{P_{avg,1\&2} - P_{p,1\&2} - \left[\pi_{avg,1\&2} - \pi_{p,1\&2}\right]} \times \underbrace{1.033^{(25-T)}}_{\text{Temperature Correction factor}} = \left[\frac{m/s}{Pa}\right]$$

where,

F is the permeate flux (QP/S)

QP is the volume rate of flow of permeate (m3/s)

S is the nominal membrane surface area (m2)

$P_{avg}$, $P_P$ are the pressures in the unit feed and permeate streams, respectively, and pavg and pp are the osmotic pressures in the unit feed and permeate (Pa)

From September 2007 to April 2009 the RO feed water was pre-treated via SSF. From this point to present the RO feed water was pre-treated via MF. On August 2009, new membranes were installed in the RO unit. Results show that the RO performance is likely influenced by the type of pre-treatment technology. The head and the tail elements of a RO unit are the most impacted due to fouling and scaling, respectively. If fouling occurs in the head elements, the pressure into the system must be increased to maintain the overall recovery.

Figure A1-12a and b show the normalized water transport coefficient for the head and tail elements of the 2:2:1:1 RO unit over a three-year period. During the 2 years in which the feed water was pre-treated by SSF, the performance of the RO unit was very unstable. After 6 months of continuous operation the A coefficient decreased by 80% (Figure A1-12). The RO unit was chemically cleaned and improvement in the A coefficient was observed. The unit ran for 5 additional months before new membranes were installed in vessel 5 and 6. After two months, the membranes in pressure vessels 5 and 6 were changed again. However, after only 2 weeks of continuously running a rapid drop in permeability was observed.

The initial value of the A coefficient after August 2009 was lower because new tighter membranes were installed (Koch Membranes TLC ULP). When the feed water was pre-treated

by Mf Ro performance was steadier. The decrease of the A coefficient in November 2009 was due to a problem with piping at the pilot plant opposed to routine operational change.

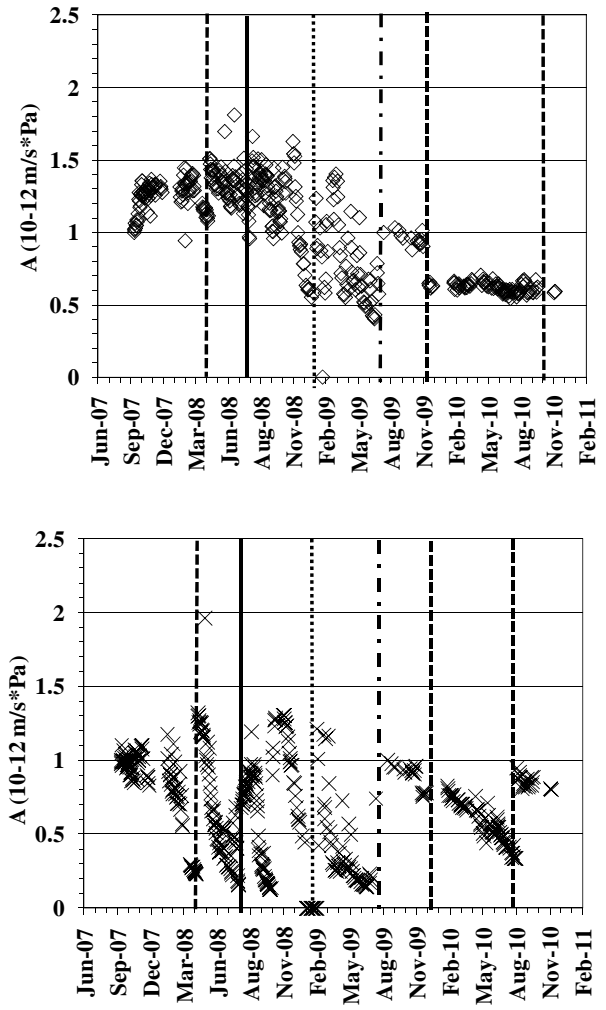


**Figure A1-12.** RO Normalized Water Permeation Coefficient (A). a. Front Elements: Pressure Vessel 1& 2 b. End Elements: Pressure Vessel 6. The continuous line shows new membranes (Hydraunatics ESPA3) were installed in vessels 5 & 6. The dashed lines show a chemical cleaning of the whole unit. The dotted line shows a chemical cleaning and new membranes in vessels 5 & 6 (Hydraunatics ESPA3). The semi-dash line shows new membranes installed (Koch Membranes TFC ULP)

## Conclusions

- The MF unit demonstrated to perform considerably more stable throughout the experiments than the SSFs. MF achieved SDI values of less than 3 for more than 95% of the time.
- Both SSF and MF produce effluent turbidity < 0.4 NTU regardless of the influent quality.

- Even though the SDI values for the north SSF improved significantly during the summer the head loss was achieved faster increasing the frequency of cleanings. Also the volume of water treated was less which increases the number of filters to treat the same amount of water.
- SSF maintenance and operation are inexpensive and do not require special skills. However, the operation of SSF depends highly on the factors that cannot be controlled, such as temperature. Therefore, uninterrupted operation of SSF is not expected. The down times of the SSFs are lengthy compared to the CIP performed to the MF.
- SSF as a pre-treatment for RO appears adequate, but not highly recommended for CAP water. The maintenance requirements of the SSF depend on temperature significantly. The algal growth affects the frequency of the cleanings. The time and water lost for each cleaning cycle has a high effect on the cost of the SSF.
- The SDI values for higher approach velocities achieved SDI values higher that the MF unit but below the value of 5 required by the RO manufactures as a good feed water for RO. It is important to note that the membranes used were in storage for a long period of time before they were installed in the unit. A well designed and properly maintain MF unit can achieve SDI values of <1 [Filmetc pdf]. However, the average value obtained using this unit was 2.2 which is less than the required - SDI = 3 - by the membrane manufactures to comply with the membrane warranty.
- RO has a steadier performance with the MF as a pre-treatment for the feed water
- MF as a pre-treatment for RO influent water proved to be an economically feasible technology.
- The cost of land would significantly increase the total cost of the SSFs as a pre-treatment for RO.

## References


**[1]** Pearson, R., et al., (1999). Third Management Plan for Tucson Active Management Area 2000-2010, Arizona Department of Water Resources.

**[2]** Barnett, T. P. and Pierce, D. W. (2008). Sustainable water deliveries from the Colorado River in a changing climate.

**[3]** Yenal, U. (2008). Doctoral Dissertation Maximizing Water Recovery during Reverses Osmosis (RO) Treatment of Central Arizona Project (CAP) Water, The University of Arizona.

**[4]** Rust, M. And McArthurs K. (2010) Slow Sand Filtration
URL: http://www.cee.vt.edu/ewr/environmental/teach/wtprimer/slowsand/slowsand.html

**[5]** Huisman and Wood

**[6]** Van Duk, J.C. and Oomer, J.H.C.M. (1978). Slow Sand Filtration for Community Water Supply in Developing Countries. Technical Paper No. 2, World Health Organization (WHO)

International Reference Centre for Community Water Supply, Voorburg (The Hague), The Netherlands.

**[7]** Moody, C., Garret B., and Holler E. (2002). Pilot Investigation of Slow Sand Filtration and Reverse Osmosis Treatment of Central Arizona Project Water. U.S. Department of the Interior, Bureau of Reclamation, Science and Technology Program Advanced Water Treatment Research Program Report No. 90.

**[8]** United States Environmental Protection Agency (EPA) (1990). Cincinnati, OH. "Technologies for Upgrading Existing or Designing New Drinking Water Treatment Facilities." Document no. EPA/625/4-89/023

**[9]** Taylor, J.S., Robert, C., Lovins, W.A., Chen, S., Kopp, K., Kothari, N. (1999). Microfiltration Productivity and Water quality in Relation to Pre-treatment, Temperature and Flux. Journal of Water Supply: Research and Technology – Aqua. Vol. 48, No. 5, pp. 191-200.

**[10]** Kim S.H., Yoon J.S., Yoon C.H. (2006). Evaluation of Microfiltration System Performance as Pre-treatment for Reverse Osmosis Seawater Desalination Through Pilot-Plant Operation. Water Science & Technology: Water Supply Vol. 6, No. 4, pp 163–169.

**[11]** Malcom Pirnie Inc., and Separation Processes Inc. (2008). Evaluation for Water Treatment Options for TDS Control, Draft Technical Memorandum.

**[12]** Memtec Group, 3M10C CMF Unit. (1997) Operation and Maintenance Manual.

**[13]** Hill, C., Personal Interview, 2010

**[14]** Density of bulk materials.
URL: www.simetric.co.uk

**[15]** Price List, for Bulk Gravels and Sands Research Triangle Raleigh NC Areas
URL: http://www.areamulchandsoils.com/price%20list%20gravels.html

**[16]** Oglebay Norton Industrial Sands, Inc. 2006; from Martin Yoklic; Silica Sand Filter Media ES 0.27-0.33 mm, UC 1.7 in 1.5 ton supersacks, with delivery

**[17]** Collins, M.R. (2002) Costing Summaries for Slow Sand Filtration and Ceramic Media Filtration. New England Water Treatment Technology Assistance Center. University of New Hampshire, Durham, New Hampshire.

**[18]** Logsdon, S. G., Kohne, R., Abel, S., and LaBonde, S. (2002) Slow sand filtration for small water systems. Journal of Environmental Engineering and Science, Vol. 1, pp. 339–348.

# Appendix 4:

Reverse Osmosis Treatment of Central Arizona Project Water: Research Program Summary 2007-2010

# Reverse Osmosis Treatment of Central Arizona Project Water: Research Program Summary 2007-2010

June 2010

Wendell P. Ela
Robert G. Arnold
James Lykins
Umur Yenal
Dongxu Yan
Andrea Corral
Justin Nixon

The University of Arizona

Department of Chemical and Environmental Engineering
1133 E. James E. Rogers Way. Harshbarger 108, Tucson, AZ 85721-0011
(520) 621-6044  (520) 621-6048 (FAX)

## 1. Introduction

Reliance on CAP water to satisfy a major fraction of the regional water demand has consequences for the quality of delivered water (Table 1.1). Salt management will in all likelihood involve a combination of processes that support or augment reverse osmosis (RO) treatment for salt separation. These might include, for example, slow sand filtration and chemical addition to prevent scaling and fouling reactions during RO treatment, post-RO treatment of brine, and so forth. Among the project objectives is long-term field testing of such process options.

The Bureau's Mobile Treatment Facility (MTF) has been in operation at the CMID/CAWCD turnout in Marana, AZ since 2007. The pilot desalination research site includes the MTF, plus slow sand filtration (SSF) or microfiltration (MF) on the front end as pretreatment options. The MF is also on loan from the Bureau. On the concentrate management side, the halophyte field site has been continuously operated since concentrate production began in 2007. In 2008 the City of Tucson purchased a pilot scale Vibratory Shear Enhanced Processing (VSEP) unit for evaluation as an alternative concentrate management option. More recently, the project team has begun to evaluate a process stream consisting of ion exchange (IX) pretreatment of CAP water followed by simulated RO treatment using the VSEP apparatus to achieve overall recoveries from 95-98%. RO/VSEP and IX/RO alternatives were compared in terms of overall water recovery and cost.

**Table 1.1** Water quality comparison - Tucson ground water and CAP water at the canal terminus

| Water Quality Constituent (mg/L) | Tucson Water Production Wells | CAP Water |
|---|---|---|
| Total Dissolved Solids | 259 | ~750 |
| Hardness (as $CaCO_3$) | 119 | 270 |
| Sodium | 40 | 112 |
| Chloride | 17 | 104 |
| Calcium | 39 | 56 |
| Magnesium | 5 | 31 |
| Sulfate | 45 | 280 |
| Alkalinity (as $CaCO_3$) | 126 | 98 |
| TOC | <1 | 3.5 |

While essential to salt management, RO treatment consumes energy and produces brine. It has been estimated that recovery during RO treatment of CAP water is limited to 75-80% to avoid membrane scaling, so that the value of water lost as brine contributes to the overall motivation for brine minimization should RO treatment of CAP water be deployed. The solubilities of calcium sulfate, calcium carbonate and barium sulfate, for example, are exceeded in brines derived from RO treatment of CAP water (Table 1.2). CAP water arrives in Tucson oversaturated with respect to barium sulfate, and it has been suggested that $BaSO_4$ precipitation limits recovery during RO treatment.

If even a third of the regional CAP allotment is RO treated without additional efforts to increase recovery, the value of water lost as brine will be ~ \$20 $M \cdot yr^{-1}$ (based on a unit value of \$1000 per acre foot). The analysis does not include the cost of brine disposal, which is

particularly relevant among inland communities like Phoenix and Tucson. Methods for increasing water recovery during salt removal include (i) pretreatment of CAP water to remove components of hardness (here $Ca^{2+}$ and $Ba^{2+}$) or (ii) post-treatment of CAP brines to separate additional water using VSEP.

**Table 1.2** Concentration/solubility data for CAP ion pairs that may contribute to membrane scaling

| *Precipitate* | *Ion Concentration* | *log (ion product)* | *log $K_{S0}$* | *Degree of Saturation* [(b)] |
|---|---|---|---|---|
| $BaSO_4(s)$ | $[Ba^{+2}] = 1.17 \times 10^{-6}$ M<br>$[SO_4^{-2}] = 2.81 \times 10^{-3}$ M | -8.48 | -10.0 | 827.83 |
| $CaSO_4(s)$ | $[Ca^{+2}] = 2.0 \times 10^{-3}$ M | -5.25 | -4.85 | 9.95 |
| $CaCO_3(s)$ | $[CO_3^{-2}] = 1.0 \times 10^{-5}$ M [(a)] | -7.7 | -8.48 | 150.64 |

(a) based on 120 mg/L carbonate alkalinity as $HCO_3^-$ and pH = 8.0.

(b) calculated as 25 X $Q_{SO}/K_{SO}$ with the assumption of RO running at 80% recovery. The value represents the approximate degree of oversaturation in the RO brine produced from CAP water.

## 1.1 Materials and methods

### 1.1.1 General

A pilot-scale research facility (Figure 1.1) was constructed 20 miles northwest of Tucson by the U.S. Bureau of Reclamation (USBR), the City of Tucson and a consortium of utilities in northwest Pima County—the Northwest Water Providers (NWWP).

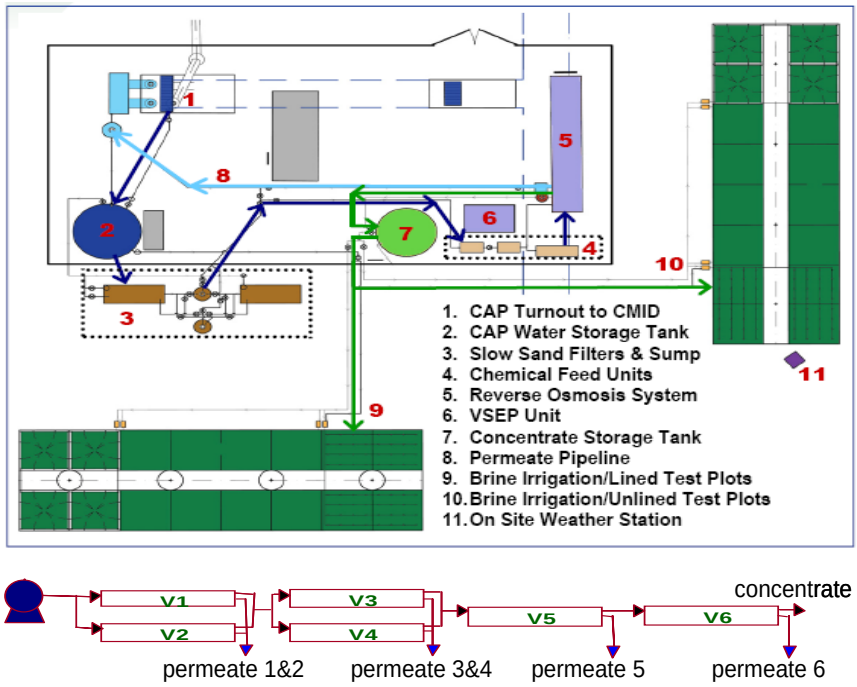


**Figure 1.1** Site plan and flow diagram, Tangerine Road Field Site. Brines generated at the field site irrigate salt tolerant vegetation. RO consists of a two-stage array (2:2:1:1). Each pressure vessel contains three 2.5-in spiral wound membranes. Influent flow is 5 gpm.

The project was designed to (i) establish the long-term (inter-seasonal) performance of RO for salt separation from CAP water at 80% recovery, (ii) compare slow sand filtration and microfiltration as pretreatment options for RO, and (iii) provide operational data with which to determine the economic feasibility of VSEP as a post-treatment of RO brine. Only the RO and VSEP units are described here. IX performance was not tested in the field but, nevertheless, a sequential treatment consisting of IX/RO was analyzed, leading to economic comparison with RO treatment (alone) and the RO/VSEP salt management alternative.

### 1.1.2 Reverse Osmosis

The pilot-scale RO unit consists of 6 pressure vessels containing a total of 18 elements in a two-stage, 2:2:1:1 configuration (Figure 1.1). Membrane elements were 2.5-inch x 40-inch polyamide thin film composite (PTFC) membranes (ESPA-2540). RO pressure requirements depend on the salinity of the feed water, water temperature, the membrane water transport coefficient (A, defined below), the design membrane flux (gallons of permeate per square foot of membrane per day [gfd]), and the target water recovery. Recovery is the percentage of influent that is recovered as permeate. Calculation of osmotic pressure follows the Morse equation:

$$\pi = \Sigma N\ R\ T$$

where, $\pi$ is the osmotic pressure [psi]
$\Sigma N$ is the sum of concentrations of all solutes [M]
R is the ideal gas constant [0.08206 L.atm/ mol.K]
T is the absolute temperature [K]

Water and salt transport coefficients are defined as follows:

$$A = \frac{Q_p / S}{P_f - P_p - (\pi_f - \pi_p)} \times TCF \left[ \frac{m/s}{Pa} \right]$$

where, $Q_p$ is the permeate flow rate ($m^3/s$)
S is the nominal membrane interfacial area ($m^2$)
Osmotic pressures are calculated based on feed and permeate chemistry (Pa)
TCF is the temperature correction factor [$1.033^{(25-T)}$]

$$B = \frac{Q_p / S \times TDS_p}{TDS_{avg} - TDS_p} \times TCF \left[ m/s \right]$$

where, $TDS_P$ is the permeate salt concentration (mg/L)
$TDS_{avg}$ is the effective salt concentration on the feed (reject) side of the membrane (mg/L)

CAP water was pretreated via slow sand filtration and fed to the RO unit at an average flow rate of 17.9 L/min. The feed pressure was ~80 psi. The flow of reject water (brine) was

maintained at 3.5 L/min to provide an adequate crossflow velocity in the final pressure vessel. The permeate flux from each element was adjusted to the design water flux, 10.9 gfd. Each element nominally contained 28 $ft^2$ of membrane surface for a permeate flow of 0.8 L/min. The six pressure vessels together produced a permeate flow of 14.4 L/min.

**Table 1.3** Reverse osmosis design and operational data

| | |
|---|---|
| Number of stages (-) | 2 |
| Number of vessels (3 elements per vessel) | 6 |
| Membrane area ($ft^2$ per element) | 28 |
| Membrane type | ESPA1 & ESPA3 |
| Water flux (gfd) | 10.9 |
| Influent flow rate (gpm) | 4.73 (17.9 L/min) |
| Feed salinity ($\mu S.cm^{-1}$) | 1000-1100 |
| Feed pressure (psi) | 80 |
| Recovery rate (%) | 80.5 |

### 1.1.3 Membrane Cleaning Procedures

Membrane cleaning procedures are summarized in an Appendix to this section.

## 1.2 Results

Nearly two years of RO performance for desalination of CAP water (Figures 1.2-1.4) suggests that scaling was observed on a time scale of months. That is, scaling was indicated by a decline in stage 2 recovery several months into the start of the overall operational period. For a more complete discussion, see results of membrane autopsy (below). The cleaning procedure applied in March 2008 temporarily restored membrane permeability, but downstream (stage 2) recovery again declined precipitously after a short period of steady operation. When the stage 2 recovery fell to 25%, the membranes were replaced and the system was operated to achieve a slightly higher overall recovery (80-85%) for four months. Near the end of that period, there was again evidence of scaling, distinguishable by preferential loss of permeability and recovery in the downstream stage, where ion concentrations reach highest levels. At that point, the membranes were again replaced, the unit was thoroughly cleaned and operation at an overall recovery of ~75% led to reasonably stable membrane performance for the next 8 months. In summary, the record of performance suggests that long-term, satisfactory RO performance is possible at recoveries approaching 80% without pretreatment to remove hardness cations. Higher recovery without water softening ahead of RO is inadvisable.

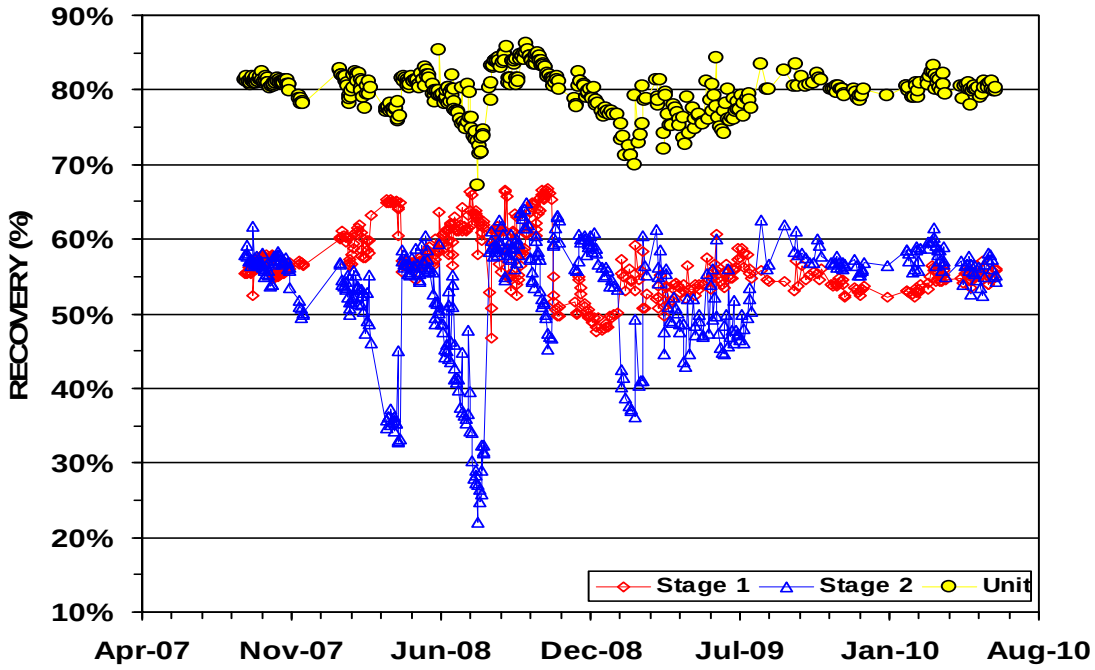


**Figure 1.2** Profile of overall and stage-specific RO recoveries during pilot-scale operation. Recovery is defined as water produced as a percent of water treated, i.e. $R = 100 \times (Q_p/Q_{in})$.

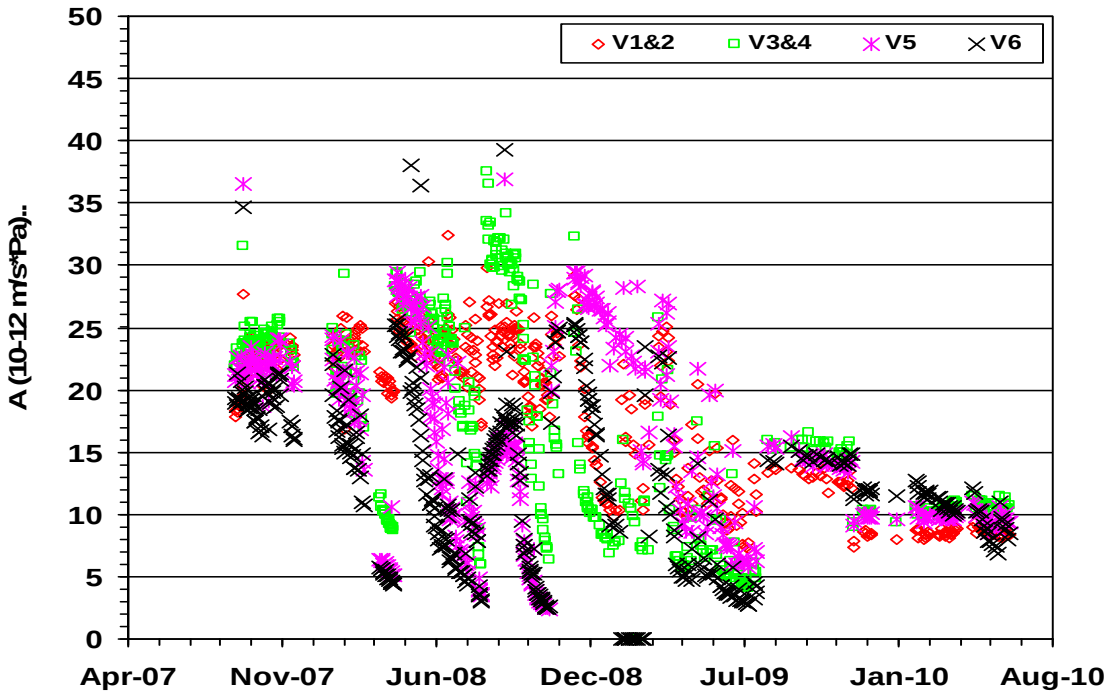


**Figure 1.3** Water transport coefficient (A) profile for RO operation (for gfd/psi, multiply y –scale by 0.0146). All values are adjusted to 25°C

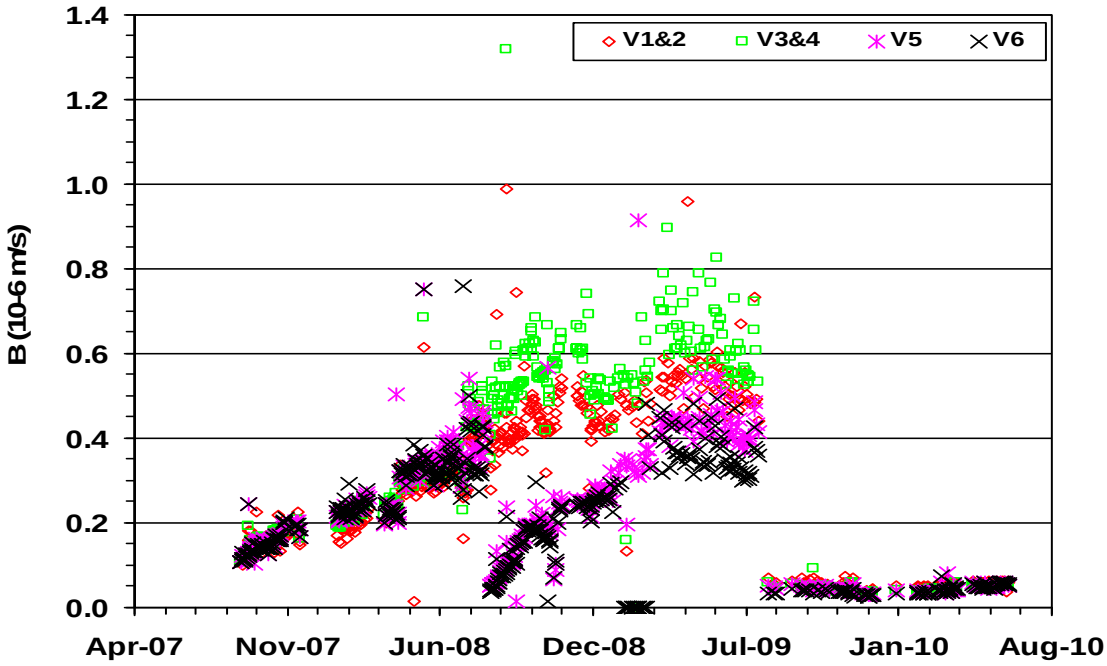


**Figure 1.4** Salt transport coefficient (B) profile at 25 $^{o}$C for the RO operation

As a check on RO unit performance, accuracy of flow measurements and salt concentration estimates a salt balance was performed around the RO unit. A reasonable salt balance (absolute value of mass balance deviation (defined below) < ~10% and normally much less) based on flow and total dissolved solids measurements was maintained across the RO unit throughout the period of study (Figure 1.5).

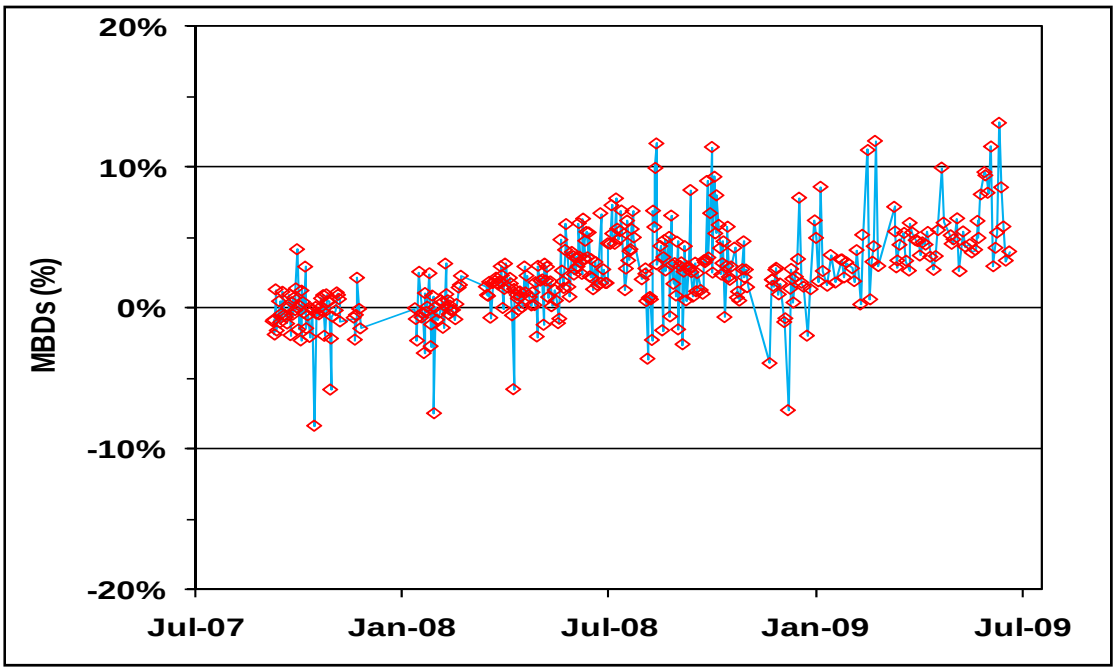

**Figure 1.5** Representative mass balance deviation profile on salt for the RO operation

$$\text{Salt Mass Balance Deviation}\,(\text{MBD}_S) = \frac{\left[Salt(in) - \sum Salt(out)\right]}{Salt(in)} \times 100[\%]$$

where, Salt(in) is the salt mass flux entering the RO unit (mg/min)
Salt(out) is the sum of salt mass fluxes leaving the reactor in permeate and brine streams (mg/min)

MBD values close to zero indicate that the flow rates of the RO (influent and effluents) are accurate as well as the conductivity values measured primarily for feed and reject streams. They also require accurate conversion of conductivity to TDS concentration. MBD values between -5% and +5% fall within the expected accuracy of measurements and TDS calculations.

The first seven months of the RO operation showed a very good salt balance through the RO system. MBD values mostly fell within -5% and +5%. By mid May 2008, roughly one and a half months after the high-pH chemical cleaning, MBD values were slightly biased toward the positive range. Values averaged +3.6% after that point. Positive MBDs might indicate an increase in the membrane porosity. The shift coincided with the onset of higher salt transport coefficients (Figure 1.4) and higher salt passage rates.

### 1.3. Post-mortem membrane analysis

To establish the causes of deteriorating membrane performance we directly inspected for surface fouling or scaling following membrane use. Membrane fragments were cut from the spiral-wound membranes used in the pilot RO unit and subjected to scanning electron microscopy (direct inspection) and energy dispersion X-ray (EDX) analysis. Material scraped from the retired pilot-scale membrane surfaces was analyzed for number of heterotrophic bacteria and fraction of inorganic and organic carbon, as indicators of a bacterial role in membrane fouling.

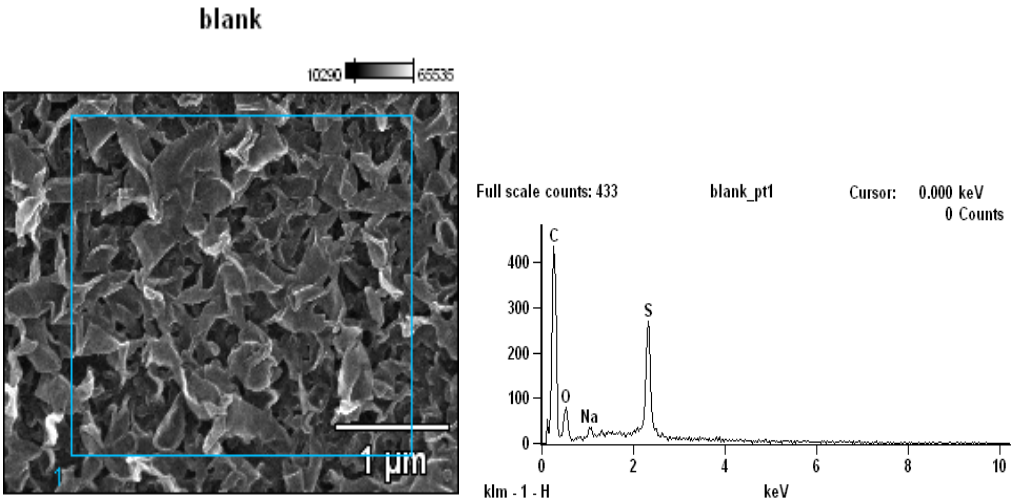


**Figure 1.6** SEM images and EDX analysis of control membrane

The control micrograph (Figure 1.6) shows the morphology of the clean membrane surface and serves as a basis for comparison only. The primary elements identified via EDX (carbon, sulfur and oxygen) conform to expectations based on polymer structure.

Fragments were cut from membranes taken out of vessels V5 and V6 in August 2008. When the membranes were replaced in the field, water permeability had degraded significantly (a value on the order of 20-25% of the original permeability coefficients). Again, the membrane fragments were analyzed via SEM and EDX. In addition, fresh samples were delivered to The Environmental Research Lab (Water Quality Center) at the University of Arizona for enumeration of total attached heterotrophic bacteria via HPC analysis. Wet foulant was scraped from the membrane surfaces. Foulant material was dried to constant weight at 105$^{o}$C prior to analysis of total inorganic and total organic carbon. The same material was analyzed at the University Spectroscopy and Inorganic Facilities via XRD.

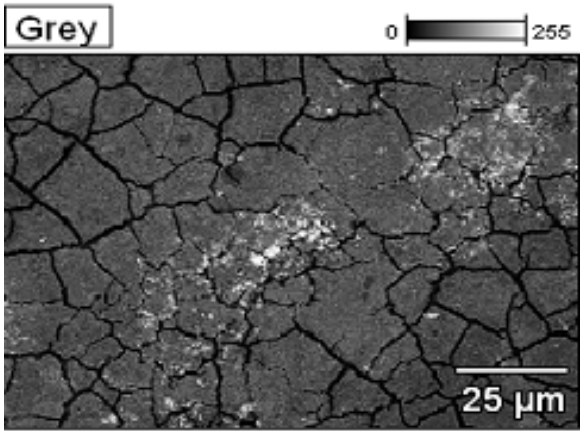


**Figure 1.7** SEM image of CAP water fouled RO membrane

SEM and EDX analyses conducted in membrane fragments from vessels V5 and V6 were similar. A typical SEM image and corresponding EDX data are provided as Figures 1.7-1.8. The light spots were apparently precipitated $BaSO_4$(s) (Figure 1.8.b). Major EDX peaks in the gray zones were dominated by silicon and aluminum, with noticeable amounts of carbon, oxygen and calcium.

EDX reports from all membrane samples indicated that silicon to aluminum (molar) ratios were relatively constant, varying from 2.0 to 2.4 (Table 1.4) The (constant) ratio suggests that deposited clays were at least partially responsible for membrane fouling. Mineral deposition on the membrane surface was heterogeneous, as indicated by the element maps (Figure 1.9). The cracks in the foulant layer that are visible in the micrographs were probably a result of sample desiccation.

**Table 1.4** Atomic percentages of elements in the foulant at surface of spent membrane

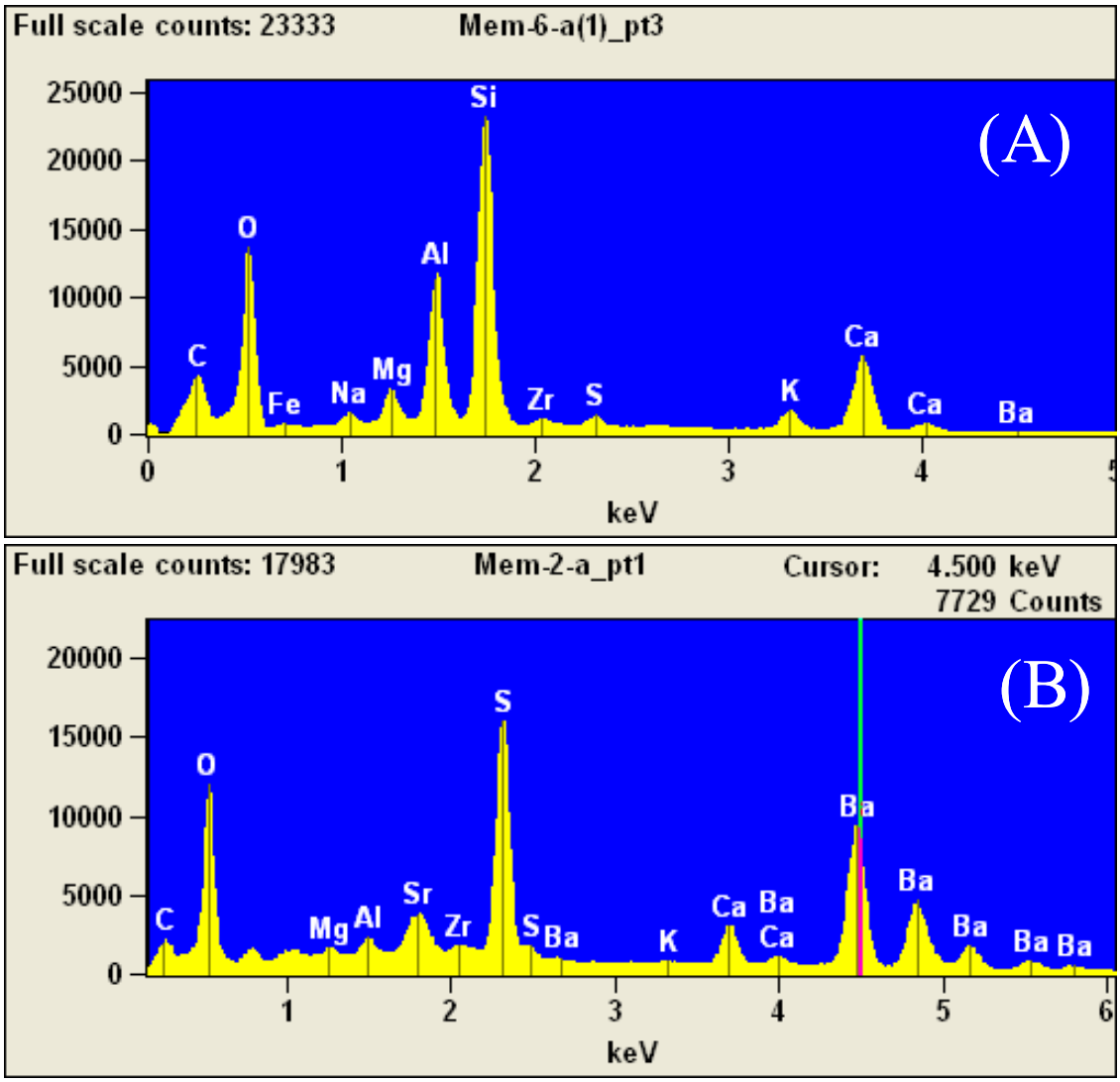


**Figure 1.8** EDX peaks produced by the foulant in the gray area (Figure 1.7) (A) and the small white area (B) shown in the SEM image.

Foulant that was scraped from the membrane surface was analyzed for mineral content using x-ray diffraction (XRD) and for organic and inorganic carbon. Representative (raw) XRD data are provided as Figure 1.10. The major peak at 27-28 degrees was identified as silicon dioxide ($SiO_2$), a major component of the membrane foulant. Clays that were identified by XRD also included potassium aluminum silicate ($KAlSiO_4$) and sodium calcium aluminum silicate. Neither calcite ($CaCO_3$) nor barite ($BaSO_4$) was detected. The sensitivity of the technique was estimated at 5% (mass ratio, mass of analyte/total mass).

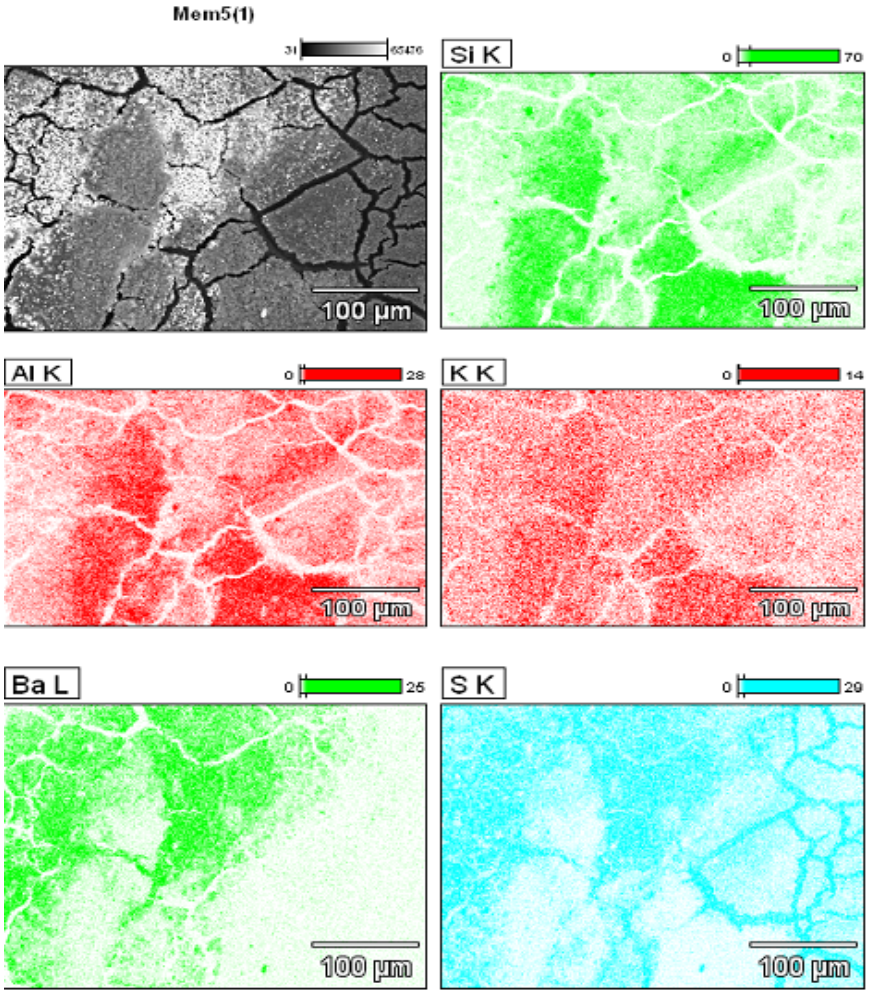


**Figure 1.9** Distribution of critical elements on the membrane surface. Data from EDX scans

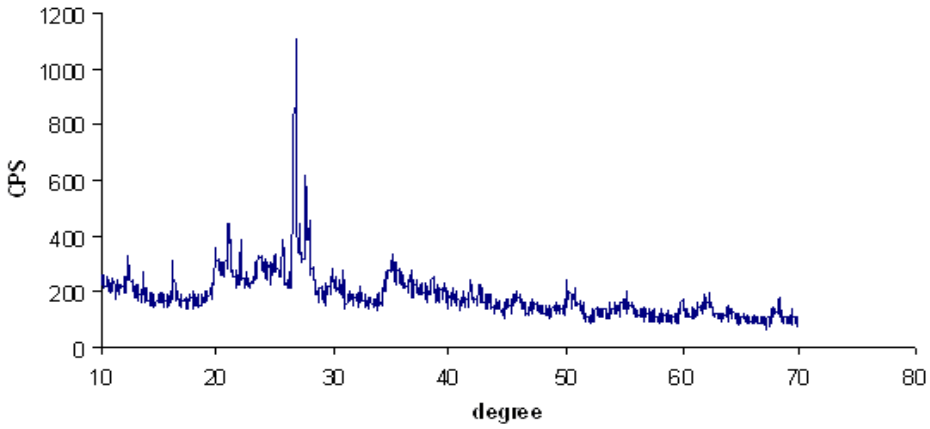


**Figure 1.10** XRD peaks of the foulant scraped off the spent membrane

HPC and fraction organic carbon data for foulant scrapings are in conflict with other measurements. Scrapings from vessel V5 (upstream and middle membranes) and V6 (downstream membrane) contained very high levels of organic and inorganic carbon (Table 1.5), suggesting that organic carbon is a major component of membrane foulant—in effect, that biomass is likely a primary contributor to membrane fouling. HPC measurements, on the other hand, were low—that culturable bacteria contribute very little to surface fouling. Taking the footprint of a single bacterium in the membrane as $2 \cdot 10^{-8}$ $cm^2$, even the highest HPC measurement ($5.1 \cdot 10^4$ $cm^{-2}$) would cover only 0.1% of the membrane surface. This result tends to support the visual evidence, in which no recognizable bacterial forms were immediately apparent, but are difficult to reconcile with the high $f_{OC}$ data.

**Table 1.5** Heterotrophic plate counts and TOC/TIC content in foulant samples scraped from the surface of a replaced membrane. Sample ID reflects membrane position in the array of vessels.

| Sample ID | TOC (%) | Total C (%) | TIC (%) | HPC (cells/$cm^2$) |
|---|---|---|---|---|
| V5-1 | 11.00 | 13.78 | 2.78 | $4.40 \times 10^4$ |
| V5-2 | ND | ND | ND | $1.73 \times 10^3$ |
| V5-3 | 11.30 | 14.29 | 3.00 | ND |
| V6-3 | ND | ND | ND | $5.10 \times 10^4$ |

As a whole, autopsy measurements suggest that the primary cause of membrane failure involved fouling with colloidal organic material. This may have been aggravated by the deposition of the clay particles derived from the slow sand filters.

### *2. Comparison of SSF and microfiltration (MF) performance for CAP water pretreatment*

Pretreatment of raw water for RO separation of soluble components is an absolute necessity for preservation of RO membrane integrity, prevention of fouling and extension of membrane life. There are, however, several ways to provide pretreatment, including SSF and MF. These two pretreatment alternatives were studied previously, leading to a conclusion that both methods performed adequately but that, land permitting, SSF was much less expensive. Because RO membrane post mortems indicated that clay particles on the RO membranes may have been derived from SSF, however, MF pretreatment was revisited in the latter phase of this investigation.

After April 2009, water to the RO unit was pretreated using MF, and a concerted effort was undertaken to compare the qualities of MF and SSF-treated water in terms of silt density index (SDI) values. The comparison was based on side-by-side tests in which the SSF overflow rate was the primary independent variable.

The SDI provides a useful indicator of colloid content in water that is prepared for RO treatment, overcoming the relative insensitivity of standard turbidity measurements. Samples for SDI measurements are passed at a constant pressure (30 psi) through a 0.45-µm membrane filter at constant temperature (± 1°C). Particle accumulation reduces the filtration rate over the 15-minute standard test period. Flow data yield a plugging factor, defined as the percentage decrease

in the flow passing through the filter compared to the original rate. SDI values are then calculated as follows:

$$SDI = \frac{PF}{t}$$

where, SDI is the silt density index [-]
PF is the plugging factor [%]; the time-dependent percentage decrease in flow rate
t is the time [minutes]

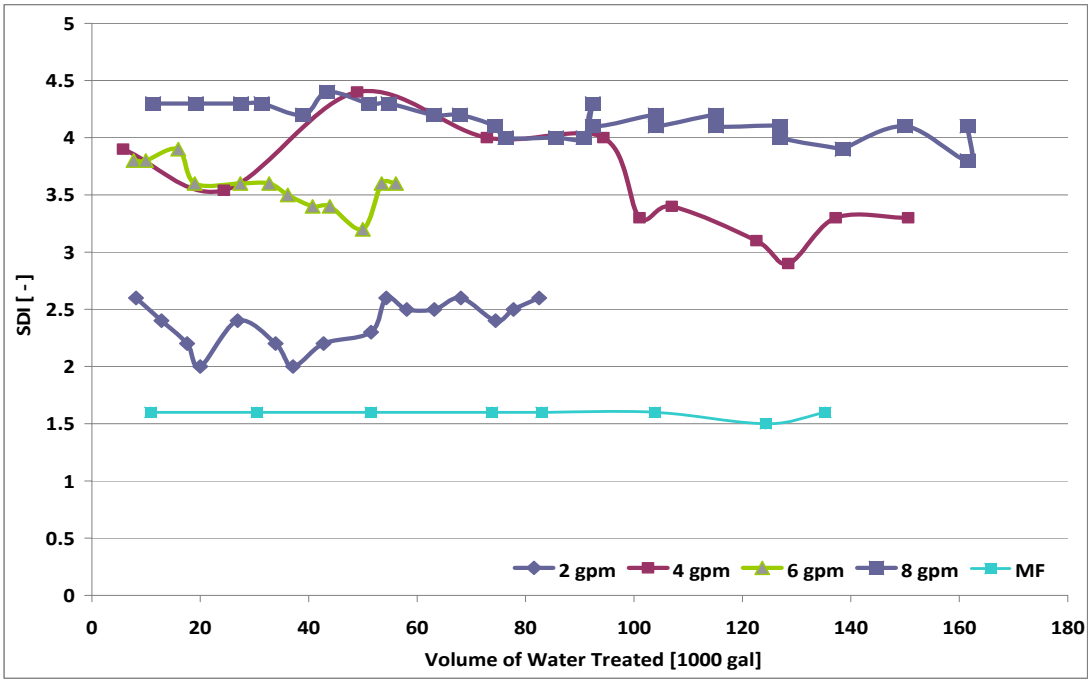


**Figure 2.1** Comparison of SSF and MF in terms of silt density index (SDI) in reactor effluent.

The SDI instrument was from Chemetec Model FPA-3300. RO membrane warranty generally depends on maintenance of SDI < 3.0 in RO influent. Values below 5.0 may be adequate to protect RO membranes from fouling due to influent particle accumulation.

Comparison of SSF and MF effluent SDI values (Figure 2.1) indicates that (i) SSF effluent quality is sensitive to the water application rate and (ii) SSF SDI values can approach those of the MF effluent if CAP water application rates are maintained at ≤ 0.027 gpm/ft$^2$.

The fluid application rate for the MF unit, 0.0165 gpm/ft$^2$ was well within the recommended range for MF operation. The normal range of SSF generation is 0.02-0.08 gpm/ft$^2$. In all cases, SDI values for MF and SSF effluents were within the range of acceptable values for downstream RO treatment, although only the MF effluent always satisfied RO membrane manufacturers' recommendations.

After MF pretreatment was initiated in April 2009, the record of time-dependent water permeation coefficients for RO treatment grew much steadier (Figure 1.3). Results suggest that the quality of MF-treated water may be superior to that SSF effluent for downstream RO separation of water-soluble components.

### *3. Minimizing water lost as RO brine – VSEP post-treatment*

VSEP (New Logic, Inc.) is a membrane separation system in which high-pressure RO or nanofiltration is used to extract additional water from highly saline solutions (Figure 3.1).

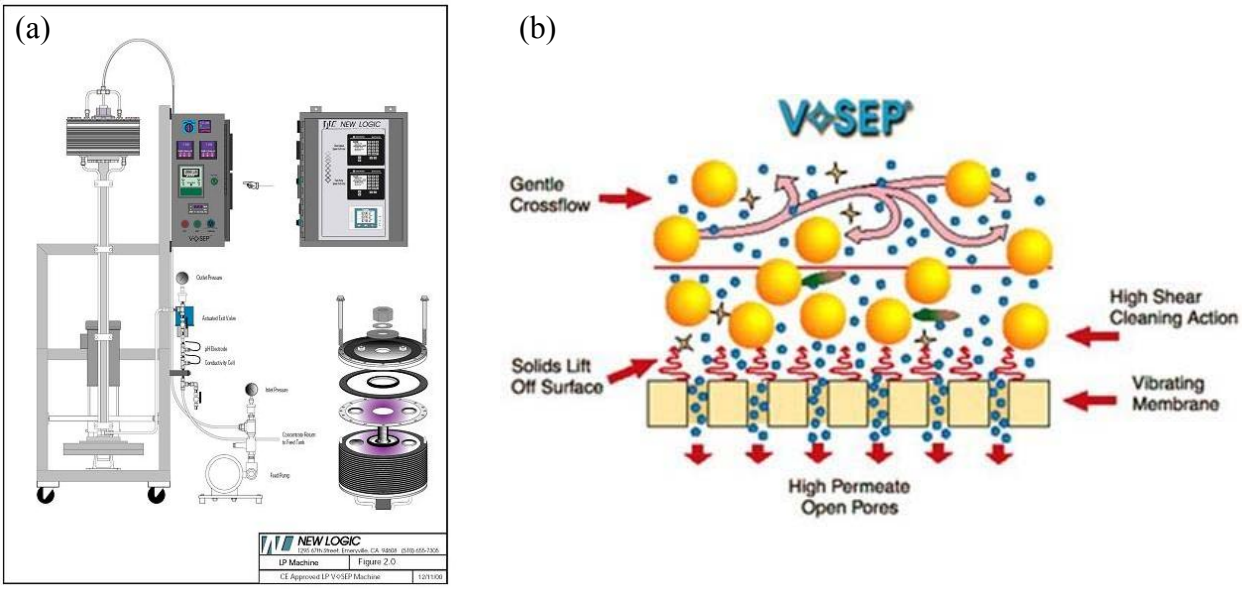


**Figure 3.1 (a)** VSEP LP reactor in pilot scale mode, (b) Principle of VSEP operation—mechanical vibration at the membrane surface produces a shear wave that prevents solids formation on membrane surfaces and scaling while forcing additional water from brines.

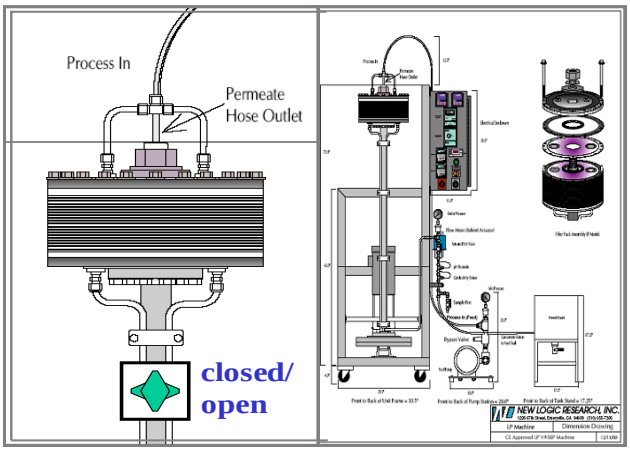


**Figure 3.2** Schematic views of the VSEP reactor and the operation of brine retention valve

The VSEP reactor was a pilot scale, LP Series unit containing 16.44 $ft^2$ of ESPA1 membrane (Hydranautics). The feed flow (RO brine) was provided at 500 psi based on preliminary testing to select an operating pressure. The unit was operated by automatically cycling the brine retention valve between its closed and open positions (Figure 3.2). With the valve closed, fluid left the reactor only as permeate. In the open-valve position, brine was briefly flushed from the unit and completely replaced with reactor influent (RO brine). During each cycle, the valve was opened (flush position) for six seconds. The length of the closed valve period was adjusted to yield target permeate recoveries. In general, average permeate flow rates were inversely related to VSEP recovery and elapsed time of operation following membrane cleaning.

Design and operational parameters for the VSEP in P-mode (pilot mode) are presented in Table 3.1.

**Table 3.1 Vibratory shear enhanced processing operational parameters**

| | |
|---|---|
| Membrane type | ESPA1 |
| Membrane surface area (sqft) | 16.44 (P-mode) |
| Conductivity of brine ($\mu S.cm^{-1}$) | 3000 – 5000 |
| Operating pressure (psi) | 500 |
| Vibration frequency (Hz) | 52.0 – 52.5 |
| Flow rate (gpm) | ~1.0 |
| Recovery rate (%) | 75 – 90 |
| Open valve period (min) | 0.1 |
| Closed valve period (min) | 1.0 – 6.9 |

VSEP recovery and the time between reactor cleanings were decision variables for VSEP operation. It was postulated that some combination of these variables would lead to economically optimal VSEP performance. Increased VSEP recovery produces additional potable water and decreases the cost of brine disposal but also lowers the average permeate flux so that more reactors are necessary to treat the same brine flow. Similarly, less frequent reactor cleaning saves on cleaning costs but, again, lowers the average VSEP permeate flux leading to purchase and operation of additional reactors. Recoveries of 89.2%, 85.7 % and 82.4 % were selected for this phase of study (overall recoveries of 98%, 97% and 96.5%), and 24-hour pilot experiments were run to establish the time-dependent permeate flux at each recovery level (Figure 3.3). Based on these results, linear relationships were established between the temperature-corrected water flux and the time of operation between membrane cleanings. Simple linear regression results are summarized (Figure 3.3).

In the 89.2% recovery experiment, for example, the length of the closed-valve period necessary to maintain recovery increased from 4.7 minutes to 6.9 minutes over 23 hours of continuous operation. The temperature-corrected water flux dropped from 59.5 gfd to 33.9 gfd over the same period. Other VSEP operating conditions were as follows: ¾-inch amplitude of torsional vibration, 500 psi operating pressure (during the closed-valve period), and 0.1 minute open-valve time. The influent TDS concentration was about 2300 mg/L, and the product water had an average TDS of 46.5 mg/L. The TDS of the concentrate was ~20,000 mg/L. A salt balance

around the reactor, defined in section 1.b, produced a positive salt mass balance deviation ($MBD_S$) ≤+5%. The temperature of the water varied between 12°C and 20°C during the day-long study, averaging 15.3 °C. The results of day-long experiments at the other recoveries were similar.

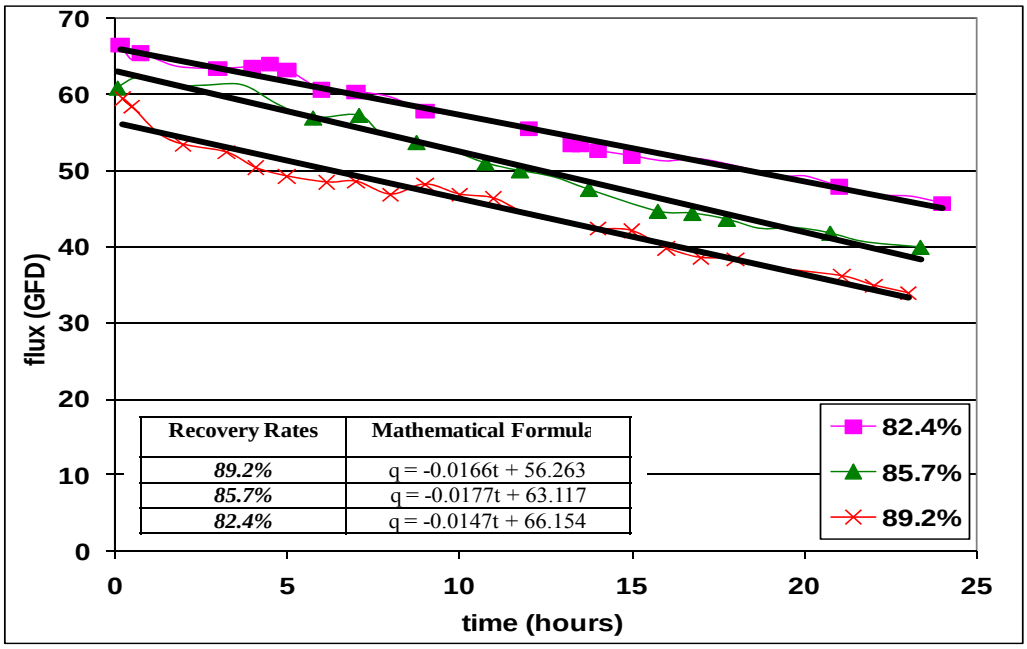


**Figure 3.3** The temperature-corrected permeate flux as a function of overall VSEP recovery and time of continuous operation following membrane cleaning. Regression lines of best fit are shown.

### *3.1 Economic analysis of VSEP option*

Three cases were selected for economic comparison—(i) RO alone, with brine disposal via enhanced evaporation, (ii) RO followed by VSEP to minimize the volume of brine for evaporative disposal, and (iii) IX before RO to achieve higher recoveries without scaling during RO. Economic and performance data for VSEP operation were derived from experiments or provided by New Logic, Inc. It is reemphasized that the long-term feasibility of recoveries >>80% via combined IX softening/RO has not yet been demonstrated, and only a theoretical treatment of RO performance and corresponding cost development is possible without addition pilot work. The analysis of IX/RO/brine disposal costs is in section 4, this report.

For cost comparison, the total flow to be treated was assumed to be 15 mgd. The period of the economic analysis was 30 years (the assumed service life of the RO vessels), and the discount operator was 0.06 $yr^{-1}$. All costs are in January 2010 dollars.

Incremental costs attributable to the RO/VSEP option include the capital and operation/maintenance costs from (i) VSEP treatment for brine minimization, (ii) augmented evaporation of residual (post-VSEP) brine and (iii) water lost as brine. A near-optimum period

of VSEP operation (between membrane cleanings) was determined as a function of VSEP recovery as follows: Fitted curves (Figure 3.3) were used to represent permeate flow rate as a function of time of continuous operation at each recovery. The total volume of permeate produced between cleaning operations, divided by the operational period plus cleaning time (Table B-1, Appendix B), yields the average permeate production rate for single VSEP device. That is,

$$Q_i = (a_i \times T^2/2 + b \times T) \times A / [(T + T_C)]$$

where $Q_i$ is average permeate flow rate for a single VSEP unit at VSEP recovery rate i [gpd]
T is the VSEP run time between cleanings [days]
$T_C$ is time required for membrane cleaning [days]
$a_i$ is the slope of the fitted relationship between flux and run time [gfd/day]
$b_i$ is the intercept (vertical axis) of the same fitted relationship [gfd]
A is the membrane area for a single VSEP unit [$ft^2$].

The number of VSEP units required ($N_i$) at recovery $R_i$ is then given by :

$$N_i = Q_{ROB} \times R_i / Q_i$$

where $Q_{ROB}$ is the total rate of brine flow from the RO process [gpd].

Not surprisingly, the average permeate flux decreases with time between successive membrane cleanings ($a_i$ values are negative).

Unit costs/manufacturer's data for the cost of full-scale VSEP reactors and VSEP operational costs are provided (Table B-1, Appendix B). Operational costs that were considered include (i) VSEP power costs—500 psi feed pressure and generation of torsional vibration (manufacturer's data), (ii) membrane cleaning and replacement costs and (iii) personnel costs. The value of water lost as VSEP brine was again taken as a system cost, estimated at $1000 per acre foot of unrecovered brine. The service life for VSEP reactors was assumed to be 10 years. For evaporation ponds and related equipment, service life was assumed to be 30 years. The largest VSEP unit manufactured by New Logic, Inc., the I-84, was used for the economics analysis. The membrane area of the I-84 unit is 1500 $ft^2$, and the cost is $250,000 per unit.

At each recovery rate for which there were pilot data ($R_i$), the annualized cost for treating 3 mgd of RO brine was calculated as a function of the period of VSEP operation between membrane cleanings (Figure 3.4). The global optimum was found at the combination of recovery and cleaning frequency that provided the lowest present value of total annualized cost. Results suggest that there is a broad operational region in which VSEP operation is near optimal—that total annualized cost is fairly insensitive to recovery in the range 80-90 percent and period between cleanings in the range of 25-40 hrs. In those ranges, the total annualized cost for the VSEP system was significantly lower ($6.6 M $\cdot$ $yr^{-1}$ versus $11.6 M $\cdot$ $yr^{-1}$) than the cost of the no-VSEP option (Table 3.2). In the RO/VSEP combined system evaluated here, only 2-4% of the CAP water treated would be lost as brine. The incremental cost of VSEP treatment is about $400

per acre foot of water treated (influent to the RO unit). The cost per unit of water recovered from RO brine is about $2400 per acre foot.

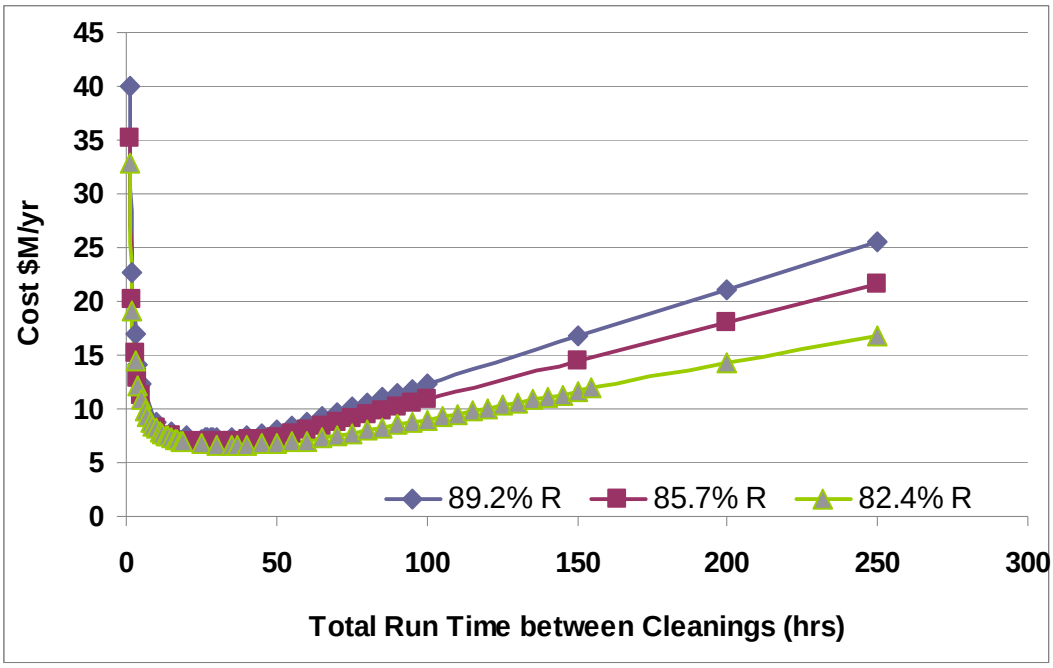


**Figure 3.4.** Annualized VSEP capital/O&M costs as a function of recovery and time of operation between cleanings.

***4. Brine minimization through IX pretreatment (softening) of CAP water***

In theory, removing hardness cations from CAP water prior to RO treatment will make it possible to drive reverse osmosis well past 80 percent recovery without precipitating $BaSO_4$(s) or $CaSO_4$(s). Ion exchange itself produces brine for disposal, however, and in communities that practice both salt management and wastewater reclamation/reuse the disposal of brines in municipal sewers is counter-productive. Ion exchange was proposed as a pretreatment for CAP water, to increase water recovery during RO and minimize RO brine volume. The IX regenerant solution will be used several times, after which the solution itself will be softened, the original ion balance restored by adding NaCl, and the solution will be used for an additional series of regeneration steps. Bench-scale IX experiments designed to confirm the feasibility of presoftening CAP water via IX involved a strong acid cation (SAC) synthetic polymeric resin manufactured by USA Resin to remove hardness ions.

Resin manufacturers suggest regeneration using 2-7 bed volumes per hour over a 1- hour period. Here the resin bed volume was approximately 2 L, and the regenerant solution consisted of 15L containing 200 g/L NaCl. The mass of calcium added to the regenerant solution during successive regeneration cycles was as illustrated (Figure 4.1). Declining mass added over the course of the experiment suggests that the solution accumulated sufficient calcium to interfere significantly with the regeneration process after a few regeneration steps. In these experiments,

the water treated in the IX column obtained by MF treatment of CAP water. Hence cation concentrations were similar to those in Table 1.1. The Figure 4.1 results suggest that under the conditions of the experiment, several regeneration steps should be possible using the same regenerant, before regenerant reconditioning is necessary to improve calcium recovery from spent IX media.

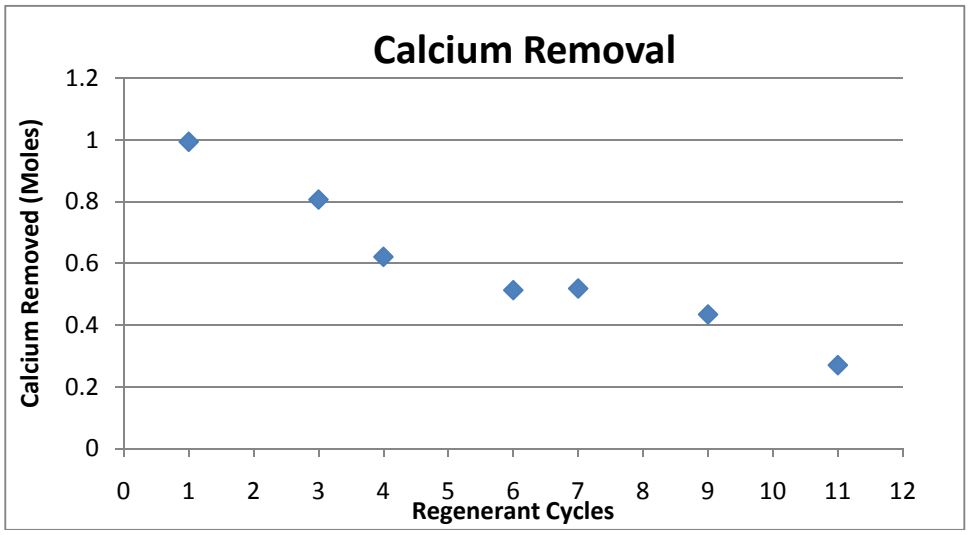


**Figure 4.1.** Calcium mass added to a recycled regenerant solution during successive regeneration steps. Declining mass suggests that the regenerant was gradually becoming saturated with calcium.

## 4.1. Materials and Methods.

### 4.1.1. Reactor description.

The city of Tucson loaned a bench-scale ion exchange reactor system (Tomar Water Systems, Inc.) to the project. The system consists of 4 columns of S40 clear PVC pipe, each with a 2-in diameter and a 32-in length. Resin capacity per vessel was 0.061 $ft^3$. Optimal flow for each column was 0.25 gpm and used in each experiment, for an overflow rate of ~11.5 $gpm/ft^2$. This is well within the norms for field-scale operation of ion exchange processes.

### 4.1.2. Ion Exchange Chromatography

A Dionex DX500 ion chromatograph was used with CD20 conductivity detector for anion and cation analyses. A 30 mM MSA solution buffered the mobile phase. Flows were regulated using an IP25 Isocratic gradient pump system. A dual head pump transports the mobile phase solution from the proportioning valve, where buffers are combined in the injection valve ahead of the ion exchange column (Model CS16). After passing through the cation exchange column, flow enters a self-regeneration suppressor (SRS). In the SRS, water is hydrolyzed at the anode to produce $H^+$ cations, and reduced at the cathode to produce $OH^-$ anions. An anion

exchange membrane is located within the suppressor, which allows the $OH^-$ to flow into the mobile phase buffer, neutralizing the $H^+$. Corresponding anions in the buffer are drawn through the anion exchange membrane to the anode side where they are removed to waste.

Software (PeakNet) for the Dionex DX500 consisted of the DX LAN program, data processing, method editor, and various other configuration/driver programs. The DX LAN communicates with the hardware via LAN lines to individual units. The DX500 can be operated from the computer (remote) or the front panels of the chromatograph itself (local). Data processing was performed after analysis. Standard solutions of known ionic composition were used to generate standard curves. In this way, retention times typical of sodium, calcium and magnesium were established. Primary cation concentrations in CAP water and CAP water following IX treatment are provided in Table 4.1. These highly preliminary results suggest that high-recovery RO treatment of the IX-pretreated water may be possible without generating calcium-containing ion products that greatly exceed their respective solubility products.

**Table 4.1.** Concentrations of primary cations in CAP water and CAP water following IX treatment using the project's bench-scale reactor.

| | | | |
|---|---|---|---|
| Source | Sodium (mM) | Magnesium (mM) | Calcium (mM) |
| CAP Feed Water | 3.79 | 1.01 | 1.27 |
| IX Effluent | 6.68 | ND[1] | ND |

[1]ND = non detect. Quantity was below the method detection limit, which was << 10 μM.

**4.1.3. Economic analysis**.

Design of the IX reactor was based on an assumed resin bed depth of 8 ft. The reactor diameter was assumed to be 12 ft, so that 12 IX units were required to treat 15 mgd at an overflow rate of 7.7 gpm/ft$^2$ (selected as design criterion based on typical water application rates for IX treatment). The calculated bed capacity for specific ions and volume to breakthrough were then determined based on an assumed resin capacity of 2.0 equivalents per liter and the composition of CAP water (Table 1.1). Results suggest that about 225 bed regenerations would be necessary per year for each IX reactor. At 10 bed volumes per regeneration, the IX process will generate about 0.5 million gallons of brine in the regeneration of all 12 reactors. This volume was added to the RO brine in order to estimate the cost of enhanced evaporation for the IX/RO alternative. It was assumed that chlorine disinfection would be unnecessary ahead of IX treatment. Resin costs, IX brine production volumes and other cost factors were as summarized (Table 4.2).

**Table 4.2** Cost parameters, regenerant volume, and cost factors for IX pretreatment

| **IX brine disposal (gal/day)** | 500,000 |
|---|---|
| Resin Price ($/m3) | $4,240 |
| Resin Lifetime (yrs) | 5 |
| IX Design Life (yrs) | 30 |
| Total Resin Volume (m3) | 307.4 |
| Total Resin Cost per Replacement | $1.30M |
| **Total Resin Cost (present worth)** | $4.26M |

Cost functions used to calculate of the total annualized (incremental) cost attributable to IX/RO and brine disposal are provided in Appendix B (Table B.2). Each cost component is a function of a single independent variable—the anticipated recovery during RO treatment of the pre-softened water. A plot of annualized cost versus recovery (Figure 4.2) indicates that economies are achieved by increasing RO recovery up to 99%, as less brine is generated for disposal and less water is lost in the process. Beyond that point, however, the energy necessary to overcome osmotic pressure in the final stage of RO dominate the calculation, leading to much higher total costs. The feasibility of 99% recovery following IX pre-softening remains to be established. IX ahead of RO treatment was predicted to increase power costs for operation of the first two stages of RO by <1%. Nevertheless, that increase is included in the analysis. The capital costs for IX, RO and augmented evaporation are the primary sources (50%) of the overall cost for the IX pre-softening alternative.

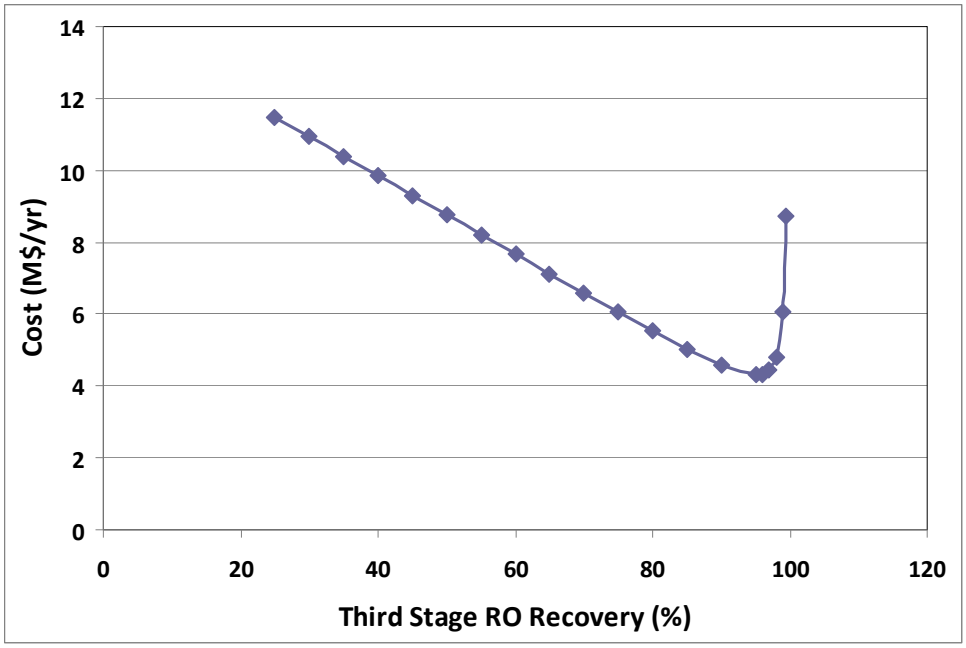


**Figure 4.2** The overall incremental cost for IX, RO and augmented evaporation as a function of recovery during reverse osmosis

## 5. Summary and Conclusions

RO brine volume was reduced from 20% to 2-4% via post-RO VSEP treatment. Under optimal conditions, RO/VSEP treatment achieved ~98% overall recovery. The total annualized cost of brine treatment was fairly insensitive to VSEP recovery in the range 80-90% and the period of VSEP operation between cleanings in the range 25-40 hrs. These values define a fairly broad window for near optimal VSEP operation under the conditions of the study. The cost of VSEP treatment to decrease brine loss to 3.5% was estimated at $394-$430 per acre foot ($1.21 - $1.32 per 1000 gal) assuming 15 MGD CAP water is treated by the treatment plant. For a hypothetical 3 MGD RO brine flow (80% recovery during RO treatement), the use of VSEP to recover additional water and reduce the volume of brine for disposal results in a savings of more than $5M/year compared to the no-VSEP brine disposal alternative (Table 5.1).

**Table 5.1. Economic Summary Including Comparison of Treatment Options**

| RO Treatment | VSEP as Post-treatment of RO | | | IX as Pre-treatment of RO | | |
|---|---|---|---|---|---|---|
| | 96.5% | 97.1% | 97.8% | 96.5% | 97.1% | 97.8% |
| $11.6M ($2.11/1Kgal) | $6.62M ($1.21/1Kgal) | $6.85M ($1.25/1Kgal) | $7.23M ($1.32/1Kgal) | $5.84M ($1.07/1Kgal) | $5.55M ($1.01/1Kgal) | $5.22M ($0.95/1Kgal) |

IX pretreatment is predicted to do even better than RO/VSEP, but there are no field data to confirm the feasibility of presumed IX/RO recoveries. Overall recoveries >>80% will be achievable if IX removes essentially all the divalent cations and no other precipitation reactions occur during RO treatment. IX used as pretreatment of RO is predicted to save and additional sum of ~$1M/yr (relative to the RO/VSEP treatment option). These values should not be accepted, however, without experimental support for the assumed IX/RO recovery.

## APPENDIX A

### High pH RO Membrane Cleaning

The cleaning procedure was carried out following an increase in the product TDS concentrations for all RO pressure vessels. The water transport coefficient (A) also declined, suggesting that membrane fouling was occurring. An increase in the differential pressures (dP) for both of the stages of the RO unit was also observed, as well as an increase in salt transport coefficient (B). (Please, refer to the results section for the related graphs.)

Sodium hydroxide (NaOH) was used to increase the pH of the cleaning solution (pH ~ 12.0), and hydrochloric acid (HCl) was use to readjust the pH to the neutral level (pH ~ 7.0). Base/acid was added to chlorine free water that was produced by running the RO temporarily without chlorine addition. Consequently, sodium sulfite ($Na_2SO_3$) was omitted from the cleaning solution recipe.

As the first step in the production of the chlorine free water, the bleach and ammonium sulfate chemical feed pumps were shut down for about 18 hours of operation immediately

preceding the cleaning steps. Both the free chlorine and the total chlorine levels in the RO influent were 0.01 mg/l before the chlorine-free permeate was accepted. The permeate tank was emptied before collecting the chlorine-free permeate. Then, 250 gallons of chlorine-free permeate was collected in that tank. Another 250 gallons of permeate was stored in an additional tank. This would provide the flushing solution at the end of the cleaning process. The pH of the cleaning solution was adjusted to 12 by adding 260 g of NaOH to the cleaning solution. Due to a technical problem with the water heater, the cleaning solution could not be adjusted to 30 $^{o}$C, as specified for membrane cleaning. The highest temperature recorded was 26 $^{o}$C.

The cleaning process consisted of four steps: (i) a low-flow flush with the basic solution, in recycle mode (ii) soak (iii) a high-flow flush with the basic solution, again in recycle mode (iv) neutral pH flush, without recycle. The low-flow flush and the high flow flush were supposed to be at 16 L/min and 16-40 L/min (reject flows), respectively. However, the low-flow flush was performed at a flow rate of 8.09 L/min at 25.9 $^{o}$C and the high-flow flush was performed at a flow rate of 11.4 L/min at 24.7 $^{o}$C. The high-pressure pump cannot be operated while running with a high-pH solution, because the pH was outside the acceptable range for pump operation to protect the membranes in normal operation. Shut down at high pH is a safety factor in the control program. The inaccessibility to the control program did not allow us to bypass this control feature. Thus the only source of water input was the RO forwarding pump, which was unable to run higher than 8.09 L/min.

A new 1-μm cartridge filter was installed on the RO forwarding pump before the cleaning process was initiated. The cleaning solution had a conductivity of 1568 μS/cm and a pH of 12.12.

The low-flow flush was performed for 1 hour. For the first 2 minutes, water was flushed to the drain. The reject and permeate flows were 7.23 L/min and 0.86 L/min, respectively, for a total flow of 8.09 L/min. The initial turbidity of the cleaning solution (before the run) in the permeate storage tank was 1.26 NTU. During the low-flow flush, a cloudy effluent was observed, especially between the 20$^{th}$ and the 45$^{th}$ minutes of the run. The turbidity of the reject water was 62.2 NTU at the 30$^{th}$ minute. The operating pressures were as follows:

**Table A.1** Operating pressures during low-flow flush step of the cleaning process

| OPERATING PRESSURES DURING LOW-FLOW FLUSH | | |
|---|---|---|
| Vessels | Influent (psi) | Product (psi) |
| 1 & 2 | 43.3 | 42.6 |
| 3 & 4 | 37.6 | 37.7 |
| 5 | 32.5 | 27.5 |
| 6 | 17.8 | 0.4 |
| Reject | 6.1 | - |

The soaking period started right after the low-flow flush run. The membranes were soaked in the cleaning solution for 2 hours. The high-flow flush followed (conductivity 1446 μS/cm and pH 11.7). The temperature was 24.7 $^{o}$C. The flow rates of the reject and product (vessel 6) waters were 9.84 L/min and 1.56 L/min, respectively, during the run, for a total flow rate of 11.4 L/min. Reject water turbidity was 21.8 NTU during the run. Operating pressures follow:

**Table A.2** Operating pressures during high-flow flush step of the cleaning process

| OPERATING PRESSURES DURING HIGH-FLOW FLUSH | | |
|---|---|---|
| Vessels | Influent (psi) | Product (psi) |
| 1 & 2 | 68.1 | 66.3 |
| 3 & 4 | 59.9 | 59.1 |
| 5 | 52.5 | 43.3 |
| 6 | 29.1 | -0.2 |
| Reject | 10.8 | - |

At the end of the high-flow flush period, the cleaning solution had a pH of 12.02 and a conductivity of 1483 μS/cm. The temperature was 23.6 $^{o}$C and the turbidity was 19.9 NTU. The spent cleaning solution was temporarily stored in the permeate storage tank. After adjusting the pH to 7.0 by addition of HCl, it was discharged to the CMID irrigation canal. The conductivity was 1000 μS/cm and temperature was 24.2 $^{o}$C.

The high-flow permeate flush was performed for half an hour as the last step of the cleaning process. During the run, the flow rates of the reject and product water were 9.80 L/min and 1.51 L/min, respectively, for a total flow of 11.3 L/min. The turbidity of the permeate water increased to 1.23 NTU in the reject line while flushing.

The RO was reinitiated (pH = 6.72; conductivity = 1103 μS/cm; temperature = 20.9 $^{o}$C; free chlorine = 0.17 mg/L; total chlorine = 0.52 mg/L, eventually increasing to 1.95 mg/L) at 11:30 PM on 04.07.2008. (3189.9 hours was the reading on the hour meter.) Recovery was 81.44 % at a total permeate flow rate of 15.27 L/min. The reject flow rate was 3.48 L/min. The cleaning process can be summarized as:

**Table A.3** Summary of the cleaning process

| STEPS OF THE CLEANING PROCESS | | | | |
|---|---|---|---|---|
| | Flow rate (L/min) | Temperature ($^{o}$C) | pH (-) | Time (hours) |
| Low-flow flush with recycle | 8.09 | 25.9 | 12.12 | 1 |
| Soaking | - | 25.9 | 11.9 | 2 |
| High-flow flush with recycle | 11.4 | 24.7 | 11.7 | 2 |
| High-flow flush with permeate water | 11.3 | 24.2 | ~7.0 | 0.5 |

## Cleaning Procedure for VSEP Membranes

Cleaning of the VSEP involves five steps. The first step of the cleaning process is a 15-minutes fresh water flush. Cold water is passed through the VSEP unit in a single-pass routine at 50 psi. Second step is the low-pH cleaning with 3% NLR 404 solution, a citric acid based solution specifically formulated to effectively remove metallic-based foulants and scaling components. The best result is obtained at between pH 2.0 and 3.0. The third step of the cleaning process is another 15-minute cold fresh water flush, and the fourth step is a high-pH cleaning with 3% NLR 505 solution, a blend of surfactants and chelating agents in a caustic liquid. The best result is obtained at between pH 11.0 and 11.5. The temperature of the cleaning solutions in steps 2 and 4 is maintained at 50 $^{o}$C throughout the 45-minute operation. The last step of the cleaning process is yet another 15-minute cold fresh water flush. In all the steps, VSEP filter pack is vibrated with a 3/4" amplitude (~52 Hz). At the end of each fresh water flush step, the pressure is increased to 300 psi while the vibration is kept constant. The permeate flow rate is measured by weighing the total amount of water collected in a jar in one minute. Permeate flows are recorded and compared to find out the success of the cleaning.

# APPENDIX B

## Functions Used to Estimate Incremental Costs for VSEP and IX Alternative Methods for Minimizing Brine Volume—Summary Tables.

### Table B.1. Summary of VSEP-related cost functions and contribution to annual cost.

| Item | Basis of Calculation | Assumptions | Contribution to Annualized Cost |
|---|---|---|---|
| **Capital costs:** | | | |
| VSEP units | $(a \times n) + \frac{a' \times n}{(1+r)^{10}} + \frac{a' \times n}{(1+r)^{20}}$ | 10-year service life. | 18%-21% |
| Disposal of brine cost (augmented evaporation ponds) | 59M$ × ($Q_{VSEP,total}$/3MGD) × $F_{30}$ | There is a linear relation between the capital cost of evaporation ponds and the flow rate of the brine to be disposed (Malcom Pirnie and Separation Processes, 2008). | 6%-12% |
| **Energy costs:** | | | |
| Pumping cost | $\left[\left(\frac{Q_{VSEP,total} \times \rho \times g \times h}{3.6 \times 10^6}\right)/\eta_s\right] \times 0.12\$/kWh \times 24hrs/d \times 365days/yr$ | The shaft efficiency of the pump is 80%. | 8%-9% |
| Vibration cost | $P_{vibration}$ × n × 0.12$/kWh × 24hrs/d × 365 days/yr | Power requirement for vibrating each VSEP unit is 12 hp | 5%-6% |
| **Cleaning costs:** | | | |
| Chemical cost | $C_{chem}$ × [24hrs/d × 365days / ($\check{T}$+$T_C$)] × n | | 12%-21% |
| Water cost | $C_{w,cleaning}$ × [24hrs/d × 365days / ($\check{T}$+$T_C$)] × n × ($C_{w,unit}$ / 3.3×$10^5$ gal/AF) | Unit value of water ($C_{w,unit}$) is 1000$/AF. | 0.4%-0.8% |
| **O&M Costs:** | | | |
| Membrane replacement cost | ($C_{memb.set}$ / 2 yrs) × n | A single set of membranes lasts for 2 years. | 18%-22% |
| O&M cost for evaporation ponds | 3.9M$ × ($Q_{VSEP,total}$/3MGD) | There is a linear relation between the O&M cost and the flow rate of the brine to be disposed. | 5%-11% |
| Personnel cost | 400K$/yr | There are 4 personnel with 8 hours shifts around the clock at the facility. | 5%-6% |
| **Miscellaneous Costs:** | | | |
| Brine cost (due to loss of water) | ($C_{w,unit}$ / 0.33 Mgal/AF) × [$Q_{VSEP,total}$ × (1 – $R_{VSEP}$)] × 365days/yr | Unit value of water ($C_{w,unit}$) is 1000$/AF. | 5%-9% |

# Appendix 5:

Water consumption, irrigation efficiency and nutritional value of *Atriplex lentiformis* grown on reverse osmosis brine in a desert irrigation district

Agriculture, Ecosystems and Environment 140 (2011) 473–483

# Water consumption, irrigation efficiency and nutritional value of *Atriplex lentiformis* grown on reverse osmosis brine in a desert irrigation district

Deserié Soliz[a,*], Edward P. Glenn[a], Robert Seaman[a], Martin Yoklic[a], Stephen G. Nelson[a], Paul Brown[b]

[a] *Environmental Research Laboratory, The University of Arizona, 2601 East Airport Drive, Tucson, AZ 85756, USA*
[b] *University of Arizona, Department of Soil, Water and Environmental Science, Shantz Bldg. 429, Tucson, AZ 85721, USA*

ARTICLE INFO

*Article history:*
Received 5 July 2010
Received in revised form 18 January 2011
Accepted 19 January 2011
Available online 18 February 2011

*Keywords:*
Lysimeters
Stomatal conductance
Transpiration
Brine reuse
Salinity
Concentrate management

ABSTRACT

Arid regions in southwestern U.S. are faced with increased water shortages with the possibility of compromised water quality. The use of impaired water resources, including saline water, for agriculture is a possibility. The halophyte forage shrub *Atriplex lentiformis* (quailbush) was irrigated over three growing seasons with brine (2.6–3.2 g $L^{-1}$ total dissolved solids) from a reverse-osmosis water treatment plant in an agricultural district in Marana, Arizona, in the Sonoran Desert, U.S. The goal was to determine if a halophyte crop could be grown productively on saline irrigation water in a way that maximized yield yet minimized excess deep percolation of salt past the root zone. Our hypotheses for this project were: (1) *A. lentiformis* could consume water at or above the potential evapotranspiration rate ($ET_o$) measured at an on-site meteorological stations; (2) need for a leaching fraction could be minimized due to the high salt tolerance of the crop; and (3) water could be presented on a constant schedule typical of the delivery from a desalination plant, with excess water presented in winter utilized in summer via the deep rooting systems of *A. lentiformis*. Three irrigation treatments were tested based on the potential evapotranspiration rate ($ET_o$): (1) plots irrigated at $ET_o$ adjusted daily via an on-site micrometeorology station; (2) plots irrigated at 1.5 $ET_o$ adjusted daily; (3) plots irrigated at a constant rate throughout the year based on the mean of annual $ET_o$. The plants produced 15–22 tons $ha^{-1}$ $year^{-1}$ of biomass and could be irrigated at the rate of $ET_o$, ca. 2 m $year^{-1}$ at this location. Drainage volumes ranged from no drainage in Treatment 1 to 12–14% of applied water in Treatments 2 and 3. It is concluded that irrigation of halophyte forage crops provide a viable strategy for extending water supplies and disposing of saline water in arid-zone irrigation districts.



## 1. Introduction

Arid regions of the world face increasing water shortages due to population growth and the need for increased agricultural production. Aridity might increase in the western US due to climate change (Cook et al., 2004), and droughts produce periodic water shortages even when long-term average water supplies are adequate (Morehouse et al., 2002). As conventional water resources become limited, the use of impaired water resources, including saline water, for agriculture has been explored (Ayars et al., 2005, 2006; Grattan et al., 2004; Grieve et al., 2004; Qadir and Oster, 2004; Shannon et al., 1997; Skaggs et al., 2006a,b). In many locations, large volumes of saline water are available from natural or secondary salinized aquifers (Ayars and Schoneman, 2006), subsurface drainage from irrigated fields (Grattan et al., 2004, 2008), from industrial sources such as cooling towers (Gerhart et al., 2006; Glenn et al., 1998) and brines from reverse osmosis (RO) plants (Jordan et al., 2009; Riley et al., 1997). Reuse of agricultural and industrial brines for crop production can be environmentally beneficial in preventing discharge of brines into natural water bodies or evaporation ponds, which can harm wildlife (Bradford et al., 1991; Hamilton, 2004).

Guidelines have been developed for the utilization of saline water on conventional crops and forages (Ayars et al., 2005; Miyamoto et al., 2005; Miyamoto and Chacon, 2006; Qadir and Oster, 2004; Shannon et al., 1997; Skaggs et al., 2006a,b). However, the low salinity tolerance of most crops limits the amount of saline water that can be applied for conventional crop production. Related to this, conventional crops require a leaching fraction to control salinity in the root zone; and as the salinity of the irrigation supply increases, the required leaching fraction also increases (Shannon et al., 1997), resulting in the potential discharge

*Abbreviations:* ANOVA, analysis of variance; AZMET, Arizona Meterological Network; CAP, Central Arizona Project; EC, electrical conductivity; ET, evapotranspiration; $ET_o$, potential evapotranspiration rate; RO, reverse osmosis; TDS, total dissolved solids; WUE, water use efficiency.

* Corresponding author. Tel.: +1 520 626 2162; fax: +1 520 573 0852.
*E-mail address:* dsoliz@email.arizona.edu (D. Soliz).

0167-8809/$ – see front matter © 2011 Elsevier B.V. All rights reserved.
doi:10.1016/j.agee.2011.01.012

of large volumes of saline water past the root zone and into the aquifer.

A lesser amount of research has explored the domestication of wild halophytes as crop plants (reviewed in Glenn et al., 1999; Masters et al., 2007; Rogers et al., 2005). One of the basic research needs is to characterize the growth and water consumption potential of halophytes to develop water management strategies for irrigation with saline water. Under natural conditions, many halophytes have low to moderate rates of growth and water consumption, as they are generally found in high-stress environments (e.g., James and Richards, 2007; Mata-Gonzalez et al., 2005; Steinwand et al., 2001, 2006). Some studies concluded that halophytes have low yield potential, limiting their usefulness as crops (e.g., Niu et al., 1995). However, field studies (Glenn et al., 1997, 1998; Glenn and O'Leary, 1985; Miyamoto et al., 1996; Noaman and El-Haddad, 2000; Watson et al., 1987) have found that at least some halophytes can have high rates of growth and water consumption, even on salinities beyond 40 g $L^{-1}$ TDS (reviewed in Glenn et al., 1999). Hence, their crop potential might be higher than has been appreciated up to now (Flowers and Colmer, 2008).

Another research need is to find halophyte species with sufficient nutritional value to replace or supplement conventional feed ingredients in animal diets. Under natural range conditions, halophytes can be valuable browse plants for ruminants (O'Connell et al., 2006; Osman et al., 2006). However, their value as irrigated forage crops has not been demonstrated (Masters et al., 2007; Rogers et al., 2005). While protein levels in halophytes can be high (e.g., Glenn et al., 1998), they can also have high mineral contents that reduce their feed value; and some species contain other anti-nutritional compounds (Masters et al., 2007). Nutritional value depends on how the crop is managed as well as on post-harvest processing and animal feeding systems (Guevara et al., 2005; Norman et al., 2008).

The present research tested the use of saline effluent from a reverse osmosis (RO) desalination test facility in the Sonoran Desert to irrigate *Atriplex lentiformis* (quailbush), a halophytic and phreatophytic C4 native shrub (Meyer, 2005). *A. lentiformis* is a valuable shrub throughout its native range in the Sonoran, Mojave, and Chihuahuan Deserts of the U.S. and Mexico (Meyer, 2005). It provides forage for livestock, wildlife habitat and has been used in revegetation and range-enhancement projects around the world (Browning et al., 2006; Gupta and Arya, 1995; Sandyswinsch and Harris, 1992). However, only a few studies have evaluated it as an irrigated crop (Bauder et al., 2008; Glenn et al., 2009; Jordan et al., 2009; Watson et al., 1987). The goal of this research was to develop irrigation and cropping methods to maximize productivity and nutritional value of *A. lentiformis* while minimizing excess deep percolation of salts. Previous research demonstrated that *A. lentiformis* could be grown in high yield over a single growing season at this location (Jordan et al., 2009). The present study extended the findings over three years and tested three different irrigation strategies both in lysimeter basins and field plots. It also compared the nutritional contents of stems, leaves, and fruits, to design a cropping strategy that maximized nutritional value of the plant parts.

## 2. Materials and methods

### 2.1. Site description

The study site is located approximately 50 km NW of Tucson, AZ in the Cortaro-Marana Irrigation District. This is a desert environment, with mean January air temperatures of 10 °C, and mean July air temperatures of 30 °C, mean annual precipitation of 263 mm, and a potential evapotranspiration rate ($ET_o$) of 2025 mm (AZMET, 2010). The soil at the site was a uniform, alkaline, sandy Pima-series loam (National Cooperative Soil Survey, 2008) formerly used to grow cotton and other field crops. The site is directly adjacent to a cotton field (unplanted during these experiments) to the south/southeast and the Central Arizona Project (CAP) irrigation canal to the north. The CAP canal delivers water from the Colorado River to the Tucson basin for agricultural and municipal use. CAP water (average TDS = 700 mg $L^{-1}$) is delivered from the canal to a reverse osmosis mobile filtration test unit supplied by the U.S. Bureau of Reclamation. Concentrate (brine) generated from the RO system (ca. 2.6–3.2 g $L^{-1}$) is supplied to a holding tank that is pumped to an irrigation system set to deliver water to test plots (Fig. 1). Altogether, test plots of *A. lentiformis* 255 $m^2$ of ground area. Plots were made as large as possible and were grouped together to minimize advection of warmer, dryer air from bare areas around the plantings, which can artificially enhance ET rates (Hagishima et al., 2007; Tolk et al., 2006). The plantings in this study had ratios of net radiation to latent heat of evaporation of 1.3 (Jordan et al., 2009), similar to the ratio expected for crops growing under well-watered conditions but not subject to advection effects (Kelliher et al., 1995; Paw and Gao, 1988; Priestley and Taylor, 1972).

### 2.2. Experimental design and plot layout

The treatment structure, rationale for each treatment, and dependent variables measured during the study are described in Table 1. Plants were grown in two sets of 4 m × 4 m plots: the first set consisted of lined, 2.5 m deep, lysimeter basins equipped with drainage tubes to quantify drainage volume and salinity; the second set of plots were in undisturbed soil. The lined (lysimeter) plots were formed by excavating the native soil, installing a 40 mL high-density polyethylene liner and divider walls in the excavated area to form individual plots, and backfilling with the original soil. Lined plots were equipped with perforated PVC drain lines in a 20 cm gravel base to convey drainage water from the bottom of the plots to sumps, in which drainage volumes could be measured and sampled.

The objective for the lysimeter plots was to determine a water balance for each irrigation strategy tested. The plots in undisturbed soil were controls to determine if plant performance in lysimeters could be extrapolated to open-field conditions. Three irrigation treatments were tested based on $ET_o$ measured on site: (1) plots irrigated at $ET_o$ adjusted daily; (2) plots irrigated at 1.5 $ET_o$ adjusted daily; (3) plots irrigated at a constant rate throughout the year based on mean annual $ET_o$. The purpose of Treatments 1 and 2 were to determine the optimal irrigation rate for biomass production while minimizing discharge past the root zone. Previous results indicated that over the first year of irrigation *A. lentiformis* could consume up to 1.3 times $ET_o$; our hypothesis for this study was that similar rates could be maintained over three years of cultivation. Irrigation volumes for Treatments 1 and 2 were adjusted each day based on $ET_o$ minus precipitation for the preceding 24 h, which was determined by an automated micrometeorology station. The purpose of Treatment 3 was to determine if plots could be irrigated at a constant rate throughout the year, typical of brine availability from RO plants and other industrial sources. Our hypothesis for this treatment was that plants would develop a deep root system that could utilize deep soil moisture in summer that infiltrated due to over-irrigation in winter. If successful, this strategy could eliminate the need to adjust irrigation volumes based on $ET_o$ throughout the year, increasing the flexibility of water managers in disposing of RO effluent.

Individual plots within a treatment were not randomized within the larger plantings, but were grouped next to each other to form 64 $m^2$ units to minimize advection effects between treatment plots and to simplify the plumbing system. Unlined plots were laid out in the same pattern as the lined plots. Each plot was planted with 16 small (mean height = 8.5 cm, approximately 3 months old),

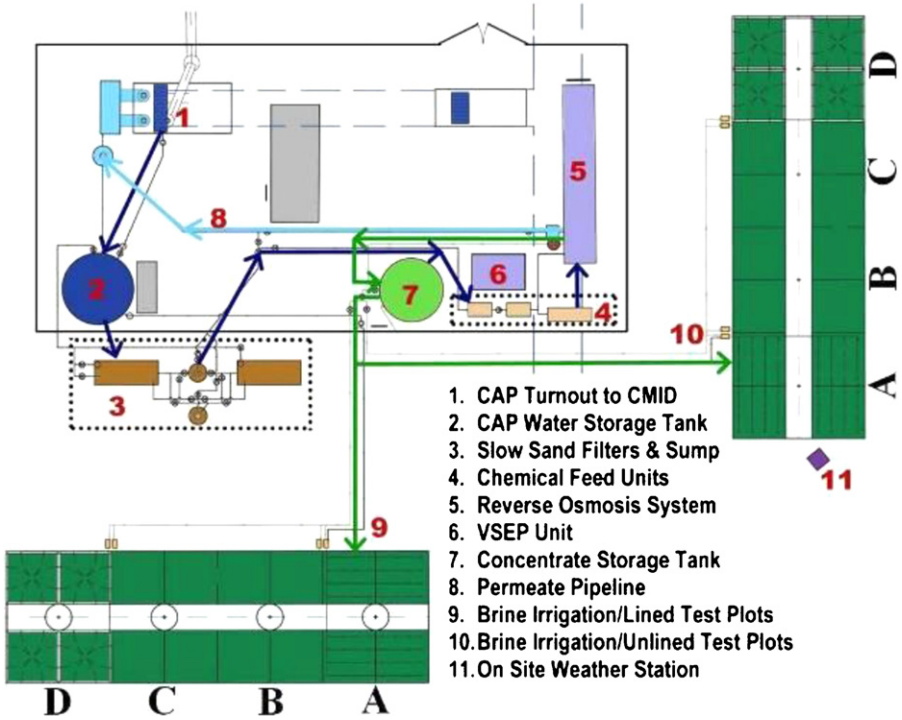


**Fig. 1.** Map of the project site showing where each treatment plot is located as well as the storage tank for the saline effluent (concentrate). A = $ET_o$, B = 1.5$ET_o$, C = ET constant and D = Turf. Turf data was not reported in this paper.

**Table 1**
Experimental design and treatment structure[a].

| Treatment | Experimental design and irrigation regime | Dependent variables |
|---|---|---|
| Lined $ET_o$ | Plants on 1 m centers in four lined, 4 m × 4 m × 2.5 m depth plots; irrigation adjusted daily to match AZMET $ET_o$ – precipitation for previous 24 h. Drainage water collected. | ET, drainage, soil moisture storage, soil moisture profiles, plant growth parameters, WUE |
| Lined 1.5 $ET_o$ | Plants on 1 m centers in four lined, 4 m × 4 m × 2.5 m depth plots; irrigation adjusted daily to match 1.5 × AZMET $ET_o$ – precipitation for previous 24 h. Drainage water collected. | ET, drainage, soil moisture storage, soil moisture profiles, plant growth parameters, WUE |
| Lined Constant Rate $ET_o$ | Plants on 1 m centers in four lined, 4 m × 4 m × 2.5 m depth plots; irrigation applied daily at a constant rate to match mean annual AZMET $ET_o$ – precipitation for the previous year. Drainage water collected. | ET, drainage, soil moisture storage, soil moisture profiles, plant growth parameters, WUE |
| Unlined $ET_o$ | Plants on 1 m centers in four unlined, 4 m × 4 m × 2.5 m depth plots; irrigation adjusted daily to match AZMET $ET_o$ – precipitation for previous 24 h. Drainage water not collected. | Soil moisture profiles, plant growth parameters, WUE |
| Unlined 1.5 $ET_o$ | Plants on 1 m centers in four unlined, 4 m × 4 m × 2.5 m depth plots; irrigation adjusted daily to match 1.5 × AZMET $ET_o$ – precipitation for previous 24 h. Drainage water not collected. | Soil moisture profiles, plant growth parameters, WUE |
| Unlined Constant Rate $ET_o$ | Plants on 1 m centers in four lined, 4 m × 4 m × 2.5 m depth plots; irrigation applied daily at a constant rate to match mean annual AZMET $ET_o$ – precipitation for the previous year. Drainage water not collected. | Soil moisture profiles, plant growth parameters, WUE |

[a] AZMET = Arizona Meteorological Station data; ET = evapotranspiration; $ET_o$ = potential ET calculated from AZMET data; WUE = water use efficiency.

greenhouse-grown *A. lentiformis* plants on 1 m spacing (16 plots per plot) in September 2006 and allowed to grow until October 2009.

### 2.3. Salinity of irrigation water and irrigation procedures

The major cations and anions in CAP inflow water, and the cation content of the RO concentrate, are listed in Table 2. Salts were concentrated 4.5 fold in the RO concentrate compared to the inflow water. Water was applied at 2 a.m. each night to deliver the predetermined fraction of $ET_o$ calculated from the previous day. Water was applied through an above-ground drip irrigation system (Hunter Industries, San Macros, CA) consisting of a storage tank equipped with a 0.6 kW pump, a 2.1 kg $cm^{-2}$ pressure reducer,

**Table 2**
Major cations and anions in Central Arizona Project (CAP) water and RO concentrate from a reverse osmosis pilot treatment plant in Marana, Arizona[a].

| Analyte (mg $L^{-1}$) | CAP | RO concentrate |
|---|---|---|
| $Na^+$ | 102 (0.69) | 462 (8.4) |
| $K^+$ | 5.41 (0.03) | 24.1 (0.48) |
| $Mg^{2+}$ | 30.6 (0.17) | 152 (2.7) |
| $Ca^{2+}$ | 75.2 (0.62) | 367.9 (6.6) |
| $Cl^-$ | 93.6 (0.55) | NA |
| $SO_4^{2-}$ | 256 (2.0) | NA |
| $NO_3^{2-}$ | 0.304 (0.007) | NA |

[a] Data are means and standard errors; sample size was 127 for CAP water and 32 for RO concentrate, representing different collection dates. Only cations were analyzed in RO concentrate. Data are from Jordan et al. (2009).

a 2.5 cm (diameter) strainer-filter, and a 2.5 cm (diameter) schedule 40 PVC distribution system to carry water to plots. Water was distributed to plants through 1.25 cm (diameter) polyvinyl tubes equipped with drip emitters (4 per plant) each delivering 3.8 liters per hour for sufficient time to meet the daily irrigation target. Irrigations were controlled by Hunter ICC 800 PL timers to deliver the correct volume of water based on 1.5 $ET_o$. The actual amount of water delivered to the plots was determined by flow meters, which were installed at the head of the irrigation lines leading to plots. Flow meters measured the total flow to each block of 4 plots making up a treatment.

### 2.4. AZMET meteorological data, calculation of $ET_o$, and irrigation timing

Meteorological data were collected from an on-site, automated Arizona Meteorological (AZMET) station (AZMET, 2010). Meteorological variables obtained as hourly or daily values included temperature ($T$, °C), vapor pressure deficit (VPD, kPa), solar radiation ($R_s$, kJ m$^{-2}$ h$^{-1}$ on an hourly basis and MJ m$^{-2}$ d$^{-1}$ on a daily basis), wind speed (m s$^{-1}$) and direction, precipitation (mm), and reference evaporation ($ET_o$, mm d$^{-1}$). Net radiation ($R_n$) was approximated as $0.77R_s$, based on an albedo value of 0.23 for short wave radiation and assuming outgoing and incoming long wave radiation were equal (Allen et al., 1996). $ET_o$ was calculated in daily time steps by a modified Penman–Montieth equation (ASCE, 2005):

$$ET_o = \frac{0.408\,\Delta R_n + \gamma(900/(T+273))u_2(e_s - e_a)}{\Delta + \gamma(1 + 0.34u_2)} \quad (1)$$

where $ET_o$ is ET of a hypothetical grass reference crop in mm d$^{-1}$; $\Delta$ is the slope of the saturation vapor pressure–temperature curve (kPa °C$^{-1}$); $R_n$ is the calculated net radiation at the top of the canopy (MJ m$^{-2}$ d$^{-1}$); $\gamma$ is the psychrometer constraint (kPa °C$^{-1}$); $T$ is the mean daily air temperature measured 1.5 m above ground level (°C); $u_2$ is the mean daily wind speed measured 2 m above ground level (m s$^{-1}$); $e_s$ is the saturation vapor pressure measured 1.5 m above ground level (kPa); and $e_a$ is the mean actual vapor pressure measured 1.5 m above ground level (kPa).

AZMET data were used to calculate the daily Marana $ET_o$ value to determine the irrigation runtimes in minutes for the *A. lentiformis* plots (described in detail in Jordan et al., 2009). A data logger program was set to start the irrigation treatments each day. Water was applied in a series of 30-min increments with 30 min between irrigation events to allow time for water to infiltrate into the soil. These 30-min cycles continued until the total runtime duration was completed, with the last cycle being a fraction of a half hour. If there was a rain event, rainfall was subtracted from the $ET_o$ value. If the rainfall exceeded the $ET_o$, irrigation was suspended until the amount of daily $ET_o$ caught up to the total of the rainfall.

### 2.5. Soil moisture measurements and water balance calculations

Soil moisture measurements were obtained monthly for each plot with a 503 DR Campbell Nuclear Neutron Hydroprobe (Campbell Pacific Nuclear International, Inc., Martinez, CA). Soil moisture was measured at 0.17 m depth intervals in one thin-walled polyvinyl chloride (5 cm internal diameter) pipe centered in each plot. The hydroprobe was calibrated by obtaining soil samples at specified depths upon coring the access ports and a corresponding neutron probe count at the specified depth after the port was installed (Jordan et al., 2009). Bulk density of soil was measured in random samples taken from plots with a volumetric soil auger and soil moisture was expressed in volumetric units (cm$^3$ cm$^{-3}$). The relationship between soil moisture and counts per minute (cpm) was:

$$\text{Soil Moisture } (\text{cm}^3\,\text{cm}^{-3}) = 2.0 \times 10^{-5}\,\text{cpm} - 0.048, \quad r^2 = 0.55 \quad (2)$$

Water balances could only be calculated for lined plots. ET in each lined plot was estimated with the following mass balance equation:

$$ET = P + I - D + \Delta S \quad (3)$$

where ET = monthly crop evapotranspiration, $P$ = precipitation determined from the meteorological station located on site; $I$ = irrigation; $D$ = drainage; and $\Delta S$ = change in soil water storage during the study period. Drainage water was collected in 16 buckets placed in the sump under the drain line from each plot. Samples of drainage water were analyzed for electrical conductivity (EC) in the laboratory with an EC meter (Markson Scientific, Inc., Henderson, NC) calibrated with NaCl standards. Water use efficiency (WUE) was calculated for both lined and unlined plots as the kg of dry biomass produced per m$^3$ of water applied (irrigation plus precipitation).

### 2.6. Soil paste extracts

EC of 1:1 (gram dry soil to mL water) soil extracts were measured in April 2008 and October 2009, encompassing two complete growing seasons. Only lined plots were measured in April 2008, while both lined and unlined were measured in October 2009. Two randomly selected plots from each treatment were measured.

### 2.7. Sampling plant biomass

Plant biomass was sampled in each plot in October 2009 and separated into woody material, stems, and leaves plus fruits. Fruits were still immature and were not separated from leaves. Stems were the small stems attached to the leaves less than 5 mm in diameter. The woody material refers to the branches and trunk of the plant. Annual production of stems was estimated by dividing final stem weights by three, since stem biomass had accumulated over three growing seasons. Leaves and fruits represented the results of a single growing season, since leaves are dropped at the end of each growing season for this species (2009).

### 2.8. Statistical analyses

Statistical analyses were carried out with Systat 11 software (Systat Software Inc, Point Richmond, CA). Data for each dependent variable were first analyzed for normal distribution by the Shapiro–Wilks Normality Text and for equality of variances among treatments by the Levene Test. Data meeting these assumptions were tested for treatment differences by analysis of variance (ANOVA). One-way, two-way or three-way analyses were used depending on the categorical variables affecting each dependent variable (see Section 3). Statistics reported for each test are $F$-values, $P$-values, and df for treatments and error. When results of ANOVAs were significant, means were separated with Tukey's Test. Data not meeting the assumptions were tested by the non-parametric Kruskal–Wallis Ranked Means Test. When results of these tests were significant, means were separated by the non-parametric Freidman Test.

**Table 3**
Summary of water use and biomass production by *Atriplex lentiformis* grown on R.O. effluent in Marana, AZ, June 2007–October 2009 (885 days)[a].

| Irrigation treatment: | Lined plots | | | Unlined plots | | |
|---|---|---|---|---|---|---|
| | 1.0 $ET_o$ | 1.5 $ET_o$ | Constant-rate $ET_o$ | 1.0 $ET_o$ | 1.5 $ET_o$ | Constant-rate $ET_o$ |
| $ET_o$ (mm) | 5334 | 5334 | 5334 | 5334 | 5334 | 5334 |
| Rain (mm) | 355 | 355 | 355 | 355 | 355 | 355 |
| Applied R.O. $H_2O$ (mm) | 4128 | 6309 | 3931 | 4221 | 5595 | 5845 |
| ET (mm) (SE) | 4897ab (30) | 5742a (524) | 3742b (369) | – | – | – |
| Drainage (mm) (SEM) | 0a (0) | 938b (494) | 534b (352) | – | – | – |
| Soil storage (mm) (SE) | −59ns (30) | −16ns (42) | 9ns (43) | – | – | – |
| Drainage (% of applied) | 0 | 14.0 | 12.5 | – | – | – |
| $ET/ET_o$ | 0.91 | 1.07 | 0.70 | – | – | – |
| Biomass ($kg\,m^{-2}$) (SE) | 7.33a (0.42) | 6.23b (1.81) | 7.20a (0.48) | 7.73a (1.17) | 4.70b (0.30) | 7.83a (1.59) |
| WUE ($kg\,m^{-3}$ $H_2O$) (SE) | 1.64a (0.094) | 0.93b (0.046) | 1.67a (0.113) | 1.59a (0.142) | 0.91b (0.067) | 1.14ab (0.231) |

[a] $ET/ET_o$ is ET expressed as a fraction of $ET_o$. WUE = water use efficiency in kg biomass per cubic meter of water added. SE = standard error. Means followed by different letters within a row are significantly different at $P < 0.05$ by Tukey's Means test.

## 3. Results

### 3.1. Cumulative water use and biomass production over the study

Table 3 gives water application rates, water use parameters, ET values, and biomass production in lined and unlined plots from 2007 to 2009. Cumulative $ET_o$ over the experiment was 5334 mm (6.02 mm $d^{-1}$ or 2197 mm $year^{-1}$) while precipitation was 355 mm (6.7% of $ET_o$). $ET_o$ at this site was about 10% higher than at the former Marana AZMET station (AZMET, 2010), probably due to advection from surrounding bare fields. Water application rates (irrigation + precipitation) generally fell short of target rates, averaging 87% of target rates across treatments. However, the plants in the Unlined Constant Rate $ET_o$ treatment were over-irrigated by 16%. Although irrigation rates were adjusted daily based on AZMET data, the accuracy of water delivery was limited by unequal flow rates through the drip emitters, which were subject to plugging and reduced flows due to buildup of salts around the emitters.

Treatment differences for ET and drainage in the lined plots were tested by the non-parametric Kruskal–Wallis test because the data were not normally distributed and the resulting variances were unequal among treatments. Both ET ($P = 0.13$, KW Statistic = 7.35, df = 2) and drainage ($P = 0.048$, KW Statistic = 6.08, df = 2) differed by treatment. Expressed as a fraction of $ET_o$ ($ET/ET_o$), ET rates ranged from 0.70 for the Lined Constant Rate $ET_o$ treatment, to 1.07 for the Lined 1.5 $ET_o$ treatment. While plants in the $ET_o$ treatment did not produce drainage water over the study, 1.5 $ET_o$ and Constant Rate $ET_o$ lost 14.5% and 12.5% of applied water as drainage, respectively. Differences in soil moisture storage over the study were small compared to application rates and were non-significant among treatments in the lined plots ($F = 0.785$, $P = 0.485$, df = 2, 9 by one-way ANOVA). Biomass production and WUE were analyzed by two-way ANOVA with Lined/Unlined and Irrigation Treatment as categorical variables. The effect of Lined versus Unlined plots were not significant either for biomass ($F = 1.16$, $P = 0.336$, df = 1, 18) or WUE ($F = 0.358$, $P = 0.557$, df = 1, 18). However, plots differed by irrigation treatment both for biomass ($F = 4.58$, $P = 0.025$, df = 2, 18) and for WUE ($F = 13.9$, $P < 0.000$, df = 2, 18). The $ET_o$ treatments produced higher amounts of biomass and had higher WUE than plants in the 1.5 $ET_o$ treatments (Table 3).

### 3.2. Time course of water use over the study

Fig. 2A shows the time course of $ET_o$ and precipitation over the study, while Fig. 2B–D show monthly values of ET, drainage, and soil storage of moisture in the lined plots. Peak summer $ET_o$ rates were 8–10 mm $d^{-1}$ while winter rates were as low as 2 mm $d^{-1}$. ET rates in all treatments tended to be higher the first summer (2007) than in 2008 and 2009. Plots in the Lined $ET_o$ treatment had peak rates of 8–9 mm $d^{-1}$. Plants in the 1.5 $ET_o$ treatment had ET rates as high as 15 mm $d^{-1}$ during summers; but winter ET rates were under 2 mm $d^{-1}$, and plants in this treatment produced drainage during the winters of 2008 and 2009. The Constant Rate $ET_o$ treatment also produced drainage during winter; hence, our hypothesis that water applied in winter could be stored in the soil and utilized in summer was not completely supported. Summer ET rates in Constant Rate $ET_o$ treatment were only 6 mm $d^{-1}$, indicating that plants were under-irrigated in summer; and the drainage data showed they were over-irrigated in winter. Nevertheless, plants in this treatment were able to discharge 87% of the applied water in ET. Except for several brief periods when the irrigation system malfunctioned (dips in the soil storage plots in Fig. 2B–D), changes in soil moisture storage were small over the study.

### 3.3. Soil moisture profiles

Soil moisture differed significantly for Lined versus Unlined ($F = 198$, $P < 0.000$, df = 1, 167) and also among Irrigation Treatment ($F = 56.8$, $P < 0.000$, df = 2, 167). The interaction term (Lined/Unlined × Irrigation Treatment) was also significant ($F = 18.3$, $P < 0.001$, df = 2, 167). For the lined plots, soil moisture was highest in the 1.5 $ET_o$ plots, lowest in the $ET_o$ plots, and intermediate in the Constant Rate $ET_o$ plots, whereas the highest soil moisture in the unlined plots was in the Constant Rate $ET_o$ plots (Table 4). Fig. 3 shows monthly soil moisture values over the study. Unlined plots had lower mean soil moisture levels than lined plots, and the 1.5 $ET_o$ treatments had higher soil moisture content than other treatments. Soil moisture levels followed a distinct seasonal pattern in the Constant Rate $ET_o$ plots, with values 50% higher in winter than in summer. The other treatments showed the same pattern but to a lesser extent.

Soil moisture levels at different depths, averaged over months, did not differ significantly by soil depth across treatments in the first 2.5 m of soil, which was common to both lined and unlined plots ($F = 0.89$, $P = 0.379$, df = 6, 12). However, during a dry-down event in July 2009, patterns of soil moisture depletion did dif-

**Table 4**
Mean soil moisture contents in the soil profile of irrigated *Atriplex lentiformis* plots across soil depths and sample dates, 2007–2009[a].

| Treatment | Mean soil moisture content ($cm^3\,cm^{-1}$) | Std. error mean |
|---|---|---|
| Lined $ET_o$ | 0.118a | 0.003 |
| Lined 1.5 $ET_o$ | 0.162b | 0.003 |
| Lined Constant Rate $ET_o$ | 0.137c | 0.004 |
| Unlined $ET_o$ | 0.086d | 0.002 |
| Unlined 1.5 $ET_o$ | 0.105e | 0.002 |
| Unlined Constant Rate $ET_o$ | 0.118a | 0.004 |

[a] Means were separated by Tukey's Test.

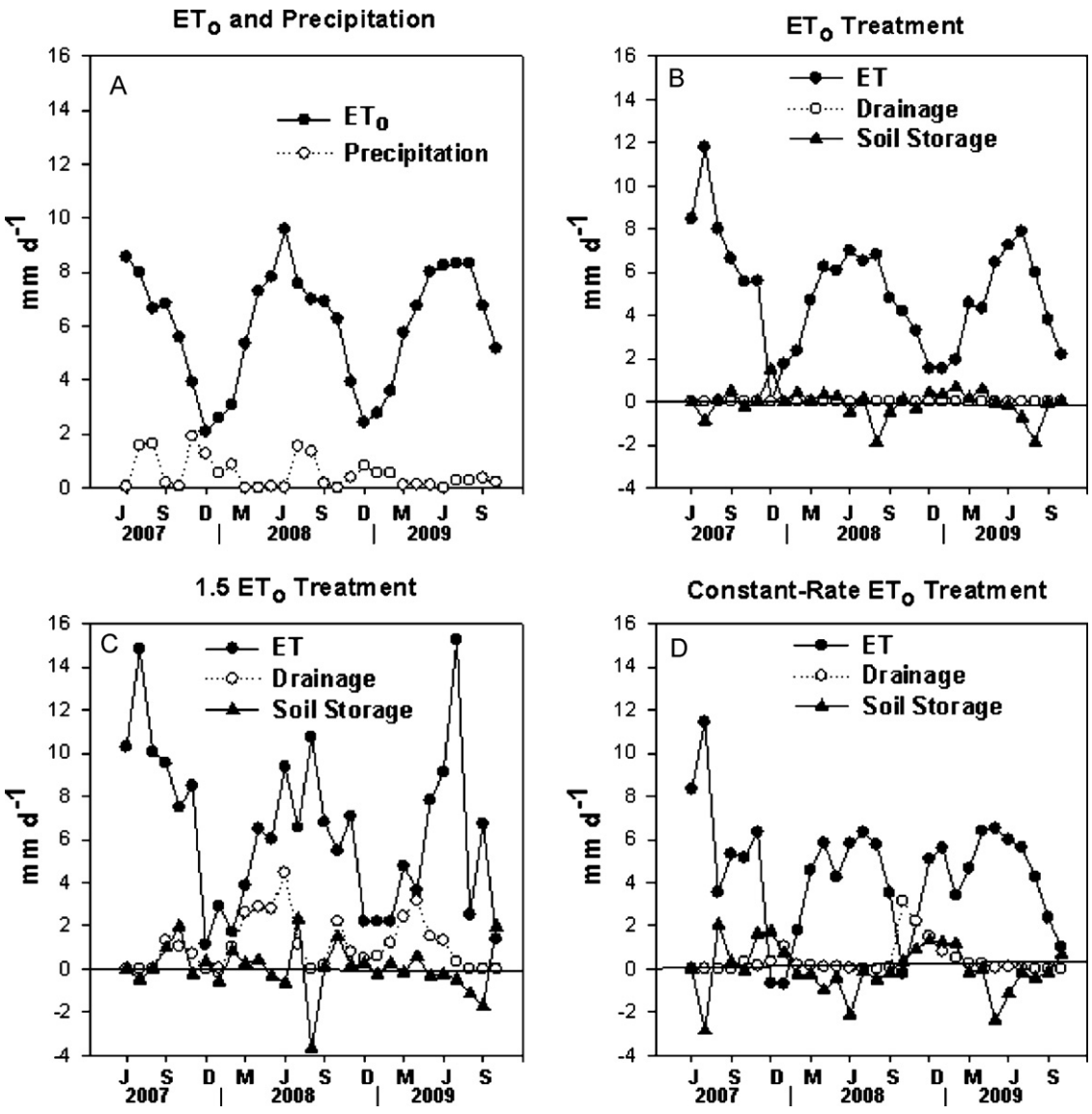


**Fig. 2.** Time course of $ET_o$ and precipitation (A), and ET, drainage and soil storage in lined plots planted with *Atriplex lentiformis* and receiving irrigation rates of $ET_o$ (B), 1.5 $ET_o$ (C) adjusted daily, or $ET_o$ presented at a constant rate over the year (D) in Marana, Arizona. Data points for B–D are monthly treatment means.

fer by soil depth, and could be used to infer rooting patterns in the plots (Fig. 4). Moisture depletion occurred in the top 1.5 m of soil, and most of the depletion was within the top meter of soil.

### 3.4. Salinity of irrigation water, drainage and soils

EC of irrigation and drainage waters differed significantly ($F = 78.7$, $P < 0.001$, df = 2, 61), with irrigation water EC (mean = 3.75 dS m$^{-1}$, std. error = 0.16) lower than drainage EC from the 1.5 $ET_o$ (mean = 6.69 dS m$^{-1}$, std. error = 0.20) or Constant Rate $ET_o$ (mean = 6.08 dS m$^{-1}$, std. error = 0.20), which did not differ significantly from each other by Tukey's Test ($P > 0.05$). Time course plots (Fig. 5) showed that irrigation EC started out low in 2007, due to the sporadic availability of RO concentrate, then was fairly constant for 2008 and 2009. Drainage EC peaked in 2008 then declined somewhat in 2009, and over the study was 1.7 times irrigation water EC. This compares to an expected value of 7.0 based on a drainage fraction of 0.14, and assuming that leaching of salts was completely efficient. The results indicate that drainage water originated largely from channeling and preferential flow through plots rather than uniform leaching.

For April 2008, data, plot soil EC differed by Soil Depth ($F = 6.67$, $P < 0.001$, df = 5, 30) but not Irrigation Treatment ($F = 0.51$, $P = 0.605$, df = 2, 30). October 2009 soil EC values differed by soil depth ($F = 5.49$, $P = 0.001$, df = 5, 35) but not by Lined/Unlined ($F = 0.00$, $P = 0.984$, df = 1, 35) or Irrigation Treatment ($F = 0.19$, $P = 0.827$, df = 2, 35). Soil EC was higher in April 2008 (mean = 2.73 dS m$^{-1}$, std. error = 157) than in October 2009 (mean = 1.69 dS m$^{-1}$, std. error = 130) ($P < 0.001$). Soil EC was highest near the surface but stabilized at 0.5 m and below (Fig. 6A). Potassium was nearly constant across depths, whereas sodium, calcium, and magnesium followed the same trend as soil EC (Fig. 6B).

### 3.5. Yield and nutritional value of leaves, stems and seeds

Dry matter production of leaves, fruits, stems, and woody material varied by treatment. Leaves and fruits accounted for about 30% of total biomass production, which ranged from 15 to

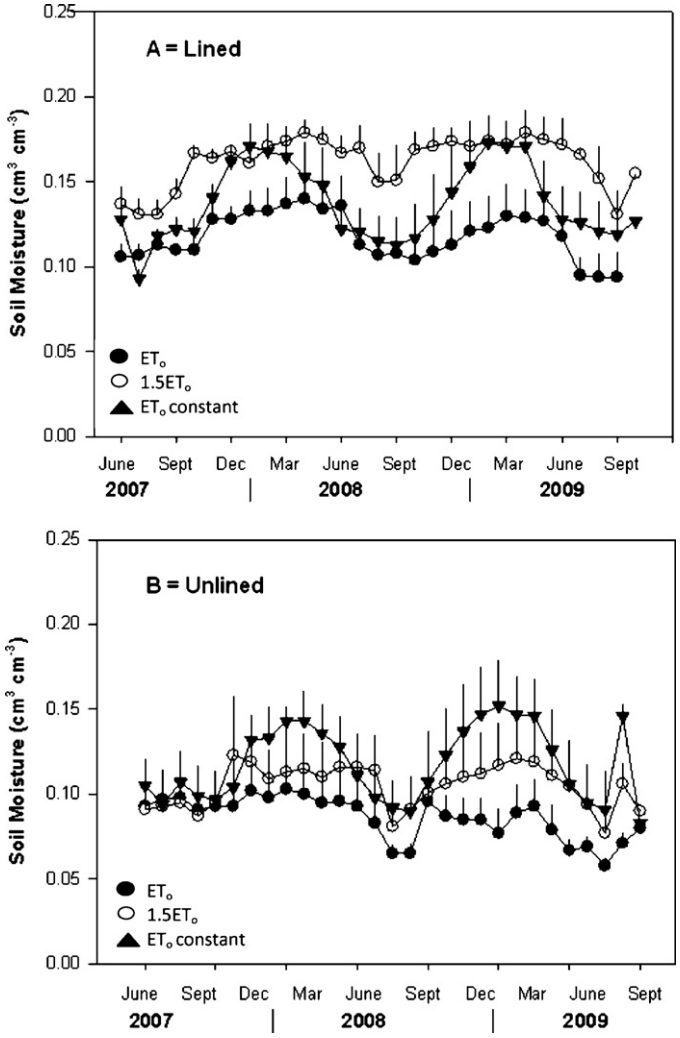


**Fig. 3.** Time course of soil moisture levels in lined (A) and unlined (B) plots planted with *Atriplex lentiformis* and receiving irrigation rates of $ET_o$ (closed circles) or 1.5 $ET_o$ (open circles) adjusted daily, or $ET_o$ presented at a constant rate over the year (closed triangles) in Marana, Arizona. Error bars are standard errors shown only in one direction to avoid overlap.

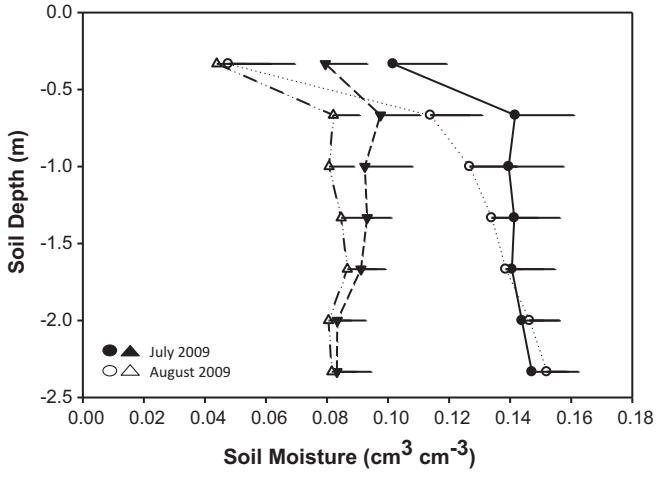


**Fig. 4.** Soil moisture depletion between July 2009 (closed symbols) and August 2009 (open symbols) during a 30 day dry-down period when irrigation was suspended. Circles show lined plots and triangles show unlined plots; error bars are standard errors shown in only one direction to avoid overlap.

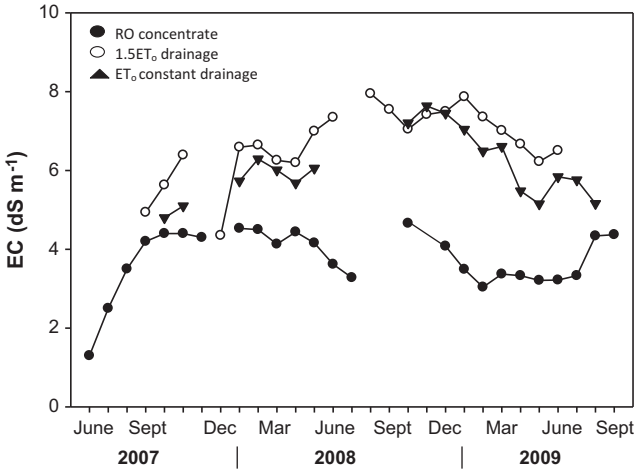


**Fig. 5.** Electrical conductivity (EC) of RO concentrate used for irrigation (closed circles) and of drainage from the 1.5 $ET_o$ treatment (open circles) and $ET_o$ constant rate (closed triangles) treatment lined plots planted with *Atriplex lentiformis* in Marana, Arizona. The gap RO concentrate data from July to October 2008, was due to lack of measurements. Gaps in drainage EC are because drainage was intermittent over the experiment.

22 t $ha^{-1}$ $year^{-1}$ among treatments (Fig. 7). As noted in Table 3, primary production was lower in the 1.5 $ET_o$ plots than in the other treatments.

Plants were dioecious, with a ratio of males to females of about 1:1. Fruits for analyses were sampled in November when fully ripe, from 6 female plants (1 from each treatment) with a 0.25 m × 0.25 m quadrant placed over a portion of the canopy. Mean seed yield was estimated at 7.4 t $ha^{-1}$ (std. error = 1.05) based on these samples. Nutritional content of plant parts are in Table 5. Leaves and seeds were higher in crude protein (13–17%) than stems (3%). Digestible carbohydrates were high in all fractions (33–36%), but acid detergent fiber, the most slowly digested fraction, was high in stems but low in leaves and fruits. Ash content was higher in leaves (28%) than fruits (18%) or stems (8.5%). Fat was low in all fractions (<1%). Contents of individual minerals were adequate for animal nutrition, but sodium, which can present problems for ruminants, was high in leaves and fruits (5.5%).

## 4. Discussion

### 4.1. Irrigation strategies for use of industrial brines

We were interested in the disposal of brine with regard to how much water *A. lentiformis* could consume and whether it could be presented on a constant delivery schedule rather than as a function of daily $ET_o$. Results over the first growing season indicated that *A. lentiformis* could be irrigated at 1.5 $ET_o$, producing high yields and minimal drainage (Jordan et al., 2009). However, over three years, this treatment had lower yield and WUE compared to plants in the $ET_o$ treatment, and produced drainage during winter in 2008 and 2009. Soil moisture levels were higher in this treatment compared to other treatments and could have been beyond the optimal limit for this desert plant. $ET/ET_o$ for this treatment was 1.07, compared to 0.91 for the $ET_o$ treatment, despite the 30% higher irrigation rate. On balance, presenting water at the rate of $ET_o$ appears to be the optimal irrigation strategy for this species. At this site, the irrigation volume could be as high as 2.0 m $year^{-1}$. The Constant Rate $ET_o$ treatment produced some winter drainage and had $ET/ET_o$ of 0.70, but produced high yields and WUE. The 12.5% drainage fraction from this treatment is not necessarily a disadvantage, as some drainage is ultimately needed to control salt levels in the rooting

**Table 5**
Proximate analyses of stems, leaves, and fruits from *Atriplex lentiformis* grown on RO effluent in Marana, Arizona[a].

| | Stems | Leaves | Fruits |
|---|---|---|---|
| Crude protein (%) | 3.01 (0.75) | 12.8 (1.85) | 17.0 (4.80) |
| Acid detergent fiber (%) | 53.0 (2.80) | 15.8 (1.44) | 16.4 (2.70) |
| Crude fiber (%) | 42.5 (2.34) | 12.7 (1.15) | 13.2 (2.16) |
| Crude carbohydrates (%) | 45.3 (0.40) | 44.0 (0.74) | 41.4 (1.67) |
| Digestible carbohydrates (%) | 35.8 (0.32) | 35.8 (1.90) | 32.7 (1.31) |
| Fat (%) | 0.78 (0.08) | 0.47 (0.16) | 0.62 (0.06) |
| Ash (%) | 8.50 (1.34) | 28.2 (1.62) | 17.8 (1.36) |
| Phosphorous (%) | 0.04 (0.00) | 0.14 (0.02) | 0.24 (0.06) |
| Calcium (%) | 1.58 (0.33) | 2.27 (0.41) | 2.03 (0.37) |
| Magnesium (%) | 0/34(0.03) | 1.44 (0.15) | 1.06 (0.02) |
| Potassium (%) | 1.09 (0.30) | 3.32 (1.84) | 3.69 (1.00) |
| Sodium (%) | 0.95 (0.27) | 5.75 (0.45) | 5.46 (0.19) |
| Copper (ppm) | 8(1) | 11(2) | 20(4) |
| Iron (ppm) | 141(5) | 204(47) | 235(82) |
| Zinc (ppm) | 22(3) | 46(20) | 58(12) |
| Manganese (ppm) | 35(5) | 194(87) | 137(57) |
| Digestible energy (Mcal $kg^{-1}$) | 2.65 (0.02) | 2.30 (0.09) | 2.31 (0.04) |
| Metabolizable energy (kcal $kg^{-1}$) | 2.19 (0.04) | 1.88 (0.08) | 1.89 (0.04) |

[a] Values are means and standard errors of three determinations per entry.

zone. Hence, this could also be a viable irrigation strategy that could allow disposal of concentrate at the same rate as it is produced.

### 4.2. Comparison of lined and unlined plots

We were concerned that growing plants in lysimeters could restrict rooting depth and drainage, leading to results that might not apply to open-field plantings. However, biomass production and WUE were comparable in lined and unlined plots. Hence, the results from lysimeter plots can be extrapolated to field planting. Furthermore, $ET/ET_o$ values were comparable to rates from open-field crops such as alfalfa in this irrigation district (AREC, 2008), indicating that advection effects due to the limited size of the planting did not artificially increase ET. However, bare soil around the site appeared to increase $ET_o$ by about 10% compared to values determined at vegetated sites within the district (AZMET, 2010).

### 4.3. Yield and nutritional value as forage

We were interested in comparing yield and utility of halophytes to conventional forages. Annual biomass yields of *A. lentiformis* both in Year One (Jordan et al., 2009) and Year Three were in the range of 15–22 metric tons $ha^{-1}$, similar to alfalfa (20.3 t $ha^{-1}$), Sudan grass (3.6 t $ha^{-1}$), and other high-yield forages (AREC, 2008). These yields were also similar to other wood biomass crops (13.8–21.8 t $ha^{-1}$) (Striker et al., 2000; Webber and Bledsoe, 2002). WUE was also high compared to conventional forages, as *A. lentiformis* is a C4 species (Osmond et al., 1980).

The utility of *A. lentiformis* lies in its potential as a forage crop. Stems were low in mineral content (8.50%) and sodium (0.95%), which can reduce the feed value of forage crops for ruminants. However, the stems were high in acid-detergent fiber (53.0%), which is difficult for ruminants to digest compared to neutral-detergent fiber, and low in protein. Furthermore, the fiber fraction made up nearly the entire total carbohydrate fraction, indicating that levels of more-digestible starches and soluble carbohydrates were very low. By contrast, leaves and fruits had relatively high mineral (28.2% leaves and 17.8% fruits) and sodium contents (5.75% leaves and 5.46% fruits), which can limit the proportions that can be used in animal diets. Fruits and seeds had protein levels within the range of alfalfa and other high quality forages, and relatively low levels of acid-detergent fibers (Table 6). Furthermore, crude fiber made up only a third of the carbohydrate fraction, indicating high levels of starch and soluble carbohydrates.

The results indicate that a cropping system for forage should maximize leaf and fruit production over woody stem material. After three years growth, woody material accounted for most of the biomass. However, leaves predominate over stems in the first growing season for *Atriplex* spp. (Bauder et al., 2008; Glenn et al., 1998; Swingle et al., 1996; Watson et al., 1987; Watson and O'Leary, 1993). Hence, the optimal cropping system should be designed either to grow *A. lentiformis* from seed as an annual forage crop, or to develop methods of partially harvesting leaves and fruits by cutting plants near the ground and allowing them to regrow on an annual basis until the bases become too woody to support good leaf production (Watson and O'Leary, 1993).

Feeding trials with *Atriplex* spp. have been successful when feed formulations are adjusted to meet animal nutritional behavior (Guevara et al., 2005; Norman et al., 2008; Swingle et al., 1996). For example, Swingle et al. (1996) reported that halophytes containing 30–40% mineral content could be added at 30% of the total diet for sheep, and could meet the forage requirement in sheep fattening diets with no reduction in meat quality or animal growth rates. However, *Atriplex* can contain anti-nutritional compounds such as saponins, non-protein nitrogen sources that can be difficult to digest, and excess sodium that limits their value as green browse

**Table 6**
Comparison of percent crude protein (CP), acid detergent fiber (SDF), Na, K and acid detergent lignin (ADL) between different forage supplements[a].

| Item | CP | Ash | ADF | Na | K | ADL |
|---|---|---|---|---|---|---|
| *Cynodon* hay | 12.3 | 8.8 | 26.1 | 0.1 | 1.5 | 6.4 |
| *Atriplex lentiformis* | 12.16 | 20.66 | 27.63 | 4.20 | 1.56 | – |
| *Atriplex nummularia* | 19.78 | 26.25 | 11.46 | 5.47 | 4.49 | – |
| *Medicago sativa* L. (alfalfa) | 17.5 | 11.5 | 28.4 | 0.009 | 2.91 | 7.9 |
| *Hibiscus cannabinus* L. (kenaf) | 11.0 | 11.8 | 41.2 | – | – | 10.5 |
| *Sorghum* spp. (Sudan grass) | 10.8 | 7.64 | 41.6 | 0.010 | 1.87 | 4.6 |

[a] Data for *Atriplex lentiformis* was an average of leaves, stems, and fruits for a plant in $ET_o$ treatment. *Cynodon* hay values were from Swingle et al. (1996); *A. nummularia* values were from Glenn et al. (1998); alfalfa and kenaf values were from Swingle et al. (1978); Sorghum values and Na and K values for kenaf were from Dann et al. (2008).

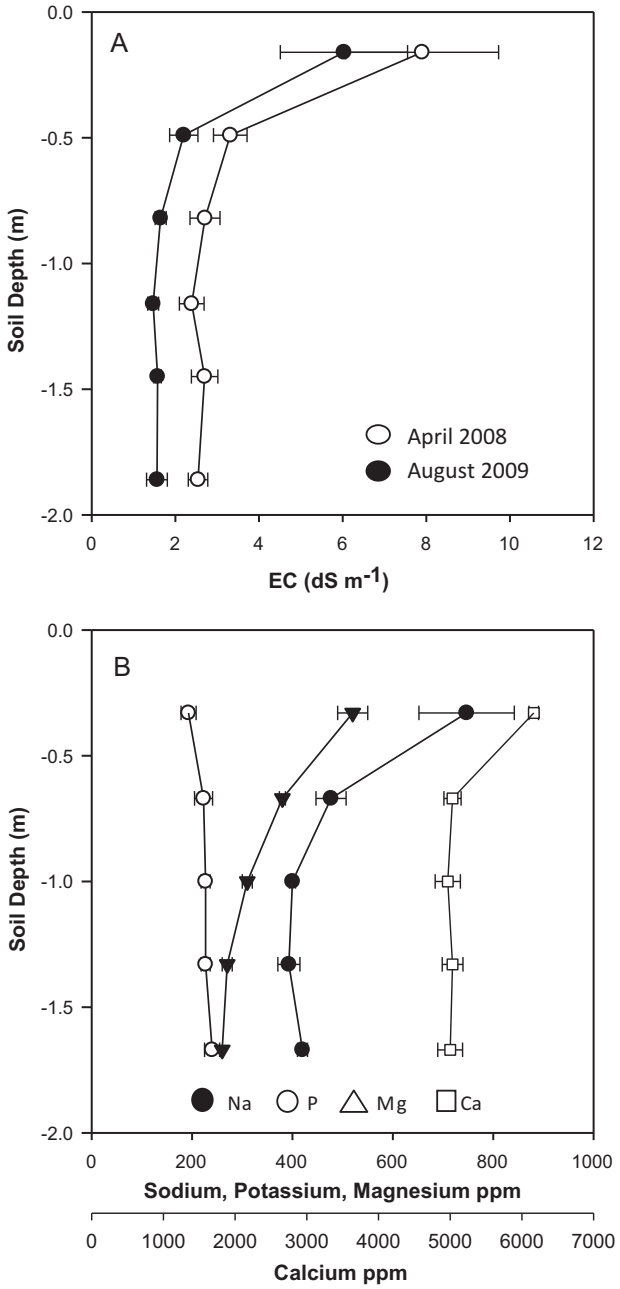


**Fig. 6.** Electrical conductivity (EC) of 1:1 soil extracts by depth averaged over all plots in April 2008 (open circles) and August 2009 (closed circles) (A); and concentration of individual cations in soils sampled in August 2009 (B). Error bars are standard errors.

plants (Masters et al., 2007; Rogers et al., 2005). The main value of *A. lentiformis* is probably as a mineral and protein supplement and forage replacement in feedlot diets for ruminants. Detailed feeding trials are needed to discover the best niche for *A. lentiformis* in commercial animal diets.

### 4.4. Sustainability of halophyte production on saline water

Over three years, the plots approached equilibrium with respect to soil salinity, since soil EC did not increase over the final growing season. Soil EC was high at the surface but reached stable values of 2–4 dS $m^{-1}$ deeper in the profile, indicating efficient downward leaching of salts. These values for 1:1 soil:water extracts can be expressed in terms of likely soil solution salinity assuming that soil moisture at field capacity is 0.15 $cm^3$ $cm^{-3}$ and that g $L^{-1}$ TDS = 0.64 dS $m^{-1}$ (Jordan et al., 2009). Calculated soil moisture salinities at the 0.5–2.5 m depths are in the range of 8.5–17.0 g $L^{-1}$, near the optimal salinities for growth of *A. lentiformis* (Miyamoto et al., 1996). Based on an irrigation salinity of 3 g $L^{-1}$, the leaching fractions required to maintain soil salinity at 17.0 g $L^{-1}$ would be 0.18, within the range produced in the two treatments that produced drainage. Ultimately, the $ET_o$ treatment should also produce drainage as it reaches equilibrium with respect to the salt tolerance limit of the plant and the salinity of the water at the bottom of the root zone.

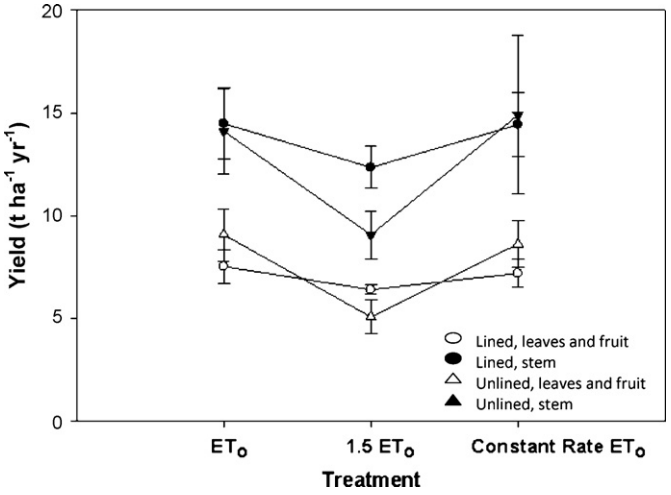


**Fig. 7.** Projected annual yield of *Atriplex lentiformis* grown in plots in Marana, Arizona showing leaves plus fruits (open symbols) and stem material (closed symbols) for lined (circles) and unlined (triangles) plots. Error bars are standard errors.

All methods of brine disposal are problematic with regard to a number of environmental issues. The use of saline water in agriculture is controversial due to the possibility of contaminating ground water supplies (Qadir and Oster, 2004; Riley et al., 1997), but has advantages over other methods of brine disposal. Agricultural drainage can become a hazard to wildlife when discharged into wetlands, evaporation ponds or reservoirs (Hamilton, 2004). Furthermore, evaporation ponds are expensive compared to reuse of saline water for crop production (Arnal et al., 2005; Jordan et al., 2009; Riley et al., 1997). Halophytes such as *A. lentiformis* have the advantage of requiring low leaching fractions due to their high salt tolerance, thereby minimizing the downward movement of salts.

The practicality and sustainability of irrigating with saline water are ultimately site specific and involve economic, agronomic, and hydrological considerations. At our study site, potable water supplies are found at depths of 100 m or greater and are separated from agricultural return-flow aquifers by confining layers (Riley et al., 1997). Furthermore, large amounts of salts are already discharged below the root zone of crops in the irrigation district using conventional water supplies (Gelt et al., 1999). Saline irrigation of halophyte crops can be managed through the use of higher irrigation volumes to ensure that salt accumulation in the soil is below the plant root zone but above any usable aquifer. Hence, irrigation of *A. lentiformis* and other halophytes appears to be an attractive beneficial use of saline water at this and similar locations in arid zone irrigation districts.

## 5. Conclusion

Based on this study, the optimal irrigation strategy for *A. lentiformis* would be $ET_o$ either presented as a function of daily $ET_o$, or with reduced efficiency as a constant rate based on annual

$ET_o$. Based on proximate analyses, *A. lentiformis* met the requirements for a supplement feed ingredient livestock, but animal feeding trials are needed to confirm this. Over the long term, irrigation of *A. lentiformis* can be projected to be a sustainable practice, with drainage volumes of about 12% achieved at equilibrium.

## References


Allen, R., Smith, M., Pruitt, W., Pereira, L., 1996. Modifications to the FAO crop coefficient approach. In: Proceedings of the ASAE International Conference on Evapotranspiration and Irrigation Scheduling , San Antonio, TX, pp. 124–132.

AREC, 2008. Arizona Crop Budgets, Pima County, http://ag.arizona.edu/arec/ext/budgets/Pima-map.html.

Arnal, J., Sancho, M., Iborra, I., Gozalvez, J., Santefe, A., Lora, J., 2005. Concentration of brines from RO desalination plants by natural evaporation. Desalination 182, 435–439.

ASCE, 2005. In: Allen, R., Walters, I., Elliot, T., Howell, D., Itenfisu, D., Jensen, M. (Eds.), The ASCE Standardized Reference Evapotranspiration Equation. ASCE, Reston, VA, http://www.kimberly.uidaho.edu/water/asceewri/ascestzdetmain2005.pdf.

Ayars, J.E., Benes, S., Basinal, L., Jacobsen, T., 2005. Drainage water. In: Ayars, J., Jacobsen, T., Basinal, L. (Eds.), A Technical Advisor's Manual. Managing Agricultural Irrigation Drainage Water. California State Water Resources Control Board, Fresno, CA, pp. 4-1–4-4, Chapter 4.

Ayars, J., Christen, E., Sooper, R., Meyer, W., 2006. The resource potential of in-situ shallow ground water use in irrigated agriculture: a review. Irrig. Sci. 24, 147–160.

Ayars, J., Schoneman, R., 2006. Irrigating field crops in the presence of saline groundwater. Irrig. Drain. 55, 265–279.

AZMET, 2010. The Arizona Meteorological Network. http://cals.arizona.edu/azmet/, last visited June, 2010.

Bauder, J., Browning, L., Phelps, S., Kirkpatrick, A., 2008. Biomass production, forage quality, and cation uptake of Quail bush, fourwing saltbush, and seaside barley irrigated with moderately saline-sodic water. Commun. Soil Sci. Plant Anal. 39, 2009–2031.

Bradford, D.F., Smith, L.A., Drezner, D.S., Schoemaker, J.D., 1991. Minimizing contamination hazards to waterbirds using agricultural drainage evaporation ponds. Environ. Manage. 15, 785–795.

Browning, L., Bauder, J., Phelps, S., 2006. Effect of irrigation water salinity and sodicity and water table position on water table chemistry beneath *Atriplex lentiformis* and *Hordeum marinum*. Arid Land Res. Manage. 20, 101–115.

Cook, E., Woodhouse, C., Eaking, C., Meko, D., Stahle, D., 2004. Long term aridity changes in the western United States. Science 306, 1015–1018.

Dann, H., Grant, R., Cotanch, K., Thomas, E., Ballard, C., Rice, R., 2008. Comparison of brown midrib sorghum-sudangrass with corn silage on lactational performance and nutrient digestibility in Holstein dairy cows. J. Dairy Sci. 91, 663–672.

Flowers, T., Colmer, T., 2008. Salinity tolerance in halophytes. New Phytol. 179, 903–905, doi:10.1111/j.1469-8137.2008.0251.x.

Gelt, J., Henderson, J., Seasholes, K., Tellman, B., Woodard, G., Carpenter, K., Hudson, C., Sherif, S., 1999. Water in the Tucson Area: Seeking Sustainability. Water Resources Research Center, College of Agriculture, University of Arizona, Tucson, AZ.

Gerhart, V., Kane, R., Glenn, E., 2006. Recycling industrial saline wastewater for landscape irrigation in a desert urban area. J. Arid Environ. 67, 473–486.

Glenn, E., Brown, J., Blumwald, E., 1999. Salt tolerance and crop potential of halophytes. Crit. Rev. Plant Sci. 18, 227–255.

Glenn, E., Mckeon, C., Gerhart, V., Nalger, P., 2009. Deficit irrigation of a landscape halophyte for reuse of saline water in a desert city. Landscape Urban Plan. 89, 57–64.

Glenn, E., Miyamoto, S., Moore, D., Brown, J., Thompson, T., Brown, P., 1997. Water requirements for cultivating *Salicornia bigelovii* Torr. with seawater on sand in a coastal desert environment. J. Arid Environ. 36, 711–730.

Glenn, E., O'Leary, J., 1985. Productivity and irrigation requirements of halophytes grown with seawater in the Sonoran Desert. J. Arid Environ. 9, 81–91.

Glenn, E., Tanner, R., Miyamoto, S., Fitzsimmons, K., Boyer, J., 1998. Water use, productivity and forage quality of the halophyte *Atriplex nummularia* grown on saline waste water in a desert environment. J. Arid Environ. 38, 45–62.

Grattan, S., Grieve, C., Poss, J., Robinson, P., Suarez, D., Benes, S., 2004. Evaluation of salt-tolerant forages for sequential water reuse systems. III. Potential implications for ruminant mineral nutrition. Agric. Water Manage. 70, 137–150.

Grattan, S., Benes, S., Peters, D., Diaz, F., 2008. Feasibility of irrigating Pickleweed (*Salicornia bigelovii* Torr) with hyper-saline drainage water. J. Environ. Qual. 37, S-149–S-156.

Grieve, C., Poss, J., Grattan, S., Suarez, D., Benes, S., Robinson, P., 2004. Evaluation of salt-tolerant forages for sequential water reuse systems. II. Plant-ion relations. Agric. Water Manage. 70, 121–136.

Guevara, J., Allegretti, L., Paez, J., Estevez, O., Le Houérou, H., Colomer, J., 2005. Yield, nutritional value, and economic benefits of *Atriplex nummularia* Lindl. plantation in marginal dryland areas for conventional forage crops. Arid Land Res. Manage. 19, 327–340.

Gupta, G., Arya, R., 1995. Performance of *Atriplex lentiformis* on a salty soil in an arid region of India. J. Arid Environ. 30, 67–73.

Hagishima, A., Narita, K., Tanimoto, J., 2007. Field experiment on transpiration from isolated urban plants. Hydrol. Process. 21, 1217–1222.

Hamilton, S.J., 2004. Review of selenium toxicity in the aquatic food chain. Sci. Total Environ. 326, 1–31.

James, J., Richards, J., 2007. Influence of temporal heterogeneity in nitrogen supply on competitive interactions in a desert shrub community. Oecologia 152, 721–727.

Jordan, F.L., Yoklic, M., Morino, K., Brown, P., Seaman, R., Glenn, E.P., 2009. Consumptive water use and stomatal conductance of *Atriplex lentiformis* irrigated with industrial brine in a desert irrigation district. Agric. Forest Meteor. 149, 899–912.

Kelliher, F., Leuning, M., Raupauch, R., Schultze, E., 1995. Maximum conductances for evaporation from global vegetation types. Agric. Forest Meteor. 73, 1–16.

Masters, D., Benes, S., Norman, H., 2007. Biosaline agriculture for forage and livestock production. Agric. Ecosyst. Environ. 119, 234–248.

Mata-Gonzalez, R., McClendon, T., Martin, D., 2005. The inappropriate use of transpiration coefficients (Kc) to estimate evapotranspiration in arid ecosystems: a review. Arid Land Res. Manage. 19, 285–295.

Meyer, R., 2005. *Atriplex lentiformis*. In: Fire Effects Information System [Online]. U.S. Department of Agriculture, Forest Service, Rocky Mountain Research Station, Fire Sciences Laboratory (Producer). Available: http://www.fs.fed.us/database/feis/.

Miyamoto, S., Chacon, A., 2006. Soil salinity of urban turf areas irrigation with saline water. II. Soil factors. Landsc. Urban Plann. 77, 28–38.

Miyamoto, S., Chacon, A., Hossain, M., Martinez, I., 2005. Soil salinity of urban turf areas irrigated with saline water. I. Spatial variability. Landsc. Urban Plann. 71, 233–241.

Miyamoto, S., Glenn, E., Olsen, M., 1996. Growth, water use and salt uptake of four halophytes irrigated with highly saline water. J. Arid Environ. 32, 141–159.

Morehouse, B., Carter, R., Tschakert, P., 2002. Sensitivity of urban water resources in Phoenix, Tucson, and Sierra Vista, Arizona, to severe drought. Clim. Res. 21, 283–297.

National Cooperative Soil Survey, 2008. Pima Series. http://www2.ftw.nrcs.usda.gov/osd/dat/P/PIMA.html (last visited October, 2008).

Niu, X., Bressan, R., Hasegawa, P., Pardo, J., 1995. Ion homeostasis in NaCl stress environments. Plant Physiol. 109, 735–742.

Noaman, M., El-Haddad, E., 2000. Effects of irrigation water salinity and leaching fraction on the growth of six halophytes species. J. Agric. Sci. 135, 279–285.

Norman, H., Masters, D., Wilmot, M., 2008. Effects of supplementation with grain, hay or straw on the performance of weaner Merino sheep grazing old man (*Atriplex nummularia*) or river (*Atriplex amnicola*) saltbush. Grass Forage Sci. 63, 179–192.

O'Connell, M., Young, J., Kingwell, R., 2006. The economic value of saltland pastures in a mixed farming system in Western Australia. Agric. Syst. 89, 371–389.

Osman, A., Bahhady, S., Hassan, N., Ghazali, F., Al Ibrahim, T., 2006. Livestock production and economic implications from augmenting degraded rangeland with *Atriplex halimus* and *Salsola vermiculata* in Northwest Syria. J. Arid Environ. 65, 474–490.

Osmond, B., Björkman, O., Anderson, D., 1980. Physiological Processes in Plant Ecology: Toward a Synthesis with Atriplex. Springer-Verlag, New York, 468 pp.

Paw, K., Gao, W., 1988. Applications of solutions to non-linear energy budget equations. Agric. Forest Meteor. 43, 121–145.

Priestley, C., Taylor, R., 1972. Assessment of surface heat-flux and evaporation using large-scale parameters. Mon. Weather Rev. 100, 81–92.

Qadir, M., Oster, J., 2004. Crop and irrigation management strategies for saline-sodic soils and waters aimed at environmentally sustainable agriculture. Sci. Total Environ. 323, 1–19.

Riley, J., Fitzsimmons, K., Glenn, E., 1997. Halophyte irrigation: an overlooked strategy for management of membrane filtration concentrate. Desalination 110, 197–211.

Rogers, M., Craig, A., Munns, R., Colmer, T., Nichols, P., Malcolm, C., Barrett-Lennard, E., Brown, A., Semple, W., Evans, P., Cowley, K., Hughes, S., Snowball, R., Bennett, S., Sweeney, G., Dear, B., Ewing, M., 2005. The potential for developing fodder plants for the salt-affected areas of southern and eastern Australia: An overview. Aust. J. Exp. Agric. 45, 301–329.

Sandyswinsch, D., Harris, P., 1992. Agroforestry and forestry on the Cape Verde Islands. Agrofor. Syst. 19, 79–91.

Shannon, M., Cervinka, V., Daniel, D., 1997. Drainage water reuse. In: Madramootoo, C., Johnson, W., Willardson, L. (Eds.), Management of Agricultural Drainage Water Quality. FAO, Rome, Chapter Four (on-line document), http://www.fao.org/docrep/w7224e/w7224e08.htm.

Skaggs, T., Poss, J., Shouse, P., Grieve, C., 2006a. Irrigating forage crops with saline waters. 1. Volumetric lysimeter studies. Vadose Zone J. 5, 815–823.

Skaggs, T., Shouse, P., Poss, J., 2006b. Irrigating forage crops with saline waters. 2. Modeling root uptake and drainage. Vadose Zone J. 5, 824–837.

Steinwand, A., Harrington, R., Groeneveld, D., 2001. Transpiration coefficients for three Great Basin shrubs. J. Arid Environ. 49, 555–567.

Steinwand, A., Harrington, R., Or, D., 2006. Water balance for Great Basin phreatophytes derived from eddy covariance, soil water, and water table measurements. J. Hydrol. 329, 595–605.

Striker, J., Rockwood, D., Segrest, S., Alker, G., Prine, G., Carter, D., 2000. Short rotation woody crops for Florida. Paper presented to Third Biennial Conference, Short Rotation Woody Crops Operations Working Group, State University of New York, Syracuse. Available on-line at http://trees.ifas.ufl.edu/SRWC-Syracuse%20NY.pdf (last visited October, 2008).

Swingle, R., Urias, A., Doyle, J., Voigt, R., 1978. Chemical composition of kenaf forage and its digestibility by lambs and *in vitro*. J. Anim. Sci. 46, 1346–1350.

Swingle, R., Glenn, E., Squires, V., 1996. Growth performance of lambs fed mixed diets containing halophyte ingredients. Anim. Feed Sci. Technol. 63, 137–148.
Tolk, J., Evett, S., Howell, T., 2006. Advection influences on evapotranspiration of alfalfa in a semiarid climate. Agron. J. 98, 1646–1654.
Watson, M., O'Leary, J., 1993. Performance of *Atriplex* species in the San Joaquin Valley, California, under irrigation and with mechanical harvests. Agric. Ecosyst. Environ. 43, 255–266.
Watson, M., O'Leary, J., Glenn, E., 1987. Evaluation of *Atriplex lentiformis* (Torr.) S. Wats and *Atriplex nummularia* Lindl. as irrigated forage crops. J. Arid Environ. 13, 293–303.
Webber, C., Bledsoe, V., 2002. Kenaf yield components and plant composition. In: Janick, J., Whipkey, A. (Eds.), Trends in New Crops and Crop Uses. ASHS Press, Alexandria, VA, pp. 348–357.

# Appendix 6:

Ruminant Digestion and the Nutritive Potential of Halophytes (*Atriplex* spp.) for use in the Feed Lots and Dairy Industry: A Literature Review

# Ruminant Digestion and the Nutritive Potential of Halophytes *(Atriplex spp.)* for use in the Feed Lots and Dairy Industry: A Literature Review

June 2010

Deserie Soliz
Mathew Kluvo

The University of Arizona

Environmental Research Laboratory
2601 E. Airport Drive, Tucson, AZ 85721-0011
(520) 626-2162, (520) 573-0852 (FAX)

**Abstract:**

*Cynodon* hay, alfalfa and Sudan grass are the most common supplements used in animal feed all around the world especially in arid and semi-arid regions. However, traditional livestock husbandry in arid regions has depended on indigenous plants, often salt tolerant species, for livestock grazing. When looking at the diversity of plant life that exist within arid and semi-arid regions within this context, *Atriplex spp*. stand out. In the desert Southwest, there are a number of indigenous halophytes that are suitable, with limits, for livestock but the stand out species are *Atriplex spp.* Research was conducted at a pilot desalination facility in Marana, AZ, to evaluate the *Atriplex lentiformis* (quail bush) for RO concentrate disposal and the use of this plant for ruminant forage.. The results showed that when compared to the most common feed supplements, *A. lentiformis* was better digested by livestock and provide a higher content of Crude Protein that traditional forage crops. Results of this review show that when mixed with a high energy/low NaCl feed, *A. lentiformis* was able to enhance the body weight of the livestock in a healthy manner. Research on *Atriplex spp*. as a portion of ruminant diets, has shown that livestock increased in body weight, and were able to maintain weight gains even without additional nutritional supplement.

**Introduction:**

This study examines the literature on ruminant digestion and processing of forage within the context of identifying the potentials and limitations for *Atriplex spp* use as a forage supplement for livestock feed. Atriplex spp. is a halophyte (salt tolerant plant) that is indigenous to the desert regions throughout the world. It has been used by native peoples for animal grazing for millennia. This review was undertaken to examine whether and how the use of this plant species has be developed, the range of applications of *Atriplex spp* or its constituents for animal feed or supplement and its potential for use as an agronomic crop.

## 1. Ruminant Digestion

Ruminants have a complex, multi-compartmented digestive tract. The first major section of a ruminant's digestive tract is the rumen (i.e. forestomach or reticorumen), which acts as a large fermentation chamber (Figure 1). It houses high concentrations of anaerobic bacteria and protozoa essential for the animal's digestion of plant matter. These rumen microbes use the fibrous and otherwise indigestible plant biomass (i.e. cellulose, hemicelluloses and lignin) as a substrate for fermentative digestion into the essential energy and nutrients which can be absorbed by the animal's intestines. It is because of these rumen bacteria that ruminant, such as cattle or sheep, are able survive on a diet consisting strictly of grass or hay (Chiba 2009). Cellulose accounts for 40-50% of the total dry weight of any plant, including *Atriplex spp*. In addition to cellulose, rumen microbes are able to metabolize all other types of carbohydrates, such as starch, sugar and other fibrous plant biomass. Because fermentation occurs under anaerobic conditions, carbohydrates are metabolized primarily into methane, carbon dioxide and three Volatile Fatty Acids (VFAs). The three VFAs are Proponic, Acetic and Butyric Acid. These VFAs provide the ruminant with 70% or more of their daily energy requirements (Chiba 2009). Unlike lipids and carbohydrates, only 50-60% of the protein in the feed is metabolized by rumen microbes. A process known as bypass protein, the remaining half of the feed pass directly through the rumen and into the abomasums (true stomach) and small intestine where the feed is digested by proteolytic enzymes in a process similar to that found in mono-gastric mammals (i.e. humans).

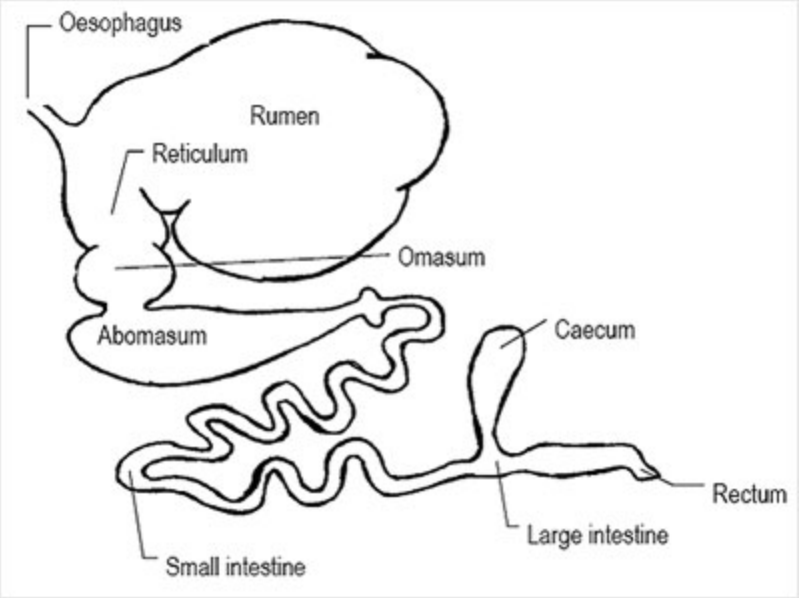


**Figure 1:**[1] Ruminant Digestive Tract

### *1.1 The breakdown of the proteins*

The dietary protein metabolized by rumen bacteria are either fermented into VFAs, in a process similar to microbial digestion of carbohydrates and lipids, or hydrolyzed by microbial enzymes into ammonia (instead of just amino acids) (Figure 2). The ammonia is then used by the microbes for their own growth and reproduction. The concentration of rumen bacteria can reach 50 billion per mL of rumen fluid while rumen protozoa can reach well over a million per mL.

[1] www.landlearnnsw.org.au/sustainability/climate-chagne/agriculture/livestock/methane

Some of these microbes are inevitably flushed out of the rumen and into the small intestine where they are digested and absorbed. The microbial biomass provides the animal with a reliable and complete supply of essential amino acids. Essential amino acids are those amino acids which vertebrates are unable to synthesize themselves but they require for survival.

### *1.2 The use of Ammonia*

Ammonia, which is produced as a byproduct of microbial metabolism, is a major source of Non-Protein Nitrogen (NPN). NPN is used for biosynthesis of microbial cells and proteins. The fact that rumen microbes break down dietary proteins all the way to Ammonia prior to resynthesizing microbial proteins shows their preference and capability for using NPN when synthesizing proteins (Diagram 2). About 40-50% of the nitrogen in *Atriplex spp.* is NPN. However, in order for NPN to be converted by rumen microbes into microbial protein, a good supply of metabolizable energy (ME) must be available in the feed. ME is needed for microbial protein synthesis because the rumen microbes cannot synthesize branched carbon chains which are the skeletons of the protein molecules. Therefore, these branched C-chains must be made available to them in their feed (Chiba 2009).

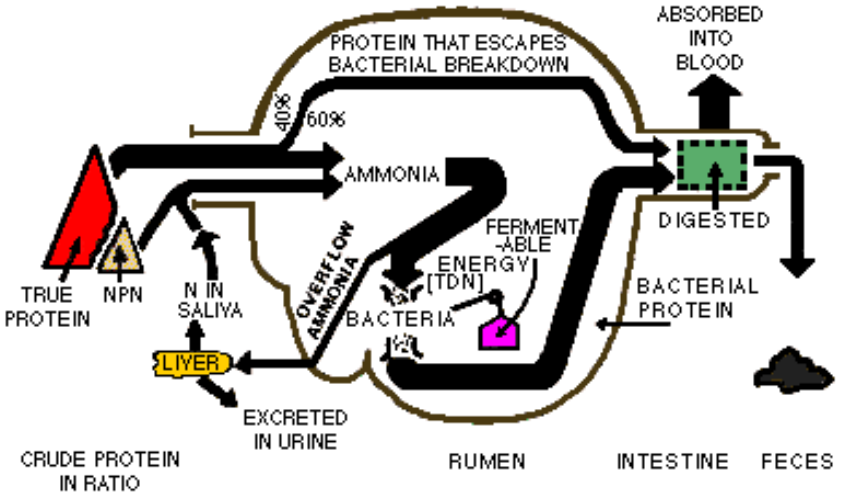


**Figure 2:[2] Ruminant Digestive Process**

## 2. *Atriplex* Literature

### *2.1. Growing Atriplex spp. using saline irrigation water*

Most halophytic plants show maximum growth at soil salinity of 20 to 25 g/L. However most halophytes show a 25-50% growth reduction when soil salinity is increased at 30 to 40 g/L (Miyamoto et al. 1994). *Atriplex spp.* are among the most productive halophytes even when irrigated with the higher levels of salinity. *Atriplex lentiformis* is the largest and most productive of the *Atriplex spp.* A hectare of *Atriplex lentiformis* can produce over 10 tons of dry matter (DM) when irrigated with water whose salinity is 40 g/L (TDS) (Masters et al. 2007).

*Atriplex spp.* produce more edible biomass per hectare than comparable, non-halophytic feed crops, such as alfalfa. In 1993, Watson and O'Leary irrigated stands of 8 species of *Atriplex*

[2] www.extension.umn.edy/distribution/livestocksystems/components/di0469-02.html

*spp.* with a salinity of 18 dS/m, or approximately 12g/L. The stands where mechanically harvested multiple times using standard alfalfa hay harvesting and baling equipment. Multiple harvests not only increased the overall productivity of each stand of *Atriplex spp.*, but the regrowth of *Atriplex spp.* stands contained a higher leaf to stem ratio than initial harvests (Watson 1990; Benjamin et al. 1995). In 7 of the species' stands including *Atriplex lentiformis,* the yield increased from the first to the second harvest. In the case of *Atriplex lentiformis,* the first harvest yielded 6.3 t/ha while the second harvest yielded 9.3 t/ha of edible biomass. However, after the third or fourth harvest yields *Atriplex spp.* stands dropped substantially. Therefore, to obtain the best results when irrigating *Atriplex lentiformis* with highly saline water, it is recommended that the stands should be uprooted and replanted following the second harvest (Watson and O'Leary 1993).

## 3. Animal Feed Potential

### *3.1 Nutritional Value of Atriplex spp. Protein content*

Due to ruminant's ability to synthesize microbial protein from Non-Protein Nitrogen, scientists often use the Nitrogen (N) content in feed to help determine its crude protein (CP). The following equation (Eq. 1) is often utilized to make the N to CP conversion. Although there are some differences reported in scientific literature on its nutritional values, in general *Atriplex spp.* are considered to be a good source of crude protein with values ranging from 9 to 24% of the dried biomass (DM) (Norman et al 2008; Guevara et al. 2006). This reflects that *Atriplex spp.* has Nitrogen content of 1.5-3.6% DM and 40-50% of the N in *Atriplex spp*. is NPN (Masters et al. 2007; Le Houérou 1991).

**Eq 1. 6.25 * (N %) DM = (CP %) DM**

The leaves and seeds of *Atriplex spp.* are much high in protein than the stems and woody parts of the plant. The Marana Project Site reports that among the *Atriplex lentiformis* grown from RO concentrate, the crude protein accounts for 13% of the dry weight (DM) of the leaves and 17% DM of the seeds. Alternatively, the stems were only 3.5% DM crude protein. This trend was consistent with *Atriplex spp.* throughout scientific literature (Table 3).

| Nutritional Values (DM) | Atriplex spp. from literature | A. Lentiformis from Marana Project | | |
|---|---|---|---|---|
| | | Seeds | Leaves | Stems |
| Protein/N(6.25) % | 9-24 | 17 | 13 | 3.5 |
| Minerals (ASH) % | 14-32 | 28 | 29 | 9 |
| ME=Kcal/kg | 280-510 | 389 | 387 | 449 |
| Crude Fiber % | 10-42 | 13 | 13 | 43 |

**Table 3 -** Nutritional values of *Atriplex spp. and A. lentiformis* grown on RO Concentrate

The crude protein value of a feed is important for livestock production because a major reduction in the intake of the feed occurs if the CP content falls below 8% DM or if N falls below 1% DM (Ben Salem et al 2004). This is due to the lack of amino acids in the feed which limits microbial reproduction in the rumen and causes a reduction in the livestock's rate of digestion. This means the ruminant cannot consume as much feed and results in a decline in the livestock's daily intake (DI) and its ability to gain weight.

### *3.2 Digestibility of Atriplex spp. on livestock*

The leaves and seeds of *Atriplex spp.* are highly digestible while their stems and woody material are not. The leaves and seeds are low in Tannins, Crude Fiber (CF) and Acid Detergent Fiber (ADF) compared to similar feed crops. Tannins reduces a protein's digestibility by inactivating microbial enzymes and forming complexes with the proteins. CF is a traditional measure of fiber content in feeds. Neutral Detergent Fiber (NDF) and Acid Detergent Fiber (ADF) are more useful measures of feeding value and should be used to evaluate forages and formulate livestock feed rations. NDF is a value for the structural components of a plant, specifically its cell walls. NDF increases as a plant matures thus comparisons between feeds using NDF can be inaccurate as it depends on the age of the plant. ADF is considered to be the best digestion category for comparisons between feed crops as it provides a value for the least digestible plant components such as lignin, cellulose and hemicellulose. The higher a feed crop's ADF value, the lower its digestibility. The leaves and seeds of the *Atriplex lentiformis* grown with the RO concentrate at the Marana Project Site had ADF values of approximately 16% DM. Comparing this value to the *A. lentiformis* stem's ADF value of 53% DM provides insight as to why the stems and woody parts of *Atriplex spp.* are much less digestible than their seeds and leaves. Throughout the scientific literature, this difference in digestibility was reported for all *Atriplex species'* leaves and seeds vs. stems.

### *3.3 Minerals and Nutrients*

According to the National Research Council (2000) there are 17 essential minerals required by beef cattle (Table 4). These 17 minerals are classified by the amount needed in their diet. Macrominerals are required in relatively large quantities, while microminerals are only required in small or trace amounts.

A Proximate Analysis is a series of laboratory tests which analyze feed to determine its nutritional value for livestock. Table 6 shows the results from the Proximate Analysis of the *Atriplex lentiformis* grown using RO concentrate from the Marana Project Site. Amongst the various nutritional categories provided by the Proximate Analysis, a list of 9 specific essential minerals are also typically included due do their importance for livestock production. The 9 minerals include Calcium, Phosphorus, Potassium, Magnesium, Manganese, Iron, Sodium, Copper and Zinc (El-Shatnawi and Turuk 2002). These minerals are the essential minerals required for ruminant production and function of structural components of bones and teeth, electrolytes in body fluids and in the metabolism of nutrients plus other major functions.

*Atriplex lentiformis* is above the critical level required for ruminant growth for all 9 of these essential minerals. In addition, *Atriplex spp.* are also high in several vitamins, including Vitamin E. Vitamin E is very important for meat quality, taste and color because it prevents the oxidation of Oxymyoglobin to Metmyoglobin following exposure to air. This anti-oxidization property of Vitamin E prevents meat from turning brown. The meat from *Atriplex spp.* fed livestock tends to remain red longer and has a higher lean to fat ratio. The latter fact is due to the protein to energy ratio in the edible biomass of *Atriplex spp.* (Pearce and Jacob 2004).

Another nutritional category provided by the Proximate Analysis of a feed is Ash. A feed's Ash value is determined by increasing the temperature of feed to the point that its Carbohydrates, Proteins, Fats and other combustible biomass are burnt away, leaving only the

feed's salt and mineral content behind. *Atriplex spp.* are invariably high in salt and mineral content with Ash values ranging from 9 to 32% of DM. Approximately half of this Ash value for all *Atriplex spp.* comes from NaCl. While sodium is an essential nutrient for livestock and NaCl is often added to $Na^+$ deficient feeds, 10% of a feed's dry matter (DM) is NaCl which it can be toxic to livestock. The National Research Council Published a report in 2005 that summarized the results of many experiments involving the affects of NaCl inclusion in the diets of various species of livestock. The results for these experiments indicate that, besides camels, cattle and sheep are the most tolerant to NaCl in their diets. Sheep can tolerate up to 10% DM of NaCl in their feed while cattle can tolerate up to 8% DM of NaCl. When NaCl content is above these values, their Daily Intake (DI) of feed is reduced, resulting in weight loss. Additionally, high salt intake can cause several chronic health problems ranging from cardiovascular disease to digestive diseases to respiratory problems (Masters et al. 2007; NRC 2000). Of course, these health problems can be avoided if *Atriplex spp.* is mixed with a low salinity feed at a level that assures an overall salt content below the animal's tolerance level. Furthermore, the importance of providing plenty of fresh water to any animal consuming a feed with any amount of *Atriplex spp.* cannot be over-emphasized.

**Table 4 -** The essential minerals needed for livestock especially beef cattle.

| **Macrominerals** | |
|---|---|
| Calcium | Potassium |
| Chlorine | Sodium |
| Magnesium | Sulfur |
| Phosphorus | |
| **Microminerals** | |
| Chromium | Manganese |
| Cobalt | Molybdenum |
| Copper | Nickel |
| Iodine | Selenium |
| Iron | Zinc |

### *3.4 Energy/Calories*

In general, *Atriplex spp.* has a very low metabolizable energy ((ME)/calorie) content compared to other more conventional livestock feeds. An extensive and wide-ranging review of scientific literature showed energy values for all *Atriplex spp.* ranging from 0.41 to 2.21 Kcal/kg DM (Le Houérou 1991; Kearl et al. 1979; Masters et al 2007; Gihad and El-Shaer 1994). *Atriplex lentiformis* grown using RO concentrate from Marana Project Site had a value on the lower side of the range, with an ME = 0.435Kcal/kg. This explains why a diet consisting of 100% *Atriplex spp.* simply does not contain enough energy/calories to allow for livestock to gain weight especially in pregnant or lactating livestock (Abu-Zanat and Tabbaa 2006). However, if the livestock's rumen microbes are given enough time to adjust to the *Atriplex spp.* diet, it can be used as maintenance feed for sheep and cattle (Le Houérou 1991). For most people who own livestock, weight gain is the goal rather than just maintenance. Thus, if *Atriplex spp.* is to provide any weight gains, it should always be mixed with other feeds to create a more complete livestock diet. Ideally, these feeds will be low in NaCl and high in ME which is the case with the most feeds found on pastures or in feedlots. The vast majority of livestock are found in one of two locations, and usually both over the course of their lives.

It is important to supplement *Atriplex spp.* into a diet with high ME content not only to provide the livestock with the calories needed to gain weight but also because extra ME improves the synthesis of proteins from NPN by microbes in the livestock's rumen. As previously mentioned, a high percentage of the Nitrogen in salt-tolerant plants is NPN in *Atriplex spp.* which accounts for 40-50% of the plant's Nitrogen (Benjamin et al. 1995). If a good supply of ME is available, rumen microbes can convert NPN into microbial proteins. The digestion of *Atriplex spp*. alone only releases a fraction of the branched C-chains needed for the rumen microbes to synthesize all the potential proteins from *Atriplex spp.* supply of NPN. When *Atriplex spp.* is added to the high calorie grain of the conventional feedlot diet, the majority of the NPN is converted to microbial protein, which can then provide well over 50% of the ruminant protein requirement (Masters et al. 2007).

## 4. Atriplex Feed Issues

### *4.1. Llivestock rumen microbes adjustment to Atriplex spp. containing, diet.*

A 1999 paper by Le Houeron explained that the differences in the feed values of *Atriplex spp.* are largely due to differences in the length of the experiments. He explains that experiments lasting 5 weeks or less, typically report a low value for *Atriplex spp.* as an animal feed. He then showed that any long-term study on the effects of an *Atriplex spp.* supplemented diet invariably resulted in improvements in livestock production. He concluded that the reason for this discrepancy is due to the time required by rumen microbes to adapt to the new *Atriplex*-based feed (Le Houérou 1991).

A perfect example of a discrepancy can be seen in the feeding trial by Chriyaa et al (1997a). During the first seven weeks of this 14-week feeding trial, the group of livestock who were fed the *Atriplex spp. s*upplemented with Wheat Straw diet lost 42 g/day. However, by the end of the 14-weeks the livestock in the same group were 250 g heavier than at the beginning. This means they gained at least 45.6 g/day during the second 7 weeks of the feeding trial. Considering that the livestock were given the same feed at the same quantity throughout the 14-week study, the only explanation would be the adaptation of the livestock and their rumen microbes to the new feed (Chriyaa et al. 1997a). Following a period of acclimation, the rumen microbes are able to quickly and efficiently digest the feed, as well as retain greater amount of the nutrients found within the feed. Furthermore, once adapted, the rumen microbes can synthesize more vitamins and nutrients, as well as create protein from the ample source of NPN found in the *Atriplex spp.* biomass.

To better understand the reason behind this increase in microbial and livestock production, one must recognize the diversity of bacteria and protozoa that constitute the populations of rumen microbes. Although many rumen bacteria can utilize several different substrates during fermentative digestion, most are specialized and prefer a single type of food. Therefore, when the ruminant's diet changes, for example from a pasture diet rich in grass and other fibrous feeds to a feedlot diet rich in the more rapidly digestible feed, the populations of Amylolytic rumen bacteria, who prefer starch, will begin to increase while the populations of Cellulolytic and Hemicellulolytic bacteria in the host's rumen will begin to decrease. This change in rumen bacteria populations takes time to reach maximum efficiency. The more extreme the change in the diet, the longer it takes for the rumen bacteria to adjust. In addition to

the three groups already mentioned, there are Proteolytic rumen bacteria, which prefer protein, as well as Sugar-utilizing and Acid-utilizing rumen bacteria populations. Table 5 shows a few of the most common species of rumen bacteria found in cattle. It is important to note this is a select list and at any one time there are up to thousands of different species of bacteria in the rumen and large intestine of cattle. Considering these are the most common rumen bacteria, it is safe to say that they are capable of using the greatest variety of different types of substrates (Chiba 2009).

**Table 5**[3]**-** ***Distribution of strains of groups of bacteria isolated from medium 98-5 inoculated with rumen contents from steers fed four diets***

| | % of total strains [1] | | | | |
|---|---|---|---|---|---|
| Group | Urea | Biuret | Urea phosphate and urea | Uric acid | Overall |
| *Bacteroides amylophilus* | 26 (2) | 1 (1) | 44 (2) | 9 (2) | 19.3 (7) |
| Anaerobic lactobacillus | 24 (3) | 20 (3) | 6 (2) | 23 (3) | 18.9 (11) |
| Facultative anaerobic lactobacillus | 3 (2) | 20 (3) | 0 | 0 | 6.4 (5) |
| *Peptostreptococcus elsdenii* | 0 | 5 (2) | 2 (1) | 0 | 1.9 (3) |
| *Streptococcus bovis* | 0 | 5 (2) | 2 (1) | 3 (2) | 2.7 (5) |
| *Bacteroides sp.* | 0 | 1 (1) | 0 | 0 | 0.4 (1) |
| *Bacteroides ruminicola* | 0 | 1 (1) | 0 | 0 | 0.4 (1) |
| *Ruminococcus albus* | 0 | 0 | 0 | 2 (1) | 0.4 (1) |
| *Ruminococcus flavefaciens* | 0 | 1 (1) | 0 | 0 | 0.4 (1) |
| *Bacteroides succinogenies* | 0 | 0 | 0 | 2 (1) | 0.4 (1) |
| *Butyrivibrio fibrosolvens* | 6 (1) | 0 | 0 | 2 (1) | 1.9 (2) |
| Atypical Butyrivibrio | 1 (1) | 0 | 0 | 0 | 0.4 (1) |
| *Borrelia sp.* | 0 | 3 (2) | 0 | 5 (1) | 1.9 (3) |
| Unknown rods | | | | | |
| Gram-negative | 21 | 15 | 13 | 22 | |
| Gram-positive or variable | 14 | 14 | 17 | 11 | |
| Unknown cocci | | | | | |
| Gram-negative | 2 | 1 | 9 | 8 | |
| Gram-positive or variable | 4 | 8 | 4 | 8 | |
| Other | 0 | 4 | 4 | 5 | |

[1] Numbers in parentheses under the different NPN sources represent the rumen samples which contained that particular bacterial group from among the total of 4 samples collected for each diet. Numbers in parentheses in the overall column indicate the sum of the appearances of each particular bacterial group for all 4 diets.

### *4.2. The leaf to stem ratio used in the feed.*

As previously discussed, the leaves and seeds of *Atriplex spp.* contain far more protein (22% vs. 3%) and far less fiber (12% vs. 40%) than the woody parts of the plant. Therefore, when the feed contains a higher leaf/seed to stem ratio it is more nutritious and digestible, thus resulting in far better livestock production. This is an important factor to note when harvesting *Atriplex spp. Atriplex lentiformis* flowers from May to September and its seeds ripen from July to October. While *Atriplex lentiformis* may hold its leaves year-round, their Nitrogen content, and thus their protein content, is the greatest in mid-summer (July) and then decreases until spring (Islam and Adams 2000; Munz 1959).

### *4.3. Feed nutritional characteristics and the inclusion % of Atriplex spp.*

Due to its high concentration of NaCl and its low energy content, feeding an animal a diet consisting of 100% *Atriplex spp.* is not productive and not typically recommended. The best results in livestock production occur when *Atriplex spp.* are mixed with a high-energy feed that contains a low NaCl concentration. The level of inclusion into this diet depends on the characteristics of the feed that it is supplemented into. A typical recommendation would be to have 50% or less of NaCl concentrations. However, when it is supplemented into low-protein,

[3] Slyter LL, RR Oltjen, DL Kern and JM Weaver. 1967. Microbial Species Including Ureolytic Bacteria from the Rumen of Cattle Fed Purified Diets. The Journal of Nurtition. 94: 68.

high- fiber feeds, such as low-quality hay or grass, inclusion levels over 80% *Atriplex spp.* have resulted in improvement in livestock production (Le Houérou 1991; Wilson and Graetz 1980).

***4.4. The inherent salt tolerance of livestock that are fed the Atriplex spp. supplemented diet.***

Some livestock are naturally more tolerant of a high salinity diet than others. The Animal Nutrition Handbook gives the following order of tolerance, from most to least:

Camel > Sheep > Goats > Cattle > Horses > Pigs > Poultry.

However, there is also a range of tolerance amongst the different species in each group of livestock as well. These differences are typically the result of the environment the animals evolved from and are adapted to; for example, species from arid environments tend to have a higher salinity tolerance. Therefore, when fed an *Atriplex spp.* supplemented diet Merino sheep and *Bos indicus* cattle will perform better, show higher weight gains and overall production than other species of sheep or cattle (Masters et al. 2007).

**Table 6:** Comparison of key nutrition component of various livestock forage crops

| Item | CP | Ash | ADF | Na | K | ADL |
|---|---|---|---|---|---|---|
| ***Cynodon* hay**[4] | 12.3 | 8.8 | 26.1 | 0.1 | 1.5 | 6.4 |
| ***Atriplex lentiformis***[5] | 12.16 | 20.66 | 27.63 | 4.20 | 1.56 | -- |
| ***Atriplex nummularia***[5] | 19.78 | 26.25 | 11.46 | 5.47 | 4.49 | -- |
| ***Medicago sativa* L. (alfalfa)**[6] | 17.5 | 11.5 | 28.4 | 0.009[7] | 2.91[7] | 7.9 |
| ***Hibiscus cannabinus* L. (kenaf)**[6] | 11.0 | 11.8 | 41.2 | -- | -- | 10.5 |
| ***Sorghum spp.* (Sudan grass)**[7] | 10.8 | 7.64 | 41.6 | 0.010 | 1.87 | 4.6 |

Not available = --. See footnote for source of values.

Table 6 lists the values for the most common nutritional categories provided by the Proximate Analysis (PA) of a feed crop for ruminant. This table compares the nutritional value of the *Atriplex lentiformis* grown using the RO concentrate at the Marana Project Site (TDS is 3500-5000mg/L) to Alfalfa, *Sorghum spp.* and Bermuda grass, all three of which were grown using clean water (TDS is less than 100mg/L). Not only is *A. lentiformis* more productive (5-10t/ha/yr), but it also more digestible and has a higher concentration of Crude Protein. The only major problems created by using *A. lentiformis* in a livestock feed are its low Metabolizable Energy/Calories and high NaCl concentrations. However, supplementing the *A. lentiformis* with a high ME, low NaCl feed at the proper inclusion percentage level, typically less than 50%, should alleviate both of these problems.

***4.5a. Atriplex spp. should be a supplement to, and not the sole ingredient of, a Livestock Feed.***

The high NaCl and the low digestible energy (DE)/calorie content found in *Atriplex spp.* biomass limit its potential to be productive as the sole ingredient in a feed for livestock. At best, a diet consisting of 100% *Atriplex spp.* will only maintain livestock weight. Alternatively, the

[4] Swingle, R.S. et al. 1996. Growth performance of lambs fed mixed diets containing halophytes ingredients. Animal Feed Science Technology. 63: 137-148.
[5] Proximate analysis of plants. 2010
[6] Swingle, R.S. et al. 1978. Chemical composition of kenaf forage and its digestibility by lambs and *in vitro*. Journal of Animal Science. 46(5): 1346-1350.
[7] Dann, H.M. et al. 2008. Composition of brown midrib sorghum-sudangrass with corn silage on lactational performance and nutrient digestibility in Holstein dairy cows. Journal of Dairy Science. 91: 663-672.

vast majority of research indicates that when it is mixed with other feeds, livestock production and live weight gain (LWG) tend to increase.

Most livestock are found in only two places: a pasture or a feedlot. Over the course of their lives most livestock, especially cattle, end up living in both. In general, they begin their lives on a pasture, with a diet primarily consisting of local grasses or hay and, when available, browse local grains, shrubs or forbs that are sometimes found on their pasture. When they reach adulthood, they are moved to a feedlot where they are fed specially formulated diets aimed at forcing them to gain as much weight as possible prior to slaughter.

The diets in both these locations can be improved when supplemented with *Atriplex spp.* However, it is important that the ratio of the *Atriplex spp.* and the other ingredients that make up the livestock's diet are such that the crude protein (CP) is at least 8% DM of the combined feed and that NaCl makes up less than 7-10% DM (Mahipala et al. 2009). If the CP content of their feed is below 8% DM, then their rumen microbes cannot reproduce at the level require for sufficient digestion. This will result in a reduction in their daily intake of the feed and thus a reduction in their daily weight gain (DWG). The same is true is the feed's NaCl content is above 8% DM for cattle or 10% DM for sheep. Due to the high CP and NaCl content of *Atriplex spp.* this is a key concept when formulating the ingredient ratios for a livestock's diet.

***4.5b. Atriplex spp. as a supplement of a common pasture diet***

Historically, on pastures in arid and semi-arid regions throughout the world, *Atriplex spp.* have been an important sources of protein and minerals for grazing livestock, especially grazing ruminants, from sheep, goats to cattle and buffalo. Since *Atriplex spp.* tend to hold their leaves year-round, they become vital sources of late-season green fodder. For this reason, *Atriplex spp.* become increasingly important as the seasons progress through the fall and winter months and the availability of grasses, grains and other more palatable feeds decreases (Shoop et al 1985; Osman et al. 2006; Gihad and El Shaer 1994)

When *Atriplex spp.* is added into a common grass-based pasture diet, animal production and daily weight gains are higher than either feed used individually. This is due to the fact that a diet of 100% *Atriplex spp.* contains low energy and high salt content which quickly limits intake. Conversely, when a diet consisting of 100% grass or hay is fed to livestock, the high fiber content limits maximum intake. If the percentage of protein in livestock feed is below 8% of Dry Matter or 8% of Organic Matter, the intake of the feed will drop substantially, resulting in weight loss (Milford and Minson 1965; Aiazzi et al. 1999). Since *Atriplex spp.* are relatively high in protein/NPN and common pasture diets have moderately high levels of ME/calories when they are combined in the correct percentage for the livestock species' nutritional requirements productivity can increase.

An insightful experiment performed by Chriyaa et al. (1997a) compared the effects of supplementing four browse species into a basal diet of Wheat Straw Hay (WSH) on the livestock production and live weight gains (LWG) of sheep found on the arid pasturelands of Morocco. The four browse supplements used in this 14-week feeding trial included *Atriplex nummularia* (SB), Alfalfa, Medic Pods, and Blue Wattle (*Acacia spp.*), each of which is commonly found on pastures in arid regions throughout Europe, Asia and N. Africa. A fifth diet consisted of the same

WSH supplemented with urea at a 1.35% DM inclusion level. Besides the control diet of 100% unsupplemented wheat straw (UWS), the urea and the four browse species were supplemented into the basal WSH diet at different inclusion levels, ranging from 27 to 37%, in order to assure that all five diets were nearly equal in Nitrogen and Crude Protein content. The N content of the five supplement diets ranged from 1.75 to 2.19% DM while CP values ranging from 71 to 90g/kg DM. All six diets were then fed to five groups of 30 sheep over a 14-week period. Each diet was analyzed to determine the total nutrient and mineral content, as well as DM, ash, CP and 6 different categories that affect the digestibility of each diet including: tannins, acid detergent insoluble nitrogen (ADIN), neutral detergent fiber (NDF), acid detergent fiber (ADF), acid detergent lignin (ADL) and in-vitro dry matter digestibility (IVDMD). The livestock were fed each diet *ad libtum.* At the end of each day, the remaining feed was weighted to determine the dry matter intake (DMI) of each diet. Each group was weighed to determine daily weight gains or losses.

During the first 7 weeks of the feeding trial, each group lost weight. The group fed the unsupplemented wheat straw (UWS) diet lost the most weight at 70 g per day and consumed the least amount of feed, with a dry matter intake (DMI) of 41g/kg. The diet of 100% un-supplemented Wheat Straw, was the one that had a CP content below (69 g per kg of DM) the threshold required for adequate rumen microbial activity (ARC 1980). This illustrates the importance of N content and CP in feed on DMI and overall livestock production. Furthermore, the fact that the livestock lost only 33 g/day when 1.35%DM Urea was added to the same Wheat Straw diet shows the importance of NPN sources in a ruminant's diet.

During the final 7 weeks of the feeding trail, each group continued to lose weight except for the group that was fed the diet supplemented with *Atriplex nummularia.* In fact, this group's daily weight gain increased so much during the second 7 weeks that even though the group lost 43 g/day during the first 7 weeks, after the 14 week trail was over the animals in the group were, on average, 250 g heavier. This translates to a 3.6 g/day weight gain over the entire 14-weeks. The group that showed the second best livestock production was the Alfalfa supplemented group. This group experienced daily weight losses of 22.0 g/day over the entire 14-week period. It should be noted that although the other group's lost weight, they lost less weight during the second seven weeks of the feeding trail. This improvement illustrates the sensitivity of the rumen microbes and the importance of allowing them enough time to adjust to new feed.

There are several reasons why *Atriplex spp.* makes such productive supplements. First of all, *Atriplex nummularia* caused the greatest increase in the livestock's daily intake, from 57.4 g per kg of livestock Body Weight (BW) to 74.6 g/kg BW. Since all five supplemented diets in this study were nearly isonitrogenous, and *Atriplex nummularia* supplemented diet contained less CP than the Urea and Alfalfa diets, this 40% increase cannot be explained solely by the feed's CP values. More important, perhaps, is the fact that *Atriplex nummularia's* low fiber content allowed for quicker and more complete digestion of the feed resulting in greater intake of the feed. Grasses, grains and most conventional feeds are high in fiber and low in N and CP, while the opposite is true for *Atriplex spp.* This is a main reason why it is such a useful supplement in these types of feeds (Chriyaa et al 1997a).

Another very important reason why the *Atriplex nummularia* group was the only one to show weight gains over this feeding trail, and why *Atriplex spp.* make such good supplements in general, is due to its increase in the feed's overall digestibility. *Atriplex nummularia* supplemented feed exhibited the best IVDMD and DDMI, which according to Waldo and Jorgensen (1981), is the best estimate for potential livestock production. When the Wheat Straw was supplemented with *Atriplex nummularia*, it increased the DM digestibility by 26% and caused a 37.2% increase in the digestibility of Crude Protein. These were by far the greatest improvements caused by the supplementation in the study. They also show how even though *Atriplex nummularia* supplemented diet did not have the highest CP content, it still allowed for the greatest overall livestock production and was the only diet that resulted in daily weight gains rather than losses. In addition to *Atriplex spp.* superior digestibility, the retention of nutrients by livestock is also vastly improved when *Atriplex spp.* is added to their feed. In the same study, N-retention went from 0.57g/day in the Unsupplemented Wheat Straw diet to 6.56 g/day when it was supplemented with *Atriplex nummularia.* The final reason why *Atriplex nummularia* was by far the best supplement in this study was the increased rate at which it allowed the DM, CP and Nutrients to be degraded and subsequently absorbed by the livestock. For example, after 72 hours only 22.6% of the Crude Protein in the Unsupplemented Wheat Straw diet was completely degraded. However when *Atriplex nummularia* was added to it, 74.4% of the CP was completely degraded and available to the livestock's intestines (Chriyaa et al. 1997b).

The study by Chriyaa et al. (1997b) explained quantitatively how and why *Atriplex spp.* are productive and useful supplements to the traditional livestock feeds typically found on pastures, i.e. grasses, grains, hay, and any high fiber low protein feed. This is excellent news for farmers and herders in arid regions where *Atriplex spp.* has been planted for range improvement and to combat the desertification and salinisation of valuable soil and cropland. Indeed, several grazing studies from Morocco show that in areas where *Atriplex spp.* was introduced to improve the surrounding rangeland and prevent soil erosion, the live weight gains in the herds of livestock surrounding these areas had greatly increased. This has spawned widespread disapproval amongst those herders whose nearby lands did not receive the *Atriplex spp.* based rangeland improvements.

Among the option to use *Atriplex lentiformis,* grown using the RO concentrate as irrigation water, is to mechanically harvest and bale the plant in a conventional fashion similar to the alfalfa harvesting process as suggested in Watson and O'Leary (1993). The growth habit of *A. lentiformis* may require alternative harvesting techniques. This is part of the current research at the Marana field site. Baling of *A. lentiformis* is one option for product development under investigation. Others include pelletizing and protein extraction. Either method will provide livestock with the additional CP and essential minerals which their diets tend to lack in sufficient quantities.

### *4.5c. Atriplex spp. as supplement to conventional feedlot diet*

While there is substantial research showing the value of *Atriplex spp.* as a feed supplement for livestock in pastures, research focused on its potential as supplement in feedlot diets, where weight gains must be maximized, is far less common. The lack of research by no means indicates a lack of potential. Most of the preliminary research in this field focuses on the processing of *Atriplex spp.* biomass to create a high protein concentrate. Presently, a group of

scientists in Argentina have had the greatest success at such *Atriplex spp.* biomass to protein concentrate processing. Through the development and specialization of selective membrane filtration, Fernández et al. (2007) are able to increase the protein content of *Atriplex lampa* leaf biomass from 21% to 85%, while decreasing its salt content from 26% to 2%. The protein concentrate (retentate) has been safely and successfully added to cattle feedlot diets resulting in greater than average weight gain (Fernández et al. 2003; Fernández et al. 2007).

The purpose of most feedlots is to fatten livestock for slaughter. In order to maximize livestock weight gain, feedlot operators must formulate specific high-energy diets that contain all of the essential minerals and nutrients required for growing livestock. To do so they utilize a "Commodity Barn", which is a combination of different feeds or "commodities" mixed at specific ratio. In order to reduce the cost per head of feeding livestock, groups of farmers, ranchers and feedlot operators combine large quantities of the most cost effective crops and feedstuffs (commodities) and house them in large weather-proof structures (barns). These commodity barns are composed of high ME/calorie feeds, typically grains or grain-based concentrates as well as "Protein Supplements" and "Mineral Premix". These ingredients are mixed together in specific rations to insure maximum livestock production at minimal cost. The premixed combinations of feedstuffs are then sold to local feedlot operators as a complete, low-cost diet for their livestock. *Atriplex spp.* biomass has the potential to effectively replace both of Protein Supplements and Mineral Premix at significantly lower costs with better results.

The protein supplement and mineral premix generated by *Atriplex spp.* biomass provide better livestock production than those used in conventional Commodity Barns because the proteins and minerals from *Atriplex spp.* are plant-based and organic and are therefore more bioavailable during digestion. The essential mineral nutrients provided by the mineral premixes currently used in Commodity Barns tend to be inorganic forms. Limestone ($CaCO_3$) provides the source of Calcium in a standard mineral premix, while Sodium Sulfate is the primary source of Sulfur. Stated previously, *Atriplex lentiformis* is above the critical level for all nine of the most important essential minerals required for ruminant growth and reproduction, including all of the minerals in a standard mineral premix. These 9 minerals include Calcium, Phosphorus, Potassium, Magnesium, Manganese, Iron, Sodium, Copper and Zinc (El-Shatnawi and Turuk 2002). Accordingly, when processed correctly, *Atriplex spp.* provides a more efficient and more readily available source of the essential minerals standard to a feedlot diet than its inorganic counterparts currently used in the mineral premix.

Within the last decade, major advancements have been made in the processing of *Atriplex spp.* biomass aimed at increasing its protein concentration. It is now possible to create a safe and viable protein supplement for use in Commodity Barns from *Atriplex spp.* leaves. As was mentioned previously about the Argentine scientist who increased protein and decreased NaCl, the feat to conduct such an accomplishment came about through the development of a "selective membrane technology" characterized by the scientists as Ultrafiltration followed by Discontinuous Diafiltration (UF-DD) (Fernández et al. 2003; Fernández et al. 2007). The membranes used throughout the UF-DD process were polyethersulfone organic membranes with a molecular weight cut-off value of 10 kD. Thus, the NaCl and other soluble salts where permitted to pass through these membranes while Amino Acids/Proteins were not. The retentate was then further processed through a process called discontinuous diafiltration (DD). During the

DD process, the retentate was diluted multiple times with liquids of alternating high and low pH. Between each dilution/pH change, the retentate was refiltered through the polyethersulfone organic membranes to further increase its protein concentration while reducing its NaCl content. This technology has made it possible to resolve the two major drawbacks of using *Atriplex spp.* as a livestock feed. It is now possible to create a plant-based protein concentrate from *Atriplex spp.* that is safer than the animal-based protein supplement commonly used by feedlot operators.

Regardless of its source, if the dry weight (DM) percentage protein in livestock's feed falls below 8% or 69 g/kg DM, the intake of the feed will drop substantially, causing the livestock to lose weight (Milford and Minson 1965; Aiazzi et al. 1999). A feed with a protein concentration of 69 g/kg DM is the threshold level given by the National Research Council (NRC) for adequate ruminant digestion. When a feed's protein concentration falls below this threshold, the reproduction of rumen microbes is reduced, which causes a reduction in the digestion of incoming feed. Thus, the livestock are forced to reduce the amount of feed they consume and are not be able to gain weight (Boutouba et al. 1990). Although rumen microbes can synthesize most of the essential amino acids from $NH_3$/NPN, they cannot synthesize them all and some essential amino acids must be supplied directly into the livestock's diets. Accordingly, protein supplements are added to livestock feed to insure maximum weight gain.

There are two types of sources of protein used in livestock diets: animal and plant. The animal-based protein supplements are typically low-quality animal parts and byproducts. In recent years, these animal-based proteins have been linked to several health problems in livestock, including diseases that can have lethal effects on the humans who eat them. The most famous of these is mad-cow disease, which was the result of cattle being fed the brains of other cattle and sheep. Fortunately, *Atriplex spp*. and other plant-based proteins provide a safe and effective alternative to those animal-based protein supplements common to the conventional feedlot diet. The plant-based proteins are typically high-protein crops such as grains or legumes that are added directly to the feed or processed to increase their protein concentration. Plant-based protein concentrates are very valuable not only because they provide the greater protein digestibility and retention than their animal-based alternatives, but they are also safer for ruminants. Because ruminants have evolved to digest and process plant proteins, they naturally prefer plant-based protein concentrates. Daily intake and weight gain tends to be higher when livestock are fed plant-based feeds, compared to animal-based feeds.

As previously mentioned, one of the most amazing features of ruminant's fermentative digestion is the fact that their rumen microbes can synthesize their own source protein from Non-Protein Nitrogen. These proteins then provide the animal with an additional source of protein. Accordingly, conventional feedlot diets use additional sources of NPN, such as urea, as low-cost dietary supplements. Studies have shown, however, that cattle receiving urea as a source of protein/NPN gain 4 times less weight and produce less milk than those receiving natural, plant-based sources of protein or NPN (Loosli and Warner 1958). Furthermore, feed-grade urea is unstable and is quickly degraded to $NH_3$. Without proper monitoring, Ammonia Toxicosis will result. Common in cattle, Ammonia Toxicosis, (bovine bonkers syndrome), is a fatal disease affecting the ruminant's Central Nervous System which causes them to stampede and act erratically before succumbing to death. Fortunately for feedlot operators, a large percentage of the Nitrogen in *Atriplex spp.* is NPN which is a safer and more productive alternative to urea as

a NPN feed supplement (Merck Veterinary Manual 2008). Ruminal Acidosis is another common and potentially fatal feedlot ailment that can be remedied by the inclusion of *Atriplex spp.* into livestock feed. It occurs when livestock, cattle in particular, are brought from their pasture into an intensive weight-gain feedlot prior to slaughter. In these feedlots, the livestock are given a high calorie diet consisting of finely ground grains, feed concentrates and a variety of dietary supplements. However, when a ruminant's diet shifts too quickly from a pasture diet of grasses and high fiber forages to a quickly digestible feedlot diet, the rapid digestion of all massive carbohydrates causes a swift increase in volatile fatty acids, specifically lactic acid. This sudden increase in lactic acid can cause a substantial drop in rumen pH which, in turn, causes a drastic shift in microbial populations from gram-negative predominance to gram-positive lactic acid producers (*Streptococcus bovis* and *Lactobacillus* sp.) thus causing a further reduction in pH. Once the pH in the rumen drops below 5.5, normal rumen microbes cannot compete with the acid resistant *lactobacii.* If luminal lactic acid concentrations exceed 100 mM, the osmolarity of the rumen increases to point at which water is drawn into the gastrointestinal tract from the systemic circulation and severe dehydration and circulatory collapse occurs in l to 2 days. However, this can be prevented by a gradual reduction in *Atriplex spp.* stem:leaf ratio in their diet as they make the pasture to feedlot transition. The stems of *Atriplex spp.* are not only high enough in fiber needed by rumen microbes to continue proper digestion but their leaves are also high in protein, a necessary component of any intensive weight-gain diet. *Atriplex spp.* natural combination of high fiber, high protein and high digestibility make it a productive and, most importantly, a safe supplement for intensive feedlots (Chiba 2009).

## 5. Conclusions

The literature reviewed provides compelling evidence that *Atriplex spp.* (including *Atriplex lentiformis* that has been successfully cultivated using Colorado River Water (CRW) RO concentrate) has potential as a supplement in livestock feed. Key considerations for using *Atriplex spp.* as a livestock feed include the salt content (a plus when incorporated in measured amounts), the protein content (comparable to other forage crops) and the digestibility (limited by salt content). However, more research in needed in: i.) the agronomic practice for growing and harvesting the plants, ii.) nutrition studies for effective incorporation into the commodities mix for feed lot and dairy operations, and iii) value added market development.

Given the water resource limits in the desert southwest, the need for water efficient methods for providing nutritional forage to the region's livestock industry, and the potential of *Atriplex spp.* to accommodate these needs, continued research that supports the development of the agronomic potential of halophytes is warranted. Combined with the need to develop and use the region's increasingly saline water resources for farming and municipal use, the development of an eco-industrial approach to municipal scale RO concentrate management has potential to provide a closed-loop, system for creating a feed crop from a waste product that is environmental benign, economically viable and socially responsible.

## References:


Abu-Zanat MMW and MJ Tabbaa. 2006. Effect of feeding *Atriplex* browse to lactating ewes on milk yield and growth rate of their lambs. Small Ruminant Research. 64: 152-161.

Agricultural Research Council (ARC). 1980. The Nutrient requirements of ruminant livestock; ARC – Commonwealth Agricultural Bureaux: Slough, England.

Aiazzi MT, A Abril, PA Torres, JA Di Rienzo and JA Argüello. 1999. Seasonal variations in chemical composition of leaves and stems of *Atriplex cordobensis* (Gandoger et Stuckert), female and male plants. Phyton-International Journal of Experimental Botany. 65: 173-178.

Benjamin RW, Y Lavie, M Forti, D Barkai, R Yonatan and Y Hefetz. 1995. Annual regrowth and edible biomass of two species of *Atriplex* and *Cassia sturtii* after browsing. Journal of Arid Environments. 29: 63-84.

Ben Salem H, A Nefzaoui and L Ben Salem. 2004. Spineless cactus (*Opuntia ficus-indica f. inermis*) and oldman saltbush (*Atriplex nummularia L.*) as alternative supplements for growing Barbarine lambs given straw-based diets. Small Ruminant Research. 51(1): 65-73.

Boutouba A, JL Holechek, ML Galyean, G Núñez-Hernández, JD Wallace and M Cardenas. 1990. Influence of two native shrubs on goat nitrogen status. Journal of Range Management. 43(6): 530-534.

Chiba LI. 2009. Rumen Microbiology and Fermentation. In LI Chiba (Ed.). Animal Nutrition Handbook. pp. 55-79. www.ag.aubun.edu/~chibale/an03microbiology.pdf.

Chriyaa A, KJ Moore and SS Waller. 1997a. Browse foliage and annual legume pods as supplements to wheat straw for sheep. Animal Feed Science and Technology. 62: 85-96.

Chriyaa A, KJ Moore and SS Waller. 1997b. Intake, digestion, and nitrogen balance of sheep fed shrub foliage and medic pods as a supplement to wheat straw. Animal Feed Science and Technology. 65: 183-196.

Dann HM, RJ Grant, KW Cotanch, ED Thomas, CS Ballard and R Rice. 2008. Comparison of brown midrid sorghum-sudangrass with corn silage on lactational performance and nutrient digestibility in Holstein dairy cows. Journal of Dairy Science. 91: 663-672.

El-Shatnawi MKJ and M Turuk. 2002. Dry matter accumulation and chemical content of saltbush (*Atriplex halimus)* grown in Mediterranean desert shrublands. New Zealand Journal of Agricultural Research. 45: 139-144.

Fernández SS, C Menéndez, S Mucciarelli and AP Padilla. 2003. Concentration and desalination of zampa (*Atriplex lampa*) extract by membrane technology. Desalination. 159(2): 153-160.

Fernández SS, C Menéndez, S Mucciarelli and AP Padilla. 2007. Saltbush (*Atriplex lampa*) leaf

protein concentrate by ultrafiltration for use in balanced animal feed formulations. Journal of the Science of Food and Agriculture. 87(10): 1850-1857.

Gihad EA and HM El Shaer. 1994. Utilization of halophytic plants for fodder production with brackish water in subtropic desert. In: VR Squires and AT Ayoub (Eds). Halophytes as a Resource for Livestock and for Rehabilitation of Degraded Lands, Nairobi, Kenya. Kluwer Academic Publishers, Netherlands. pp. 77-96

Guevara JC, LI Allegretti, JA Paez, OR Estevez, HN Le Houérou and JH Silva Colomer. 2005. Yield, nutritional value, and economic benefits of *Atriplex nummularia* Lindl. plantation in marginal dryland areas for conventional forage crops. Arid Land Research and Management. 19(4): 327-340.

Islam M and Adams MA (2000*)* Nutrient distribution among metabolic fractions in 2 *Atriplex spp.* Journal of Range Management. 53: 79-85.

Kearl LC, LE Harris, H Lloyd, MFA Farid and MF Wardeh. 1979. Arab and the Middle East Tables of Feed Composition. Damascus: The Arab Centre for The Studies of Arid Zones and Dry Lands, The league of Arab States, p. 554.

Le Houérou HN. 1991. Feeding shrubs to sheep in the Mediterranean arid zone: intake, performance and feed value. In IVe Congrès International des Terres de Parcours. Montpellier, France. pp. 623– 628.

Loosli JK and RG Warner. 1958. Distillers grains, brewers grains, and urea as protein supplements for dairy rations. Journal of Dairy Science. 41: 1446-1450.

Mahipala MBPK, GL Krebs, P McCafferty and K Dods. 2009. Effects of increasing the inclusion level of *Atriplex amnicola* in the diet of sheep. Animal Production Science. 49(11): 1029-1034.

Masters DG, SE Benes and HC Norman. 2007. Biosaline agriculture for forage and livestock production. Agriculture, Ecosystems and Environment. 119: 234-248.

Merck Veterinary Manual. 2008. www.merckvetmanual.com/mvm/index.jsp.

Milford and Minson. 1965. The energy value of ryegrass and cocksfoot assessed by a slaughter technique with lambs. British Journal of Nutrition. 19: 373-382.

Miyamoto S, EP Glenn and NT Singh. 1994. Utilization of halophytic plants for fodder production with brackish water in subtropic desert. In: VR Squires and AT Ayoub (Eds). Halophytes as a Resource for Livestock and for Rehabilitation of Degraded Lands, Nairobi, Kenya. Kluwer Academic Publishers, Netherlands. pp. 43-75.

Munz PA. 1959. A California flora. University of California Press, Berkeley.

National Research Council (NRC). 2000. Nutrient Requirements of Beef Cattle. 7th Eds. National

Academy Press. Washington, DC.

Norman HC, DG Masters, MG Wilmot and AJ Rintoul. (2008) Effect of supplementation with grain, hay or straw on the performance of weaner Merino sheep grazing old man (*Atriplex nummularia*) or river (*Atriplex amnicola*) saltbush. Grass and Forage Science. 63(2): 179-192.

Osman AE, F Bahhady, N Hassan, F Ghassali and T Al Ibrahim. 2006. Livestock production and economic implications from augmenting degraded rangeland with *Atriplex halimus* and *Salsola vermiculata* in northwest Syria. Journal of Arid Environments. 65(3): 474-490.

Pearce K and R Jacob. 2004. Saltbush lifts sheep meat vitamin content. Farming Ahead. 153: 63.

Shoop MC, RC Clark, WA Laycock and RM Hansen. 1985. Cattle diets on shortgrass ranges with different amounts of fourwing saltbush. Journal of Range Management. 38: 443-449.

Slyter LL, RR Oltjen, DL Kern and JM Weaver. 1967. Microbial species including ureolytic bacteria from the rumen of cattle fed purified diets. Journal of Nutrition. 94: 185-192.

Swingel RS, AR Urias, JC Doyle and RL Voigt. 1978. Chemical composition of kenaf forage and its digestibility by lambs and *in vitro*. Journal of Animal Science. 46(5): 1346-1350.

Swingle RS, EP Glenn and V Squires. 1996. Growth performance of lambs fed mixed diets containing halophyte ingredients. Animal Feed Science Technology. 63: 137- 148.

Waldo DR and NA Jorgensen. 1981. Forages for high animal production: Nutritional factors and effects of conservation. Journal of Dairy Science. 64: 1207-1229.

Watson MC. 1990. *Atriplex* species as irrigated forage crops. Agriculture, Ecocsystems and Environment. 32: 107-118.

Watson MC and WO O'Leary. 1993. Performance of *Atriplex* species in the San Joaquin valley, California, under irrigation and with mechanical harvests. Agriculture, Ecosystems and Environment. 43: 255-266.

Wilson AD and Graetz RD. 1980. Cattle and sheep production and supplementation of *Atriplex-Vestiara* (Saltbush) community. Australian Journal of Agricultural Research. 31(2): 369-378.

www.extension.umn.edu/distribution/livestoclsystems/components/di0469-02.html.

www.landlearnnsw.org.au/sustainability/climate-change/agriculture/livestock/methane.

# Appendix 7:

Sustainable Irrigation Strategies for the Forage Halophyte, *Atriplex lentiformis*

# Sustainable Irrigation Strategies for the Forage Halophyte, *Atriplex lentiformis*

Deserié Soliz[a,*], Edward P. Glenn[a], Martin Yoklic[a], Janick F. Artiola[b], Stephen G. Nelson[a]

[a]Environmental Research Laboratory, The University of Arizona, 2601 East Airport Drive, Tucosn, AZ 85756, USA
[b]University of Arizona, Department of Soil, Water and Environmental Science, Shantz Bldg. 429, Tucson, AZ 85721, USA

*Corresponding author. Tel: 520-626-2162; Fax: 520-573-0852; EM: dsoliz25@msn.com

## Abstract

The forage halophyte, *Atriplex lentiformis*, was grown in field and greenhouse trials to determine yield, water use, and leaching requirements in response to deficit irrigation with saline water. In field trials, *A. lentiformis* had a maximum yield of 24.4 t $ha^{-1}$ when irrigated with brine from a reverse osmosis plant (3 g $L^{-1}$ TDS) at an irrigation rate of 1.0 $ET_o$ (approximately 2 m $yr^{-1}$) in an irrigation district in Marana, Arizona. Higher application rates reduced water use efficiency (WUE) and yield, while WUE increased on lower rates. Greenhouse trials under well-watered conditions showed that the apparent zero-point-salinity for yield was 47.3 g $L^{-1}$ TDS. A further greenhouse experiment was conducted in which plants in sealed pots were grown to the wilting point on a single applications of water. The experiment was conducted at different salinities to see if salinity and water stress were additive factors in reducing yield and WUE. To the contrary, yield and WUE actually increased as a function of salinity, perhaps due to conversion from C3 to C4 photosynthesis over the salinity range (noted in other studies with *A. lentiformis*). Using a simple linear model of salinity vs. irrigation treatment from the literature, we projected yields, water use and drainage values for *A. lentiformis* grown on three salinities (3, 10 and 20 g $L^{-1}$ TDS) and six irrigation volumes ranging from 0.25 to 1.5 $ET_o$. On the lowest salinity, *A. lentiformis* will maintain productivity with minimal discharge of drainage on 0.8 $ET_o$ irrigation. On higher salinities, yield can be maintained only at higher water application rates and the discharge of drainage increases. A mass balance determined for the field plots showed that lysimeter basins had not yet reached equilibrium conditions after three years, and most of the salt applied in the irrigation water was still stored in the root zone. We conclude that xerohalophytes such as *A. lentiformis* could greatly extend the useful range of salinities under which forage crops can be grown in arid-zone irrigation districts.

*Keywords:* soil salinity, halophytes, *Atriplex*, desalination, reverse osmosis

## 1. Introduction

### *1.1 Use of saline water for crop production*

Large volumes of saline water are produced in agricultural districts and by industrial facilities, including reverse osmosis plants and power plant cooling towers. Salinities of these sources range from mildly saline (e.g. < 5 g $L^{-1}$ for typical agricultural return flows and reverse osmosis brines) to quite saline (e.g. 10-20 g $L^{-1}$ for concentrated agricultural and industrial brines). Numerous studies have demonstrated that saline water can be used to produce conventional crop and landscape plants on the lower salinities (Ayars et al., 2006; Gerhart et al., 2006; Miyamoto et al., 2005; Miyamoto and Chacon, 2006; Qadir and Oster, 2004; Shannon et al., 1997). Water management becomes a concern when irrigating with saline water, however.

Conventional crops require a leaching fraction (LF) to control salinity in the root zone. According to a steady-state model widely used in agriculture (Ayers and Westcot, 1985), the leaching requirement (LR) is a function of the salinity of the irrigation supply and the threshold salinity tolerance of the crop:

$$LR = S_w / S_t - S_w \quad (1)$$

where $S_w$ is the salinity of the irrigation water and $S_t$ is the threshold salinity of the soil solution at which yields begin to decline for a given crop. The total irrigation requirements for maximum yield ($Y_{max}$) is:

$$I_v = ET_{max} + LR \quad (2)$$

where $I_v$ is irrigation volume and $ET_{max}$ is crop evapotranspiration at its maximum yield potential. Since $ET_{max}$ is dependent on meteorological conditions, $ET_{max}$ can be expressed in terms of $ET_o$:

$$ET_{max} = k\, ET_o \quad (3)$$

where $ET_o$ is potential ET determined from meteorological data and k is the crop coefficient, the empirically-determined ratio of $ET_{max}$ to $ET_o$ at a given stage of crop development for a particular crop.

When LR and $ET_{max}$ are large, irrigation volumes increase and large volumes of saline drainage water can be discharged past the root zone. The drainage water can damage aquifers, or in irrigation districts with drainage systems, it must be recovered and handled as a waste product (Beltran, 1999). Furthermore, in arid regions agricultural water users must often compete with urban water users for scarce supplies.

Recently, farmers in arid zone irrigation districts around the world have begun practicing deficit irrigation of crops to conserve water supplies (often of necessity due to inadequate deliveries during national water shortages) (Fereres and Soriano, 2006; Geerts and Raes, 2009). Deficit irrigation applies less water than could be consumed by the crop under pristine conditions. Often, however, near-maximal yields can be preserved because water use efficiency (WUE) and harvest index typically increase for a crop grown under water stress. The amount of actual ET ($ET_a$) under deficit irrigation is typically 60-80% of $ET_{max}$.

Salinity can become a major constraint to the practice of deficit irrigation. If suboptimal volumes of irrigation water are supplied, salts tend to accumulate within the root zone. This is why conventional irrigation recommendations call for a generous LR to maintain actual yields ($Y_a$) at 90% to 100% of $Y_{max}$ (Ayers and Westcot, 1985). There is concern that under-irrigating will produce conditions of secondary salinization within the root zone that will eventually lead to very low yields or crop failure (Beltran, 1999). Furthermore, salt stress and moisture stress are often considered as additive stress factors (e.g., Allen et al., 1998; Nimah and Hanks, 1973; Letey et al., 1985; Letey and Dinar, 1986; Bresler, 1987, Bresler and Hoffman, 1986; Cardon and Letey, 1994; Pang and Letey, 1998) that can severely curtail crop yields under deficit irrigation with saline water.

Contrary to Ayers and Westcot (1985), recent transient-state analyses (Letey et al., 2011) show that the so-called steady-state model used to estimate LR results in an over-estimate of the LR needed to support high yields. Furthermore, experiments with several crops show that plant-irrigation-relationships can be highly self-regulating. For example, Shani and Dudley (2001) showed that corn, melon and alfalfa could be irrigated with water ranging from 0.6 g $L^{-1}$ to 6 g $L^{-1}$ salt at irrigation volumes ranging from 0.2 to 1.7 $ET_o$. Contrary to expectations, salt and moisture stresses were not additive in reducing crop yield and interactive effects were not noted. Under deficit irrigation (up to 0.6 $ET_o$), $Y_a$ values were similar across salinities, and were limited only by the available water. At the higher levels of irrigation yields diverged as a function of salinity. Simple linear models could predict yield based on the limiting nature of water or salt stress under a given irrigation scenario.

Dudley et al. (2008) showed that under deficit irrigation these crops produce a minimum LF that increases with the salinity of the irrigation water. Under flood irrigation, salts accumulate at the bottom of the root zone. Eventually salinity in the soil water at the bottom of the root zone reaches the zero yield potential point ($S_{max}$), the theoretical salinity at which water uptake and growth ceases (Ayers and Westcot, 1985). This saline water exits the root zone as the LF. However, growth and water uptake continue in the upper portion of the root zone where salinities are lower (see also Letey et al., 2011). The same principle applies to other forms of irrigation (e.g., drip) but the geometry of salt distribution in the root zone is different (Mmolawa and Or, 2000).

Shani and Dudley (2001) and Dudley et al. (2008) found that under that under deficit irrigation, there is a maximum amount of salt that can be stored in the root zone. Above this value crops will reduce transpiration and leaching will occur, and more extensive yield loss will not occur from repeating the irrigation schedule. They showed that for melon, a salt-sensitive crop, LF values were 0.11 to 0.54 on irrigation salinities of 0.8 g $L^{-1}$ to 6 g $L^{-1}$ when irrigated at $ET_{max}$ without a LR. Yield reductions across this salinity range were 40% to 80% of $Y_{max}$ but yields were sustainable over time.

*1.2 Halophytes to extend the salinity range*

Halophytes can greatly extend the useful salinity range for crop production (Glenn et al., 1999); with some species maintaining productivity on salinities exceeding seawater (e.g., 40 g $L^{-1}$) (OLeary et al., 1985). Xerohalophytes are plants capable of tolerating both moisture and salinity stress simultaneously and they could be especially valuable in deficit irrigation schemes. Several xerohalophtes in the genus *Atriplex* have high yields and produce useful forage material on a wide range of salinities (Glenn et al., 1999). In previous studies we showed that *Atriplex*

*lentiformis* Torr. (quailbush) produced 24.4 t $ha^{-1}$ $yr^{-1}$ of biomass on irrigation volumes equal to potential ET ($ET_o$) (ca. 2 m $yr^{-1}$) when irrigated with mildly saline brine (ca. 3 g $L^{-1}$) from a reverse osmosis desalination plant in a three-year lysimeter trial in a Sonoran Desert irrigation district in Marana, Arizona (Jordan et al., 2009; Soliz et al., 2011). The same species was successfully grown under extreme deficit irrigation (0.2 $ET_o$) with mildly saline irrigation water (1.2 g $L^{-1}$) in a five year field trial in the Mohave Desert in Twenty-Nine Palms, California (Glenn et al., 2009). Plants grew slowly but formed a nearly closed canopy within the first three years of irrigation. At the other extreme of salinity, when irrigated with hypersaline seawater (40 g $L^{-1}$) in a coastal desert environment at Puerto Penasco, Mexico, yields of 18 t $ha^{-1}$ $yr^{-1}$ were obtained when plots were flood irrigated daily (OLeary et al., 1985).

*A. lentiformis* clearly has potential as a saline water crop to be used under diverse scenarios of conventional and deficit irrigation management and over a wide salinity range. However, the effects of salinity on growth and WUE and the interactions between salinity and moisture stress have not been systematically explored for this species as they have for crop plants. In this paper, we combine greenhouse experiments with previously collected field data to develop yield and water use functions for *A. lentiformis* under irrigation volumes ranging from 0.25 to 1.5 $ET_o$, at irrigation salinities of 3, 10 and 20 g $L^{-1}$, covering the practical range of irrigation and salinities that might be encountered in field applications for this plant. We take the model of Dudley et al. (2008) in projecting yields as a function of salinity under optimal and deficit irrigation scenarios. The greenhouse and field results show that WUE increases markedly with both increasing salinity and decreasing irrigation volumes. Contrary to salinity being an additive stress, moderate salinities enhance the ability of the plant to extract water from a drying soil. The modeling results show that this plant can be grown productively under deficit irrigation even on highly saline water.

## 2. Materials and Methods

### *2.1 Greenhouse growth experiments*

Two experiments were conducted in a greenhouse at the Environmental Research Laboratory in Tucson, Arizona. The greenhouse has approximately 80% light transmission and is heated in winter and evaporatively cooled in summer. For both experiments, seeds were germinated in trays on fresh water then transplanted to pots filled with a mixture of medium texture sand and potting mix (Sunshine Mix No. 1, Sun Gro Horticulture, Bellevue, Washington) (2:1 by volume).

Experiment One was designed to determine the growth response to salinity under optimal irrigation conditions. This experiment was conducted in June and July, 2010 in 4 L capacity pots, following methods described in Glenn and OLeary (1984) and Vasquez et al. (2006). Five replicate plants per treatment were irrigated with solutions containing 0.25 g $L^{-1}$ soluble fertilizer (Mir Gro, 20% N -20% P - 20% K, plus trace metals, Scotts Miracle-Gro, Inc., Marysville, Ohio) and NaCl to produce treatment salinities of 0 g $L^{-1}$ (no added NaCl), 5 g $L^{-1}$, 10 g $L^{-1}$, 20 g $L^{-1}$ and 30 g $L^{-1}$ NaCl. Pots were arranged in a block design on a greenhouse bench with the five blocks arranged along a small temperature gradient from the pad end to the fan end of the greenhouse. They were irrigated daily with 1 L of solution, which produced sufficient drainage to keep the pots within 10% of the target salinity throughout the experiment. The experiment lasted 30 days, at which point plants on the fastest growing treatment had filled the pots with root

mass and plants were ca. 40-50 cm in height. Plants were cut at the soil line, and shoots were oven dried to constant weight to determine dry biomass production and cation and anion content (Soil, Water and Planting Testing Laboratory, University of Arizona, Tucson, AZ).

Experiment Two was designed to test the combined effect of salt stress and moisture stress on plant growth and water use efficiency, to define the lower limit of moisture content and the upper limit of salinty at which plants could extract water from the soil solution. Plants (four replicates per treatments) were grown to the wilt point in sealed pots using methods described in Glenn and Brown (1998). Each pot (2 L capacity) was lined with plastic sheeting to prevent drainage and filled with 1600 grams of air-dried soil plus potting mix. Each pot received 800 ml of treatment solution. Treatment solutions were made up in distilled water containing 0.5 g Mir Gro soluble fertilizer, plus NaCl to produce treatment salinities of 0 g $L^{-1}$, 5 g $L^{-1}$, 10 g $L^{-1}$, 20 g $L^{-1}$ and 30 g $L^{-1}$. The plastic enclosing the soil was sealed across the top of the pot, except for a small opening to receive the transplant. After planting, the plastic cover was drawn around the plant stem and the surface of the pot was covered with white styrofoam packing chips as an additional vapor barrier, and the pot was wrapped in aluminum foil as a heat shield. Control pots were prepared the same as treatment pots but did not receive transplants. Analyses showed control pots contained approximately 730 mg of total dissolved solids, containing 125 mg $Na^{+}$, 90 mg $K^{+}$, 50 mg $Ca^{+2}$, and 23 mg $Mg^{+2}$ per pot at the start of the experiment.

Pots were randomly assigned to treatment, based on a random number table. Experiment Two was conducted from March to May, 2007 (before Experiment One). Plant heights and pot weights were determined approximately weekly. Plants were harvested when they showed signs of wilting, and when pot weights no longer decreased from week to week, indicating they had ceased to remove water from the pot.

On harvest, plant shoots were processed as in Experiment One. Then the soil in each pot was removed, mixed thoroughly, and sampled to determine residual moisture content and salt content. Residual moisture content was determined by oven drying a 10 g soil sample. The dried sample was then extracted in 50 ml of distilled water and electrical conductivity (EC) was determined with a Markson EC meter (Markson Scientific, Inc., Henderson, North Carolina) calibrated with standards of NaCl covering the range of salinities encountered in the extracts. These readings were used to determine grams of NaCl per gram soil and per gram residual soil moisture in each pot at harvest.

### *2.2 Statistics and other calculations for greenhouse experiments*

WUE (g dry weight shoots per kg water) was calculated from the g dry weight of shoots per pot divided by the kg water used per pot minus the mean loss of water from control pots. Growth and water use characteristics of *Atriplex* species were analyzed by one-way analysis of variance (ANOVA) with salinity as the independent variable. Treatment effects were considered significant if $P < 0.05$. Linear and curvilinear equations were fitted to data using curve fitting software in SigmaPlot.

### *2.3 Mass balance of field plots based on sodium*

A mass balance for each field irrigation treatment in Soliz et al. (2011) was conducted by analyzing the irrigation supply, soil, plant tissue and surface litter for $Na^{+}$ after three years of irrrigation in each treatment in lined lysimeter tanks. $Na^{+}$ in soil was measured at 30 cm depth

increments over the first 2 m of soil profile in samples pooled by treatment across replicates. $Na^+$ in soil was expressed in units of kg $m^{-2}$ using a bulk density of soil of 1.4 g $cm^{-3}$ (Jordan et al., 2009) to calculate weight of soil in the profile. $Na^+$ in plant tissue and leaf litter was measured in whole plants and 0.0626 $m^2$ surface samples, respectively, from individual plots. Plant $Na^+$ was expressed in units of kg $m^{-2}$ based on the biomass yield in each plot reported in Soliz et al. (2011). $Na^+$ in the irrigation and drainage water were estimated from the electrical conductivity (EC) of samples taken approximately monthly for the irrigation supply and when available for the drainage water. The relationship between EC (dS $m^{-1}$) and mg $L^{-1}$ $Na^+$ was based on an analysis of irrigation water showing that 1 dS $m^{-1}$ = 0.12 mg $L^{-1}$ $Na^+$, with $Na^+$ accounting for 19% of total salts in the irrigation supply.

*2.4 Model for deficit irrigation scenarios*

Yield and water use functions were modeled using values for $Y_{max}$, $ET_{max}$, WUE, $S_t$, $S_{max}$ from field and greenhouse data. Equations were based on those in Dudley et al. (2008), Allen et al. (1998) and Ayers and Westoct (1985). We modeled the yield and water use response of *A. lentiformis* to three salinities (3 g $L^{-1}$, 10 g $L^{-1}$ and 20 g $L^{-1}$) and six irrigation scenarios with $I_v$ = 0.25 $ET_o$, 0.5 $ET_o$, 0.75 $ET_o$, 1.0 $ET_o$, 1.25 $ET_o$ and 1.5 $ET_o$. We modeled results over an idealized annual cycle of irrigation after the soil-water system reached equilibrium conditions rather than over individual irrigation cycles, and we did not consider effects of soil matrix potential or differential water uptake by roots at different soil levels in the calculations, as these effects are not known for *A. lentiformis* (see Results and Discussion). We assumed a linear relationship between transpiration and yield (Dudley et al., 2008) except at $I_v$ above 1.0 $ET_o$ where yields decrease due to lowered WUE (Soliz et al., 2011). Effects of precipitation were not considered in this generalized model.

Following Dudley et al. (2008) we approximated LF, the fraction of $I_v$ that becomes too saline to support growth and transpiration, as:

$$LF = S_w/S_{max} \quad (4)$$

We calculated $Y_a$ as:

$$Y_a = Y_{max} (I_v - LF\ I_v)/ET_{max} \quad (5)$$

and:

$$ET_a = I_v - LF \quad (6)$$

We set $ET_{max} = ET_o$ based on field results. We assumed $Y_a$ was proportional to $ET_a$ at $ET_a$ of $ET_o$ or less. However, irrigation with 1.5 $ET_o$ lowered yields in the field by 15% due to decreased WUE, so for $ET_a$ above $ET_o$ we diminished $Y_a$ below $Y_{max}$ in proportion to excess water delivery (Soliz et al., 2011).

Equation (5) diminishes $Y_a$ and $ET_a$ below $Y_{max}$ and $ET_{max}$ based on the amount of water available to support transpiration under a given salinity and irrigation volume scenario, using the value of $S_{max}$ determined in the greenhouse studies as the salinity for zero growth and transpiration. When $S_w$ approaches $S_{max}$, $Y_a$ becomes 0. For each scenario, we adjusted $I_v$ and

$S_w$ for the amount of water and salts left behind by the previous annual irrigation cycle (Dudley et al., 2008). We considered the rooting depth as 1 m and that soil moisture content at field capacity was 0.1 $m^3$ $m^{-3}$ based on neutron probe measurement (Soliz et al., 2011). We considered that the residual salinity of that water was $(S_w + S_{max})/2$ (Ayer and Westcot, 1985), and used these values to adjust $I_v$ and $S_w$ for each irrigation scenario (Duldey et al., 2008).

## 3. Results and Discussion

### *3.1 Relative yield, drought tolerance and WUE versus salinity in greenhouse trials*

When irrigated daily with saline water in Experiment One, *A. lentiformis* plants had maximum biomass production on 5 g $L^{-1}$ (10.8 g per plant), and decreased production above or below this salinity (Figure 1) ($F = 26.0$, $P < 0.001$, df = 4, 10). The decrease in yield above 5 g $L^{-1}$ was a linear function, with a linearly-extrapolated value for zero yield at 47.3 g $L^{-1}$. Hence, in Equation (4), $S_t$ = 5 g $L^{-1}$ and $S_{max}$ = 47.3 g $L^{-1}$. Alfalfa is plotted on the same graph for comparison (based on literature values) (Ayers and Westocot, 1985); *A. lentiformis* has about five times higher salt tolerance than alfalfa. $Na^+$ and $Cl^-$ increased in above-ground biomass as a function of salinity (Figure 2) but only the $Cl^-$ increase was significant ($F = 27.2$, $P = 0.004$, df = 4,10). Total salts ranged from 14.8 % of dry matter on 5 g $L^{-1}$ to 24.3 % on 30 g $L^{-1}$, with the treatment effect marginally insignificant ($F = 2.98$, $P = 0.073$, df = 4, 10).

Experiment Two was designed to detect the limits for growth and water use under combined salt and moisture stress. We tested the hypothesis that salt and drying were additive stress factors for *A. lentiformis*. We predicted that salinity would have a negative effect on final biomass yield and WUE, and that plants on saline solutions would leave more water behind in pots at the wilt point than plants grown without added salts. Plants in sealed pots with a limited water supply grew more slowly than in Experiment One, requiring 48 – 60 days to reach their wilt points, with final shoot dry weight ranging from 0.7 to 2.8 g among treatments. The results were the opposite of our starting hypotheses. Final biomass actually increased with salinity ($F = 26.0$, $P < 0.001$, df = 4, 10), with the data fitting a hyperbolic rise-to-a-maximum function (Figure 3A). Plants on the 5 g $L^{-1}$ treatment had the highest water use, consuming nearly all of the 800 ml added to the pot (Figure 3B). Control pots without plants had very low water loss. Plants on the 0 g $L^{-1}$ treatment had the highest soil moisture content at the plant wilt point (i.e., they left the most water behind). Plants on 5 g $L^{-1}$ had the lowest final soil moisture (ca 0.02 g $g^{-1}$), while plants on 10 – 30 g $L^{-1}$ treatments had final soil moisture values of 0.07 – 0.09 g $g^{-1}$ (Figure 3C) ($F = 4.50$, $P < 0.001$, df = 4, 10). WUE increased markedly with salinity (Figure 3D) ($F = 24.5$, $P < 0.001$, df = 4, 10). Final soil salinities at the wilt point were about 3-4 times higher (Figure 4) than the predicted zero point of 47.3 g $L^{-1}$ extrapolated from Experiment One. It is likely that setting $S_{max}$ at 47.3 g $L^{-1}$, derived from linear extrapolation in Experiment One, is an underestimate of the true zero point for growth and transpiration of this species. Moisture and salt stress were clearly not additive stress factors in terms of plant growth and survival for *A. lentiformis*. Just the opposite, interaction effects were positive: salinity enhanced yield and WUE, and drying appeared to increase $S_t$.

The data are not at all typical of conventional crop responses to salinity. However, they are consistent with other physiological studies of euhalophytes, which show that these plants are typically stimulated by moderate salinity levels relative to their growth on non-saline water (Flowers, 1985; Glenn et al., 1999). The reason for this stimulation is not known, but might be

related to the need for the plants to take up cations and anions (particularly $Cl^-$) to support osmotic adjustment (Glenn and Brown, 1998). Regarding the increase in biomass production and WUE as a function of salinity in Experiment Two, this might be related to a shift from C3 to C4 photosynthesis over the salinity range. Zhu and Meinzer (1999) grew *A. lentiformis* on a salinity gradient from 0 to 34 g $L^{-1}$ NaCl and reported a similar growth response to ours. They also showed that the ratio of ribulose-1,5-bisphosphate carboxylase/oxygenase (Rubisco) activity to that of phosphoenolpyruvate carboxylase (PEPC) decreased from 0.96 in plants grown at 0 g $L^{-1}$ NaCl to 0.37 in plants grown at 34 g L-1 NaCl because PEPC activity on a leaf area basis increased linearly with increasing salinity, while Rubisco activity remained relatively constant. These data indicate a marked shift from the C3 pathway for photosynthesis (using Rubisco) at low salinity to the C4 pathway (using both PEPC and Rubisco) at high salinities, leading to a higher WUE and, under the conditions of our experiment, higher final biomass production. Similar results were reported for the C4 xerophyte, *Atriplex halimus*, grown on a salinity gradient (Alla et al., 2011). An increased salt tolerance of plants on drying soils relative to growth under non-limiting water conditions was also noted for the halophyte *Sesuvium portulacastrum* (Slama et al., 2008).

### *3.2 Field data for $ET_{max}$, $Y_{max}$, WUE and rooting depth*

In field experiments in Marana, *A. lentiformis* was grown in 16, 4 m x 4 m x 2.5 m depth drainage lysimeters for three years on three irrigation treatments (four lysimeters per treatment) (Jordan et al., 2009; Soliz et al., 2011): 1.0 $ET_o$, adjusted daily to match Penman-Monteith $ET_o$ determined at an on-site meteorological station; 1.5 $ET_o$ adjusted daily; and 1.0 $ET_o$ presented as a constant daily fraction of annual $ET_o$ from the previous year's data (i.e., $ET_o$/365). The purpose of the first two treatments was to determine $Y_{max}$ and $ET_{max}$, while the constant-rate $ET_o$ treatment was designed to see if irrigation water could presented on a constant schedule, as would be produced from an industrial source, with excess water supplied in winter used to support summer $ET_a$, taking advantage of the deep root system of *A. lentiformis*. The irrigation source was effluent from a reverse osmosis plant at about 3 g $L^{-1}$ salinity. Results are summarized in Table 1. $Y_{max}$ was 24.4 t $ha^{-1}$ $yr^{-1}$ dry shoot biomass at $ET_a = ET_o$. Yield actually decreased on the 1.5 $ET_o$ treatment to 15 t $ha^{-1}$ $yr^{-1}$. The constant-rate $ET_o$ and 1.5 $ET_o$ treatments produced drainage but over three years the 1.0 $ET_o$ treatment did not. As a result, the experiment produced different values of $ET_a$ and $Y_a$ for each treatment, allowing WUE to be plotted as a function of $ET_a$ (Figure 5). Similar to results with salinity, WUE increased with diminished water supply.

### *3.3 Models of yield and water use functions under different irrigation scenarios*

Results of model calculations are in Tables 2- 4 and the trends are illustrated in Figure 6. The yield response (Figure 6A) is very similar in form to that determined for melons by Dudley et al. (2008), except that the scales of the independent variables are stretched for *A. lentiformis*. Irrigation volumes ranged from 0.6 ETo to 1.4 ETo for melons, but 0.25 ETo to 1.5 ETo for *A. lentiformis*. Salinities ranged from 0.8 g $L^{-1}$ to 6 g $L^{-1}$ for melons but 0 g $L^{-1}$ to 20 g $L^{-1}$ for *A. lentiformis*. Melons had 80% yield reduction when irrigated with 6 g $L^{-1}$ water at a rate of 1.0 $ET_o$, whereas those conditions were near the optimal for biomass yield of *A. lentiformis*. When irrigated at 1.5 $ET_o$, *A. lentiformis* could maintain yields from 15-24 t $ha^{-1}$ $yr^{-1}$ across the salinity

range, but with high rates of discharge of water and salts past the root zone. Under water-limiting conditions, LF for plants on 3 g $L^{-1}$, 10 g $L^{-1}$ and 30 g $L^{-1}$ were 0.086 – 0.141, 0.226 – 0.275 and 0.432 – 0.456, respectively, depending on irrigation scenario within each salinity.

The optimal scenario to maximize yield and minimize drainage was an irrigation rate of 1.0 $ET_o$ at $S_w$ of 3 g $L^{-1}$ at 1.0 $ET_o$. This would make *A. lentiformis* a good candidate for high-yield forage production using mildly saline agricultural or industrial brines. On the other hand, under extreme deficit irrigation *A. lentiformis* will remain viable across the salinity range, making it a good candidate for absorbing low rates of brine discharge with minimal leaching past the root zone if yield is not a concern (Glenn et al., 2009).

### *3.4 Salt balance in field lysimeters after three years of irrigation*

The projected results in Figure 5 and Tables 2-4 are highly idealized. We conducted a salt balance with respect to $Na^+$ to determine actual patterns of salt uptake and discharge in lysimeter tanks (Figure 6). Over the first three growing seasons, none of the treatments approached equilibrium conditions expected from Tables 2-4. Tanks in the 1.0 $ET_o$ treatment did not produce drainage over three years, and nearly all the $Na^+$ was retained in the soil profile. Plants on the 1.5 $ET_o$ treatment produced drainage (mean EC = 6.69 dS $m^{-1}$), with about 0.8 kg $Na^+$ discharged in drainage water. However, this is lower than the 1.8 kg $Na^+$ expected for this irrigation treatment in Table 2 (e.g., 19% of 9 kg total salts). The constant-rate $ET_o$ treatment produced a small amount of drainage (mean ET = 6.08 dS $m^{-1}$) in winter, when the storage capacity of the soil profile was exceeded and $ET_a$ was low. Longer-term experiments with halophyte crops are needed to work out the agronomic details.

## 4. Conclusion

The performance of *A. lentiformis* over the range of salinities and irrigation volumes should be tested under actual field conditions, but the results of the greenhouse studies show that it is extremely salt tolerant and that water stress and salinity both enhance WUE; it can be grown under both high-salinity and low-salinity irrigation under a wide range of irrigation scenarios. There is a need to develop best agronomic practices to produce *A. lentiformis* as a high-quality forage acceptable to the animal feed industry. Animal feeding trials have shown that halophyte forages can substitute for conventional forages and are good range plants for livestock, but so far they have not been produced in sufficient quantity or quality to be evaluated as commercial feed ingredients. Previous results showed that $ET_{max}$ was highest Year One, and that plants became progressively woodier and had lower nutrient value with age. Hence, it might be more feasible to treat this as an annual rather than a perennial crop. Other xerohalophytes likely share the same traits as *A. lentiformis*, and candidate species should be drawn from the local flora when possible to avoid needless plant introductions to new locations.

## References

Alla, M. M. N., Khedr, A. H. A., Erag, M. M., Abu-Alnaga, A. Z., Nada, R. M., 2011. Physiological aspects of tolerance in *Atriplex halimus* L. to NaCl and drought. Acta Physiologiae Plantarum 33, 547-557.

Allen, R. G., Pereira, L. S., Raes, D., Smith, M., 1998. Crop evapotranspiration: Guidelines for computing crop water requirements – FAO Irrigation and drainage paper 56. Food and Agriculture Organization of the United Nations, Rome.

Ayers, J., Christen, E., Sooper, R., Meyer, W., 2006. The resource potential of in-situ shallow ground water use in irrigated agriculture: a review. Irrig. Sci. 24, 147-160.

Ayers, R. S., Westcot, D. W., 1985. Water quality for agriculture. FAO Irrig. Drain. Paper 29, Rev. I. FAO, Rome, Italy.

AZMET. 2010. The Arizona Meteorological Network. http://cals.arizona.edu/azmet/. (last visited June, 2010).

Beltran, J., 1999. Irrigation with saline water: benefits and environmental impact. Agricultural Water Management 40, 183-194.

Bresler, E., 1987. Application of conceptual model to irrigation water requirement and salt tolerance of crops. Soil Sci. Soc. Am. J. 51, 788-193.

Bresler, E., Hoffman, G., 1986. Irrigation management for salinity control: Theories and tests. Soil Sci. Soc. Am. J. 50, 1552-1560.

Cardon, G., Letey, J., 1994. Plant water uptake terms evaluated for soil water and solute movement models. Soil Sci. Soc. Am. J. 32, 1876-1880.

Fereres, E., Soriano, M. A., 2006. Integrated approaches to sustain and improve plant production under drought stress. Journal of Experimental Botany 58, 147-159.

Flowers, T. J. 1985. Physiology of halophytes. Plant and Soil. 89, 41-56.

Title: Deficit irrigation as an on-farm strategy to maximize crop water productivity in dry areas
Author(s): Geerts S, Raes D
Source: **AGRICULTURAL WATER MANAGEMENT** Volume: **96** Issue: **9** Pages: **1275-1284** Published: **SEP 2009**

Gerhart, V., Kane, R., Glenn, E., 2006. Recycling industrial saline wastewater for landscape irrigation in a desert urban area. J. Arid Environ. 67, 473-486.

Glenn, E. P., Brown, J. J., 1998. Effects of soil salt levels on the growth and water use efficiency of *Atriplex canescens* (Chenoposiaceae) in drying soil. American Journal of Botany 85, 10-16.

Glenn, E., Brown, J., Blumwald, E., 1999. Salt tolerance and crop potential of halophytes. Crit. Rev. Plant Sci. 18, 227-255.

Glenn, E., Mckeon, C., Gerhart, V., Nagler, P., Jordan, F., Artiola, J. 2009. Deficit irrigation of a landscape halophyte for reuse of saline waste water in a desert city. Landscape and Urban Planning 89, 57-64.

Glenn, E. P., OLeary, J. W., 1984. Relationship between salt accumulation and water content of dicotyledenous halophytes. Plant Cell and Environment 7, 253-261.

Jordan, F. L., Yoklic, M., Morino, K., Brown, P., Seaman, R., Glenn, E. P., 2009. Consumptive water use and stomatal conductance of *Atriplex lentiformis* irrigated with industrial brine in a desert irrigation district. Agric. Forest Meteor. 149, 899-912.

Letey, J, Dinar, A., 1986. Simulated crop-production functions for several crops when irrigated with saline waters. Hilgaria 54, 1-32.

Letey, J., Dinar, A., Knapp, K.C., 1985. Crop-water production function model for saline irrigation waters. Soil Sci. Soc. Am. J. 49, 1005-1009.

Letey, J., Hoffman, G. J., Hopmans, J. W., Grattan, S. R., Suarez, D. L., Corwin, D. L., Oster, J. D., Wu, L., Amrheim, C. 2011. Evaluation of soil salinity leach requirement guidelines. Agricultural Water Management 98, 502-506.

Miyamoto, S., Chacon, A., Hossain, M., Martinez, I., 2005. Soil salinity of urban turf areas irrigated with saline water: I. Spatial variability. Landsc. Urban Plann. 71, 233-241.

Miyamoto, S., Chacon, A., 2006. Soil salinity of urban turf areas irrigation with saline water - II. Soil factors. Landsc. Urban Plann. 77, 28-38.

Mmolawa, K., Or, D. 2000. Root zone solute dynamics under drip irrigation: A review. Plant and Soil 222, 163-190.

Nimah, M., Hanks, R. J., 1973. Model for estimating soil, water, plant and atmosperic interelations: I. Description and sensitivity. Soil Sci. Som. Am. Proc. 37, 522-527.

OLeary, J. W., Glenn, E. P., Watson, M. C., 1985. Agricultural production of halophytes with seawater. Plant and Soil 89, 311-321.

Pang, X. P., Letey, J., 1998. Development and evaluation of EN-VIRO-GRO, an integrated water, salinity and nitrogen model. Soil Sci. Soc. Am. J. 62, 1418-1427.

Qadir, M., Oster, J., 2004. Crop and irrigation management strategies for saline-sodic soils and waters aimed at environmentally sustainable agriculture. Sci. Total Environ. 323, 1-19.

Shani, U., Duley, L. M. 2001. Field studies of crop response to water and salt stress. Soil Sci. Soc. Am. J. 65, 1522-1528.

Shannon, M., Cervinka, V., Daniel, D., 1997. Drainage water reuse, in: Madramootoo, C., Johnson, W. and Willardson, L. (Eds.), Management of Agricultural Drainage Water Quality, FAO, Rome, Chapter Four (on-line document, no page numbers). http://www.fao.org/docrep/w7224e/w7224e08.htm.

Slama, I., Ghnaya, T., Savoure, A., Abdelly, C., 2008. Combined effects of long-term salinity and soil drying on growth, water relations, nutrient status and proline accumulation of *Sesuvium portulacastrum*. Comptes Rendus Bologies 331, 442-451.

Soliz, D., Glenn, E. P., Seaman, R., Yoklic, M., Nelson, S. G., Brown, P., 2011. Water consumption, irrigation efficiency and nutritional value of *Atriplex lentiformis* grown on reverse osmosis brine in a desert irrigation district. Agric. Ecosyst. Environ. 140, 473-483.

Vasquez, E. A., Glenn, E. P., Guntenspergen, G. R., Brown, J. J., Nelson, S. G., 2006. Salt tolerance and osmotic adjustment of *Spartina alterniflora* (Poaceae) and the invasive M haplotype of *Phragmites australis* (Poaceae) along a salinity gradient. American Journal of Botany 93, 1784-1790.

Table 1. Water use and yield of *Atriplex lentiformis* grown for 3 seasons (885 days) in drainage lysimters in an irrigation district in Marana, Arizona. Water units are cumulative over the experiment are are in units of mm $m^{-2}$. Means followed by different letters within a row are significantly different at $P < 0.05$ by Tukey's test. Data are from Soliz et al. (2011).

| **Irrigation Treatment:** | **1.0 $ET_o$** | **1.5 $ET_o$** | **Constant Rate $ET_o$** |
|---|---|---|---|
| **ETo (mm)** | 5334 | 5334 | 5335 |
| **Rain (mm)** | 355 | 355 | 355 |
| **Applied Water @ 3 g $L^{-1}$ TDS** | 4128 | 6309 | 3931 |
| **ETa (mm)** | 4897ab | 5742a | 3742b |
| **Drainage (mm)** | 0a | 934b | 534b |
| **Soil Storge Mmm)** | -59 | -16 | 9 |
| **Biomass** | 7.33a | 6.23b | 7.20a |

Table 2. Approximate mass balance calculation for *Atriplex lentiformis* grown on different annual irrigation volumes determined as a function of potential ET ($ET_o$ = 2 m $yr^{-1}$) and at a irrigation salinity of 3 g $L^{-1}$ TDS. The table assumes that maximum biomass yield is 24.4 tons $ha^{-1}$ when 2.0 m of water is consumed and that yield and water consumption decrease linearly with irrigation volumes. It also assumes that the maximum salinity at which the plant can extract water is 47.3 g $L^{-1}$ TDS and that above that water above that salinity exits the root zone as drainage. Volumes of water and weights of salt are per $m^2$ of ground area.

| **Treatement (x $ET_o$)** | **Applied $H_2O$ (m $yr^{-1}$)** | **Consumed $H_2O$ (m $yr^{-1}$)** | **Drained $H_2O$ (m $yr^{-1}$)** | **Drainage Fraction** | **Yield (tonne $ha^{-1}$ $yr^{-1}$)** | **Drainage Salinity (g $L^{-1}$)** | **Drained Salts (kg $m^{-2}$ $yr^{-1}$)** |
|---|---|---|---|---|---|---|---|
| **1.5** | 3.0 | 2.0 | 1.0 | 0.333 | 17.3 | 9 | 9 |
| **1.25** | 2.5 | 2.0 | 0.5 | 0.200 | 24.4 | 15 | 7.5 |
| **1.00** | 2.0 | 1.83 | 0.17 | 0.086 | 22.3 | 47.3 | 5.6 |
| **0.75** | 1.5 | 1.36 | 0.14 | 0.093 | 16.6 | 47.3 | 4.2 |
| **0.5** | 1.0 | 0.89 | 0.11 | 0.106 | 10.9 | 47.3 | 2.8 |
| **0.25** | 0.5 | 0.43 | 0.071 | 0.141 | 5.2 | 47.3 | 1.4 |

Table 3. Same as Table 3 but irrigation salinity is 10 g $L^{-1}$.

| Treatement ($x ET_o$) | Applied $H_2O$ ($m\ yr^{-1}$) | Consumed $H_2O$ ($m\ yr^{-1}$) | Drained $H_2O$ ($m\ yr^{-1}$) | Drainage Fraction | Yield (tonne $ha^{-1}\ yr^{-1}$) | Drainage Salinity ($g\ L^{-1}$) | Drained Salts ($kg\ m^{-2}\ yr^{-1}$) |
|---|---|---|---|---|---|---|---|
| **1.5** | 3.0 | 2.0 | 1.0 | 0.333 | 24.4 | 30 | 30 |
| **1.25** | 2.5 | 1.93 | 0.57 | 0.226 | 23.5 | 47.3 | 25 |
| **1.00** | 2.0 | 1.54 | 0.46 | 0.230 | 18.7 | 47.3 | 19.9 |
| **0.75** | 1.5 | 1.15 | 0.35 | 0.235 | 14.1 | 47.3 | 15.1 |
| **0.5** | 1.0 | .75 | 0.25 | 0.246 | 9.2 | 47.3 | 9.9 |
| **0.25** | 0.5 | .36 | 0.14 | 0.275 | 4.4 | 47.3 | 5.2 |

Table 4. Same as Table 1 but irrigation salinity is 20 g L-1. The drainage fraction under salinity limited conditions is now 20/47.3 = 0.42.

| Treatement ($x ET_o$) | Applied $H_2O$ ($m\ yr^{-1}$) | Consumed $H_2O$ ($m\ yr^{-1}$) | Drained $H_2O$ ($m\ yr^{-1}$) | Drainage Fraction | Yield (tonne $ha^{-1}\ yr^{-1}$) | Drainage Salinity ($g\ L^{-1}$) | Drained Salts ($kg\ m^{-2}\ yr^{-1}$) |
|---|---|---|---|---|---|---|---|
| **1.5** | 3.0 | 1.70 | 1.30 | 0.432 | 20.7 | 47.3 | 59.6 |
| **1.25** | 2.5 | 1.41 | 1.09 | 0.434 | 17.2 | 47.3 | 49.7 |
| **1.00** | 2.0 | 1.13 | 0.87 | 0.437 | 13.8 | 47.3 | 39.7 |
| **0.75** | 1.5 | 0.84 | 0.66 | 0.441 | 10.2 | 47.3 | 29.8 |
| **0.5** | 1.0 | 0.54 | 0.46 | 0.456 | 6.5 | 47.3 | 19.9 |
| **0.25** | 0.5 | 0.26 | 0.24 | 0.471 | 3.2 | 47.3 | 9.9 |

Figure Captions

Figure 1. Growth response of *Atriplex lentiformis* to salinity in a greenhouse experiment in Tucson, Arizona. Error bars are standard errors of means. Alfalfa data (included for comparison) are from Ayers and Westcot (1985).

Figure 2. Cation (A) and anion (B) content of *Atriplex lentiformis* shoot tissues grown along a salinity gradient in a greenhouse experiment in Tucson, Arizona. In (A) closed circles are sodium, open circles are potassium, open triangles are calcium and closed triangles are magnesium. In (B) closed circles are chlorine, open circles are sulfate, open triangles are nitrate and closed triangles are phosphate. Error bars are standard errors of means.

Figure 3. Shoot biomass yield (A), water usage (B), final soil moisture content (C) and water use efficiency (D) of *Atriplex lentiformis* grown to the wilt point along a salinity gradient in sealed pots in a greenhouse experiment in Tucson, Arizona. Error bars are standard errors of means. (B) shows evaporation losses from control sealed pots without plants.

Figure 4. Final salinity of the remaining soil solution in sealed pots in which *Atriplex lentiformis* was grown to the wilt point along a salinity gradient in a greenhouse experiment in Tucson, Arizona. Error bars are standard errors of means.

Figure 5. Water use efficiency of *Atriplex lentiformis* plants grown for three years in lysimeter tanks in an irrigation district in Tucson, Arizona. WUE was calculated as shoot biomass yield divided by actual evapotranspiration. Data points are for the three irrigation treatments tested in Soliz et al. (2011). Error bars are standard errors of means.

Figure 6. Equilibrium projections of yield (A), the drainage fraction (B), drainage volume (C) and salt discharge (D) of *Atriplex lentiformis* grown under deficit irrigation scenarios at three irrigation salinities (3, 10 and 20 g $L^{-1}$ TDS). Projections are based on a linear model (Dudley et al., 2008) using a salinity of 47.3 g L-1 as the salinity at which growth and transpiration go to zero.

Figure 7. Approximate $Na^+$ balance for *Atriplex lentiformis* grown in drainage lysimeters for three years in an irrigation district in Marana, Arizona under three irrigation treatments. Drainage values are shown as negative numbers to denote discharge below the root zone. Error bars are standard errors of means.

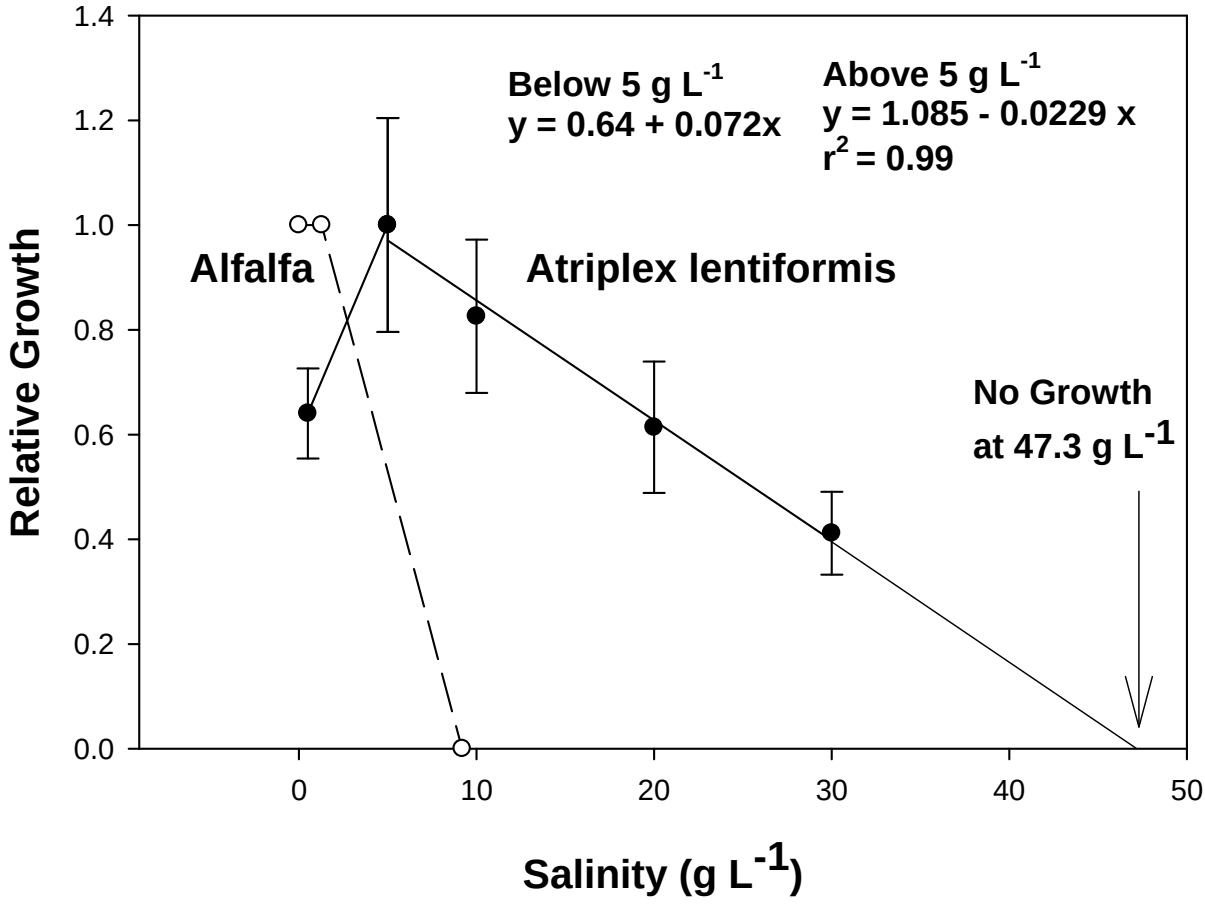
Below 5 g L-1
y = 0.64 + 0.072x
Above 5 g L-1
y = 1.085 - 0.0229 x
r2 = 0.99
Alfalfa
Atriplex lentiformis
No Growth
at 47.3 g L-1
Relative Growth
Salinity (g L-1)
0.0
0.2
0.4
0.6
0.8
1.0
1.2
1.4
0
10
20
30
40
50

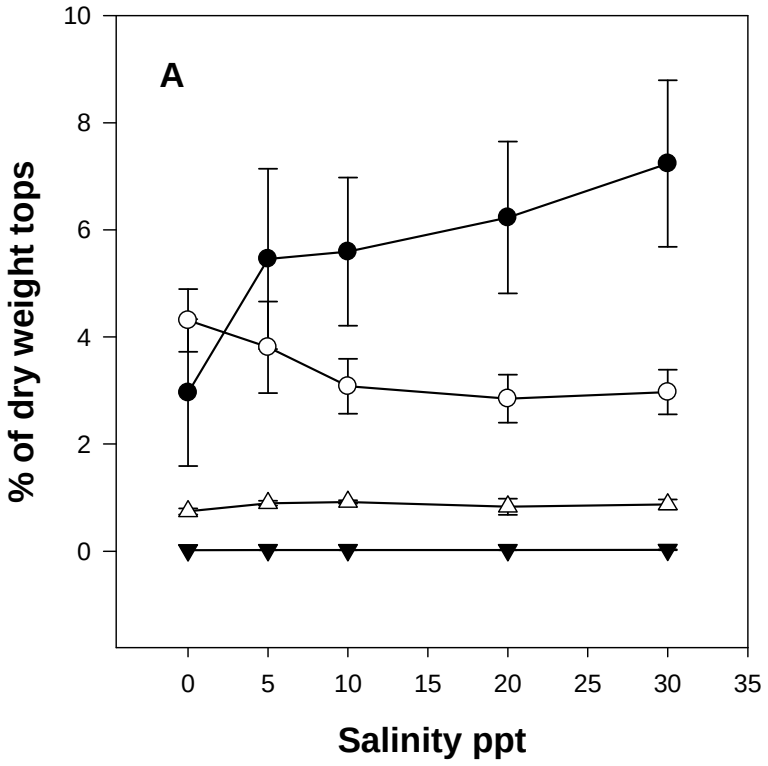
A
% of dry weight tops
Salinity ppt
0
2
4
6
8
10
0
5
10
15
20
25
30
35

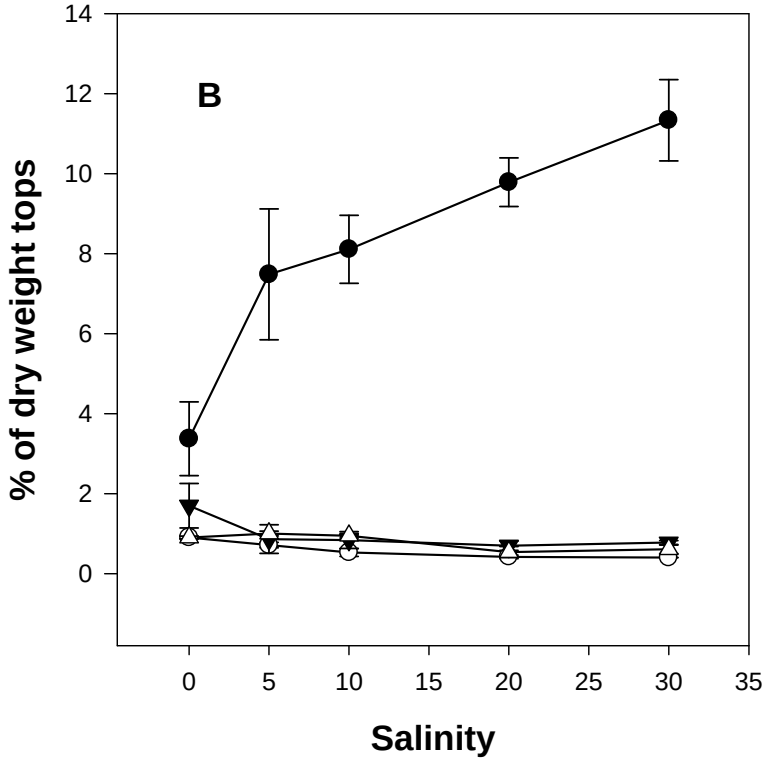
B
% of dry weight tops
Salinity
0
2
4
6
8
10
12
14
0
5
10
15
20
25
30
35

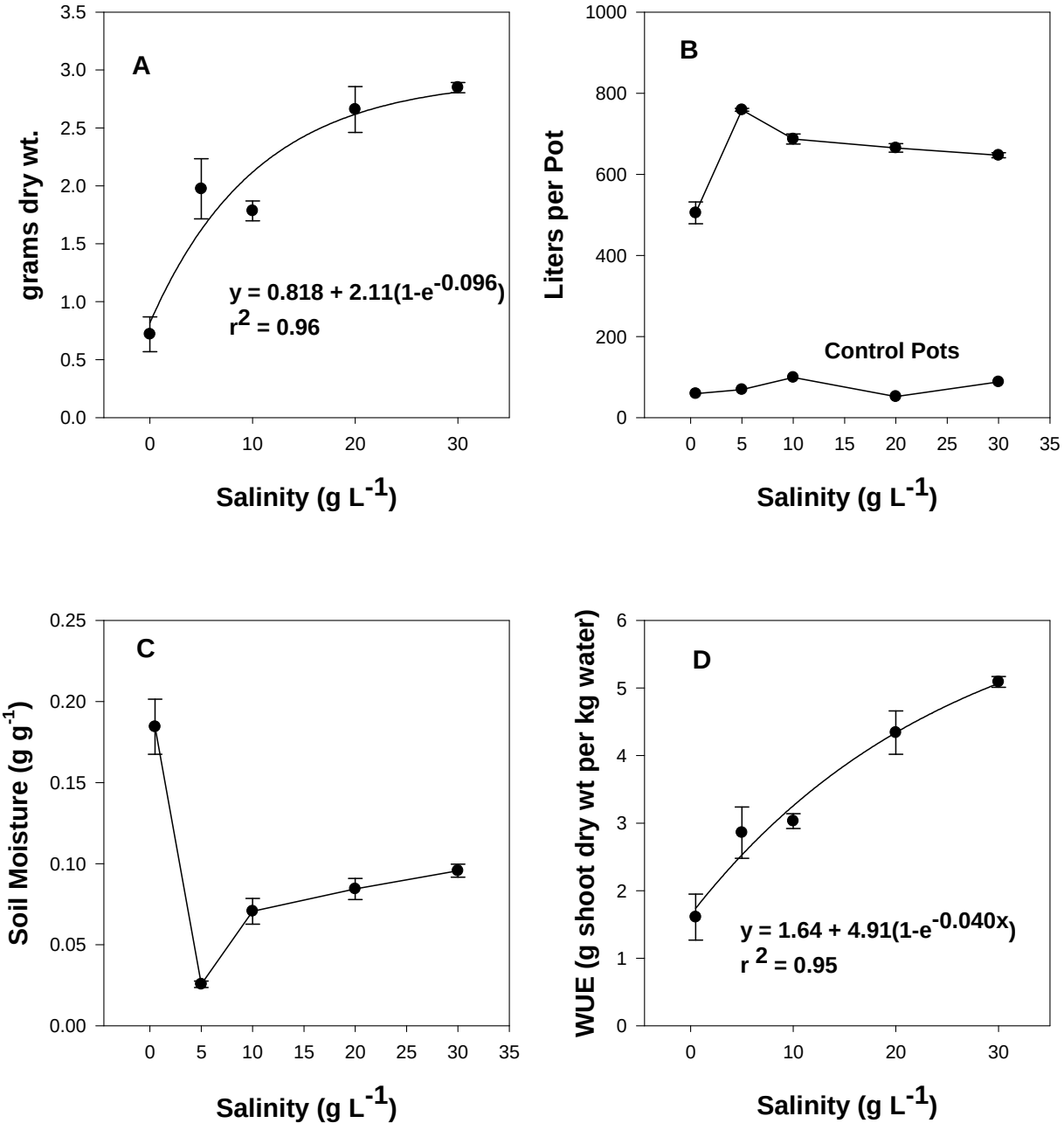
A
grams dry wt.
y = 0.818 + 2.11(1-e-0.096)
r2 = 0.96
Salinity (g L-1)
B
Liters per Pot
Control Pots
Salinity (g L-1)
C
Soil Moisture (g g-1)
Salinity (g L-1)
D
WUE (g shoot dry wt per kg water)
y = 1.64 + 4.91(1-e-0.040x)
r 2 = 0.95
Salinity (g L-1)

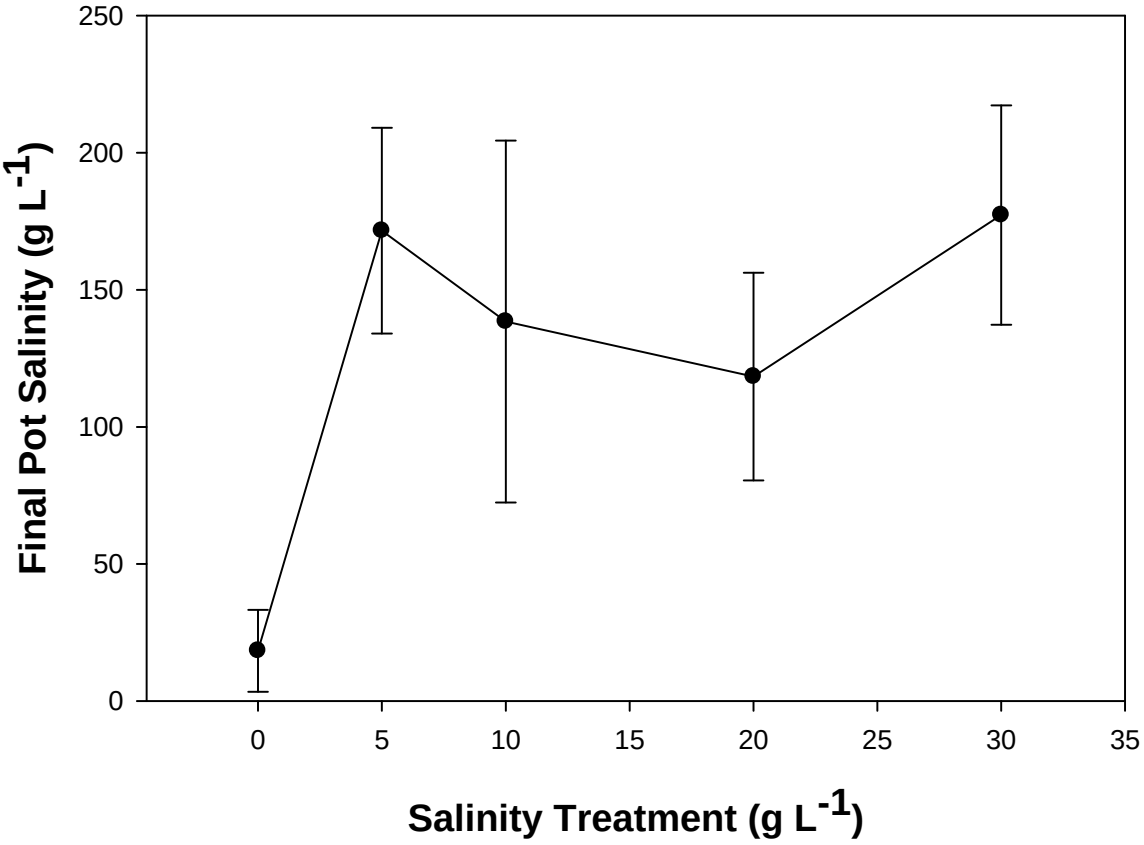
Final Pot Salinity (g L-1)
250
200
150
100
50
0
0
5
10
15
20
25
30
35
Salinity Treatment (g L-1)

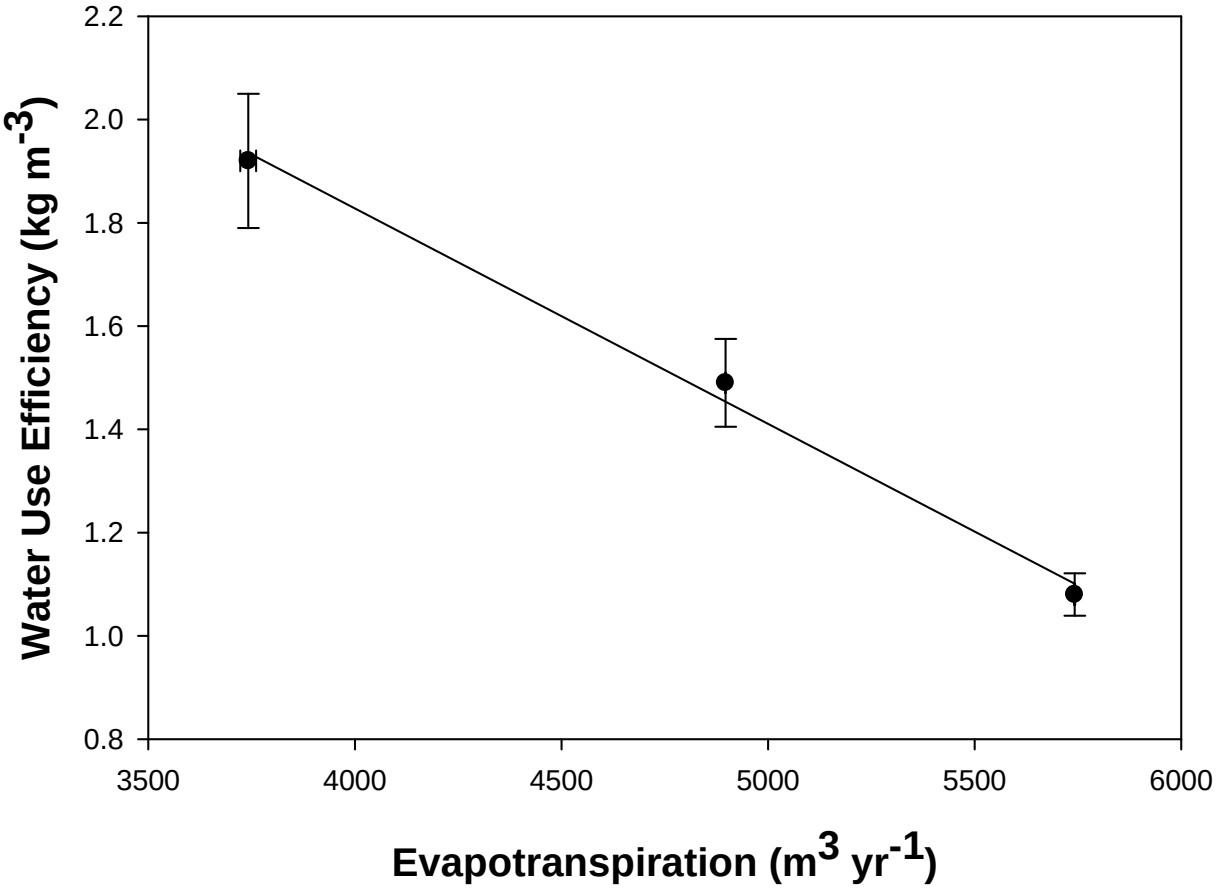
Water Use Efficiency (kg m-3)
2.2
2.0
1.8
1.6
1.4
1.2
1.0
0.8
3500
4000
4500
5000
5500
6000
Evapotranspiration (m3 yr-1)

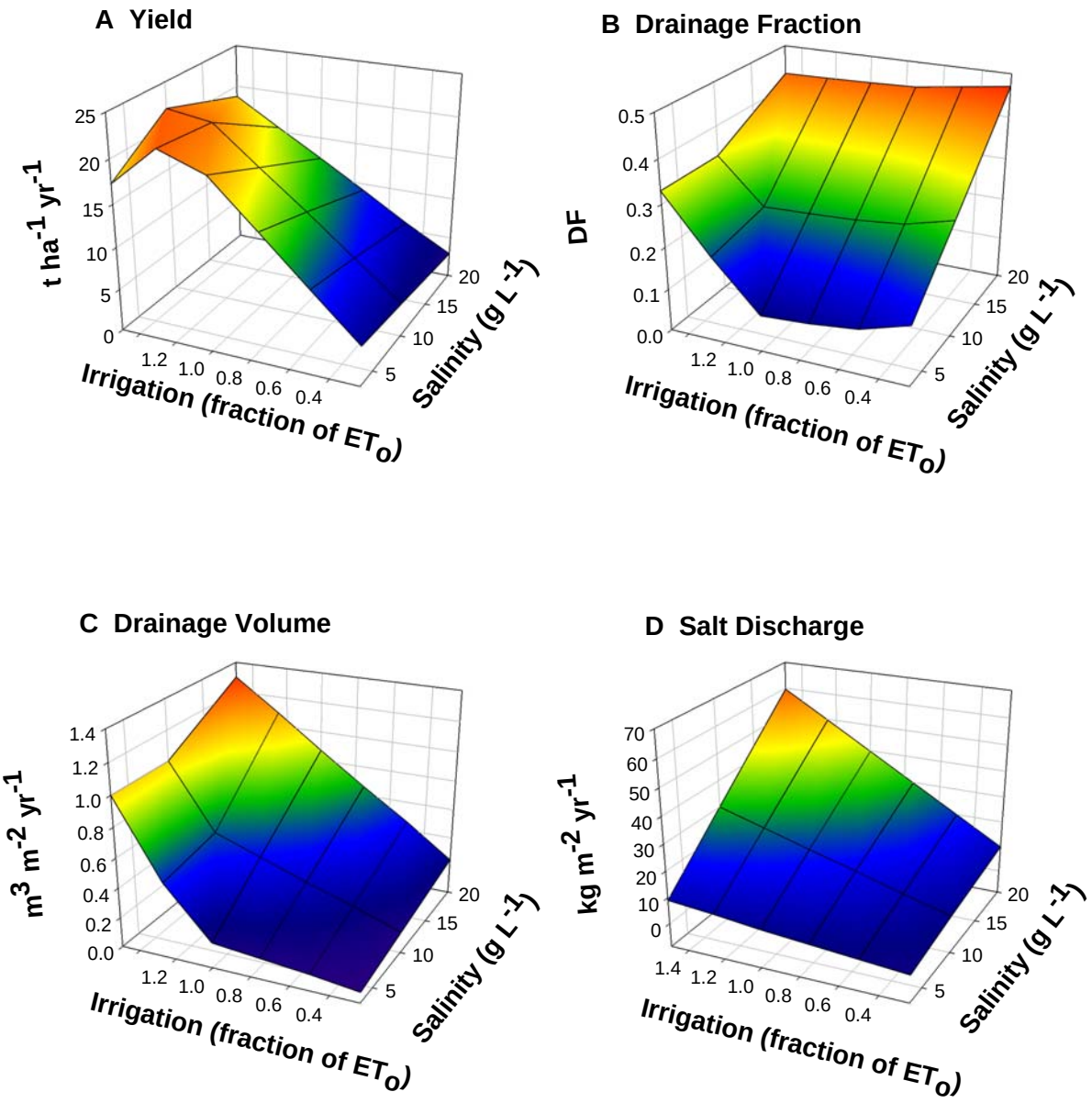
A Yield
t ha-1 yr-1
25
20
15
10
5
0
1.2
1.0
0.8
0.6
0.4
Irrigation (fraction of ETo)
5
10
15
20
Salinity (g L-1)
B Drainage Fraction
DF
0.5
0.4
0.3
0.2
0.1
0.0
C Drainage Volume
m3 m-2 yr-1
1.4
1.2
1.0
0.8
0.6
0.4
0.2
0.0
D Salt Discharge
kg m-2 yr-1
70
60
50
40
30
20
10
0

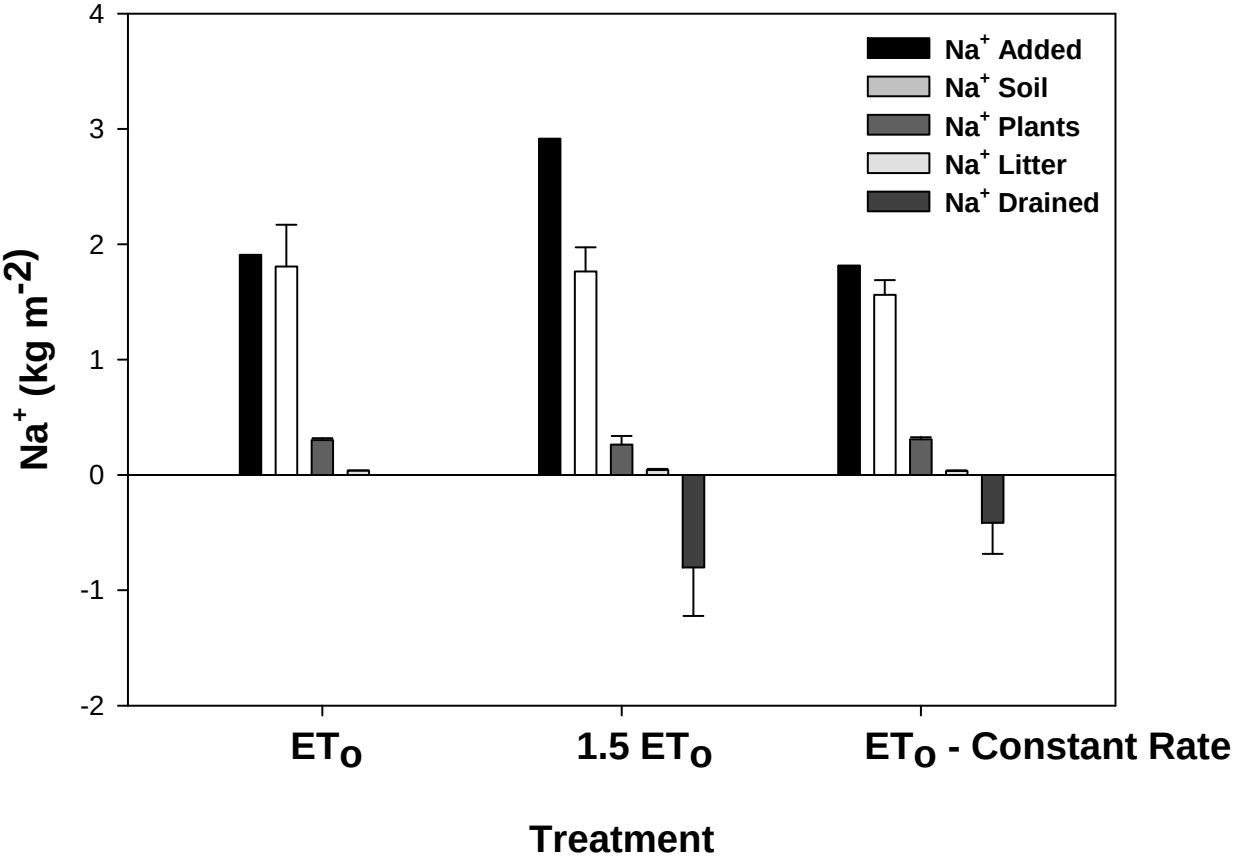
4
3
2
1
0
-1
-2
Na+ (kg m-2)
Na+ Added
Na+ Soil
Na+ Plants
Na+ Litter
Na+ Drained
ETo
1.5 ETo
ETo - Constant Rate
Treatment

# Appendix 8:

Bio-Assays of Aquaculture Species using Reverse Osmosis Concentrates: Preliminary Findings and Growth/Survivability of two Halophyte Species using RO and VSEP Concentrates

# Bio-Assays of Aquaculture Species using Reverse Osmosis Concentrates: Preliminary Findings

# And

# Growth/Survivability of two Halophyte Species using RO and VSEP Concentrates

Deserie Soliz and Steve Nelson

Short-term bio-assays with shrimp (*Litopenaeus vannemei*) and tilapia (*Oreochromis niloticus*).

Shrimp (*Litopenaeus vannemei*) long-term bio-assay with growth rate test.

Growth of Red Orach *(Atriplex hortensis)* irrigated with reverse osmosis concentrates.

Growth of Quail bush (*Atriplex lentiformis*) irrigated with reverse osmosis concentrates.

## Introduction:

A series of small, bench top, viability experiments were conducted in the Spring of 2010. These preliminary studied looked at the viability of shrimp and tilapia in RO and VSEP concentrates produced at the Desalination Research Facility, Marana Field site. In addition, greenhouse studies compared the growth rate of *Atriplex lentiformis* on CWR, RO concentrates and CWR, VSEP concentrate. A heritage salad crop (annual) *Atriplex hortensis* was also evaluated on the two RO concentrates.

These studies provided a preliminary look at the survivability of the aquatic species and the response of the *Atriplex spp*. to differing irrigation salinities. Additional in depth studies are underway on the growth of tilapia on various RO concentrates.

## Short-term bio-assays with shrimp (*Litopenaeus vannemei*) and tilapia (*Oreochromis niloticus*).

**Objective:** To determine survival of young tilapia and un-fed post larval shrimp in two reverse-osmosis (RO) concentrates (CAP RO and VSEP) and a control using artificial seawater at a similar salinity. These were preliminary experiments designed to provide information for future, in-depth, experiments to validate the potential use of reverse osmosis concentrates and brines in aquaculture production.

**Materials and Methods:** The shrimp bioassays were conducted in thirty, 250-mL Erlenmeyer flasks, each with 150 mL of water. Aluminum foil was used to cover the top of each flask to ensure that the shrimp would not jump out. There were three treatments, two of which were concentrates and one was a control group in artificial seawater at 20 ppt. The concentrates include one of 3 ppt salinity and the other was a Vibratory Shear Enhanced Processing (VSEP) concentrate at about 16 ppt. Each of the treatment groups had 10 flasks with the appropriate water and one post-larval Pacific white shrimp (*Litopenaeus vannemei*). The shrimp were obtained, through the courtesy of Dr. Donald Lightner, from the West Campus Agricultural Center of the University of Arizona. The original source of the shrimp post-larvae was the Oceanic Institute in Hawaii. Prior to the bioassays, the shrimp were maintained in 20 ppt artificial seawater for several days and fed commercial feed for post-larval shrimp. The shrimp were not fed during the bioassay. Each day the number of surviving shrimp and mortalities in each group were counted.

For the Tilapia bioassays, four 10 gallon glass aquariums with 30 liters of treatment water in each were used. The treatments were: 1) VSEP concentrates at a salinity of 10 ppt; 2) artificial sea water at 20 ppt, 3) reverse osmosis (RO) concentrate at approximately 3 ppt; and 4) artificial sea water at 3 ppt. Each tank was supplied with aeration from a commercial aquaculture air pump also with a biological (gravel and oyster shell) filter. Each tank was stocked with five small (5-8 cm standard length) Tilapia (*Oreochromis niloticus*) per tank. The Tilapia were obtained, courtesy of Dr. Kevin Fitzsimmons, from the aquaculture facilities at the Environmental Research Laboratory (ERL) of the University of Arizona. The fish were not fed during the bioassay. Each day, fish mortalities were recorded for each tank.

**Results and discussion:**

*Shrimp bioassay* - Mortality of the shrimp was 80% within 48 hours in the flasks containing VSEP concentrate, while all of the shrimp survived in the other treatments over the same time. Thus, the VSEP concentrate appears to be unsuitable for use in the aquaculture production of marine shrimp. The RO concentrate had salinities considerably lower than optimum for this species, but the shrimp are able to survive in this water. Additional studies of other shrimp species may be more suitable for use in a concentrate based aquaculture systems are warranted.

Shrimp bio-assay experiment

*Tilapia bioassay* - The Tilapia at salinities of 20 ppt (using salt for artificial seawater) appeared un-healthy and the mortality in the 96-hour bioassay was 60%. However, survival was good in the RO and VSEP concentrate trials. This bioassay indicates that it would be worthwhile to conduct growth tests and longer term bioassays with tilapia in both concentrates. The demonstration at Marana has shown that these tilapia survive and can reproduce in the RO concentrate. Additional tests are waiting the spawning of tilapia in the ERL aquaculture facility. Spawning of the fish is temperature dependent, so fry should be available the arrival of summer temperatures.

## Shrimp (*Litopenaeus vannemei*) long-term bio-assay with growth rate test

**Objective:** To determined survival un-fed post larval shrimp in a reverse-osomosis concentrate and in control tanks of artificial seawater at similar and different salinities. These were preliminary experiments designed to provide information for future, in-depth, experiments examining the potential use of reverse osmosis concentrate in aquaculture production.

**Materials and Methods:** For this experiment nine 75 liter fish tanks with covers were used. Bio filters for these tanks were constructed from plastic container, Plexiglas, PVC pipe and gravel. Three tanks each were filled with water at 20 parts per thousand (ppt), reverse osmosis (RO) concentration, which was approximately 3 ppt and artificial sea water at 3 ppt respectively. Each tank was provided with 10 small larval Pacific white shrimp (*Litopenaeus vannemei*). The shrimp were obtained, through the courtesy of Dr. Donald Lightner, from the West Campus Agricultural Center of the University of Arizona. The original source of the shrimp post-larvae was the Oceanic Institute in Hawaii.

The tank biofilters were acclimated initially with tilapia (*Oreochromis niloticus*) before the shrimp were added. The tilapia were used to inoculate the tanks with microorganisms to process ammonia from aquatic species waste into nitrite. The tilapia were feed every day and monitored to see if any mortality occurred. No mortalities were recorded and the Tilapia were returned to their original tank.

The location where the shrimp bio-assays took place was at the Environmental Research Laboratory (ERL). The area at the ERL that the shrimp experiments were taken place was in the Fleischmann building in the back lab where the radioactive equipment is stored. The shrimp were feed every day adding about 35 pellets of shrimp food to each tank. Mortality was monitored in each tank daily. More shrimp were added to any tank that lost more than 50% of the shrimp in the beginning of the experiment to keep the experiment consistent within the first week. One of the RO tanks (# 5) had 100% mortality within the first 24 hours of the experiment. This tank was restocked after the water was changed and the filter cleaned. Each tank's water was tested once a week for nitrite and ammonia build up as well as the pH of the water.

**Results and Discussion:**

When examining all of the data, it was observed that the artificial sea water at 20 ppt is suitable for the shrimp to survive in. The data showed that the shrimp had difficulty surviving within the RO concentrate water. Replacement of some of the shrimp had taken place within the first 48 hours of the experiment. Eventually, the tank water was changed out and need shrimp were added. The change in water and cleaning of the tank did not change the results that had been witnessed. The tanks filled with artificial sea water at 3 ppt did very well with the shrimp. The shrimp did not seem to have any problems living in water at a low salinity level as 3 ppt. The overall results illustrated that larval Pacific white shrimp will not handle RO concentrate but can live in low salinity water when made from artificial sea salts. See graph below to see the shrimp survival rate at the end of the experiment.

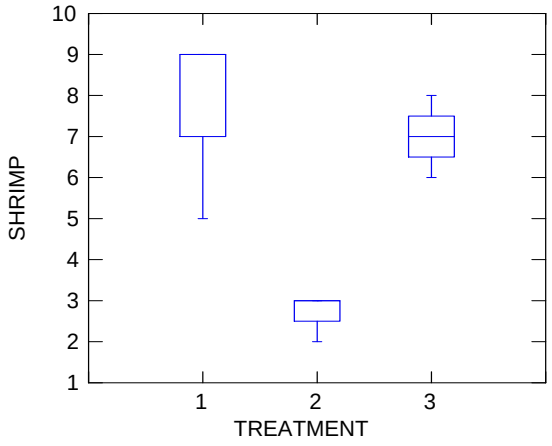


1 = 20ppt – Seawater Salt Mix
2 = 3.5 ppt – RO Concentrate
3 = 3.0 ppt – Seawater Salt Mix

## Growth of Red Orach *(Atriplex hortensis)* irrigated with RO concentrates.

**Objective:** Determine viability of red orach, a heritage leaf vegetable similar to spinach, irrigated with three saline water sources. Irrigation treatments: 3ppt concentrate from a reverse osmosis (RO) concentrate with chemical fertilizer, 3ppt RO concentrate from a fish production tank, and Tucson city water with added fertilizer.

**Materials and Methods:**

The *Atriplex hortensis* seeds used for the experiment were obtained from the Condor Seed Company in Yuma, AZ. The seeds germinated the seeds in individual compartments of seedling trays. Three seeds per compartment were planted and thinned upon germination to one seedlings per compartment. The seeds were planted February 17, 2010 and the trays set in the nursery area of the halophyte greenhouse at the Environmental Research Laboratory of the University of Arizona. The seed and seedlings were watered by an automatic sprinkler system three times per day. The seeds germinated in 2-3 days.

When the seedlings were approximately 1 cm in height, they were transplanted to individual, 4 liter pots filled with a potting soil mix. Each pot was assigned randomly (through use of a random numbers table) to one of three treatments: 1) Tucson city water with added fertilizer; 2) reverse osmosis (RO) concentrates with added fertilizer; and 3) and RO concentrate from a fish culture tank. The commercial fertilizer added to the first two treatments (Miracle Gro) was according the manufacture's recommendation for potted plants. Each pot was irrigated three time per week with 1 liter of the treatment solution. There were 12 plants per treatment (36 pots in total). The plants were harvested when there was evidence that they were beginning to bolt. Each entire plant, including roots was harvested and weighed. The plants were then dried to constant mass at 70 degrees Celsius. The final above-ground dry biomass and the dry mass of roots of each plant were determined with an electronic balance and compared among treatments using One-Way Analysis of Variance.

*Atriplex Hortensis*, Red Orach, Mountain Spinach

The tank used for rearing the fish was approximately 184 gallons. The fish that were used in the fish tank were from the aquaculture lab at the Environmental Research Laboratory (ERL). We weighed and measured 20 small fish and 24 medium fish. Wet and dry weight of the plants were taken at the start the project. These weights help determine the total weight change of the plants

over time. The weight measurements help determine if one of the plants is retaining more water that the others and if that makes a difference in it growth.

**Results and Discussion:**

When examining the results of the One-Way Analysis of Variance that we conducted, we noticed that there was a significant difference between the different irrigation treatments. There was a small difference between the treatments using Tucson water plus Miracle Gro and RO concentrate plus Miracle Gro. Whereas, *A. hortensis* grown on RO concentrate from the Tilapia tank grew quicker and fuller and were generally more vigorous than the other two irrigation treatments. See graph and picture below.

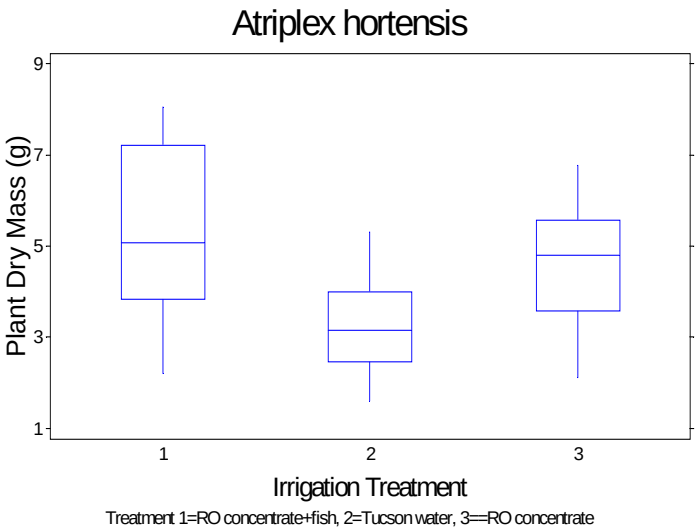


## Growth of Quail bush (*Atriplex lentiformis*) irrigated with RO concentrates.

**Objective:** To compare the growth of quail bush irrigated with three water sources. The first was a 3ppt concentrate from a reverse osmosis (RO) concentrate with added fertilizer, the second was the vibratory shear enhanced processing (VSEP) with added fertilizer and the third was Tucson city water with added fertilizer.

**Materials and Methods:**

For this experiment, 20 small green pots three liters each were used. 15 *A. lentiformis* that were originally planted on January 27, 2009 were used. Five *A. hortensis* that were originally planted on February 17, 2009 were used. The seeds for the *A. hortensis* were obtained from the Condor Seed Company in Yuma, AZ. The seeds for the *A. lentiformis* were taken from another project in Marana, AZ. The plants that were planted within the green pots were chosen at random.

The plants were separated into three different irrigation treatments. The irrigation treatments were tap water (Tucson Water) with Miracle Gro, reverse osmosis (RO) concentrate with Miracle Gro and vibratory shear enhanced processing (VSEP) with Miracle Gro. The five *A. hortensis* were being irrigated only with VSEP with Miracle Gro water since we had previously tested the plant on RO with Miracle Gro water. For each plant, 500 mL of water with a teaspoon of Miracle Gro were used for irrigation. Irrigation regiment was on a Monday, Wednesday and Friday schedule. Watering did not take place on the weekends.

Similar plants in size to the test plants were taken for wet and dry weights of the plants at the start of the project. The irrigation process started on March 22, 2009. Initial height measurements of the plants were taken. Height measurements were taken every week to monitor the growth

process of each plant. Some of the plants needed to be transplanted in the first few days due to the plants not able to survive the initial transplant from a small tray to the pots.

**Results and Discussion:**

When examining the data, it was observed that the plants being irrigated with Tucson water plus Miracle Gro grew quicker than any other irrigation treatment. When comparing RO concentrate plus Miracle Gro versus VSEP plus Miracle Gro, it was noticed that the plants given RO concentrate plus Miracle Gro grew much more than the plants given VSEP plus Miracle Gro. The plants given VSEP plus Miracle Gro had difficult first few weeks accepting the VSEP water due to the amount of salt content that was within the water. It was not until between week 3 and week 4 did the plants start to grow. The overall conclusions for this project are that the plants did very well with regular city water plus Miracle Gro while it had a slow start on the two salinity waters. Between the two salinity waters, plants given VSEP will take awhile before any growth or production can be seen while plants given RO concentrate will grow but at a slower rate than regular city water. See graphs below.

When observing to see if *A. hortensis* would be able to survive when watered with VSEP, it was observed that it would survive some times. Five pots of *A. hortensis* were tested on VSEP and it was noticed that they did not start to flourish until week 4. Even with the plants starting to flourish, they were still the smallest plants and had a difficult time with the salinity of the VSEP plus Miracle Gro that was provided to it. Overall, it is not recommend to use higher salinity waters on a plant like *A. hortensis* due to it difficulty with the amount of salts.

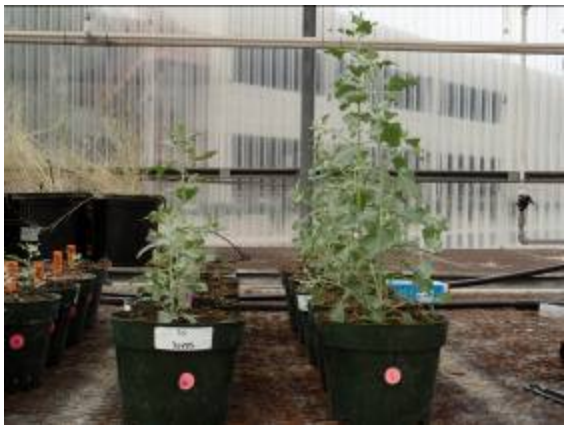

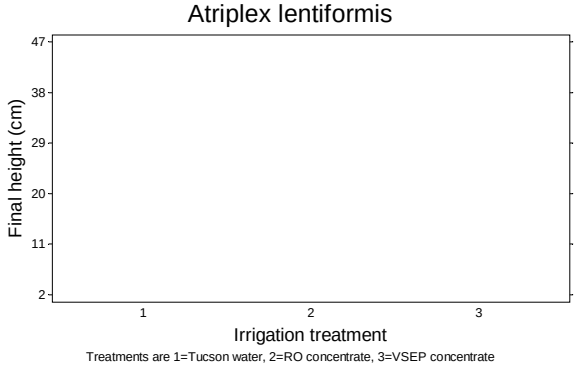


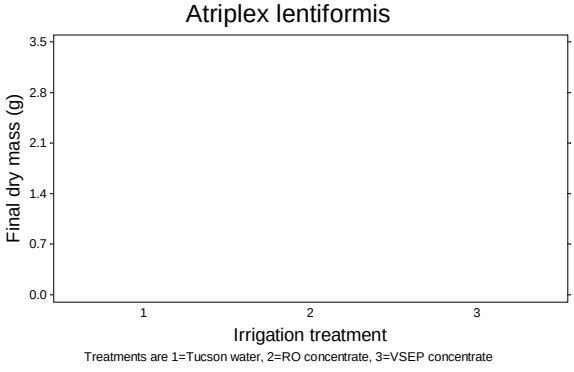

# Appendix 9:

Ion Exchange Pre-Treatment of Reverse Osmosis Feed Water Using Regenerant Recycle

Department of Chemical and Environmental Engineering,
University of Arizona

# *Ion Exchange Pre-Treatment of Reverse Osmosis Feed Water Using Regenerant Recycle*

By: James Lykins

# Table of Contents

# Ion Exchange Pre-Treatment of Reverse Osmosis Feed Water Using Regenerant Recycle

As Arizona's population grows and current water supplies are stretched, the full allocation of Arizona's Central Arizona Project (CAP) water allotment must be utilized and new water resources need to be tapped. If brackish water resources are to play a greater role in regional water supply, salt management will become a major issue in the state. The Salt River and Central Arizona Project (CAP) canal together bring over 1 million tons of salt per year into central and southern Arizona. Since little leaves, salt accumulates in regional aquifers and soils. The salt concentration in CAP water can be lowered ahead of potable use so that the salt carried by the CAP water does not degrade higher quality groundwater resources. To address this, investigations have been undertaken to evaluate reverse osmosis (RO) desalination of CAP water and salt management strategies for the RO residuals. Ion exchange has been proposed as a method for pre-treating CAP water to increase water recovery during reverse osmosis treatment and to minimize the resultant brine volume. Pilot-scale investigations in Tucson indicate that with conventional RO desalination of CAP water, recovery is limited to 80%. If scale-forming cations are removed prior to RO treatment, the expected maximum water recovery is over 90%. Both RO and ion exchange produce a brine waste, and therefore treatment and disposal of wastes from these processes should be considered as a single problem. In the study reported here, (i) regenerant reuse and (ii) augmentation of IX regenerant by RO brine are explored in this context. Results suggest that a sodium regenerant solution can be reused, with periodic softening, to regenerate a strong acid cation exchange resin. Further, it has been determined that the RO concentrate can be used to augment regenerant solutions if sufficient supplementary sodium is added.

## 1.0 Introduction

Reverse osmosis (RO) is the only economically viable desalting process for widespread use in the United States. It has been widely employed in the last two decades for treatment of waters with high total dissolved solids (TDS). Current limitations to water recovery through reverse osmosis include scaling and fouling of the reverse osmosis membranes. Precipitation can occur in feed water with high concentrations of dissolved ionic species when the ionic are concentrated through the reverse osmosis process. This type of scaling limits the reverse osmosis recovery because the production of scale will foul the surface of the membrane inhibiting transmembrane transport of water. In many reverse osmosis applications, the production of concentrate (brine) is a key determinant of process economic feasibility (Kaakinen, 1984). Brine disposal is expensive because it often requires large evaporation ponds or deep well injection which may dominate the cost of a reverse osmosis plant (Kaakinen, 1984). Therefore, a primary driver in any reverse osmosis project is brine minimization and optimization of recovery.

Ion exchange pre-treatment is frequently an economically feasible method for improving water recovery by reverse osmosis systems treating saline water sources (Kaakinen, 1983). For example, at the Yuma Desalting Plant the high total dissolved solids concentration in the feed water limits water recovery during desalting operations without pre-treatment. High calcium and sulfate concentrations cause gypsum ($CaSO_4$) to precipitate on the membranes. For this reason, recovery was limited to around 80%. However, with the addition of ion exchange pre-treatment of the feed water, the maximum recovery was found as 92.89% (Kaakinen, 1983). At La Verkin Springs, the

Bureau of Reclamation demonstrated the feasibility of ion exchange to minimize brine and improve recovery for a desalting operation designed to lower the salinity of the Colorado River. At La Verkin Springs, the addition of ion exchange pre-treatment allowed for recoveries of up to 92%, verifying the potential of ion exchange pre-treatment as a method for brine minimization and improved recovery (Kaakinen, 1984).

## 2.0 Background

The Central Arizona Project (CAP) was designed to bring water into southern Arizona, primarily for farming with human consumption as a secondary demand. As Tucson's population grows; however, more of Arizona's CAP allocation will be utilized to serve water to the general public. With the full utilization of Arizona's allocation of CAP water, it becomes critically important to manage effectively the supply of water and salt into Arizona. Currently, the University of Arizona is operating a pilot scale reverse osmosis facility integrated with bench-scale laboratory studies to experiment with salt management and water recovery of CAP water using RO technology. The ongoing experimental investigations include determining the economic feasibility of Vibratory Shear Enhanced Processing (VSEP) for water recovery from brine, the relative merits of slow sand filtration and microfiltration for CAP water pre-treatment, the mechanism of anti-scalants, and the fouling and scaling limitations to recovery due to the specific nature of CAP water. After reverse osmosis treatment, aquifer storage and recovery of reverse osmosis treated water is also being investigated as a means for water storage and blending with native ground water. This pilot scale reverse osmosis plant is capable of treating approximately 5 gpm of CAP water.

The Bureau of Reclamation has shown that ion exchange pre-treatment can be used to minimize brine volume and improve water recovery through reverse osmosis. In order to meet the growing demand for water and the need to minimize brine volume this study seeks to investigate the economic feasibility and applicability of ion exchange pre-treatment of CAP water ahead of reverse osmosis while recycling the ion exchange regenerant stream. Due to the nature of CAP water, the following investigations are required to determine the applicability of ion-exchange pretreatment with regenerant recycle. (1) Establish the limits of regenerant reuse to reduce the sodium chloride (NaCl) costs associated with regeneration. (2) Extend regenerant reuse through periodic lime soda softening. (3) CAP water also contains around 6 mg/L of dissolved silica (CAP water quality). The effect of this dissolved silica on strong acid cation exchange resins is unknown and needs to be investigated to ensure there are no adverse effects. (4) The Bureau of Reclamation has also shown that the reverse osmosis brine can be used as a supplement to the sodium chloride regenerant. The low TDS of CAP water might make this prospect less feasible; however, the potential of brine salts as regenerant supplements was investigated in the work. (5) Finally, the expected reverse osmosis recovery with ion exchange pre-treatment needs to be determined to calculate the economic feasibility of the proposed pre-treatment process. (6) Combining the results of the experiments, the study will determine the economic feasibility and applicability of ion exchange pre-treatment for Central Arizona Project feed water to a reverse osmosis plant.

## 3.0 Ion Exchange Regenerant Reuse and Softening

### *3.1 Introduction*

Reuse of sodium chloride regenerant has been used effectively for arsenic removal using anion exchange resins (Robins, 2001). It is expected that the same concept can be applied to the strong acid cation (SAC) exchange resin used for the pre-treatment of CAP water. Due to the competition of cations for the SAC resin sites, as cations accumulate in the regenerant solution, the regeneration efficacy will begin to decreases. When the decreased regeneration capacity of the resin makes continued recycle cost prohibitive, the regenerant solution can be softened with lime soda ash and reused. This method of regenerant recycling and softening has the potential to improve significantly the economic feasibility of ion exchange pre-treatment.

The following experiments seek to show that ion exchange can be used to reduce the ions from CAP source water that participate in scaling reactions during reverse osmosis. A second objective is, to show that the regenerant (NaCl) solution can be reused for multiple regeneration cycles. Regenerant use was then extened by precipitation of hardness cations (i.e., $Ca^{2+}$, $Ba^{2+}$, $Sr^{2+}$ for CAP water) in the regenerant solution when the regeneration efficacy declines. To improve regenerant strength sodium chloride may be added to maintain the desired sodium concentration.

Several experimental objectives were explored using bench-scale ion exchange equipment. The first was to find and apply and applicable model to ion exchange data. Second was to determine the long term effect of reusing and softening the regenerant

solution. A secondary objective was to determine whether counter or co-current regeneration effected the utilization of the regenerant solution.

*3.2 Background*

The initial experiments performed involved a Purolite C-100E SAC resin for the removal of calcium from a synthetic solution containing calcium chloride. The feed calcium chloride varied throughout experimentation to reduce the time to equilibrium. Several areas of ion-exchange were explored using this resin including the potential for regenerant reuse and precipitation of calcium from the regenerant solution using the lime soda ash procedure. Further, countercurrent and co-current regeneration techniques were explored to determine an optimal method for regenerating the resin. The reaction describing the exchange of calcium and sodium can be represented as:

$$Ca^{2+} + 2\overline{Na^{+}} \leftrightarrow \overline{Ca^{2+}} + 2Na^{+}$$

Where the equilibrium (selectivity coefficient) is expressed as:

$$K_{Na^{+}}^{Ca^{2+}} = \frac{\overline{C}_{Ca^{2+}} C_{Na^{+}}^{2}}{\overline{C}_{Na^{+}}^{2} C_{Ca^{2+}}}$$

Where a bar indicates resin phase concentration.

Finally, the data obtained were modeled using an equilibrium expression of the following form (REF):

$$\frac{\overline{X}_{Ca^{++}}}{\left(1-\overline{X}_{Ca^{++}}\right)^{2}} = K_{Na^{+}}^{Ca^{++}} \frac{\overline{C}}{C} \frac{X_{Ca^{++}}}{\left(1-X_{Ca^{++}}\right)^{2}} \qquad (1)$$

Where C is the total cation concentration of the solution (eq/L) and $\overline{C}$ is the total ionic capacity of the resin (for C100E this is 1.9 eq/L). The term $\overline{X}_{Ca^{++}}$ is the fraction of calcium on the resin defined as $\frac{\left[Ca^{++}\right]}{\overline{C}}$ and $X_{Ca^{++}}$ is the fraction of calcium in the

solution defined as $\frac{[Ca^{++}]}{C}$. The term $K_{Na^+}^{Ca^{++}}$ is the selectivity coefficient for the exchange of calcium for sodium on the resin.

The lime soda ash softening procedure used for softening the regenerant was based on the procedure outlined by Masters and Ela (Masters and Ela, 2007). The first step is the addition of lime ($Ca(OH)_2$) for the removal of aqueous $CO_2$. In this step, the pH is adjusted above 10.33 (the $pK_a$ for $H_2CO_3$). The reaction is:

$$CO_2(aq) + Ca(OH)_2 \leftrightarrow CaCO_3(s) + H_2O$$

Following the pH adjustment, lime is added for the removal of calcium carbonate hardness through the precipitation of calcium carbonate as follows:

$$Ca^{2+} + 2HCO_3^- + Ca(OH)_2 \leftrightarrow 2CaCO_3(s) + 2H_2O$$

The magnesium carbonate hardness is also removed by the addition of lime:

$$Mg^{2+} + 2HCO_3^- + Ca(OH)_2 \leftrightarrow 2CaCO_3(s) + Mg(OH)_2(s) + 2H_2O$$

The calcium and magnesium noncarbonate hardness can then be removed through the addition of soda ash ($Na_2CO_3$) as follows:

$$Ca^{2+} + Na_2CO_3 \leftrightarrow CaCO_3(s) + 2Na^+$$

$$Mg^{2+} + Na_2CO_3 + Ca(OH)_2 \leftrightarrow CaCO_3(s) + Mg(OH)_2(s) + 2Na^+$$

The resulting suspension contained dissolved sodium chloride plus the solids of calcium carbonate and magnesium hydroxide. The solids were removed via filtration. The softened regenerant solution was then reused. Water loss from the sludge was replaced using a additional water and sodium chloride to achieve the same initial conductivity (211 ms/cm).

*3.3 Results and Discussion*

The first experiments conducted were designed to examine the capability of directly reusing the regenerant solution. This was done by loading a measured amount of resin (1.23 L) with a synthetic calcium solution. Equilibrium was obtained through a recycling loop. The synthetic calcium solution consisted of 0.0088 M $CaCl_2$ in deionized water for cycle 1-2 and approximately 0.031 M $CaCl_2$ for cycles 3,4,5,7,8 and 9 using calcium chloride dihydrate ($CaCl_2$-$2H_2O$). A cycle consists of an equilibrium regeneration phase followed by an equilibrium-loading phase. Each cycle consisted of a regeneration with a sodium chloride (initially 100 g/L NaCl) solution that was also allowed to come to equilibrium. Finally, the resin capacity was defined and calculated as the amount of calcium removed from the loading solution. In the first two experiments (cycles) no sodium chloride was added to the regenerant to make up for the sodium removed due to exchange. In the third and fourth experiments, sodium chloride was added to make up for the calculated loss of sodium due to exchange with the resin. This was calculated based on the increase in equivalents of calcium in the regenerant solution[*]. After cycle 4, the resin capacity had decreased by approximately one half its initial value as depicted in Figure 1.

[*] The sodium chloride addition only made up for the sodium lost due to ion exchange, however significantly more sodium was lost due to dilution in the columns from water in the cartridge filter

**Figure 1. Resin Capacity vs. Cycle #**

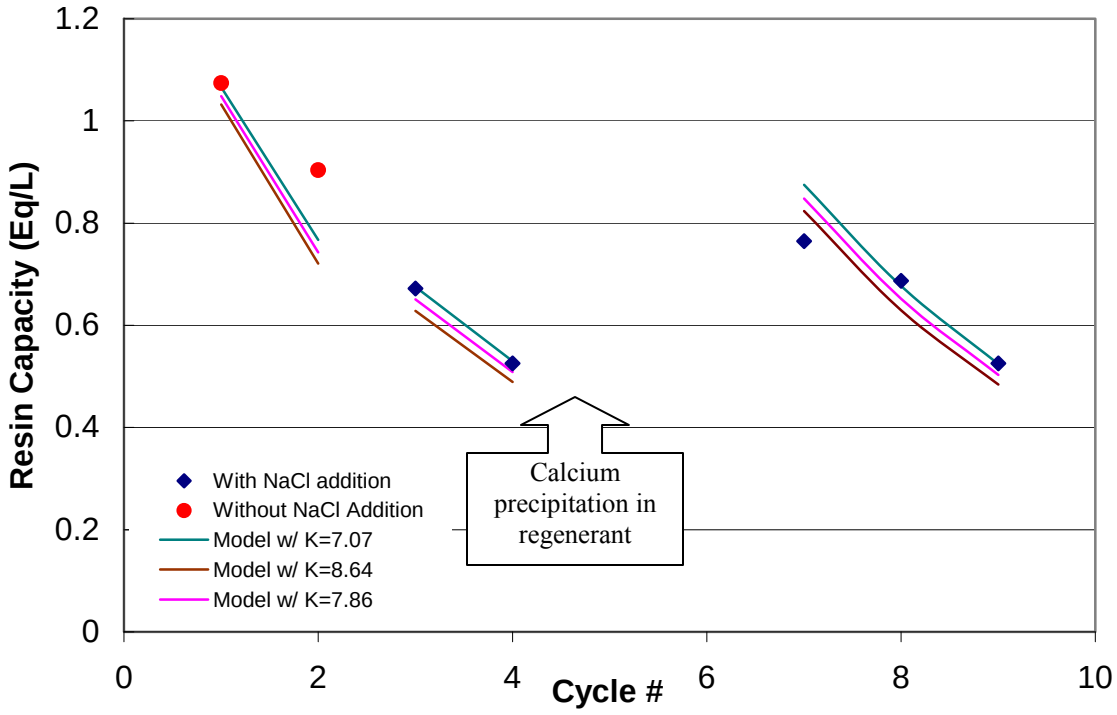


As Figure 1 depicts, the resin capacity did not return to its initial value. This is due to the decreased salt concentration in the regenerant. Further, the model still fits the data and therefore the resin still achieved the same equilibrium distribution that indicates there is no effect on equilibrium due to the softening process.

Due to the very large decrease in resin capacity, calcium was precipitated from the regenerant solution after cycle 4. This was done by adjusting the pH above 10.33 and adding soda ash ($Na_2CO_3$). The supernatant liquid was then siphoned off for use, and the pH was returned to between 5 and 6.

After the softening step, a new experimental method was used to examine the breakthrough curve of calcium for this particular system. This was done by creating a

calcium chloride solution (0.011 M or 445 mg/L $Ca^{2+}$) and passing it once through the ion exchange column rather than in a recycle loop. Samples were then taken at set periods to produce the breakthrough curve depicted in Figure 2.

**Figure 2.** Calcium vs. Time in Effluent (Cycle 6)

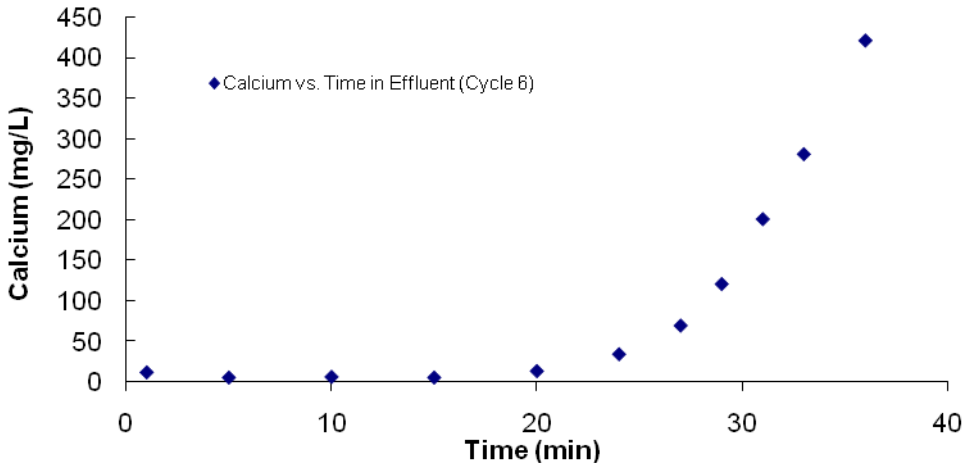


As Fig. 2 depicts, breakthrough began to occur between 20 and 24 minutes with a solution containing approximately 445 mg/L calcium. The experiment for cycle five was done similarly; however, data collection was hampered due to equipment problems. Following these two experiments, the recycling loop was used to generate equilibrium data in subsequent experiments (see cycles 7-9 in Figure 1).

The next experiments conducted were performed to determine the optimum regeneration mode, countercurrent or co-current (up flow and down flow respectively). These experiments were conducted using the previous method of regenerating and loading within a recycle loop. The calcium was first precipitated from the regenerant solution. A fresh solution was not made because the regenerant strength was not a variable in this

experiment. The resin capacities, as defined earlier, were then compared between the two regeneration methods as depicted in Figure 3.

**Figure 3.** Counter vs. Cocurrent Regeneration

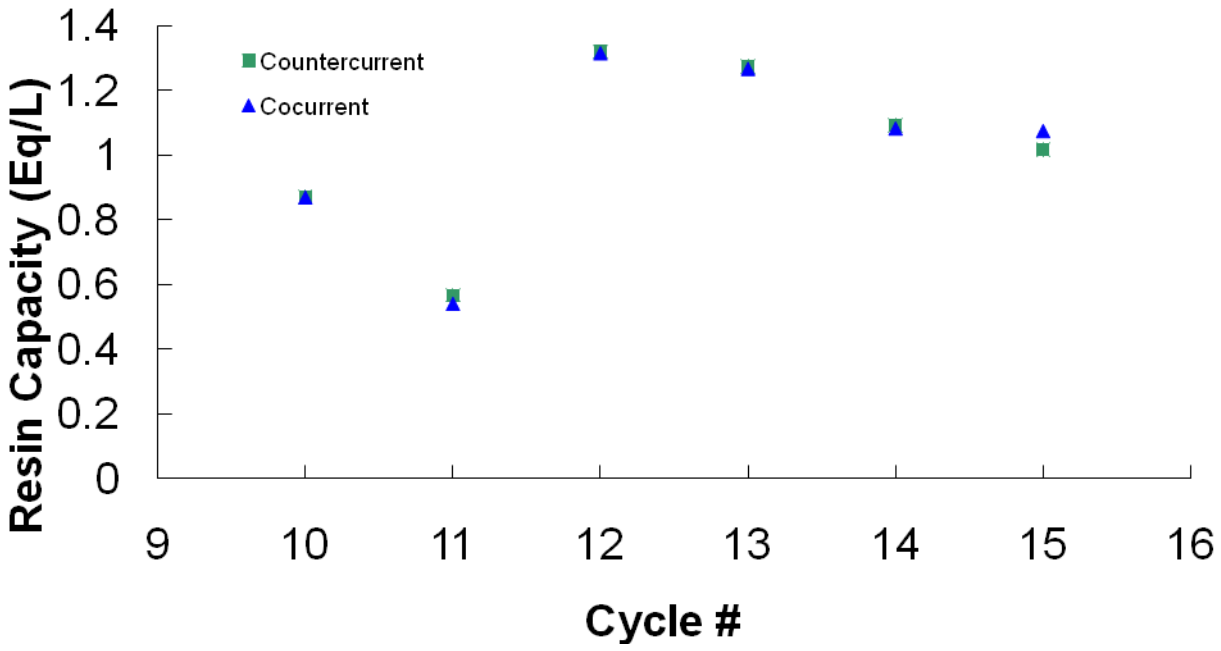


Following cycle 11, a fresh regenerant solution was used. As shown (Figure 3), there was no operational benefit to regenerating either countercurrent or co-current to the loading flow. This agrees with equation 1, since the equilibrium expression is not a function of direction of flow. In practice, since the regenerant will be conserved, regeneration would be done in a recycle mode, using the simplest configuration and method of regenerant addition.

Finally, the model described by equation 1 was used to calculate a selectivity coefficient ($K_{Na^+}^{Ca^{++}}$) for the Purolite C100E resin. The error was minimized between the model and the experimental results by varying $K_{Na^+}^{Ca^{++}}$ using excel's solver function. The calculated selectivity coefficient was approximately 7.86 using the data from cycles 3-4 and 6-9.

Typical $K_{Na^+}^{Ca^{++}}$ values for SAC resins are between 3-6. Figure 1 shows the effect of variation in $K_{Na^+}^{Ca^{++}}$ by plus or minus 10% on the theoretical relationship.

It was determined that the selectivity coefficient was very sensitive to experimental error based on a sensitivity analysis. Therefore, to better calculate the selectivity coefficient for this resin the scale of the experiment (reactor size) was reduced. A selectivity coefficient of 3.08 was calculated by using a small amount of resin, still allowing the loading and regenerant solutions to come to equilibrium.

Sources of error were introduced in the data due to the inability to completely drain water from the ion exchange column. Approximately 1.65 L of each solution (loading, regenerate, rinse) remained in a cartridge filter as well as approximately 1.5 L of solution in miscellaneous tubing. In some cases the fraction of the total volume remaining in the system after draining was approximately 0.3. This affected the loading for example because the loading solution was mixed with several liters of regnerant solution limiting the transport of calcium onto the resin. This had a large impact on the results; however, calcium and sodium concentrations were calculated accounting for this dilution factor.

Using what was learned on the larger scale, the equilibrium experiments with regenerant reuse and softening were repeated on a much smaller scale. In these experiments, 76 mL of Purolite C100E resin was used in a chromatography column. The resin was loaded using 2 L of a synthetic calcium chloride solution containing approximately 3 g/L calcium. The regenerant solution was initially 2 L containing 200 g/L NaCl. Volume of

regenerant was reduced to 1 L after cycle 17 to speed up the experiment. Sodium chloride was added after each cycle to maintain a constant initial sodium chloride concentration of 200 g/L. The required amount of sodium chloride to add after each regeneration cycle was calculated based on the increase in calcium in the regenerant solution. For every equivalent of calcium removed from the resin (measured by increase in calcium in the regenerant) an equivalent of sodium was added as sodium chloride. The resin was rinsed after each loading and regeneration cycle with deionized water. The lime soda ash softening process was employed each time the regeneration efficacy decreased by more than 15%. The calcium concentration in the regenerant increased monotonically across several regeneration cycles between softening events (Figure 4).

**Figure 4.** Calcium Accumulation in Regenerant

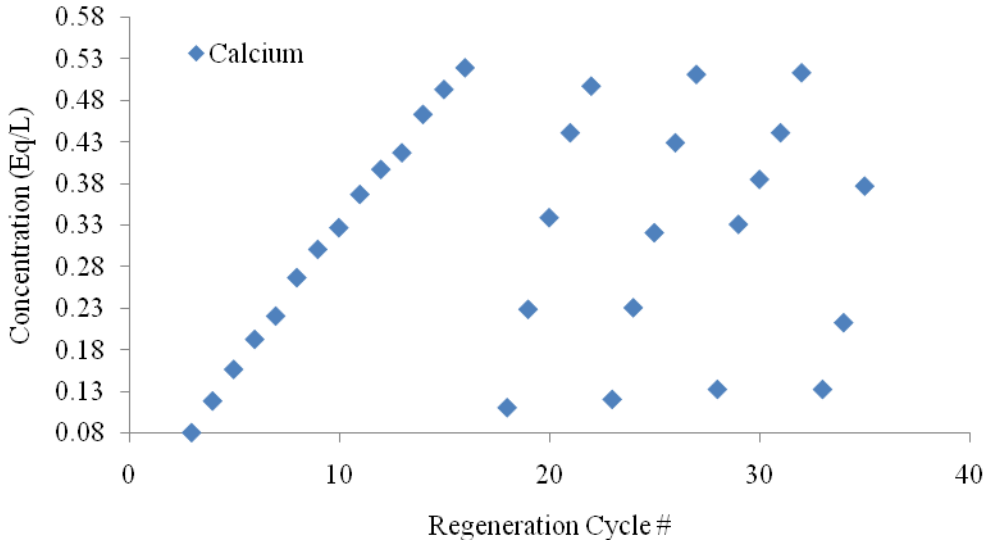

As expected, the resin calcium loading capacity decreased as calcium increased in the regenerant solution (Figure 5) based on the equilibrium model in Equation 1 with a selectivity coefficient of 10.25 (as calculated from the experimental data using a least squares regression analysis).

**Figure 5.** Modeled Equilibrium Loading Capacity

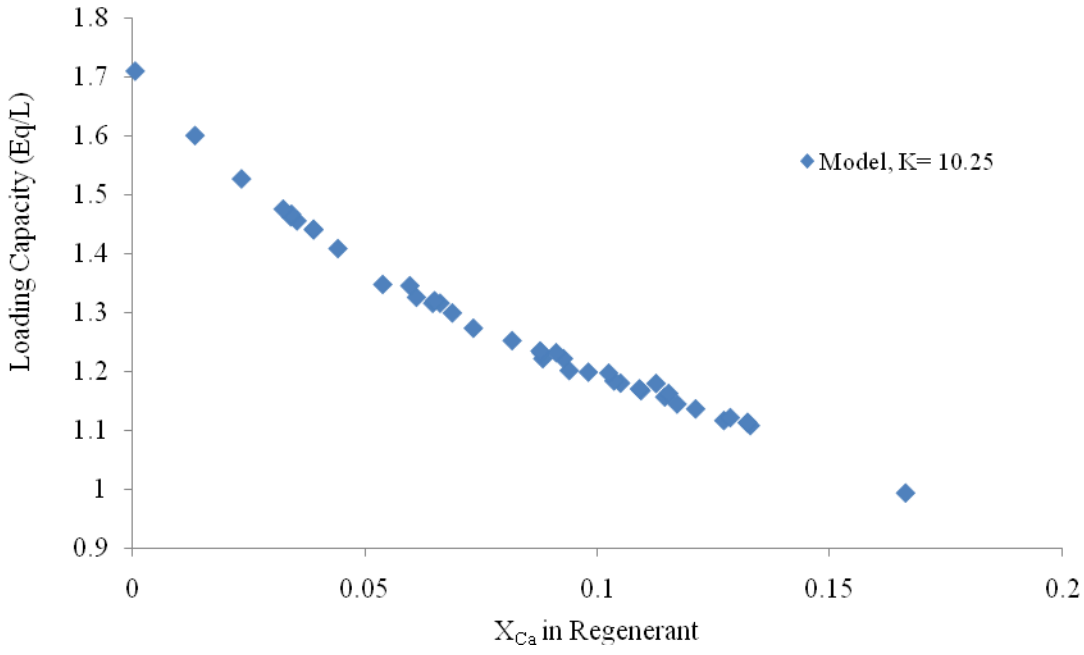


The modeled results shown in Figure 5 are not a smooth curve because of the slight variations in sodium concentration in the regenerant solution. The expectation was that ion exchange would be governed by equation 1 with a constant K independent of time, number of precipitations, or calcium content in the regenerant solution. That is, despite periodic softening, the resin performance would not be adversely affected and the selectivity coefficient would be constant.

**Figure 6.** Equilibrium Loading Capacity

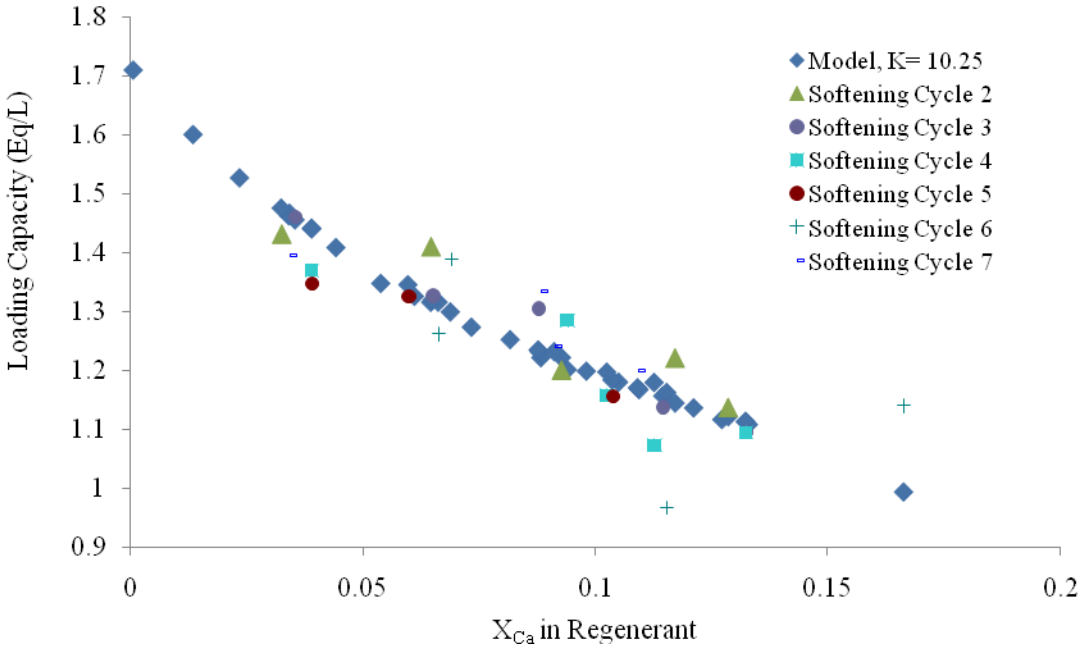


Figure 6 indicates that the performance of the resin continued to follow Equation 1 through seven softening steps. It is clear that the softening procedure does not affect the resin selectivity coefficient with time and therefore the resin performance is constant.

*3.4 Conclusions*

Experiments show that the potential for reusing spent regenerant. They also show that divalent cations can be removed from the sodium chloride regenerant solution using the lime soda ash softening procedure. There is no difference between operating in countercurrent or co-current modes during regeneration if regeneration reactions are allowed to reach equilibrium. It is therefore recommended that the simplest regeneration configuration be used. Finally, equilibrium modeling of the ion exchange process was done using selectivity coefficients and minimizing the error between data and model. This resulted in a selectivity coefficient of 3.08 using a small jar experiment and 10.25 using small scale columns.

## 4.0 Dissolved Silica Effects on Strong Acid Cation Exchange Resins

### *4.1 Introduction*

The water chemistry of silica is complex. Dissolved silica can exist in many forms, but it exists primarily as silicic acid. Due to the dissociation of silica, silicic acid is negatively charged in the neutral pH range. For example metasilicilic acid:

$$H_2SiO_3 \leftrightarrow HSiO_3^- + H^+$$

Further, silica can form 'gels' if the concentration is sufficiently high or the salt content of the water is high enough to stabilize these gels (Papirer, 2000). The formation of these gels is important in the ion exchange processing of waters containing dissolved silica because they may have an adverse effect on the performance of the resin. For a strong acid cation exchange resin, silicic acid will not bind to the resin in the traditional sense due to its negative charge; however, there may be some mechanism for silica gels to occupy the sites on the SAC resin. Further, the resin beads may promote gel formation due to the high local salt concentration at the surface of the resin during exchange since the concentration of cations on the resin is 1.9 eq/L compared to the bulk solution which can be significantly lower. These gels may degrade performance. If ion exchange kinetics are adversely affected by the silica, broader breakthrough curves will be the result.

### *4.2 Background and Methods*

The concentration of dissolved silica in CAP water is approximately 6 mg/L. A loading solution containing six times this concentration (approximately 36.5 mg/L) of dissolved silica as well as six times the concentration of calcium and magnesium in CAP water was used to determine the potential adverse effects of the dissolved silica on the performance

of the ion exchange resin. If the silica itself or the silica gel occupies any of the resin sites, a loss of resin capacity and/or a decrease in cation affinity would be expected with time, as the silica or gel accumulates on resin adsorption sites. Regeneration was done using a 1 L solution of 200 g/L NaCl. The loading solution contained the blend of magnesium, calcium and silica at three times the concentration in CAP water in a 15 L volume to saturate the resin. The loading solution and the regenerant solution were re-circulated through the column until equilibrium was reached. The resin was rinsed with deionized water after regeneration and loading. The experimental setup consisted of a chromatography column containing 78 mL of Purolite C100E ion exchange resin. Regenerant reuse and lime soda ash softening were employed as described previously.

Following sixteen cycles (regeneration followed by loading), visible silica gels were observed on the top of the resin bed as well as floating in the column. The presence of these gels may lengthen the diffusion path of the salts to the surface of the ion exchange resin thereby decreasing the overall mass transfer rate. A breakthrough experiment was designed to determine whether the presence of these gels had an adverse effect on the kinetics of the resin. Following the final loading cycle, 15 L of a loading solution containing 1000 mg/L calcium was passed once through the column to load the resin with calcium. Following this, 7 L of a regenerant solution containing 200 g/L of sodium chloride was passed once through the column to regenerate the sites with sodium ions. Finally, a breakthrough curve was generated by passing 15 L of a 1000 mg/L calcium loading solution through the column and taking samples at set intervals. This procedure

was performed again using a fresh batch of resin to develop a control breakthrough curve for comparison.

A separate experiment to investigate whether dissolved silica or silica gel occupies the resin sites was also performed. In this experiment, 50 mL of Purolite C100E resin was rinsed with deionized water and loaded with 0.5 L of a synthetic solution containing 23.07 g of dissolved calcium chloride dihydrate. The resin was then regenerated using 302 mL of deionized water containing 60.4 g NaCl. Following this 'conditioning' of the fresh resin, the resin was split into two separate 19 mL fractions. One fraction was loaded with 1.22 g of sodium metasilicate nonahydrate in 0.30 L of deionized water (the pH was adjusted to 6.35 with HCl). The second fraction was loaded with 0.50 g NaCl in 0.30 L of deionized water so that both fractions were in a solution containing the same concentration of sodium ions. The media fractions were then dewatered and approximately 1.1-1.2 g of resin was placed in five 10 mL sample tubes (each fraction). Finally 8.80 mL of a loading solution of 17.99 g of calcium chloride dihydrate in 0.5 L of water was added to each sample tube and allowed to equilibrate with the resin. Finally, the equilibrium calcium concentrations were measured in each sample tube to determine the equilibrium distribution of calcium on the resin. Wet resin was also measured and dried to determine the percentage of water weight in each resin sample.

*4.3 Results and Discussion*

The first equilibrium experiment used a column and loading solutions containing dissolved silica at six times the concentration in CAP water resulted in the buildup of visible silica gels on the resin and floating in the column. Figure 7 shows the concentration of magnesium and calcium in the regenerant versus the cycle number.

Figure 7. Cation Accumulation in Regenerant

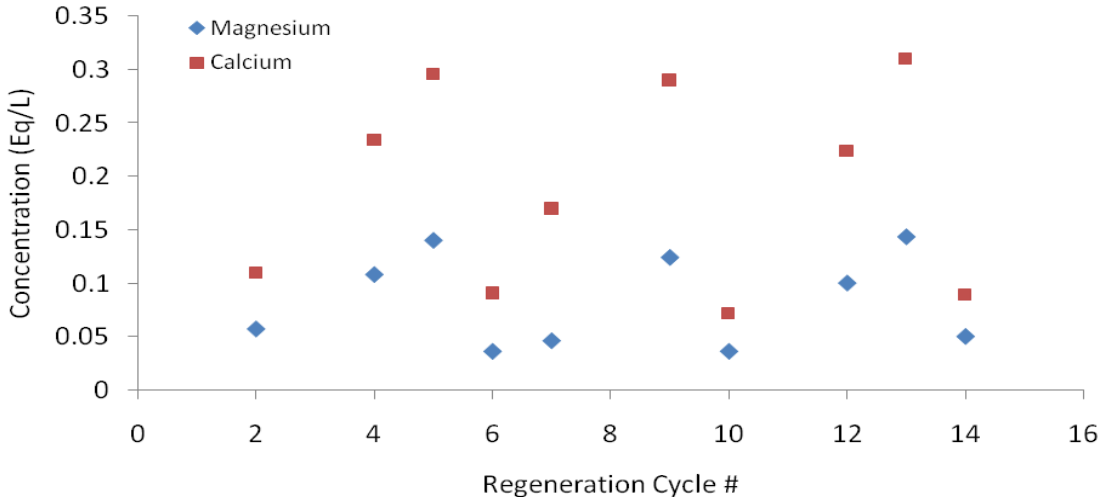


The magnesium and calcium cations accumulated in the regenerant solution until they were removed by the lime soda ash softening process. Figure 8 shows both the modeled and the experimental loading performances as a function of the fraction of calcium in the regenerant solution.

**Figure 8.** Hardness Loading Capacity

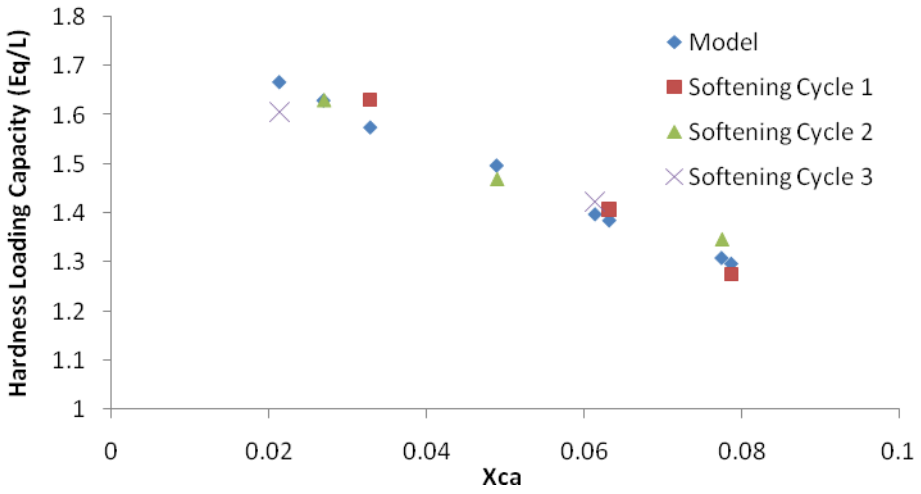


There was essentially no deviation over time from the modeled equilibrium. The affinity factors did not change over time. Silica accumulation on the resin had no apparent effect on cation affinity for the resin. Despite the build up of silica on the resin, the loading performance was the same. Therefore there was no cumulative effect; however, the sites may have initially saturated with silica and we would expect to see a constant loading performance as well if this were the case.

In the second type of equilibrium silica experiment multiple small samples of resin were soaked in a silica solution. In addition, replicate control resin samples were soaked in deionized water with a small amount of sodium. Figure 9 illustrates the loading capacity results for these samples.

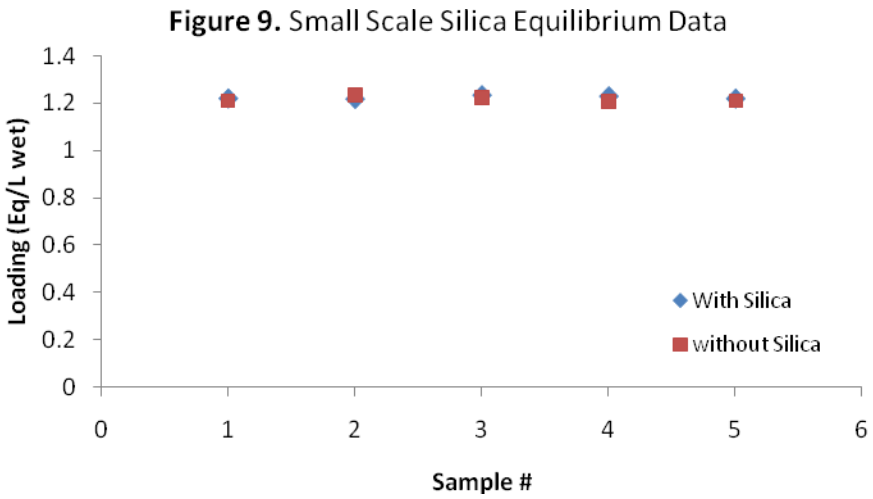


As Figure 9 depicts, the difference in loading capacity between the resin samples loaded with silica and the control resin samples is not significant.

Following the equilibrium experiments, the resin that had been loaded with silica was used in a breakthrough experiment to determine if there had been a change in the kinetics of the resin adsorption due to build up of silica. Figure 10 shows the breakthrough curves for the silica loaded resin and the fresh resin control.

**Figure 10.** Breakthrough Curves

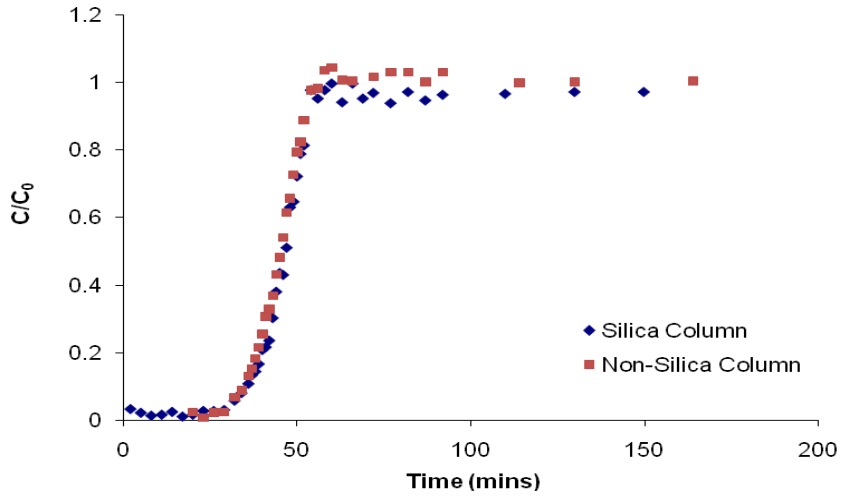


Again, results were essentially indistinguishable.

*4.4 Conclusions*

The presence of dissolved silica in CAP water was investigated as a source of potential adverse effects on a strong acid cation exchange resin. The potential for silica gels to form and occupy sites on the resin or to limit the diffusion of rates of salts to the surface of the resin was investigated. The equilibrium experimental results indicate that there are no adverse effects on the affinity of the ion exchange resin for calcium. The affinity factors, and therefore the equilibrium state of the resin, did not change with time or with silica gel formation. There was essentially no difference between resin soaked in a saturated silica solution and in the control solution.

The sorption kinetics of the resin containing silica gel was also investigated to determine how the presence of the silica gels affected the mass transfer of the salts to the resin surface. Breakthrough curves for the treated and untreated (control) resins were

essentially identical. These experiments show that the silica levels in CAP water should not adversely affect the ion exchange resin performance.

## 5.0 Investigation of Improved Recovery using Ion Exchange Pre-Treatment

### *5.1 Introduction*

The Bureau of Reclamation has shown that ion exchange pre-treatment greatly increases the maximum possible recovery during RO treatment of CAP water. Thus, the cost of ion exchange pretreatment may be more than balanced by reduced water loss and lower brine disposal costs.

For CAP water, brine minimization is especially important. The CAP canal carries 1 million tons of salt into central and southern Arizona each year. Management of this salt is necessary to protect future water quality. Expected recovery using ion exchange pre-treatment is an important component of overall understanding of the salt management economics.

### *5.2 Background and Methods*

The primary factors limiting water recovery during reverse osmosis are the onset of precipitation (scaling) and the energy costs because extracting the last bit of water requires more energy to overcome the osmotic pressure. The recovery at which precipitation begins during reverse osmosis treatment of CAP water is important to estimating the potential for improving water recovery. Maximum recovery experiments were carried out in a plate and frame reactor using an ESPA 1 membrane. To measure maximum recovery, the CAP water was concentrated through the reverse osmosis system

by discarding permeate until precipitation occurred. The onset of precipitation was indicated by an increase in turbidity and a decrease in upward slope of the time-dependent conductivity curve. Cross flow velocities were maintained at levels similar to those of the field experiments. The volume of water remaining when precipitation occurred was used to calculate the maximum recovery as follows:

$$\%\,\mathrm{Recovery} = 100 * \left(1 - \frac{V_{final}}{V_{initial}}\right)$$

This experiment was repeated using ion exchange treated CAP water to determine the expected increase in recovery due to ion-exchange pre-treatment. This experiment is ongoing and results are not yet available.

## 6.0 Potential for using Reverse Osmosis Brine to Regenerate Ion Exchange Resin

### *6.1 Introduction*

At the Yuma Desalting Plant, the Bureau of Reclamation showed that reverse osmosis brine can be used to supplement regeneration of the ion exchange resin (Kaaniken, 1983). Brine from the reverse osmosis process contained concentrated sodium cations with a concentrated suite of anions found in CAP water. A major anion found in CAP water is sulfate ($SO_4^{2-}$). The presence of sulfate can cause gypsum precipitation during regeneration due to the increased concentration of calcium that arises during resin regeneration. This problem was addressed in the Bureau of Reclamation report, which indicated that sufficient fluid velocities during regeneration and a clarifier causes the precipitation to occur outside the column so as not to scale the ion exchange resin.

The potential use of reverse osmosis brine to supplement regeneration of the ion exchange resin increases process feasibility by reducing the need for supplemental sodium chloride.

*6.2 Background and Methods*

A high TDS in the Yuma Desalting Plant feed water translates to a high sodium concentration in the brine, which is then more effective for regeneration of the resin. Based on expected recovery of 90%, the concentration of sodium in the reverse osmosis brine will be about 2.7 g/L. Approximately 16 bed volumes of this solution will be required to regenerate the exhausted ion exchange resin. With vibratory shear enhanced processing, the concentration would increase further, but the solution volume would also decrease.

The potential for supplemental regeneration was investigated by concentrating 30 gallons of ion exchange treated CAP water to approximately 3 gallons (90% recovery) using reverse osmosis plate and frames. 1 L of this brine was then used to regenerate 73.5 mL of Purolite C100E saturated with calcium. The resin was then reloaded using 3 L of a 4 g/L calcium solution to determine the loading capacity after regeneration.

*6.3 Results and Discussion*

Regeneration of the resin with the synthetic reverse osmosis brine produced a loading capacity of approximately 0.33 Eq/L (originally about 1.2 eq/L). Gypsum precipitation was observed during regeneration. However, the kinetics of the precipitation were slow enough to produce gypsum primarily in the feed reservoir to the column. Although regeneration capacity using the reverse osmosis brine was limited, any amount of

regeneration using this method saves on the amount of sodium chloride required for the regeneration step because it allows for regeneration of up to ¼ of the sites prior to using the primary regenerant solution. There has to be a secondary step unless all of the sites are regenerated to their previous capacity or the regeneration will be progressively less effective.

### *6.4 Conclusions*

Using reverse osmosis brine as regenerant resulted in a renewed loading capacity of just 0.33 Eq/L after reaching equilibrium with the regenerant solution. This improves the ion exchange process feasibility and economic feasibility due to the reduced NaCl requirement.

## 7.0 Ion Exchange Breakthrough Modeling for Binary and Multi-component Feed Waters

### *7.1 Introduction*

The design of ion exchange columns relies heavily on equilibrium adsorption models as well as extensive laboratory work with small scale columns. Rapid small scale column tests (RSSCTs) can produce viable scale up parameters for granular activated carbon adsorption columns (Crittenden, 1986). These rapid small scale column tests are also applicable to other adsorption processes such as ion exchange to predict breakthrough patterns and scale up laboratory results. These tests can reduce the experimental time and costs associated with performing detailed pilot-scale studies.

The RSSCTs require knowledge of the physical mechanisms that dominate the adsorption process. For ion exchange processes, a constant-pattern wave model with a constant driving force effectively simulates breakthrough in (binary) multivalent systems (Lee,

2007). The constant-pattern wave model predicts the dynamic behavior of an ion exchange column for various operating conditions.

Many ion exchange feed waters are not ideal binary mixtures of solutes. Therefore, it becomes necessary to develop a model that can predict breakthrough curves for operating conditions in which the feed water consists of multiple, heterovalent solutes. Development of this model will allow for faster design of RSSCTs based on predicted breakthrough curves for the multi-component system, which in turn makes ion exchange design and scale up faster and less expensive.

*7.2 Background*

The general form of the equation describing the dynamic behavior of an ion exchange column can be derived from a series of transient mass balances on a volume element (Lee, 2007). This equation is derived based on assumptions that no chemical reactions occur in the column, there are no co-ions or non-ionic species in the resin interior, the resin does not shrink or swell, flow through the column is an ideal plug flow, only mass transfer by convection and at the boundary layer is significant, the temperature in the column is uniform and constant, the flow rate is constant and the activity coefficients are 1 (Lee, 2007). Further, this model assumes that the resin is non-porous and there is no internal resistance to transport. The resulting partial differential equation describing the adsorption of a cation is:

$$\left(\frac{1-\varepsilon}{\varepsilon}\right)\left(\frac{\overline{C}}{C}\right)\frac{\rho\partial y_M}{\partial t}+\frac{\partial x_M}{\partial t}+u_0\frac{\partial x_M}{\partial Z}=0 \qquad (1)$$

Where ε is the void fraction of the ion exchange bed, $\overline{C}$ is the total cation capacity of the resin (stationary phase), C is the cation concentration in the mobile phase, ρ is the density of the ion exchange resin, $y_M$ is the cation equivalence fraction on the stationary-phase, $x_M$ is the metal equivalence fraction in the mobile phase and $u_0$ is the linear velocity of the fluid. This equation represents the dynamic adsorption behavior of the system as a function of time (t) and position in the column (Z) (Lee, 2007).

To describe the ion-exchange rate, a constant driving force model is used as shown by:

$$\left(\frac{1-\varepsilon}{\varepsilon}\right)\left(\frac{\overline{C}}{C}\right)\frac{\rho\partial y_M}{\partial t} = K_L a(x_M - x_M^*) \tag{2}$$

where $K_La$ is the overall mass-transfer coefficient and $x_M^*$ is the mobile phase cation equivalence fraction that is in equilibrium with the resin surface fraction, $y_M$.

Finally, the $x_M^*$ is a function of $y_M$ as described by the following equation for a binary system with a divalent cation (M) and a monovalent cation (H) (Lee, 2007):

$$x_M^* = 1 + \frac{K'_{MH}}{2y_M}(1-y_M)^2 - \frac{1-y_M}{2}\sqrt{\frac{4K'_{MH}}{y_M} + \frac{K'^{\,2}_{MH}}{y_M^{\,2}}(1-y_m)^2} \tag{3}$$

The term $K'_{MH}$ is a modified equilibrium constant defined as (Lee, 2007):

$$K'_{MH} = K_{MH}\frac{\overline{C}}{C} = \left(\frac{y_M}{x_M}\right)\left(\frac{x_H}{y_H}\right)^2 \tag{4}$$

Equations (1) - (3) can be used to describe the dynamic behavior of the system with the following initial conditions and boundary condition:

$x_M = y_M = 0$ at t = 0 (Initial Condition)

$$x_M = x_{M,F} \quad \text{at } z = 0 \qquad \text{(Boundary Condition)}$$

where $x_{M,F}$ is the cation equivalence fraction in the feed.

An analytical solution to equation (1) is complicated; however, a simpler numerical solution can be found by using the method of lines to discretize the equation. To solve equation (1) in this manner, the length of the column is split into nodes from i = 0 at the beginning of the column to i = n + 1. The length of each node is then described by h = L / (n+1). The cation equivalence fraction as a function of height must be discretized as follows:

$$\left(\frac{\partial x_M}{\partial Z}\right)_i = \frac{x_{m,i+1} - x_{m,i-1}}{2h} \tag{5}$$

With $\alpha = \left(\frac{1-\varepsilon}{\varepsilon}\right)\left(\frac{\overline{C}}{C}\right)\rho$, equation (1) becomes:

$$\alpha \frac{dy_{m,i}}{dt} + \frac{\partial x_{m,i}}{\partial t} + u_0\left[\frac{x_{m,i+1} - x_{m,i-1}}{2h}\right] = 0 \tag{6}$$

With equations (2) and (6) we get the following relationship for the metal equivalence fraction at node i as a function of time:

$$\frac{dx_{m,i}}{dt} = -u_0 \frac{x_{m,i-1} + x_{m,i-1}}{2h} - K_L a(x_{m,i} - x^*_{m,i}) \tag{7}$$

Equation (2) becomes:

$$\frac{dy_{m,i}}{dt} = \frac{K_L a}{\alpha}(x_{m,i} - x^*_{m,i}) \tag{8}$$

Integration of equations (7) and (8) yield the cation equivalents fraction as a function of time for the mobile and stationary phases respectively.

$$x_{m,i}^{j} = \left[ -u_0 \frac{x_{m,i+1}^{(j-1)} - x_{m,i-1}^{(j-1)}}{2h} - K_L a(x_{m,i}^{(j-1)} - x_{m,i}^{*(j-1)}) \right] \Delta t + x_{m,i}^{(j-1)} \quad (9)$$

$$y_{m,i}^{j} = y_{m,i}^{(j-1)} + \frac{K_L a}{\alpha}(x_{m,i}^{(j-1)} - x_{m,i}^{*(j-1)}) \quad (10)$$

Where j is the present time step and j-1 and j+1 indicate the past time step and future time steps respectively as represented by $t_j = t_{j-1} + \Delta t$.

This numerical solution can now be applied to nonlinear isotherms and eventually expanded to multiple component systems to effectively model breakthrough behavior.

*7.3 Results and Discussion*

In order to verify the numerical solution, it was necessary to compare the results of an analytical solution to those given by Equation 9. Therefore, the constant-pattern wave approach model used by Lee et. al. and adapted as described previously was used to predict the breakthrough curve for a feed containing a constant source of pure divalent cations ($x_i = 1$) assuming a linear isotherm where $y_i = x_i^*$. The results of this comparison are shown in Figure 11 for a distance of 0.14 cm into the column.

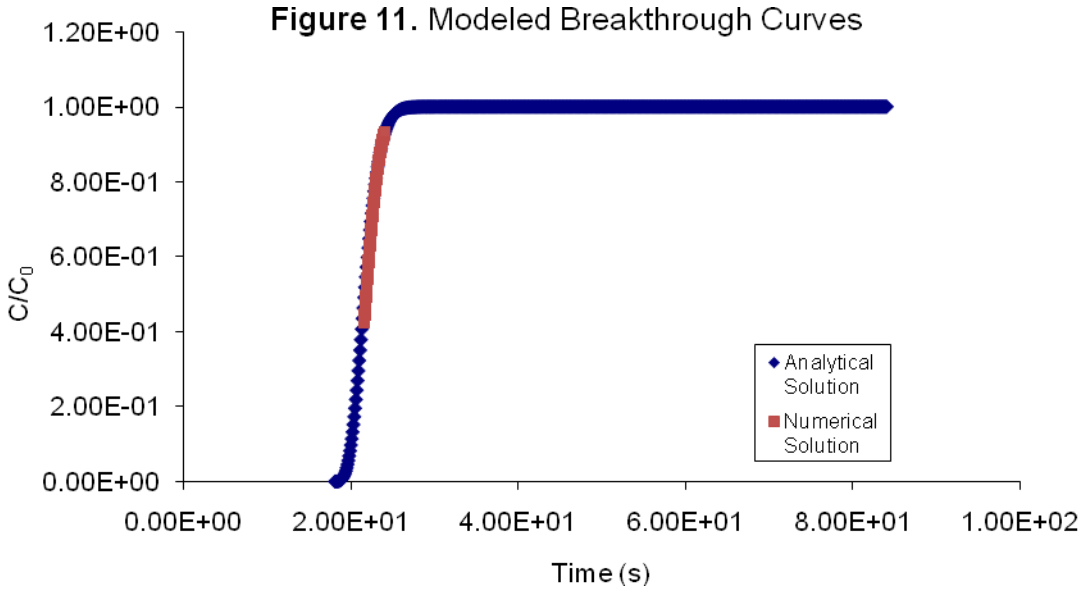


**Figure 11.** Modeled Breakthrough Curves

As Figure 11 illustrates, the breakthrough curves for the analytical and numerical solutions match up well for a linear isotherm. The next step in modeling the breakthrough curve is to expand the numerical solution to non-linear isotherms. This is usually the case for ion exchange systems. Further, the model needs to be adjusted to account for multiple species competing for sites on the resin surface.

*7.4 Conclusions*

Modeling of ion exchange breakthrough curves is an important step in being able to predict the dynamic behavior of small and larger scale systems. Accurate prediction of breakthrough times and the length of the mass transfer zone is crucial in scaling up designs of ion exchange columns. A knowledge of the breakthrough pattern for each component in a complex mixture allows for more effective bed utilization prior to regeneration. Further, it allows for predicting the long-term behavior and efficacy of a regenerant solution that is continually reused and accumulates cations.

An analytical and numerical solution for modeling the breakthrough curve for a single species in a divalent system with a linear isotherm has been presented. Further, it is believed that this numerical solution can be expanded to non-linear isotherms as well as to multiple component systems. Future work with this model will allow for accurate prediction of breakthrough times for multiple components in a complex system.

## 8.0 Economic Feasibility of Ion Exchange Pre-Treatment of CAP Water

### *8.1 Introduction*

It has been shown that ion exchange pre-treatment is a scientifically feasible method for improving water recovery from a reverse osmosis system. The benefits to using ion exchange pre-treatment are the decreased brine volume and higher water recovery. A common and expensive method for brine treatment is an evaporation pond. Due to the decreased brine volume, much smaller evaporation ponds will be required to treat the brine and remove the salts. Brine treatment is especially important in southern Arizona where salt accumulating in groundwater is a big threat to future water supplies.

Since ion exchange is considered a beneficial process as a pre-treatment add on to a reverse osmosis system in terms of brine minimization, it is necessary to determine whether the ion exchange process is economically beneficial. The basis of an economic analysis can be the value of decreasing the brine volume and recovering extra water compared to the long-term cost of installing, operating, and maintaining an ion exchange pre-treatment system. Therefore, an economic analysis was performed for a hypothetical reverse osmosis system treating a feed CAP water at 20 MGD.

### *8.2 Background*

As mentioned earlier, the benefits of an ion exchange pre-treatment system are twofold. First brine minimization leads to smaller evaporation ponds required for treating the reverse osmosis brine. Second, the improved water recovery leads to a significant water savings that is also economically valuable. These benefits can be assigned a monetary value and then compared to the overall cost of an ion exchange system.

This economic analysis was done by estimating the capital costs for the ion exchange system required to treat 20 MGD of CAP water. The method of column design was adapted from Water Treatment Principles and Design and used to determine the required amount of resin, columns, and column size to treat the 20 MGD of water (Crittenden, 2005). Following determination of the system requirements, the capital costs were estimated using relationships for vertical vessels (Seider, 2004). The capital cost for the resin was estimated as \$4,240 $m^3$ (Ion Exchange Chemistry and Operation). Finally, the capital cost of the regenerant storage tank was estimated using a correlation to volume (Seider, 2004). Other capital costs were assumed negligible in comparison or were assumed already in place since this system will be added on to an existing system. It was assumed that the ion exchange process will allow for an increase in recovery from 80% to 92%. Finally, operations and maintenance were estimated and an economic analysis was performed with a 20-year lifetime at an 8% discount rate to determine an overall net present value for the benefits and costs of the ion exchange pre-treatment system.

### *8.3 Results and Discussion*

The economic analysis performed was based on several key factors. First, the size of the equipment drove the total capital investment; however, the total capital investment was

small in comparison to the lifetime cost of operation and maintenance. The components of the capital cost are shown in Table 1.

**Table 1 –** Capital Costs for Ion Exchange Equipment

| **Vertical Vessels** | |
|---|---|
| Shell thickness, $t_s$ (in) | 1 |
| Material of Construction | Stainless Steel 316 |
| Diameter, $D_i$ (in) | 196.9 |
| Height, L (in) | 177.2 |
| Weight of Vessel (lbs) | 60117 |
| Empty Vessel Cost, $C_v$ ($) | $105,367.03 |
| Platforms and Ladders, $C_{PL}$ ($) | $15,136.09 |
| Materials Factor, $F_M$ | 2.1 |
| Number of Vessels | 7 |
| Purchase Cost, $C_P$ (mid-2000 $) | $1,592,857.57 |
| Purchase Cost, $C_P$ (Sep-2008 $) | $2,461,652.21 |
| **Resin** | |
| Total Bed Volume ($m^3$) | 131.4 |
| Resin Cost ($/$m^3$) | $4,237.76 |
| Total Resin Capital Cost (1997-$) | $557,002.31 |
| Total Resin Capital Cost (Sep 2008-$) | $876,379.09 |
| **Regeneration Tank** | |
| Tank Volume (gall) | 56630 |
| Type | Floating Roof |
| NaCl (lbs) | 681,439 |
| NaCl Cost ($/lb) | $0.02 |
| NaCl Cost ($) | $13,629 |
| Purchase Cost, $C_P$ (mid-2000 $) | $99,560.34 |
| Purchase Cost, $C_P$ (Sep-2008 $) | $167,492.47 |

The biggest cost for the system was the lifetime cost of chemical addition. This includes lime, soda ash, sulfuric acid, and the sodium chloride required for regeneration. These

costs over 20 years added up to a net present value of approximately $54 million and are shown in Table 2.

**Table 2 –** Feedstock Costs

| **Feedstocks** | |
|---|---|
| Soda Ash (lbs/yr) | 23922561.73 |
| Soda Ash Cost ($/lb) | $0.1647 |
| Soda Ash Cost ($/yr) | $3,940,045.92 |
| Lime (lbs/yr) | 6699175.416 |
| Lime Cost ($/lb) | $0.1756 |
| Lime Cost ($/yr) | $1,176,375.20 |
| Sulfuric Acid (lbs/yr) | 5017412.933 |
| Sulfuric Acid Cost ($/lb) | $0.0469 |
| Sulfuric Acid Cost ($/yr) | $235,316.67 |
| NaCl (lbs/yr) | 5021858.635 |
| NaCl Cost ($/lb) | $0.02 |
| NaCl Cost ($/yr) | $100,437.17 |
| Energy cost per Regen Cycle ($/cycle) | $45.35 |
| Regen Cycles per year | 865.4205501 |
| Energy Costs ($/yr) | $39,246.82 |
| **Total Annual Cost** | **$5,491,421.78** |

In comparison, the capital investment had a net present value of approximately $16.9 million. The estimated value of the decreased evaporation pond size and increased water recovery are shown in Table 3.

**Table 3 –** Value of Water Savings and Evaporation Pond Savings

| **Evaporation Ponds** | |
|---|---|
| Cost for 13.5 mgd (2007-$) | $98,800,000.00 |
| Cost for 20 mgd at 92% Recovery (2007-$) | $27,480,755.81 |
| Cost for 20 mgd at 80% Recovery (2007-$) | $47,620,360.44 |
| Cost for 20 mgd at 92% Recovery (2008-$) | $31,848,177.03 |
| Cost for 20 mgd at 80% Recovery (2008-$) | $55,188,499.19 |
| **Capital Cost Savings (2008-$)** | **$23,340,322.15** |

| **Water Value** |
|---|

| | |
|---|---|
| Water Value ($/ft$^3$) | $0.0889 |
| Water Saved at 92% Recovery (ft$^3$/yr) | 117,104,167.1 |
| **Capital Saved ($/yr)** | **$10,410,560.45** |

Finally, overall total capital investment was calculated using Lang factors (Seider, 2004). With estimations for the required operations and maintenance, the overall net present value of the ion exchange pre-treatment process can be calculated and is shown in Table 4.

**Table 4 –** Economic Analysis Results

| **Lifetime Analysis** | |
|---|---|
| Lifetime (yrs) | 20 |
| Discount Rate (%) | 8 |
| O&M Net Present Value | -$20,191,034.19 |
| Feedstock Net Present Value | -$53,915,588.52 |
| Total Capital Investment | -$16,861,569.38 |
| Water Savings Net Present Value | $102,212,417.10 |
| Evaporation Pond Savings | $23,340,322.15 |
| **Net Lifetime Savings** | **$34,584,547.18** |

Overall, a net savings of $34.6 million are realized by instituting an ion exchange pre-treatment process. It can be seen from Table 4 that the driver of the savings is the value of the water saved with an increase of 12% recovery.

*8.4 Conclusions*

Ion exchange pre-treatment is a scientifically and economically feasible method for improving water recovery from reverse osmosis treatment plants. An economic analysis on treating a 20 MGD supply of CAP water revealed that the economic benefits of ion exchange pre-treatment outweigh the additional costs incurred. A net present value for the savings/earnings was calculated to be approximately $34.6 million over a 20 year lifetime. It was determined that the biggest driver of the cost was chemical addition. If

further regenerant saving techniques can be implemented, like using the reverse osmosis brine, this process becomes significantly more economically advantageous. Economically and scientifically, ion exchange is a feasible process for brine minimization and improving water recovery.

Literature Cited

Crittenden, J. C. "Design of Rapid Small-Scale Adsorption Tests for a Constant Diffusivity." Journal WPCF 58 (1986): 312-19.

Crittenden, John C., R. R. Trussell, David W. Hand, Kerry J. Howe, and George Tchobanoglous. Water treatment principles and design. Hoboken, N.J: John Wiley, 2005.

"ION EXCHANGE CHEMISTRY AND OPERATION." Ion Exchange Systems and Equipment. REMCO Engineering Water Systems and Controls. 8 May 2009 <http://www.remco.com/ix.htm>.

Kaakinen, John W., and Paul E. Laverty. Cation Exchange Pretreatment Studies for High Recovery - Yuma Desalting Plant. Tech. no. REC-ERC-82-11. Yuma: U.S. Department of the Interior - Bureau of Reclamation, 1983.

Kaakinen, John W. Cation-Exchange Pretreatment Studies for La Verkin Springs. Tech. no. REC-ERC-84-12. La Verkin Springs: U.S. Department of the Interior - Bureau of Reclamation, 1984.

Lee, I-Hsein, Yu-Chung Kuan, and Jia-Ming Chern. "Prediction of ion-exchange column breakthrough curves by constant-pattern wave approach." Journal of Hazardous Materials 152 (2007): 241-49.

Masters, Gilbert M., and Wendell P. Ela. Introduction to Environmental Engineering and Science (3rd Edition). Upper Saddle River: Prentice Hall, 2007.

Papirer, Eugene. Adsorption on silica surfaces. New York: Marcek Dekker, 2000.

Robins, Robert G., Tadahisa Nishimura, and Pritam Singh. "Removal of Arsenic from Drinking Water by Precipitation, Adsorption or Cementation." Technologies for Arsenic Removal from Drinking Water (2001): 31-42.

Seider, Warren D. Product and process design principles synthesis, analysis, and evaluation. New York: Wiley, 2004.

# Appendix 10:

Use of Ion Exchange Softening with Regenerant Recycle
as Pretreatment for Reverse Osmosis
Desalination of Central Arizona Project Water

# Use of Ion Exchange Softening with Regenerant Recycle as Pretreatment for Reverse Osmosis Desalination of Central Arizona Project Water

Justin Nixon, M.S. Report

Environmental Engineering, 2010

## Abstract

To meet projected water demands within Arizona, full allocation of Central Arizona Project (CAP) water must be utilized. As brackish water resources play a greater role in regional water supply, salt management is a major issue in the state. Together, the Central Arizona Project (CAP) canal and the Salt River bring over 1 million tons of salt per year into central and southern Arizona. Since little leaves, salt accumulates in regional soils and aquifers. To address these concerns, investigations have been performed to evaluate reverse osmosis (RO) desalination of CAP water and salt management strategies for RO residuals. Ion exchange is a potential method for pre-treating CAP water to increase water recovery during reverse osmosis treatment and to minimize the resultant brine volume. Pilot-scale investigations in Tucson have indicated tradition RO treatment of CAP water is limited to 80% recovery. If scale-forming cations are removed prior to RO treatment, the expected maximum recovery is above 90%. Both RO and ion exchange produce a brine waste, and therefore treatment and disposal of wastes from these processes are considered as a single problem. In the study reported here regenerant reuse is explored. Results suggest that a sodium regenerant solution can be reused, with periodic softening, to regenerate a strong acid cation exchange resin. The results suggests the pretreatment of CAP water using IX before RO desalination can increase water recovery to over 97%. In a comparative economic analysis, it was found that IX pretreatment was preferred relative to RO plus brine evaporation ponds or RO plus VSEP and brine evaporation ponds, if the RO recovery was equal or greater than 96%.

## Introduction

Reverse Osmosis is the most common and widespread method of desalination. Non-mechanical limitations to desalination include scaling and fouling of RO membranes. Precipitation can occur in feed water with high concentrations of dissolved ionic species when concentrated through reverse osmosis process. Scaling limits reverse osmosis recovery because the precipitated salts inhibit transmembrane water flux. The production of concentrate (brine) is a primary determinant of economic feasibility (Kaakinen & Laverty, 1983). Evaporation ponds are the primary method for brine disposal. These are expensive due to land requirements and the brine disposal cost typically is a significant fraction of the overall reverse osmosis plant cost. Therefore, brine minimization and recovery optimization are primary drivers for the RO process.

Ion exchange pre-treatment potentially serves as an economical method for improving RO recovery. For example, the Yuma Desalting Plant water recovery was limited due to high concentration of total dissolved solids. High calcium and sulfate concentrations cause gypsum (CaSO4) to precipitate on the membranes. As a result, recovery was limited to approximately 80%. However, the addition of ion exchange pretreatment of the feed water produced a maximum recovery of 92.89% (Kaakinen & Laverty, 1983)

At La Verkin Spring, The Bureau of Reclamation demonstrated the feasibility of ion exchange to minimize and improve recovery for a desalting operation designed to lower the salinity of the Colorado River (Lykins, 2009). It was found that ion exchange pre-treatment allowed for recoveries of up to 92%, indicating ion exchange pretreatment as a method for brine minimization and improved recovery (Kaakinen & Laverty, 1983)

# 1. Background

### 1.1 Overview

Local ground water in accessible aquifers of the Tucson Active Management Area (TAMA) contains 200-300 mg/L of total dissolved solids (TDS) **Table 1.1**. These waters have traditionally been served to the public following disinfection. To meet projected water demands, TAMA utilizes Central Arizona Project (CAP) water. When CAP water enters the Tucson area it contains ~750 mg/L TDS. CAP utilization in the TAMA will bring at least 200,000 metric tons of salt annually to the Tucson area. (Pearson, 1999) This accumulation of salt will remain in the area due to Tucson's location at the southern terminus of the CAP canal. Without salt management steps, the average salinity of TAMA will double over a 50-year period. (**Figure 1.1**) (Pearson, 1999).

**Table 1.1** CAP water quality – comparison to Tucson well data

| Water Quality Constituent (mg/L) | Tucson Water Production Wells | CAP Water |
|---|---|---|
| Total Dissolved Solids | 259 | ~750 |
| Hardness (as CaCO3) | 119 | 270 |
| Sodium | 40 | 112 |
| Chloride | 17 | 104 |
| Calcium | 39 | 56 |
| Magnesium | 5 | 31 |
| Sulfate | 45 | 280 |
| Alkalinity (as CaCO3) | 126 | 98 |
| TOC | <1 | 3.5 |

The addition of CAP water to the TAMA has already increased TDS levels in delivered water and as a result membrane treatment is necessary to maintain average TDS levels near 450 mg/L (Yenal, Maximizing Water Recovery During Reverse Osmosis (RO) Treatment of Central Arizona Project (CAP) Water, 2009).Though essential to salt management, reverse osmosis requires a significant amount of energy and produces brine. RO treatment of CAP water is limited to 75-80% to avoid membrane scaling (Malcolm Pirnie Inc., and Separation Processes Inc., 2008). Tucson has no ready sink for RO brines, so disposal costs will add significantly to cost of RO treatment.

**Figure 1.1** The water supply/demand projections for the TAMA. The geographic boundaries of the TAMA are shown in the map at right.

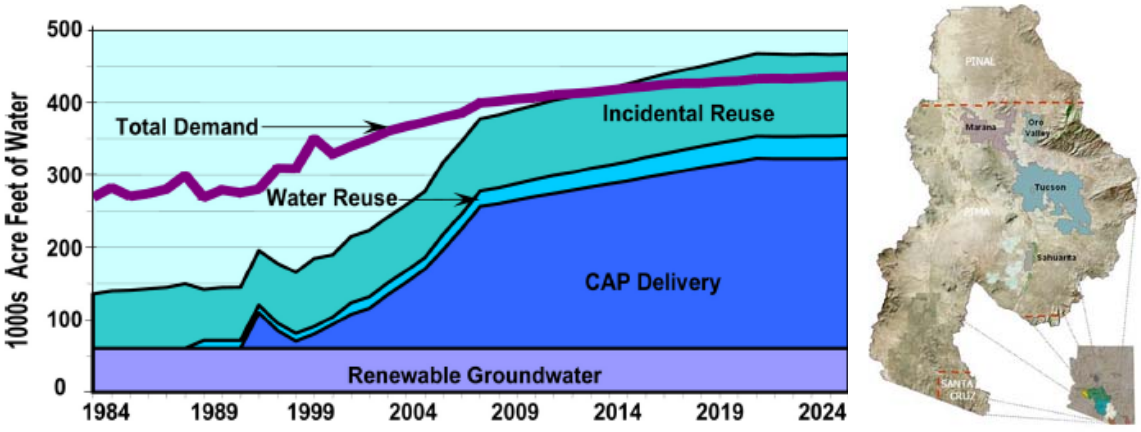

**Table 1.2** Concentration and solubility data for CAP water species that may contribute to membrane scaling (Yenal, Maximizing Water Recovery During Reverse Osmosis (RO) Treatment of Central Arizona Project (CAP) Water, 2009)

| *Precipitate* | *Ion Concentration* | *Log (ion product)* | *log $K_{s0}$* | *Degree of Saturation [(b)]* |
|---|---|---|---|---|
| $BaSO_4(s)$ | $[Ba^{+2}] = 1.17 \times 10^{-6}$ M<br>$[SO_4^{-2}] = 2.81 \times 10^{-3}$ M | -8.48 | -10.0 | 827.83 |
| $CaSO_4(s)$ | $[Ca^{+2}] = 2.0 \times 10^{-3}$ M | -5.25 | -4.85 | 9.95 |
| $CaCO_3(s)$ | $[CO_3^{-2}] = 1.0 \times 10^{-5}$ M [(a)] | -7.7 | -8.48 | 150.64 |

(a) based on 120 mg/L carbonate alkalinity as $HCO_3^-$ and pH = 8.0.

(b) calculated as $25 \times 10^{[\log(\text{ion product}) - \log KS0]}$. The value represents the approximate degree of over saturation in the RO brine produced from CAP water assuming 80% water recovery.

Early precipitation of solids from CAP water is caused by the high cation levels of calcium and barium. **Table 1.1** displays the solubility products of common membrane scalants $BaSO_4$, $CaSO_4$, and $CaCO_3$. Pre-RO softening to remove divalent cations that contribute to membrane scaling will allow greater recoveries during RO treatment. This report examines this strategy to minimize brine volume via ion exchange pretreatment of CAP water

The project includes operation of pilot-scale facilities, located on Tangerine Road, approximately 20 miles north of the city of Tucson on I-10. The facilities were constructed and provided by U.S. Bureau of Reclamation (USBR), the City of Tucson, and the water utilities based in northwest Pima County consisting of the Metropolitan, Marana, Oro Valley and the Flowing Wells Irrigation District. Pilot-scale facilities for desalination of CAP water include slow sand filtration (SSF), microfiltration (MF), ion exchange unit, chemical addition to prevent membrane scaling and fouling, reverse osmosis and VSEP treatment of RO brine.

## 1.2 Brine minimization through IX pretreatment (softening) of CAP water

In theory, removing hardness cations from CAP water prior to RO treatment will make it possible to drive reverse osmosis well past 80 percent recovery without precipitating $BaSO_4(s)$ or $CaSO_4(s)$. (Malcolm Pirnie Inc., and Separation Processes Inc., 2008). Ion exchange itself produces brine for disposal, however, and in communities that practice both salt management and wastewater reclamation/reuse the disposal of brines in municipal sewers is counter-productive. Ion exchange was proposed as a pretreatment for CAP water, to increase water recovery during RO and minimize RO brine volume. The IX regenerant solution will be used several times, after which time the solution itself will be softened, the original ion balance restored by adding NaCl, and the solution will be used for an additional series of regeneration steps. Bench-scale IX experiments designed to confirm the feasibility of pre-softening CAP water via IX involved a strong acid cation (SAC) synthetic polymeric resin manufactured by USA Resin to remove hardness ions.

## 1.3 Ion Exchange Theory

Ion exchange is a process in which resin beads containing exchangeable cations or anions are contacted with an electrolyte solution to change the ion composition of the solution. The process has been used in water softening by exchanging hardness ions for sodium ions and demineralization of water by removing both cations and anions. Other applications include separation of products from bioreactors and recovery of metals from dilute solutions. (McCabe, Smith, & Harriott, 2005)

Most processes use synthetic ion-exchange resins, although some natural materials such as clays and zeolites have natural ion-exchange capability. Synthetic resins are prepared from organic polymers such as cross-linked polystyrene to which ionizable groups have been added (McCabe, Smith, & Harriott, 2005). Cation exchangers include weak acid resins with carboxylic acid groups ($-COO^-$), and strong-acid resins with sulfonic acids with ($-SO_3^-$). Anion exchanger materials can have weak-base amine groups (-N+H3) or strong-base ammonium groups [-N+(CH3)3].

In both cation and anion exchange resins, the acid or base groups are chemically bonded to the resin matrix which gives the resin a high concentration of fixed positive or negative charges. These charges are balanced by mobile counterions such as $Cl^-$, $OH^-$, or $NO_3^-$ for anion resins or $H^+$, $Na^+$, or $Ca^{2+}$ for cation resins, maintaining electrical neutrality within the resin particles. Ion exchange takes place when the activity of ions in the feed solution differs from that of the ions in the resin phase (McCabe, Smith, & Harriott, 2005).

Resins are insoluble in water, but they swell in aqueous solution to an extent depending on the electrolyte concentration within the feed solution, concentration of fixed charges, and degree of cross-linking. (McCabe, Smith, & Harriott, 2005). Extent of resin swelling varies with each manufacturer. For sulfonic acid resin with a moderate degree of cross-linking, the swollen volume of the Na-form resin in dilute solution is about 1.8 times its dry volume and has 45 percent porosity. While swelling is desirable to increase diffusion rates inside the particles, swelling decreases the capacity of resin per unit volume of bed. Resins are characterized as spherical beads ranging in size between 0.3 and 1.2 mm. (McCabe)

## 1.4 Equilibria (Background)

The capacity of an ion exchange resin is the number of exchangeable groups per unit mass (or volume) of resin. Ion exchange is a reversible process in which the counterion in the resin is replaced by a different ion within the feed solution. Cation exchange of a sodium-form resin with a monovalent ion $A^+$ is defined by the following reaction

Monovalent exchange $$\boldsymbol{A^+ + NaR \Leftrightarrow AR + Na^+}$$

Equilibrium constant, K, for the reaction is expressed in terms of activities or the product concentrations and activity coefficients

$$\boldsymbol{K = \frac{c_{Na^+} c_{AR}}{c_{A^+} c_{NaR}} \times \frac{\gamma_{Na^+} \gamma_{AR}}{\gamma_{A^+} \gamma_{NaR}}}$$

For dilute solutions, the activity coefficients do not change much with concentration, and a simple concentration-base equilibrium constant is used.

$$K' = \frac{c_{Na^+} c_{AR}}{c_{A^+} c_{NaR}}$$

When a monovalent ion is replaced by a divalent ion, each new couterion balances two charged sites on the resin.

Divalent exchange $$B^{2+} + 2NaR \Leftrightarrow BR_2 + 2Na^+$$

$$K' = \frac{(c_{Na^+})^2 c_{BR_2}}{c_{B^{2+}} (c_{NaR})^{2+}}$$

## 1.5 **Reactor Description.**

The City of Tucson loaned a bench-scale ion exchange reactor system (Tomar Water Systems, Inc.) to the project. The system consists of 4 columns of S40 clear PVC pipe, each with a 2-in diameter and a 32-in length. Resin capacity per vessel was 0.061 $ft^3$. Optimal flow for each column was 0.25 gpm, producing an overflow rate of ~11.5 $gpm/ft^2$. This is well within the norms for field-scale operation of ion exchange processes. In the field application a Memcor microfiltration unit was used to pretreat the CAP water before the ion exchanger. The microfiltration unit operates with membranes at pore size of 0.2 microns. The filtrate of MF unit enters a 55 gallon tank, designated as the IX feed tank illustrated in **Figure 1.2**

When in operation, a rotary vane pump provides CAP water to the IX system with a maximum flow of 1 gpm. Columns of the IX unit are filled in upflow direction. Bottom manifold is closed preventing water drainage. Columns 1-4 operate in in parallel while only columns 3&4 can operate in both series and parallel. To switch there is valve that allows the effluent of column 3 to enter column 4.

**Figure 1.2** Ion exchange setup at the Pilot Plant Facility

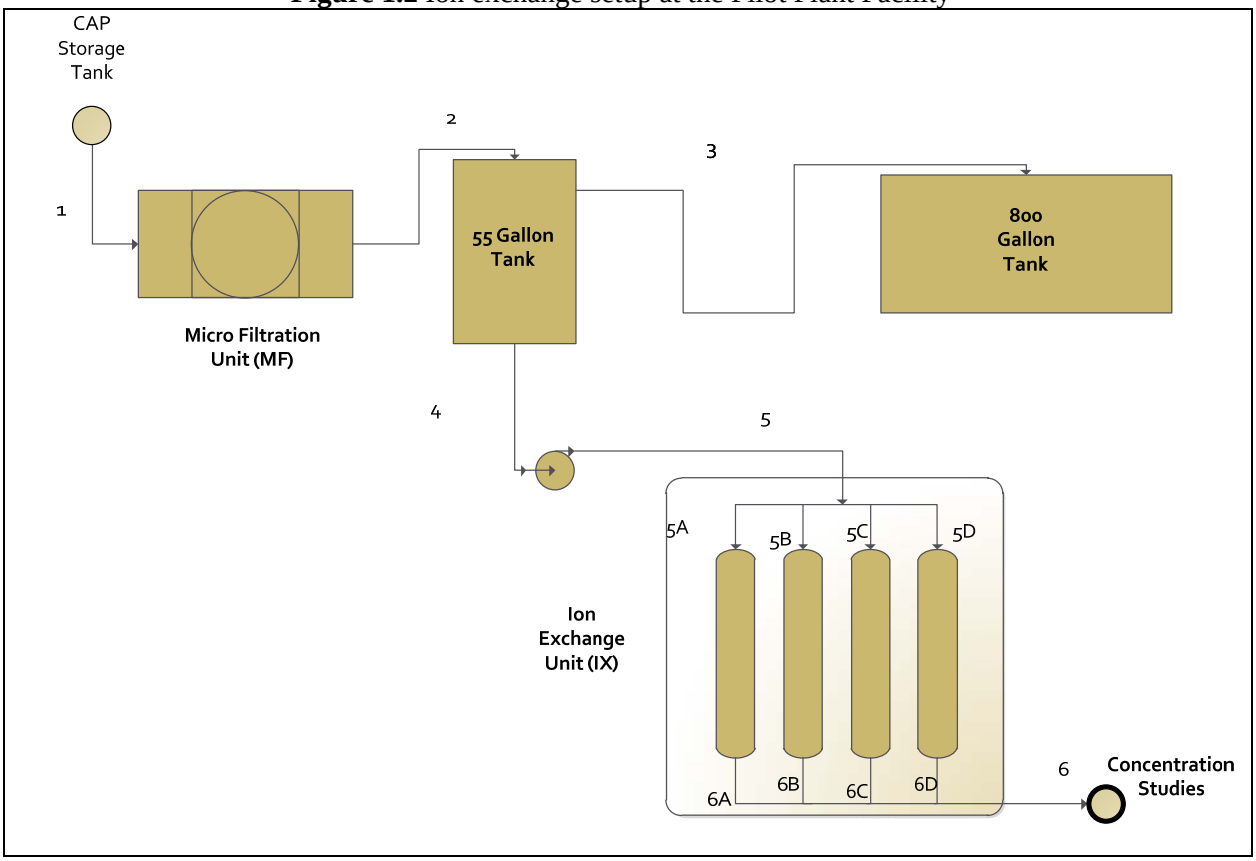

## 1.6 Normal (Softening) Mode

**Figure 1.3** illustrates the ion exchange operation performed at the field site. The Memcor Microfiltration unit provides CAP water to the ion exchange indicated as stream 1 (S1) in the figure. Prior to entering the exchange columns, the MF filtrate enters a cartridge filter indented as E-1 in the figure. This reduces particulates which could potentially interfere with resin binding sites. The CAP water exits filter (E-1) as stream 2 (S2) and enters pump P-1. Pump P-1 is capable to providing 1 gpm flow to the TOMAR ion exchange unit indicated by steam 3 (S3).

Stream 3 is divided 4 streams indicated by streams S3.1-S3.4. Streams S3.1-S3.4 enters four ion exchange columns. Not that each streams have corresponding valves which allow restrict flow each column. In other words, the system is able run however many columns that are needed. The four columns are labeled C1, C2, C3, and C4 on the following figure. Each column is provided CAP water by streams S3.1, S3.2, S3.3, and S3.4 respectively. Within each column the hardness ions are exchanged with sodium. Effluent streams for each column are indentified by S4.1-S4.4. C which all combine as stream 5 (S5) entering 400 gallon tank indicated in previous BFD (**Figure 1.2**) Note, prior to running in normal mode, ion exchange columns must be filled from bottom to top. This is described and illustrated in the Regeneration Mode section. Once the columns are filled, Tomar system is ran in normal mode described below.

To operate normal mode, open Valve-V1 located to top right hand corner of the Tomar system. This provides MF treated CAP water to the IX unit as indicated by Stream 1 (S1) in the figure below. Initially valve V-7 is closed preventing water from exiting the system. Valve V-7 is red and located below the manifold that combines the effluent of each column. Close valve V-4 and open valve V-3 which allow columns to be filled from bottom flow. Both valves located above the pump towards the bottom of IX system. Each valve is labeled with arrows indicating the direction the handles must be turned to operate either regeneration or normal mode.

Experiments were performed one column at a time. Valves V6.1-V6.4 are used to fill columns C1-C4 respectively. The following description applies to column 1 only, though each column can be operated in similar fashion. Close valves V6.2-V6.4 to isolate restrict flow to column 1 only. Also close valves V5.1-V5.4 which regulates flow into columns 1-4 through the top of each column. These valves are characterized as black knobs located on the front panel of IX unit.

Once the valves are adjusted, turn on pump by turning the off/on switch located on the front panel. Once the pump is on, adjust the bypass valve V-2 to regulate flow into the IX unit. If valve V-2 is fully closed, water is feed into column 1 at 1 gpm, which is too fast and will cause resin to back towards the top of the column. If V-2 is fully opened, the pump is not able to provide enough water to fill column 1. Must adjust valve V-2 in between these two extremes to fill the column 1.

As the column fills, make sure to rid the column of air bubbles to ensure water has complete contact with the resin bed. This is achieved by reasonably tapping the column until the air bubbles exit through the top of the column.

Once the column is filled, turn off the pump by turning the off/on switch. Close valve V-3 and open valve V-4 by turning the yellow valve handles above pump to normal mode position indicated by the arrows

labeled on the handles. This orientation will allow water to enter the top of the column 1illustrated in the figure as stream 3.1 (S3.1)

Turn on pump and open valve V-7 to run system in normal operation. Flow through column 1 will exit through the drain which a pipe is located at the bottom right hand corner of the IX unit. The drain nozzle is below the manifold on which houses valves V6.1-V6.4 located. A ½ '' ID pipe is connected to the drain nozzle to transport IX effluent to 55 gallon barrel. A submersible pump transports the IX effluent to the an 800 gallon tank located north of the VSEP shed for future use in VSEP concentration study.

The flowrate is measure with a graduated cylinder and a stop watch. Most of the experiments were with a single column with flowrate between 1000-1200 ml/min. To set flowrate, adjust bypass valve V-2 to regulate flow to pump P-1. Also adjust valve V-5.1 to regulate flow into top of column 1. Initially samples were taken every 2 hours. Calcium concentrations of the effluent were determined by EDTA titration which is explained in the Hardness detection of the report. Calcium concentrations were determined for the Feed CAP water as well.

When the effluent calcium equaled to that of CAP feed, saturation was obtained. Once saturation is obtained, turn off IX unit by turning the off/on switch located on the front panel of the IX unit. Close valve V-7 and V-1 to prevent leaking of water. At this point the system is ready for regeneration which is described in next section.

Eventually, a method was implemented allowing resin capacity to be calculated without constant sampling. The tomar system was operated in identical fashion as described above. Samples were taken a few hours after the start of operation. Change occurred when effluent flow indicated by Stream 5 was diverted to VSEP Tank and an additional barrel. Flow entering the additional barrel was slight in comparison (approximately 20 ml/minute) with total flow diverted to VSEP Tank. Flow diverted to additional was collected over a period of 24 hours. Water collected in barrel was mixed using paint stirrer for approximately 5 minutes. Water from this barrel is titrated at site along with feed sample and initial effluent samples.

Once calcium concentrations are determined, a mass balance is performed to determine amount of calcium removed which is described in future section (will show example plot and calculations). Once calcium removal is calculated changes in resin capacity are plotted as function of regenerant uses and calcium accumulation in regenerant.

**Figure 1.3 Normal (Softening) Mode**

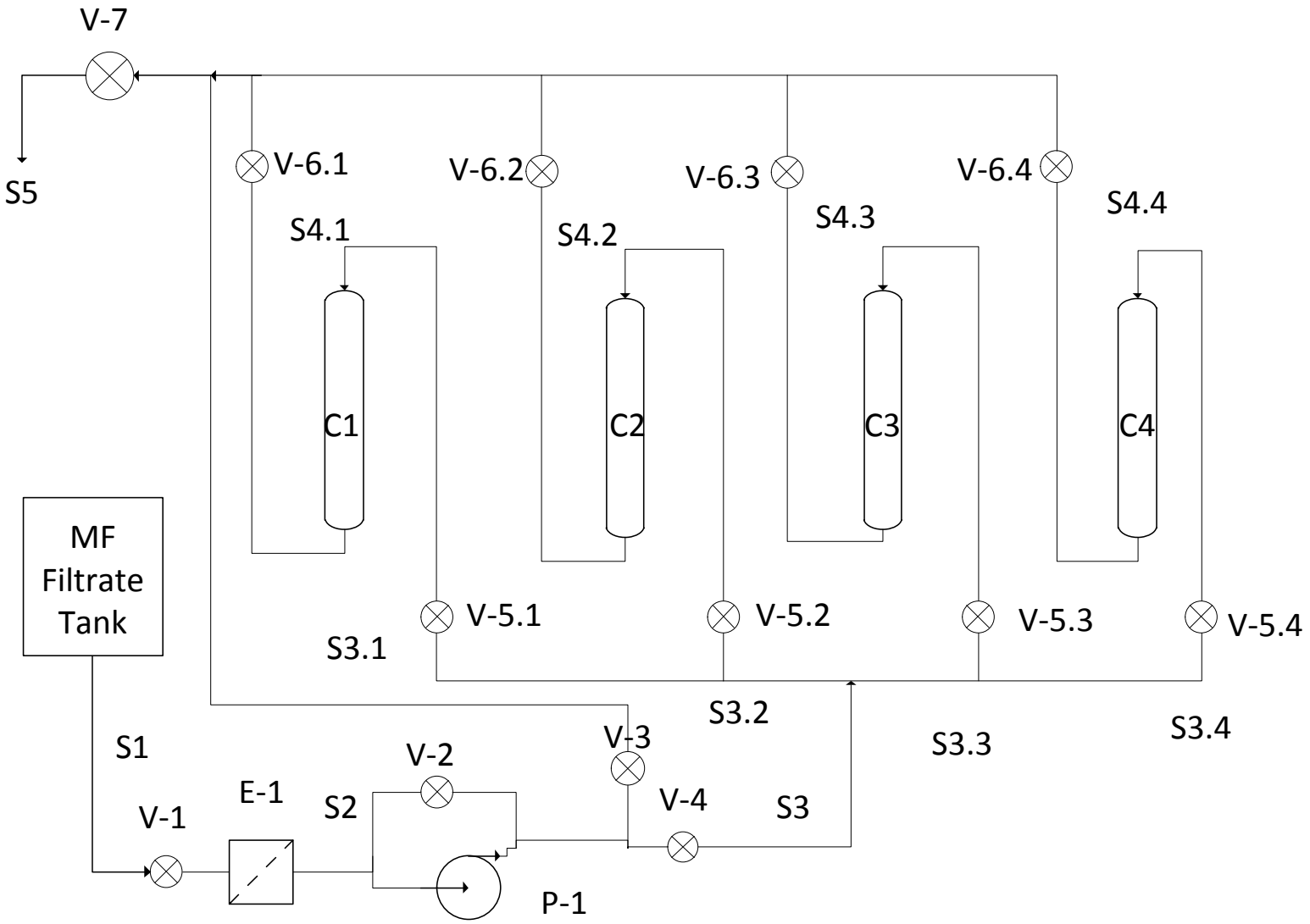

## 1.7 Regeneration Mode

According to manufacturer, the recommended volume of regenerant solutions is 2-7 BV with a regeneration time of 1 hour. Experiments were performed using resin bed volume of approximately 2 L. Regeneration solution fulfilled the high end of 7.5 bed volume requirement and added 3000 grams of Morton softening salt to 15 L of DI water. A paint stirrer is used to mix the regenerant solution for approximately 5 minutes. The IX unit is capable of regenerating all columns in parallel and columns 3&4 in series. However, regenerations were performed one column at a time resulting in four separate regeneration solutions. The regeneration of column 1 is described in **Figure 1.4**, though regenerations of remaining columns are performed in similar fashion.

A 50 L tank, provided by TOMAR systems, is attached to a 1gpm pump, located on metal stand beneath the columns, by ½ '' ID PVC Pipe. The tank is attached pvc pipe with a quick connect fitting.The rotary vane pump included with the Tomar system is connected to power source on the front panel of the system. The power source has power cord which is plugged into one of the various electrical outlets within the shed that houses MF unit. Prior to turning on the pump, it is necessary to adjust a series of valves.

Valve V-7 is located in the bottom right corner of the IX system. This valve is connected to a manifold that combines the effluent of each column. This valve must be closed, otherwise the regenerant will exit through the drain pipe. Valves V-3 and V-4 are adjusted in way that orients both valve handles perpendicular to the flow lines. These valves have yellow handles and are labeled with arrows indicating the orientation they must be in to operate in regeneration mode. This orientation opens valves V-3 and closes valve V-4. This allows the regenerant solution to enter the bottom of the exchange columns in the upflow direction.

Each column has an isolation valve located on a manifold of the drain pipe. These valves are illustrated in the following figure as valves V6.1-V6.4 correspond to columns C1-C4 respectively. To regenerate column 1, open valve V-6.1 and close valve V6.2-V64. Also close valves V6.2-V6.4. These valves regulate flow into columns C2-C4 during normal mode.

Once the valves are closed, turn the pump on by turning switch located on front panel of IX unit. This allows pump P-1 to provide regenerant solution to column 1 through stream 3 (S3). Valve V-2, is a globe valve attached to pump P-1 that regulates flow to pump. If V-2 is fully closed, the regenerant will enter column 1 at approximately 1gpm. This flowrate is too fast and will not only cause high pressure but will exceed the recommended flowrate suggested by manufacturer. Manufacturer suggests regeneration run time of 1 hour. A regenerant flowrate of approximately 250 ml/min allows the 15 L regenerant solution to single pass through the column. If valve V-2 is fully open, the regenerant solution will not be able to fill the column. Must adjust flow between the two extremes to fill column at adequate flowrate.

Valve V-5.1 is also used to regulate flow through column 1. If fully closed flow is prevented from exiting the top of column 1. Opening valve V-5.1 allows regenerant solution to exit the top of column1 and flow into a 20 L paint bucket which holds the regenerant till future use. As regenrant solution flows into bucket, a graduated cylinder and stop watch is used to ensure flow is approximately 250 ml/min. As the water level lowers in regenerant tank, head loss may require readjustment of valves V-2 and V-6.1.

During regeneration check flowrate every 15 minutes and adjust flow as need to ensure constant flow of 250 ml/min.

Once regeneration time reaches 1 hour, the regenerant tanks should be nearly empty ( there will always be a small portion remaining in the tank since regenerant exits tank a few centimeters from the its bottom. Turn off pump by turning power switch on front panel of IX unit. Empty the remaining few milliliters of regenerant from the tank into the regenerant storage bucket. There will be some regenerant remaining in the column 1. To collect, disconnect the ¼ '' ID PVC pipe that enters the base of column 1 indicated as stream 4.1 (S4.1) on the figure. Use a container to collect the regenerant that drains from column 1. To speed this process, disconnect the ¼'' ID PVC attached to the top of column 1, indicated by stream 5.1 (S5.1) on the figure.

Once the regenerant within Column 1 is collected add this portion into the storage bucket. Mix contents with a paint stirrer for approximately 5 minutes. Collect a sample (approximately 20 ml) of the regenerant solution to perform titrations for calcium determination and IC analysis. Once calcium concentration is obtained, add equivalent amount of NaCl to regenerant to replenish sodium concentration. Repeat this process after every loading cycle.

**Figure 1.4 Regeneration Mode**

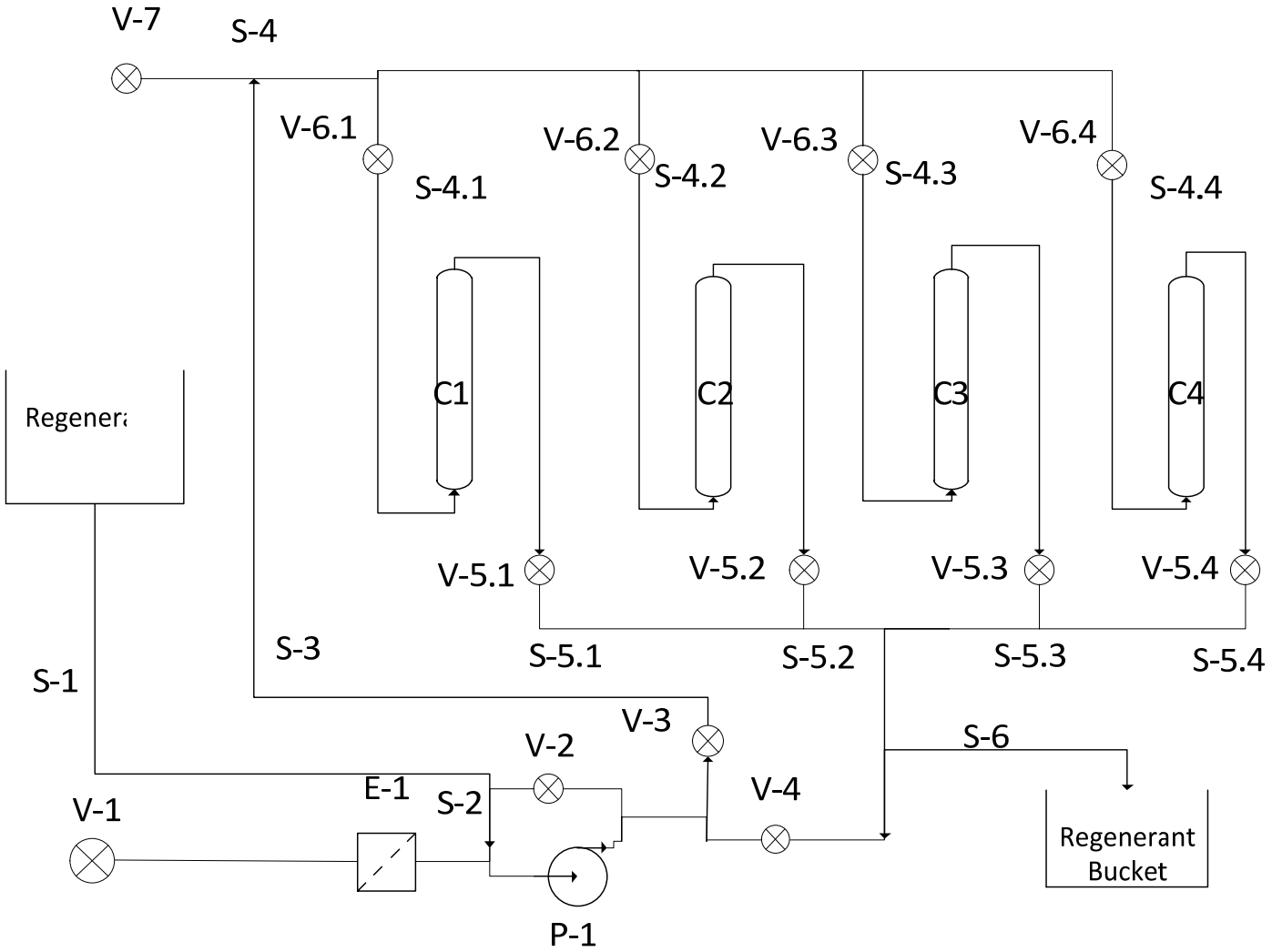

## 1.8 Regenerant Softening

Hardness ions accumulate in the regenerant solution during reuse. As a result, resin capacity decreases, which increases the frequency of regenerations. Lime and soda ash softening involves the precipitation of hardness ions within the regenerant solution. Once precipitated, the hardness ions are removed by filtration and the regenerant solution can be reused. Prior to this, calcium concentration in regenerant solution is used to calculate the amount of lime and soda ash that is needed.

The softening procedure followed method outlined by (Masters & Ela, 2008). The first step is the addition of lime ($Ca(OH)_2$) for the removal of aqueous $CO_2$. In this step, the pH is adjusted above 10.33 (the $pK_{a2}$ for $H_2CO_3$). The reaction is:

$$CO_2(aq) + Ca(OH)_2 \leftrightarrow CaCO_3(s) + H_2O \qquad \text{(Eq. 1)}$$

Following the pH adjustment, lime is added for the removal of calcium carbonate hardness through the precipitation of calcium carbonate as follows:

$$Ca^{2+} + 2HCO_3^- + Ca(OH)_2 \leftrightarrow 2CaCO_3(s) + 2H_2O \qquad \text{(Eq. 2)}$$

The magnesium carbonate hardness is also removed by the addition of lime:

$$Mg^{2+} + 2HCO_3^- + Ca(OH)_2 \leftrightarrow 2CaCO_3(s) + Mg(OH)_2(s) + 2H_2O \qquad \text{(Eq. 3)}$$

The calcium and magnesium noncarbonate hardness can then be removed through the addition of soda ash ($Na_2CO_3$) as follows:

$$Ca^{2+} + Na_2CO_3 \leftrightarrow CaCO_3(s) + 2Na^+ \qquad \text{(Eq. 4)}$$

$$Mg^{2+} + Na_2CO_3 + Ca(OH)_2 \leftrightarrow CaCO_3(s) + Mg(OH)_2(s) + 2Na^+ \qquad \text{(Eq. 5)}$$

The softening results in a suspension containing dissolved sodium chloride and solids of calcium carbonate and magnesium hydroxide. The solids were removed via filtration and the softened regenerant solution was reused. Water loss from the sludge was replaced and sodium chloride was added as necessary to maintain the initial concentration of 200 g/L NaCl

*Sample Calculation*

Calcium removal for each loading experiment was calculated from breakthrough curves listed in appendix A. The amount removed in each loading/regeneration cycle was summed to calculate the cumulative calcium in the regenerant solution. It was assumed magnesium was removed in the same proportion due to having similar equilibrium (K) values. Using the softening method outlined by Ela and Masters, the following table was generated to balance the softening equations 1-5. For the example it is assumed a cumulative mass of 6 moles of $Ca^{2+}$ was in the regenerant solution at the time of softening.

**Table 1.3**Softening Balance

| *Component* | *Amount (moles)* | *Lime* | *Soda Ash* | *CaCO3* | *Mg (OH)2* |
|---|---|---|---|---|---|
| ***CO2*** | 0 | 0 | 0 | 0 | 0 |
| ***Ca-CH*** | 0 | 0 | 0 | 0 | 0 |
| ***Mg-CH*** | 0 | 0 | 0 | 0 | 0 |
| ***Ca-NCH*** | 6 | 0 | 6 | 6 | 0 |
| ***Mg-NCH*** | 6 | 6 | 6 | 6 | 0 |

Since the regenerant solution was made with 15 L of distilled water, it was assumed the carbonate hardness was non-existent. Likewise $CO_2$ was considered negligible due to lack of carbonate.

$$6\ mol\ Na_2CO_3 \times \frac{106\ g\ Na_2CO_3}{mol\ Na_2CO_3} = 636\ g\ Na_2CO_3$$

$$6\ mol\ Ca(OH)_2 \times \frac{74\ g\ Ca(OH)_2}{mol\ Ca(OH)_2} = 444\ g\ Ca(OH)_2$$

636 grams of lab grade $Na_2CO_3$ and 444 grams of lab-grade $Ca(OH)_2$were added to the bucket that held the regenerant solution used during the column 1 experiments. A paint stirrer was used to mix the regenerant solution for approximately 15 minutes. The resulting suspension was left alone to settle for two days. After this elapsed time, most of the particles settled to the bottom of bucket as a white sludge leaving a clear, supernatant layer of regenerant solution.

The top layer was siphoned with ½ ‘’ ID tube into another 20 L paint bucket. This process was performed in such way not to disturb the white precipitate layer that had settled towards the bottom. Only 10 Liters of the original 15L regenerant solution was retrieved. The remaining volume of precipitates was disposed of while the recovered 10 L solution was filtered to remove suspended particles. Softened solution was filtered using vacuum pump, 1000 ml Erlenmeyer flask with nozzle for vacuum pump, and numerous glass fiber filters.

To restore regenerant volume to 15 L, a 5 L solution of 200g/L NaCl was added to the softened regenerant. The softened regenerant also needed additional sodium chloride to replenish the sodium removed during previous regenerations. Ion exchange chromatography should be used to determine sodium content of softened regenerant to determine amount of NaCl needed to reach 200 g/L. An alternative method is to add enough NaCl to reach a conductivity of 211 mS/cm.

## 1.9 Hardness Determination

When EDTA (ethylenediaminetetraacetic acid or its salts) is added to water containing both calcium magnesium ions, it combines first with the calcium that is present. Therefore, the calcium ion can be determined directly using EDTA when the pH is made significantly high so that the magnesium precipitates as $Mg(OH)_2$ and an indicator is used which combines to calcium only. Murexide indicator

was used to give a color change at a point where all the calcium complexes with the EDTA at a pH of 12-13.

A sample is added to an Erlenmeyer flask along with a magnetic stir bar and enough DI water for a total volume of 50 ml. 0.1 grams of Murexide indicator is added to the flask giving a pink color. Three milliliters of 1.0 M NaOH solution is added to the flask to raise the pH of its contents above 12. A buret is used to titrate the solution using 0.01 M EDTA solution. The titration endpoint is reached when the contents in flask change from pink to purple. There is a mole to mole ration between the amount of EDTA used and the amount of calcium within the sample. The sample volume used for titration depends on the its concentration. When determining the calcium concentration within the regenerant solution, only 1 ml is needed due to the rapid accumulation of calcium with regenerant reuse. However calcium concentrations within the IX effluent and CAP require larger sample volumes to so that enough EDTA is used for adequate determination.

## 1.10 Ion Exchange Chromatography

A Dionex DX500 ion chromatograph was used with CD20 conductivity detector for anion and cation analyses. A 30 mM MSA solution buffered the mobile phase. Flows were regulated using an IP25 Isocratic gradient pump system. A dual head pump transports the mobile phase solution from the proportioning valve, where buffers are combined in the injection valve ahead of the ion exchange column (Model CS16). After passing through the cation exchange column, flow enters a self-regeneration suppressor (SRS). In the SRS, water is hydrolyzed at the anode to produce $H^+$ cations, and reduced at the cathode to produce $OH^-$ anions. An anion exchange membrane is located within the suppressor, which allows the $OH^-$ to flow into the mobile phase buffer, neutralizing the $H^+$. Corresponding anions in the buffer are drawn through the anion exchange membrane to the anode side where they are removed to waste.

Software (PeakNet) for the Dionex DX500 consisted of the DX LAN program, data processing, method editor, and various other configuration/driver programs. The DX LAN communicates with the hardware via LAN lines to individual units. The DX500 can be operated from the computer (remote) or the front panels of the chromatograph itself (local). Data processing was performed after analysis. Standard solutions of known ionic composition were used to generate standard curves. In this way, retention times typical of sodium, calcium and magnesium were established. Primary cation concentrations in CAP water and CAP water following IX treatment are provided in Table 4.1. These highly preliminary results suggest that high-recovery RO treatment of the IX-pretreated water may be possible without generating calcium-containing ion products that greatly exceed their respective solubility products.

## 1.11 Concentration of IX effluent via Plate and Frame RO

Lab-scale experiments were performed to simulate RO treatment of CAP water pretreated with ion exchange. Two plate and frame units in series were used to concentrate IX pretreated CAP water. Permeate produced by the two RO units was collected and discarded. The concentrate was recycled back to the feed tank. The feed tank conductivity as a function of RO recovery was measured.

The plate and frame study is illustrated in **Figure 1.5**. The feed tank is filled with 10 L of IX treated CAP water. Feed water is provided to a positive displacement pump P-1as stream 1 (S-1). Pump P-1 provides water to the first plate and frame vessel. This vessel contains flat membrane manufactured by Sachaem. The membrane was cut from a larger spiral wound membrane in a rectangular shape with 4''× 6''dimensions. It is placed between two metal plates. Feed water travels along the membrane surface by crossflow. The applied pressure between the two plates allows water to permeate through the membrane. Permeate from the 1st RO is indicated in figure as S-3.

However the membrane flux is low relative to crossflow velocity. Most of the water exits 1st RO as concentrate. The concentrate exiting from 1st plate and frame is introduced as the influent solution of the 2nd Plate and Frame RO. This is indicated in figure as S-4. The 2nd plate and frame operates in similar fashion as the first RO. An applied pressure allows produces permeate stream S-6 that is collected and discarded as along with permeate from 1st RO S-3. The concentrate from 2nd RO is recycle back to the feed tank indicated by S-7 in the figure.

As time passes the volume of the feed solution decreases as permeate is produced and feed conductivity increases feed tank becomes more concentrated.

**Figure 1.5** Block-Flow Diagram of Plate and Frame Study

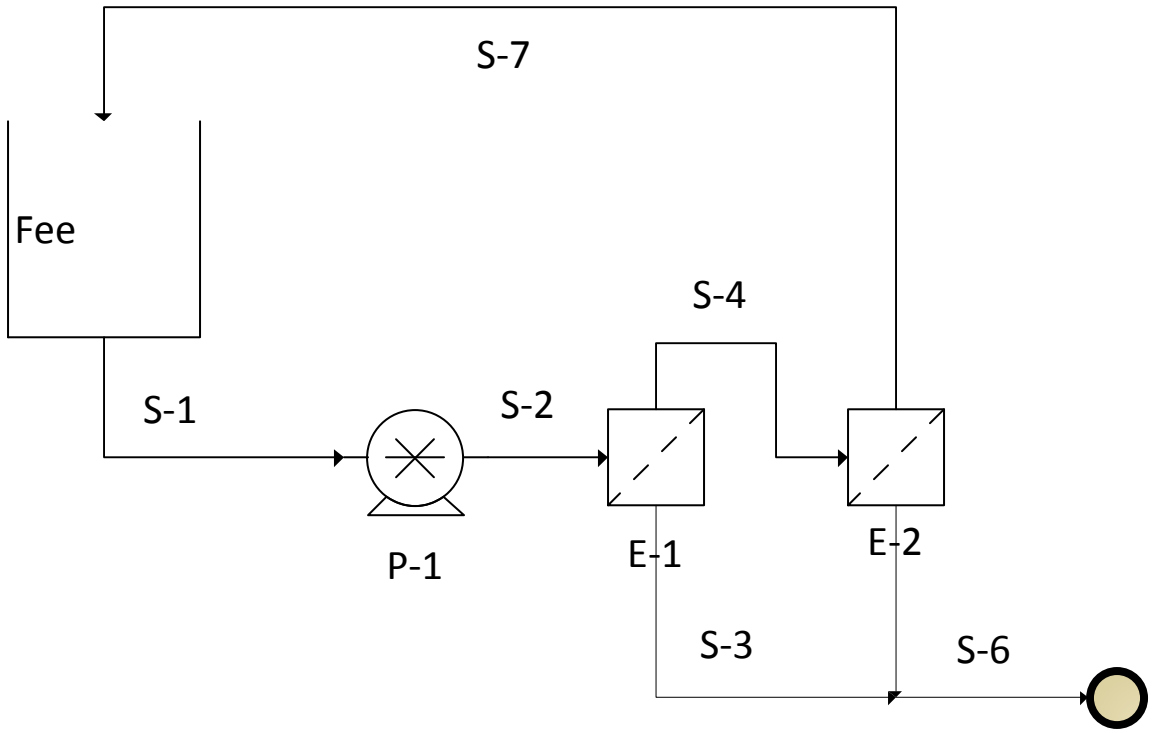

# 2. Results

## 2.1 Calcium Removal for CAP water

During the softening process, calcium effluent concentrations are below detection leve1. When breakthrough occurs, calcium begins to appear in the effluent. Once saturation occurs, the effluent concentrations should match influent concentrations. Figure 3.1 illustrates breakthrough curve for a single column containing 1.7 liters of USA brand resin. The effluent calcium concentration was plotted as a function of water treated. The volumetric flowrate was kept near constant - ranging between 1000 ml/min to 1200 ml/min. It is possible to calculate the amount of calcium retained by the resin by integrating the area under the feed concentration curve and above the breakthrough curve. The area is approximated by multiplying the volume of water treated by the influent feed concentration. Breakthrough curves for four series of ion exchange experiments are found in Appendix A.

**Figure 2.1** Ion exchange breakthrough curve for CAP water using an exchange column with a resin bed volume of 1.7 L.

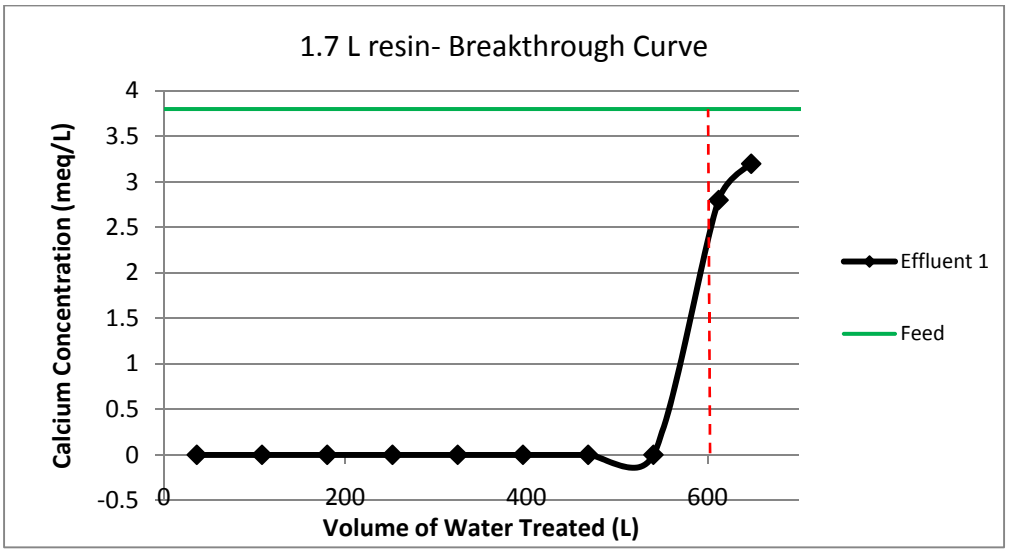


The loss of resin capacity with increase in the polyvalent cation concentration in the regenerant (before softening) was monitored and plotted. It was found that the loss of capacity was sensitive to the concentration of sodium in the regenerant solution. If no make-up sodium was added after each regeneration to maintain the sodium concentration constant in the regenerant, there was a markedly more rapid loss of resin capacity as illustrated by the figure below

**Figure 2.2** Resin exchange capacity during multiple loading/regeneration cycles with and without sodium chloride make-up after each cycle.

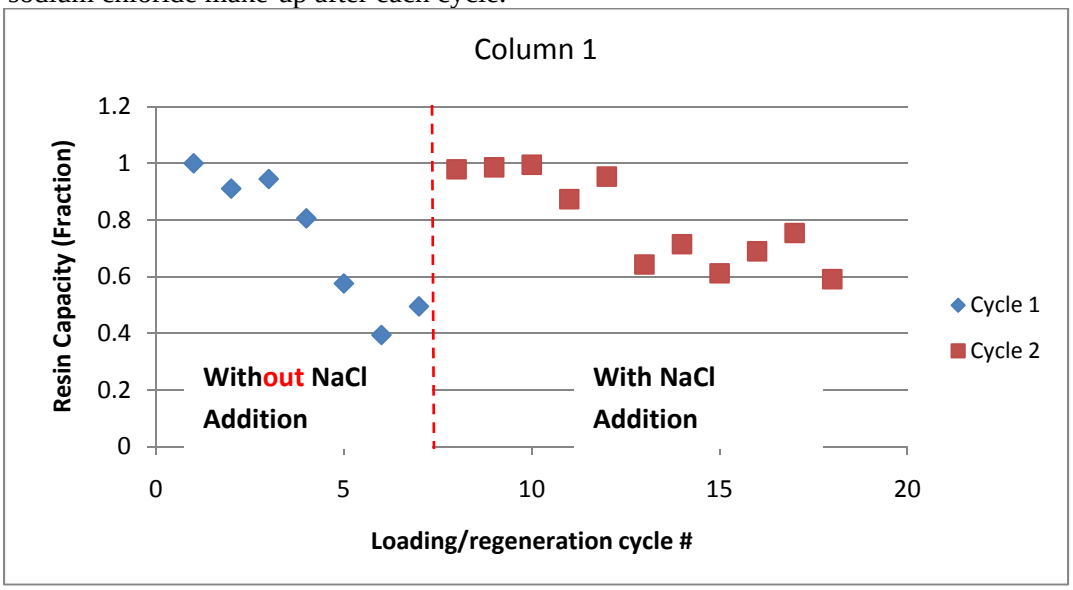


During the first cycle, resin capacity decreased immediately with each regeneration. Once resin capacity dropped to 40% capacity, the regenerant solution was softened to remove accumulated hardness ions. Once the regenerant was softened, NaCl was added to re-establish a concentration of 200 g/L NaCl (3.42 mol/L $Na^+$) and in the second experiment, the NaCl concentration was brought back-up to 200 g/L after each loading/regeneration cycle.

## 2.2 Bench-Scale Calcium Removal

Bench-scale experiments were conducted in the lab using same SAC resin used in the field. Resin was exposed to a loading solution containing only calcium cations to determine its capacity. Once saturated, the resin was regenerated using a highly concentrated NaCl solution. Resin Capacity was monitored as a function of regenerant reuses. Once capacity was below about 85%, the regenerant solution underwent a softening procedure to remove calcium the accumulated calcium and reach initial capacity. Figure below plots decrease resin capacity as function of number of loading/regeneration cycles.

**Figure 2.3** Resin exchange capacity for bench-scale calcium treatment during multiple regenerant softening periods (Montemayor, 2010).

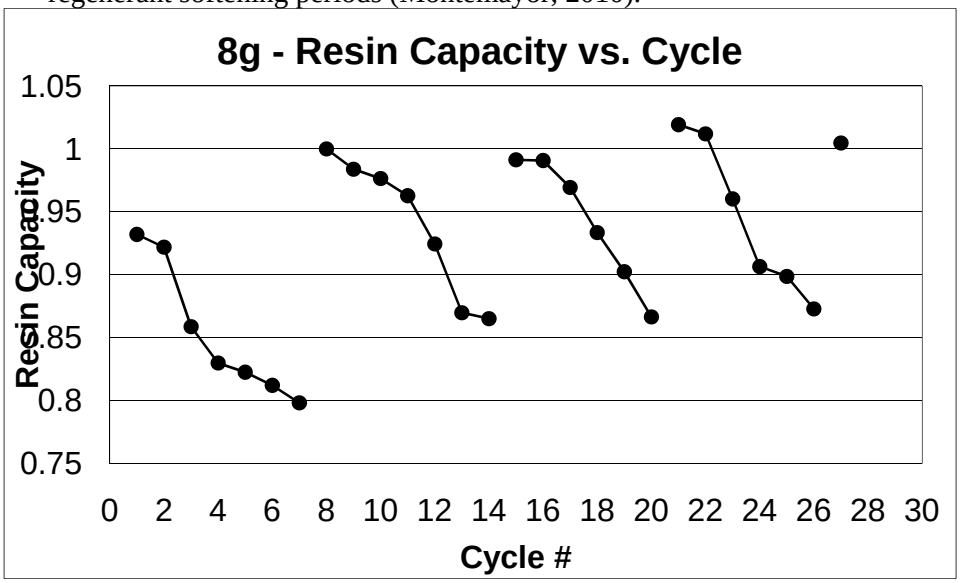


## 2.3 Ion Exchange Chromatography

The following figure displays an ion chromatograph (IC) of the IX CAP feed water after microfiltration. Method analysis indicates that peaks occurring at 10, 18, and 25 minutes are sodium, magnesium, and calcium respectively. The MF sample was diluted by a factor ten once since standard distribution curves only apply to 0 to 100 M range. Figure 3.5 displays the chromatograph for the ion exchange effluent.

**Figure 2.4** Ion Chromatograph of MF treated CAP water

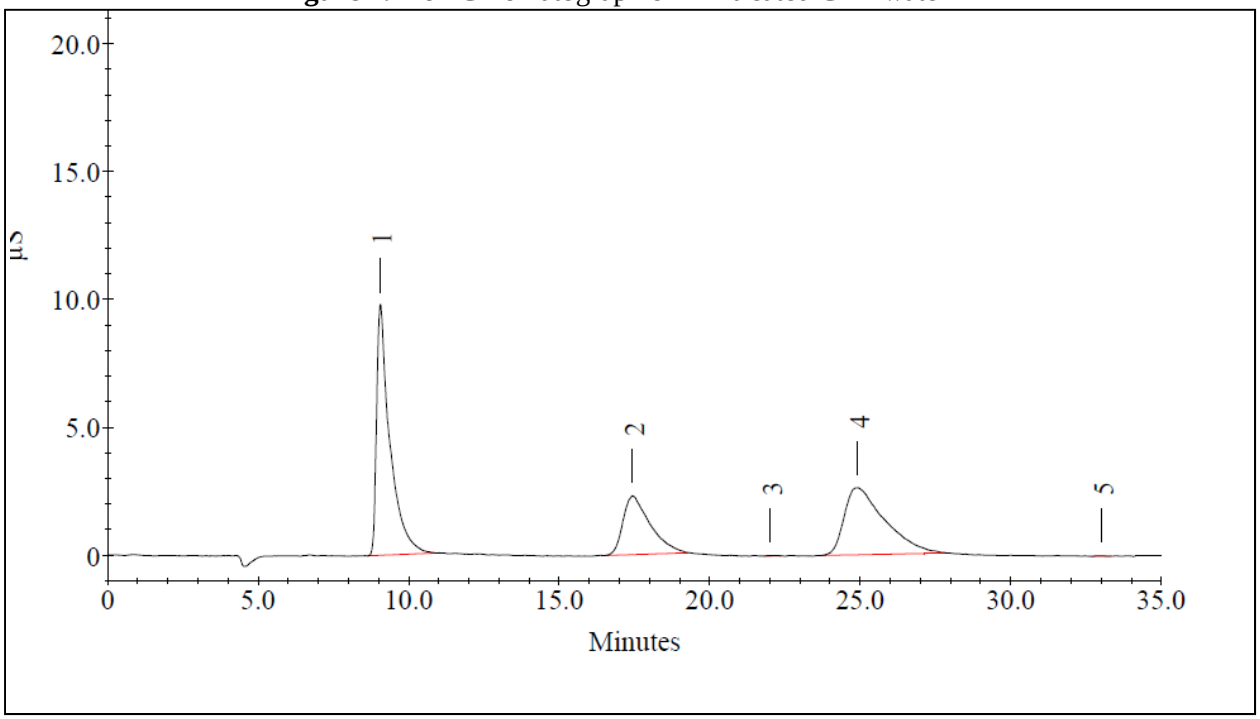


**Figure 2.5** Ion Exchange Chromatograph of IX treated CAP water

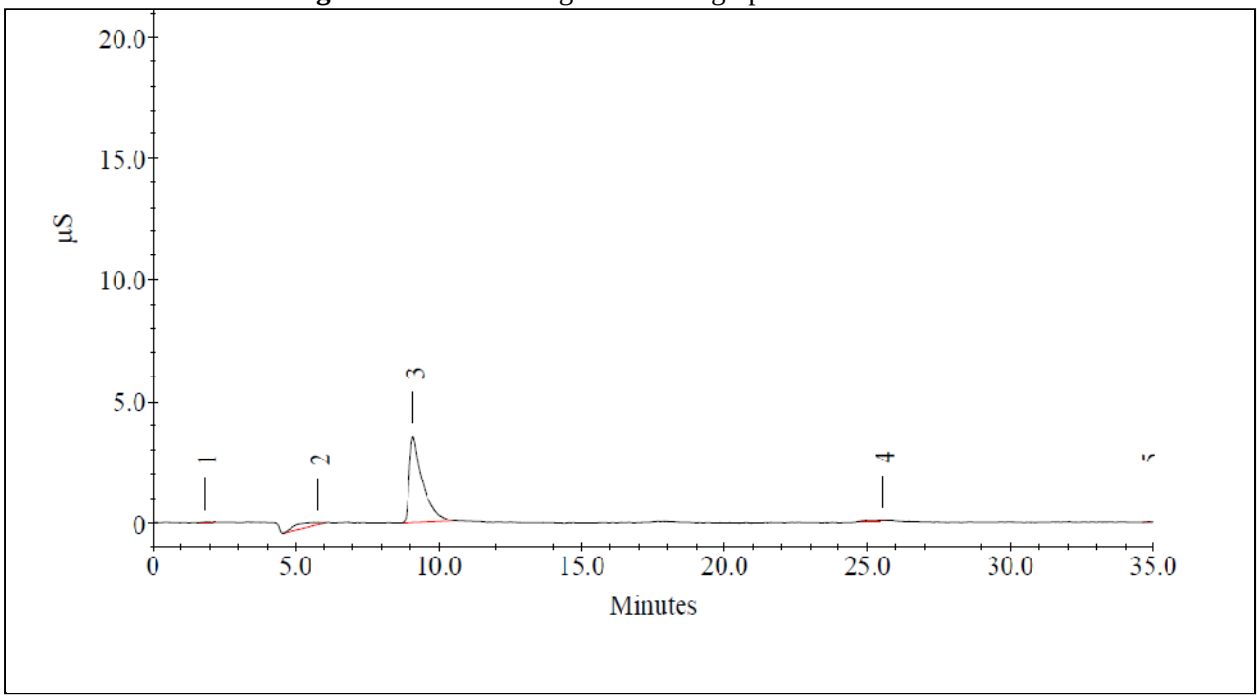


In the ion exchange effluent sodium is indicated by the sole peak at about 9.5 minutes. There are smaller peaks indicated but none are above the detection limit. Cation concentrations of both raw CAP water and softened CAP water were calculated from peak areas displayed in **Figure 2.4** and **Figure 2.5** . Standards prepared from reagent grade, dry salts were prepared and run through IC to produce standard curves from

which the concentrations of the various cations in the samples could be calculated. Ion compositions for CAP water pre- and post-IX treatment are displayed in Table 2.1

**Table 2.1** Concentrations of primary cations in CAP water and CAP water following IX treatment.

| | | | |
|---|---|---|---|
| Source | Sodium (mM) | Magnesium (mM) | Calcium (mM) |
| CAP Feed Water | 3.79 | 1.01 | 1.27 |
| IX Effluent | 6.68 | ND[1] | ND |

[1]ND = non detect. Quantity was below the method detection limit, which was << 10 µM.

## 2.4 Concentration and Induction Time Evaluation

Vibratory Shear Enhance processing (VSEP) was developed by New Logic, Inc. The process increases liquid/solid separation showing a significant improvement in the recovery fraction over conventional RO treatment. During VSEP, the brine or slurry is processed in a semi-batch mode between membrane leaf elements. Vibration of the membrane causes a shearing effect which lifts solids from the surface, thus retarding the onset of permeation loss due to build-up of solids on the membrane surface. This high shear cleaning action reduces membrane scaling while preserving water flux. (Yenal, Maximizing Water Recovery During Reverse Osmosis (RO) Treatment of Central Arizona Project (CAP) Water, 2009)

**Figure 2.6** Schematic view of the intense shear waves produced on the face of the membrane as a result of the vibration

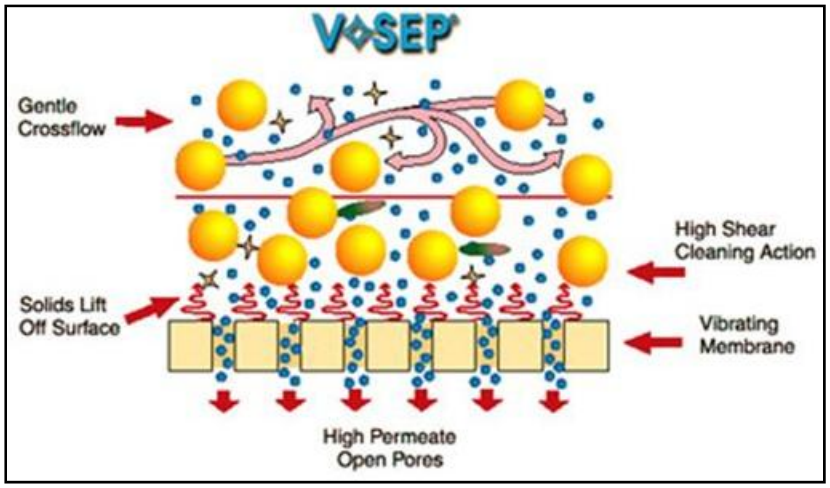


In desalination applications VSEP is conventionally used as a post treatment of RO brine for brine minimization. However, in this project VSEP was used as means to quickly concentrate IX treated CAP water to allow evaluation of the degree of precipitation at various recovery fractions. VSEP treatment of softened CAP water at 98% recovery was conducted for a duration of 24 hours. During this operation

properties were monitored such as permeate flux, concentrate flux, and conductivities of the influent, permeate, and concentrate stream. Data can be found the Appendices. Permeate flux of pre-softened CAP was compared to VSEP treatment of RO brine (from raw CAP) at 89% giving an equivalent overall recovery of 98%. (**Figure 2.7**)

**Figure 2.7** Comparative Flux of VSEP treated IX effluent to RO Brine

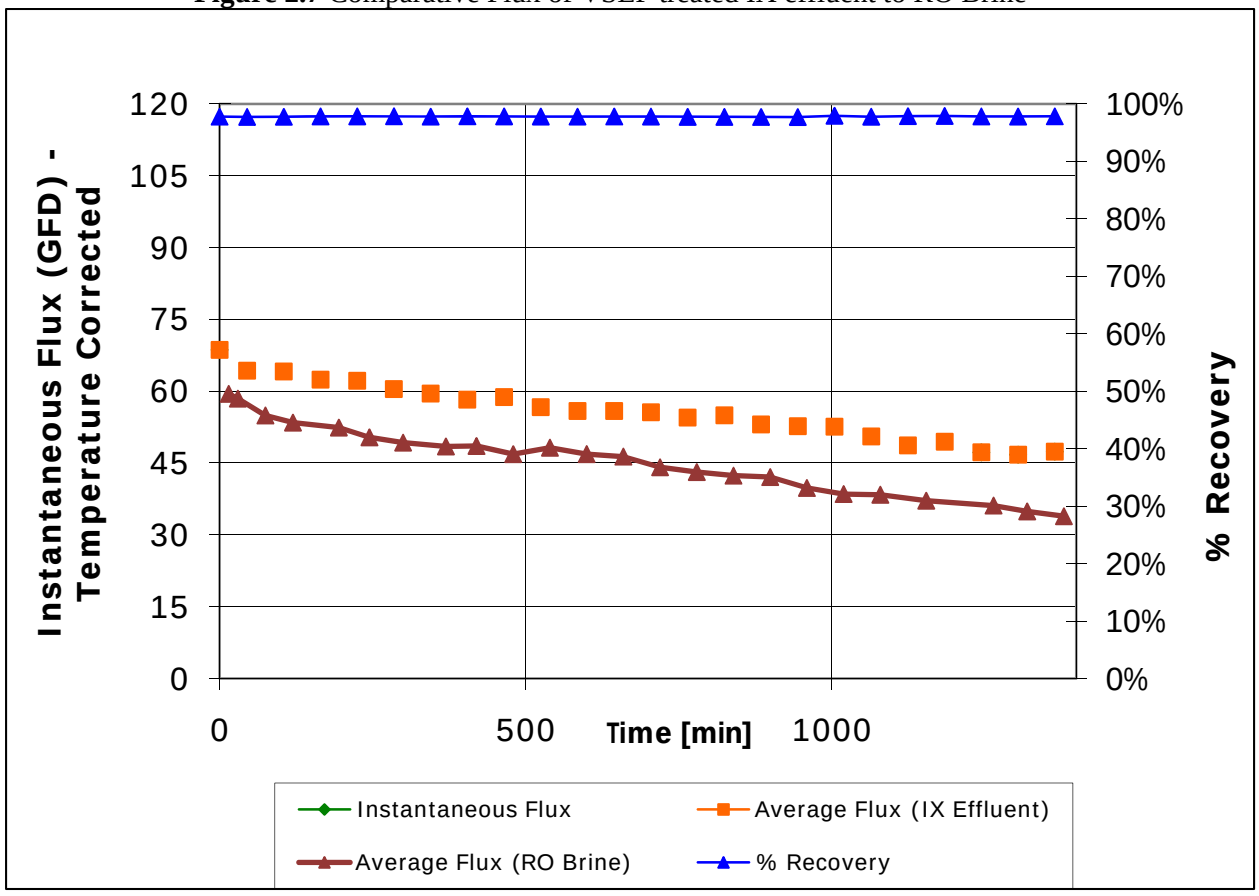


### 2.4.1 Induction Tests

When precipitation occurs in an aqueous solution, the light absorbance of the water increases. If precipitation does not occur, the solution maintains a constant absorbance as it is concentrated. Induction tests were performed to monitor absorbance of CAP water, pretreated with IX, and then concentrated using VSEP. The VSEP effluent was collected at various recoveries. Figure 3.9 shows the results of induction tests performed on VSEP brine at various recoveries.

**Figure 2.8** Absorbance versus time of VSEP generated brine of IX pretreated CAP water at 90, 95, and 96.1% recoveries (Xu, 2010)

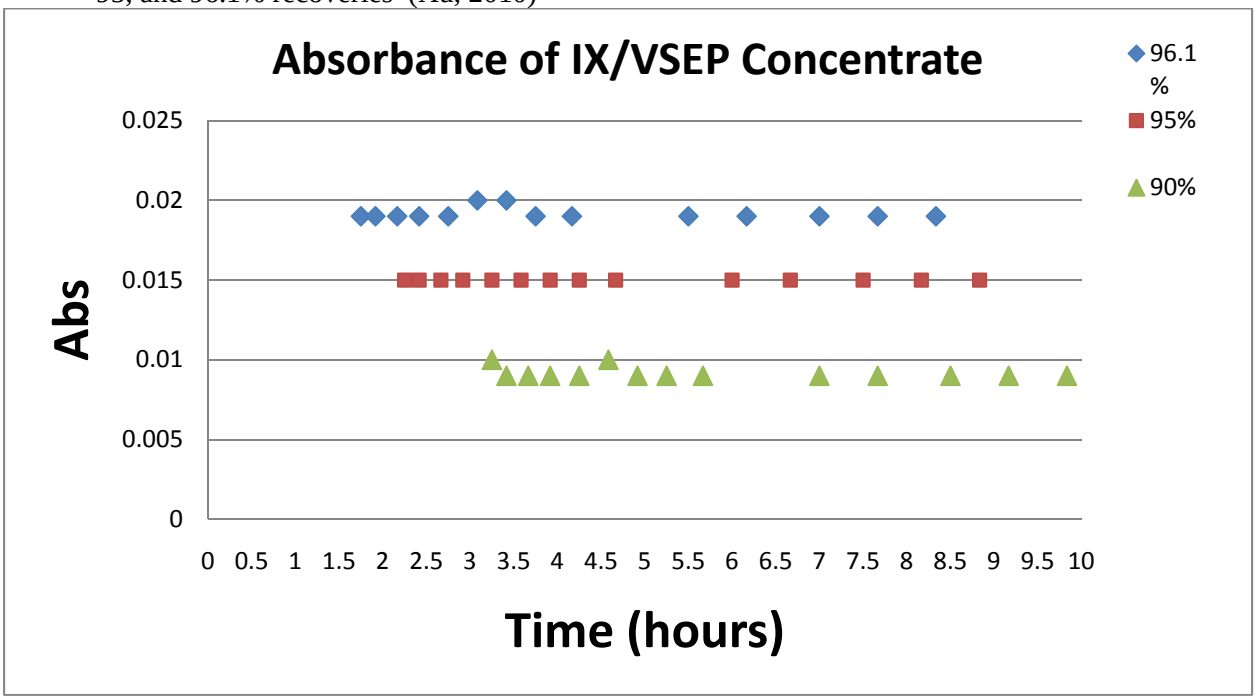


Constant absorbance indicates that no precipitation occurs within the brine during the period analyzed. Figure 3.9 indicates that softened CAP water may undergo RO treatment to recoveries up to 96.1% without membrane scaling. Additional, induction tests were performed at higher recoveries and are displayed in Figures 3.10 and 3.11. The absorbances of these brines were monitored for approximately 5 hours.

**Figure 2.9** 5-hour Induction of VSEP generated brine of IX pretreated CAP water at 95.6, 97.3, and 98.3% recoveries (Xu, 2010)

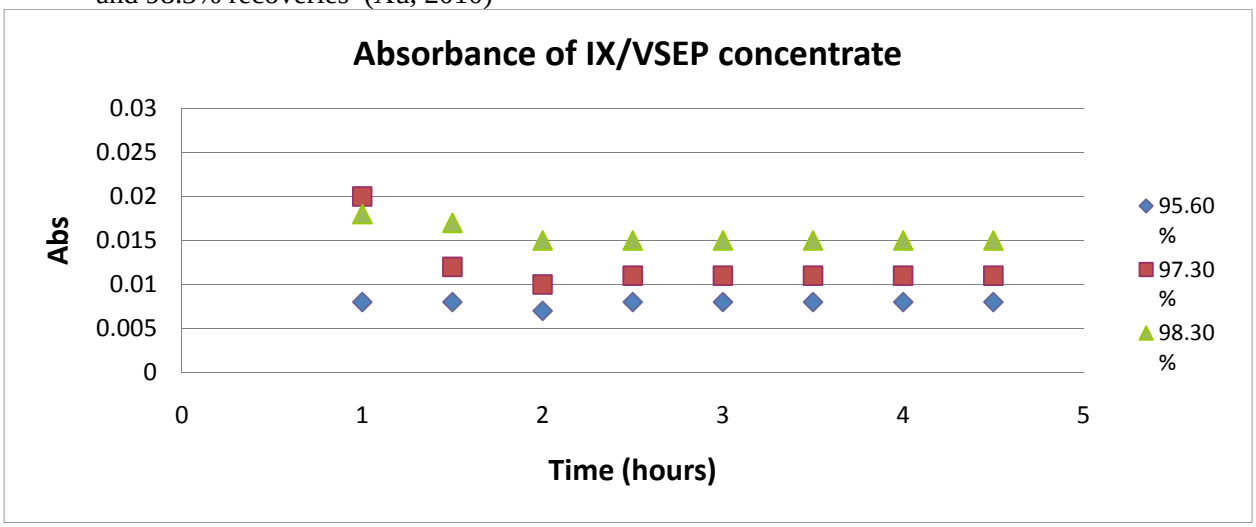

Representative induction tests were continued for a total time of 50 hours. Absorbance remained stable 45.5 hours after the test's start. Further monitoring at 48 and 50 hours resulted in stable absorbance indicating no precipitation occurred during induction period.

**Figure 2.10** 50-hour Induction of VSEP generated brine of IX pretreated CAP water at 95.6, 97.3, and 98.3% recoveries (Xu, 2010)

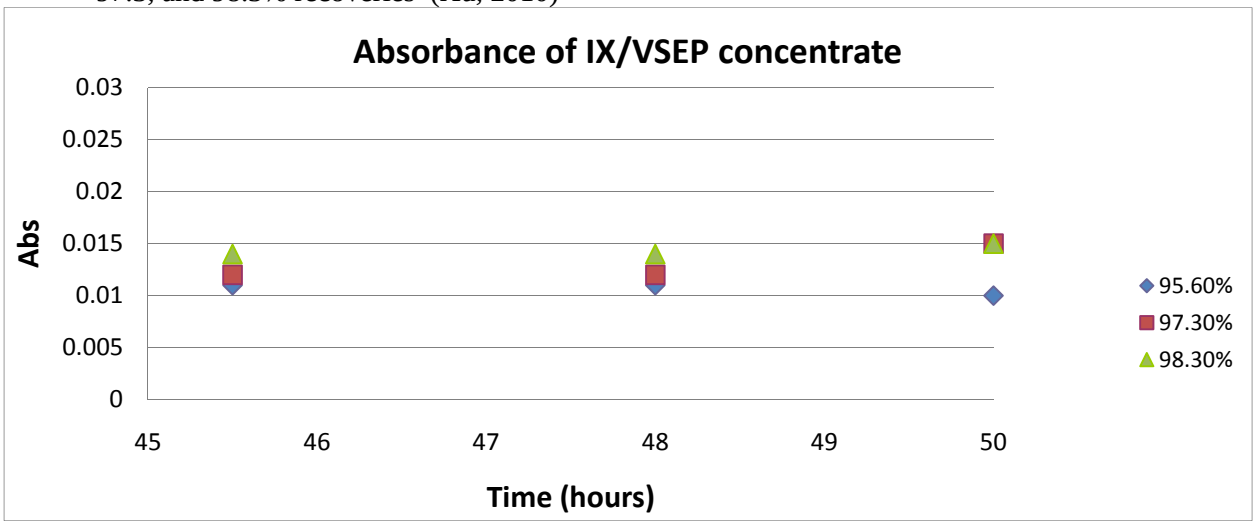


Stable absorbance at 98.3% suggests that softened CAP water may undergo RO treatment to recoveries up to 98.3% without membrane scaling

### 2.4.2 X-ray Diffraction (XD)

Potential scalants, $BaSO_4$, $CaCO_3$, $CaSO_4$, and $SrSO_4$, are in crystalline form when precipitated. The atomic planes of crystal cause an incident beam of X-rays to interfere with one another as they leave the crystal. This phenomenon is called X-Ray Diffraction (XRD). English physicists Sir W.H. Bragg and his son Sir W.L. Bragg explained why cleavage faces of crystals appear to reflect S-ray beams at certain angles of incidence (theta, θ ) and individual mineralogic species produce unique interference patterns of X-rays. Their explanation is mathematically formulated in Bragg's law:

$$n\lambda = 2dsin\theta$$

The variable d is the distance between atomic layers in a crystal, and the variable is the wavelength of the incident X-ray beam; n is an integer. This observation is an example of X-ray wave interference. (Anderson, 2010)

XRD measures the average spacing between layers or rows of atoms to determine the orientation of a single crystal or grain. Softened CAP water was concentrated to 98.3% recovery using VSEP. The concentrated brine was collected and dried by drying a sample in an oven at 80˚C. Once dry, the crystals were submitted for XRD analysis at The University of Arizona, Scanning and Imaging Facility. Phase identification of crystals was conducted by obtaining XRD pattern for the sample. The resulting data was compared with known standards in the JCPDS file, which are for random orientations (there are more

than 50,000 JCPDS cards of inorganic materials. (Anderson, 2010). XRD analysis identified that VSEP concentrate at 98.3% recovery contained significant masses of only halite (NaCl) and sodium carbonate sulfate ($3Na_2{:}CO_3{:}2SO_3$). This suggests that IX treatment successfully removed the divalent cations within CAP water, which prevents the membrane scalants discussed in Table 1.2.

### 3.5 Precipitation Modeling

USGS provides a free model to predict precipitation reactions during the concentration of water. PHREEQC is computer program written in the C programming language that is designed to perform a variety of low-temperature aqueous geochemical calculations. PHREEQC is based on an ion-association aqueous model and has capabilities for transport calculations involving reversible reactions which includes aqueous, surface complexation, solid-solution and ion-exchange equilibria. (Parkhurst & Appelo, 1999)

PHREEQC was used to model the precipitation of salts expected in CAP water during RO treatment. Calculations were performed using the ion composition of CAP water displayed in Table 2.1. Figure 3.12 displays the moles precipitated as function of RO recovery. The x-axis is plotted on log-scale to better illustrate the concentration curves for each precipitate.

**Figure 2.11** PHREEQC Modeling of CAP water: Concentration of Precipitated Salts as function of RO Recovery (Shroads)

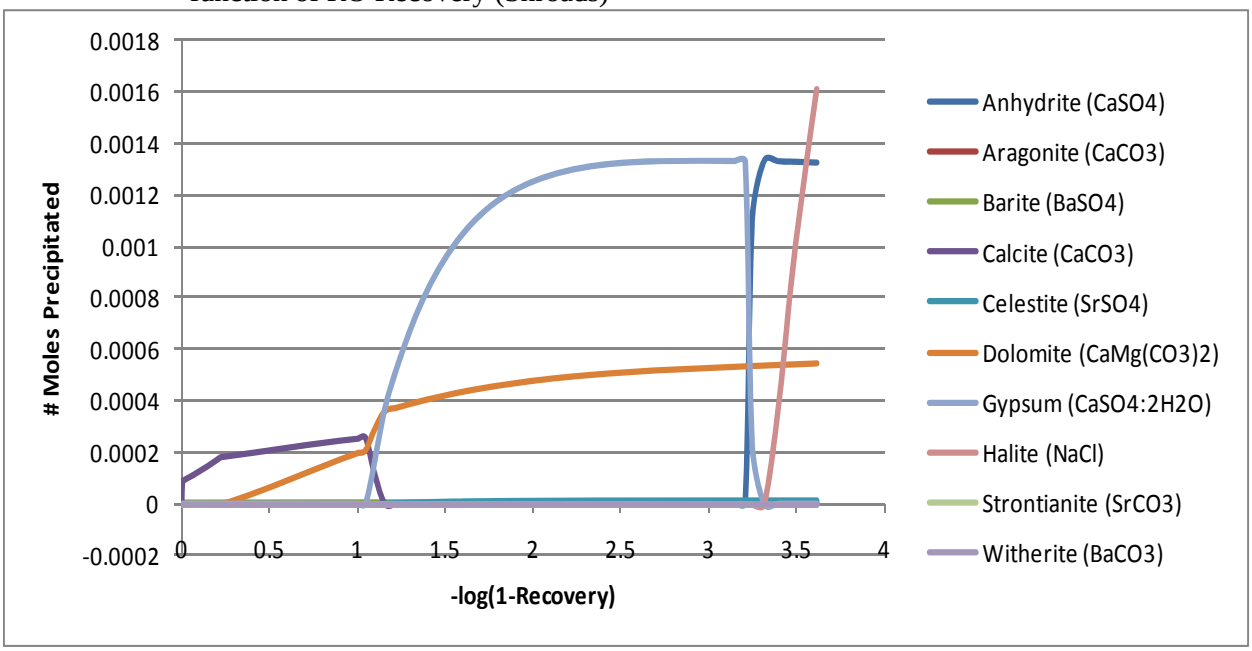


Due to the divalent cations within CAP water a variety of precipitates form when CAP water is concentrated. Precipitation is governed by $K_{SO}$ solubility constants. As recovery increases water reduction causes $Q_{SO}$ to exceed $K_{SO}$. In general, precipitation increases as recovery increases. However, some precipitates will redissolve to form other precipitates i.e. gypsum will decrease proportionally as anhydrite increases.

PHREEQC was also used to model precipitation that occurred in IX pretreated CAP water during RO treatment. Calculations were performed using the ion composition of CAP after IX treatment displayed in Table 2.1. It was assumed that the calcium and magnesium concentrations were reduced to the detection level of 10 µM. It was also assumed that other multivalent cations such as barium were removed in the same proportion of calcium. Figure 3.13 displays the moles precipitated as function of RO recovery.

**Figure 2.12** PHREEQC Modeling of IX-Treated CAP water: Concentration of Precipitated Salts as function of RO Recovery (Shroads)

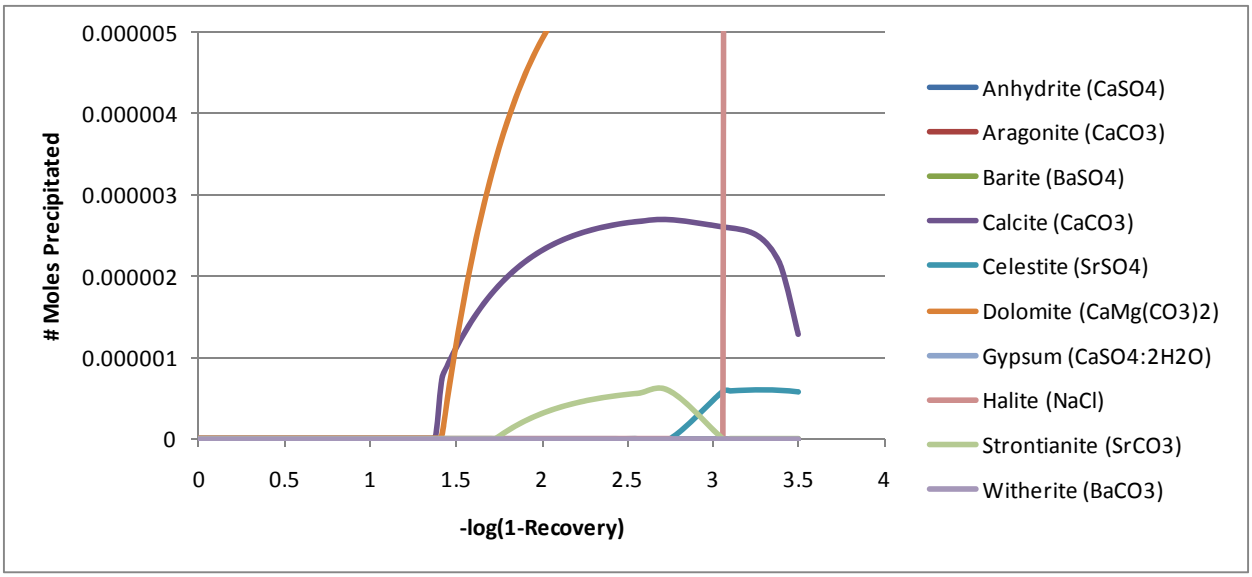


Due to the low concentration of multivalent cations in IX treated CAP water, the concentration of precipitates are over an order of magnitude lower than those predicted in non-IX treated CAP water. Note the assumption that magnesium and calcium concentrations are at detection level is a worst case scenario. It is possible (and likely based on the previously described induction time results) that the IX treatment of CAP water provides concentrations well below the detection levels.

# 3. Economic Analysis

The total treatment plant capacity is assumed as 15 MGD and kept consistent with the no-VSEP option and VSEP as brine minimization option. The whole 15 MGD is assumed to be treated by IX in order to increase the RO recovery. The first two stage RO is assumed as running at 80% recovery and the addition of a third stage RO was assumed to be constructed, run and operated at different recoveries.

The increase in the power requirement due to the increase in the osmotic pressure after the ion exchange is taken into account for both of the first two stages of RO and the third stage RO that is an addition to the system because of the higher recovery possible after IX treatment. However the cost for increase in the power requirement for the first two stages of the RO is less than 1% of the overall cost in the optimum case. The pumping cost for the third stage RO is about 14%. The capital costs for IX, RO and evaporation ponds make up the significant portion of the overall cost - approximately 50% of it. The construction and

the manufactured equipment costs for pressure ion exchange units are summarized in Table 5.1. The cost for each category is scaled up to January 2010 using ENR cost index except for the manufactured equipment cost.

$$Cost_{1979} \times \frac{Index_{2010}}{Index_{1979}} = Cost_{2010}$$

**Figure 3.1** Cost categories and related cost curves for pressure ion exchange unit

| **Construction Cost for Pressure Ion Exchange** | | |
|---|---|---|
| **Cost Category** | **Cost Equation** | **For 15 MGD** |
| Manufactured Equipment '10[1] | 153820x + 438838 | $2,746,138 |
| Excavation and Sitework '79 | 70.368x + 752.05 | $1,808 |
| Concrete '79 | 211.06x + 2517.5 | $5,683 |
| Steel '79 | 330.01x + 3985.5 | $8,936 |
| Labor '79 | 8282.2x + 3956.3 | $128,189 |
| Pipe and Valves '79 | 11625x + 20501 | $194,876 |
| Electrical and Instrumentation '79 | 14800x + 1479.2 | $223,479 |
| Housing '79 | 6165.7x + 30422 | $122,908 |
| Miscellaneous and Contigency '79 | 12880x + 9687.4 | $202,887 |
| **TOTAL '10** | | **$5,368,338** |

Courtesy of Malcolm Pirnie Inc..

Design of the IX reactor was based on an assumed resin bed depth of 8 ft. The reactor diameter was assumed to be 12 ft, so that 12 IX units were required to treat 15 mgd at an overflow rate of 7.7 gpm/ft$^2$ (selected as design criterion based on typical water application rates for IX treatment). The calculated bed capacity for specific ions and volume to breakthrough were then determined based on an assumed resin capacity of 2.0 equivalents per liter and the composition of CAP water (Table 1.1). Results suggest that about 225 bed regenerations would be necessary per year for each IX reactor. At 10 bed volumes per regeneration, the IX process will generate about 0.5 million gallons of brine in the regeneration of all 12 reactors. This volume was added to the RO brine in order to estimate the cost of enhanced evaporation for the IX/RO alternative. It was assumed that chlorine disinfection would be unnecessary ahead of IX treatment. Resin costs, IX brine production volumes and other cost factors were as summarized (Figure 3.1).

**Table 3.1** Cost parameters, regenerant volume, and cost factors for IX pretreatment

| | |
|---|---|
| **IX brine disposal (gal/day)** | 500,000 |
| Resin Price ($/m3) | $4,240 |
| Resin Lifetime (yrs) | 5 |
| IX Design Life (yrs) | 30 |
| Total Resin Volume (m3) | 307.4 |
| Total Resin Cost per Replacement | $1.30M |
| **Total Resin Cost (present worth)** | $4.26M |

Cost functions used to calculate of the total annualized (incremental) cost attributable to IX/RO and brine disposal are provided in Appendix B of the report by (Yenal, Corral, Nixon, Arnold, & Ela, 2010). Each cost component is a function of a single independent variable—the anticipated recovery during RO treatment of the pre-softened water. A plot of annualized cost versus recovery (**Figure 3.2**) indicates that economies are achieved by increasing RO recovery up to 99%, as less brine is generated for disposal and less water is lost in the process. Beyond that point, however, the energy necessary to overcome osmotic pressure in the final stage of RO dominate the calculation, leading to much higher total costs. The feasibility of 99% recovery following IX pre-softening remains to be established. IX ahead of RO treatment was predicted to increase power costs for operation of the first two stages of RO by <1%. Nevertheless, that increase is included in the analysis. The capital costs for IX, RO and augmented evaporation are the primary sources (50%) of the overall cost for the IX pre-softening alternative.

**Figure 3.2** The overall incremental cost for IX, RO and augmented evaporation as a function of recovery during reverse osmosis

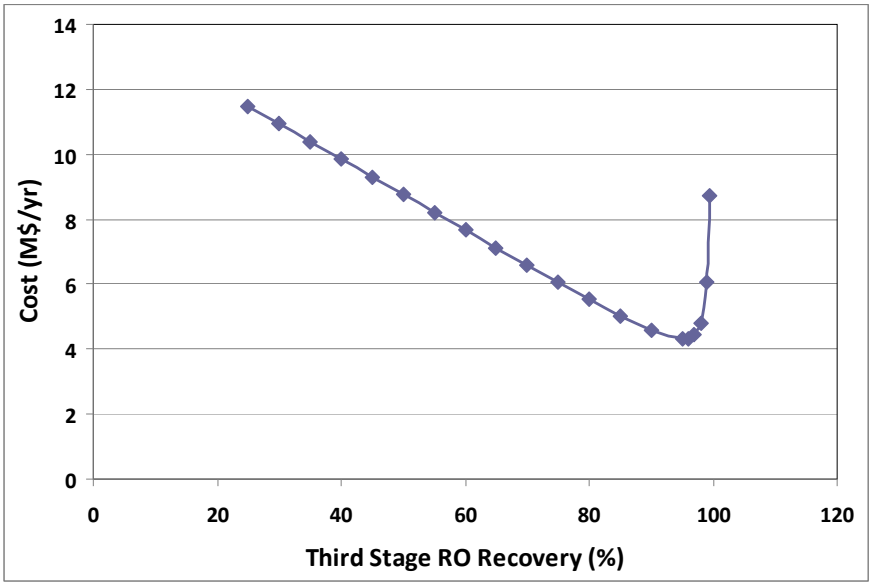

The economic analysis for the RO/IX option is compared with those of the RO only and RO/VSEP option **Table 3.2** Summary of the economic analysis. Detailed economics for these two options can be found in report by (Yenal, Corral, Nixon, Arnold, & Ela, 2010).

**Table 3.2** Summary of the economic analysis

| **RO Treatment** | **VSEP as Post-treatment of RO** | | | **IX as Pre-treatment of RO** | | |
|---|---|---|---|---|---|---|
| | **96.5%** | **97.1%** | **97.8%** | **96.5%** | **97.1%** | **97.8%** |
| $11.6M ($2.11/1Kgal) | $6.62M ($1.21/1Kgal) | $6.85M ($1.25/1Kgal) | $7.23M ($1.32/1Kgal) | $5.28M ($0.96/1Kgal) | $4.99M ($0.91/1Kgal) | $4.66M ($0.85/1Kgal) |

# Appendix A. Breakthrough Curves

A.1 Column 4 Experiments

The following figures plot effluent calcium concentrations as a function of volume of water treated. All columns used in experiments have equal resin bed volume of 1.7 Liters (wet).

Figure A.1.1 Breakthrough Curve for 1st experiment using column 4

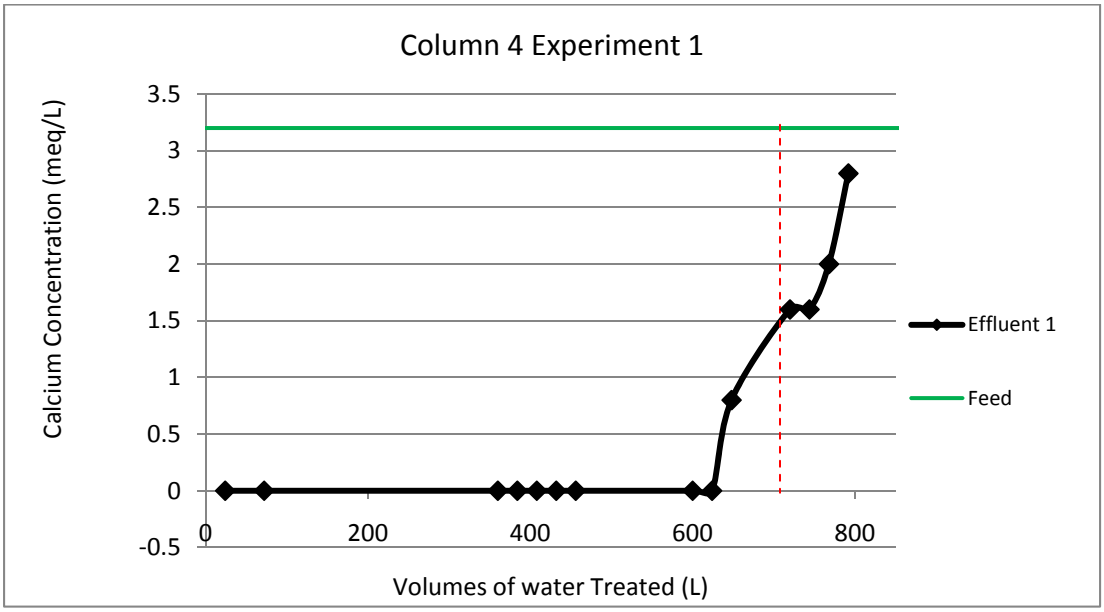


Sample Calculation

Find Midpoint between the volumes right before breakthrough and the volume where the last

$$Effective\ Volume = \frac{648 + 792}{2} L = 708\ L$$

$$Calcium\ Removed = 708\ L \times 3\ \frac{meq}{L} \times \frac{eq}{1000\ meq} \times \frac{1\ moles\ Ca^{2+}}{2\ eq}$$

Calcium removed 1.062 moles. Calculations for following breakthrough curves were calculated in similar fashions

Figure A.1.2 Breakthrough Curve for 2nd experiment using column 4

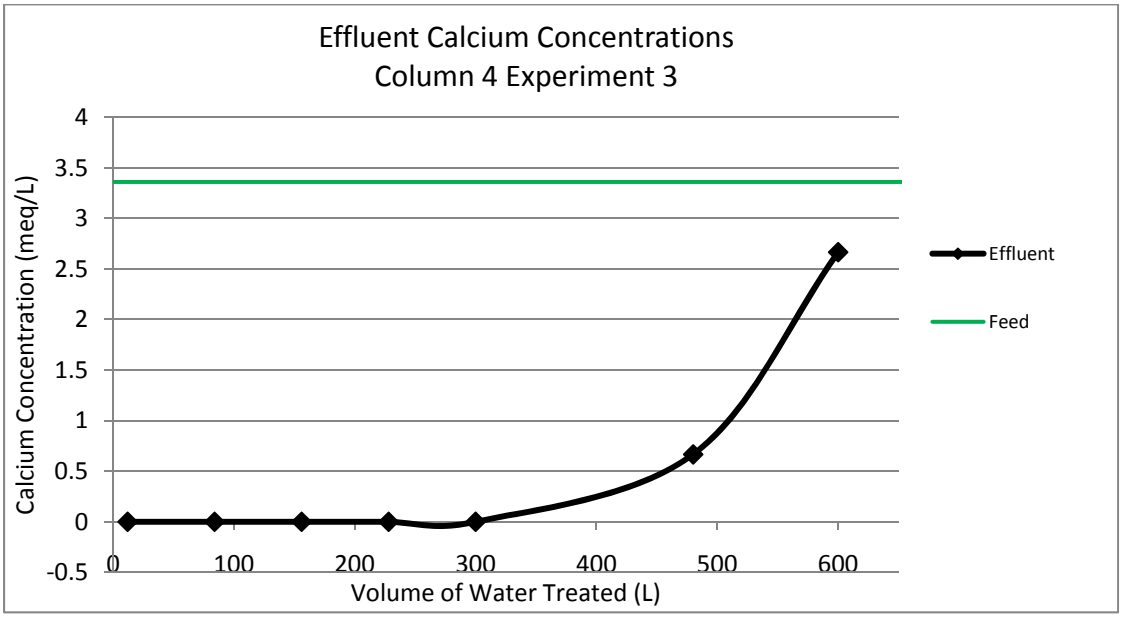


Column 4 Experiment 3: 0.8064 moles of calcium removed

Figure A.1.3 Breakthrough Curve for 4th experiment using column 4

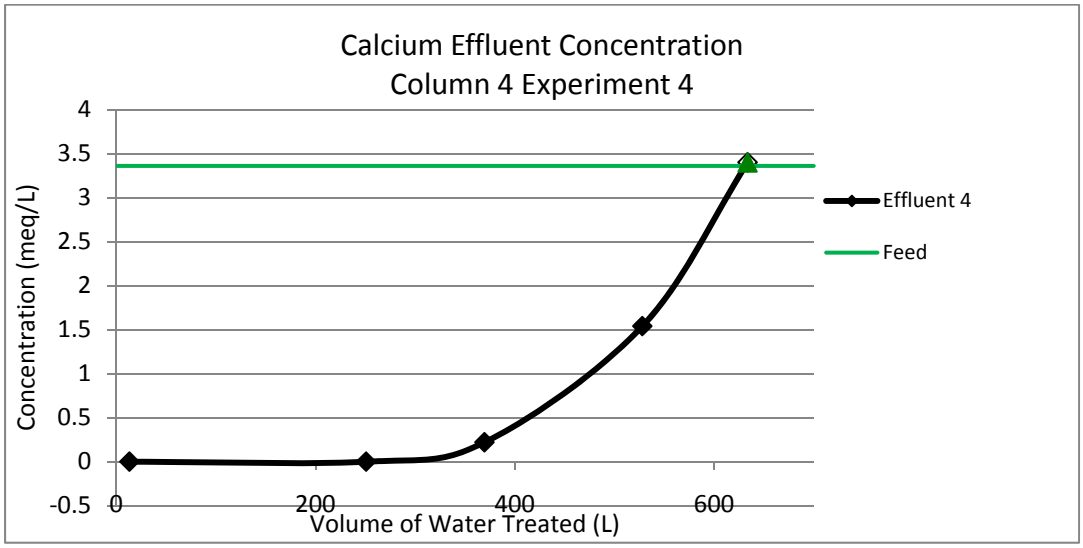


Column 4 Experiment 4: 0.6209 mole of Calcium removed

Figure A.1.4 Breakthrough Curve for 6th experiment using column 4

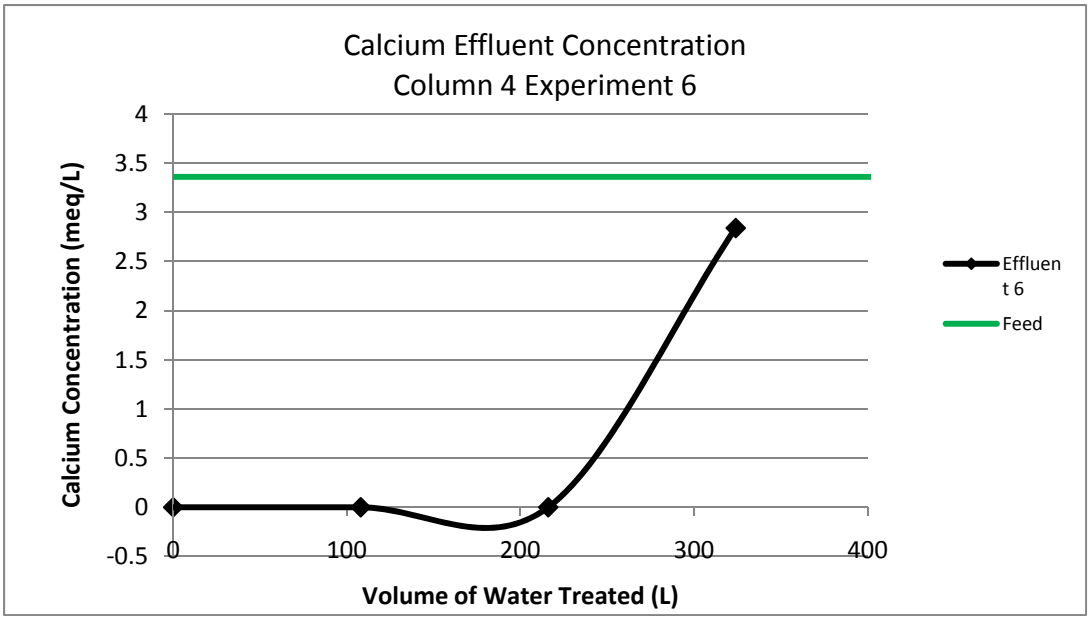


Column 4 Experiment 6: 0.513 moles of Calcium removed

Figure A.1.5 Breakthrough Curve for 7th experiment using column 4

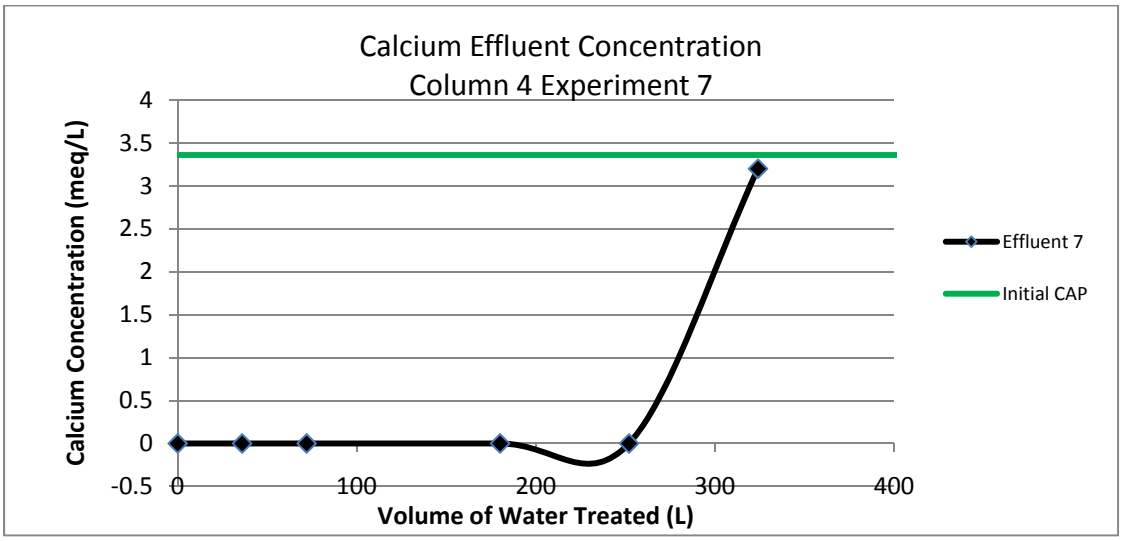


Column 4 Experiment 7: 0.518 moles of Calcium removed

Figure A.1.6 Breakthrough Curve for 9th experiment using column 4

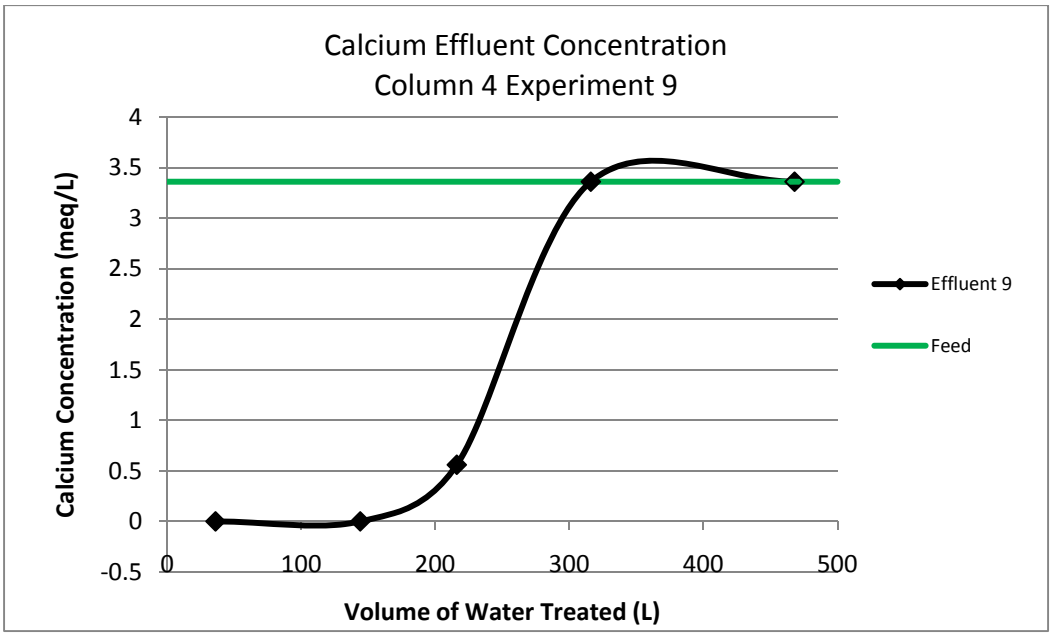


Column 4 Experiment 9: 0.433 moles of Calcium removed

Figure A.1.7 Breakthrough Curve for 11th experiment using column 4

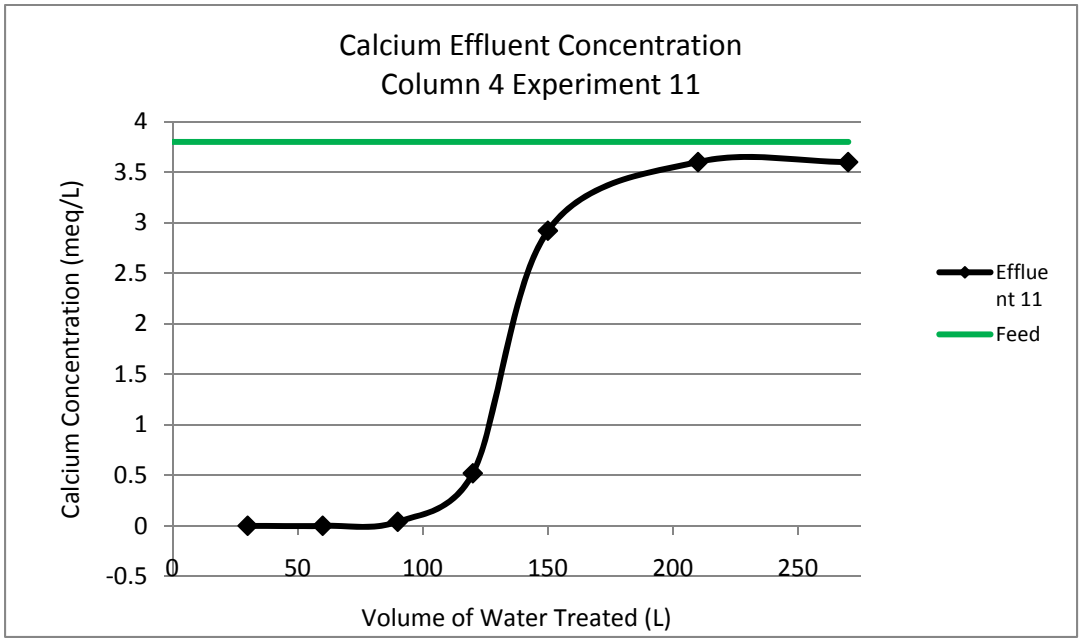


Column 4 Experiment 11: 0.27 moles of Calcium removed

Following Figure displays calcium removal as function of regenerant cycles for Column 4 experiments.

Figure A.1.8 Resin Capacity of Column 4 as a function of Regeneration Cycles

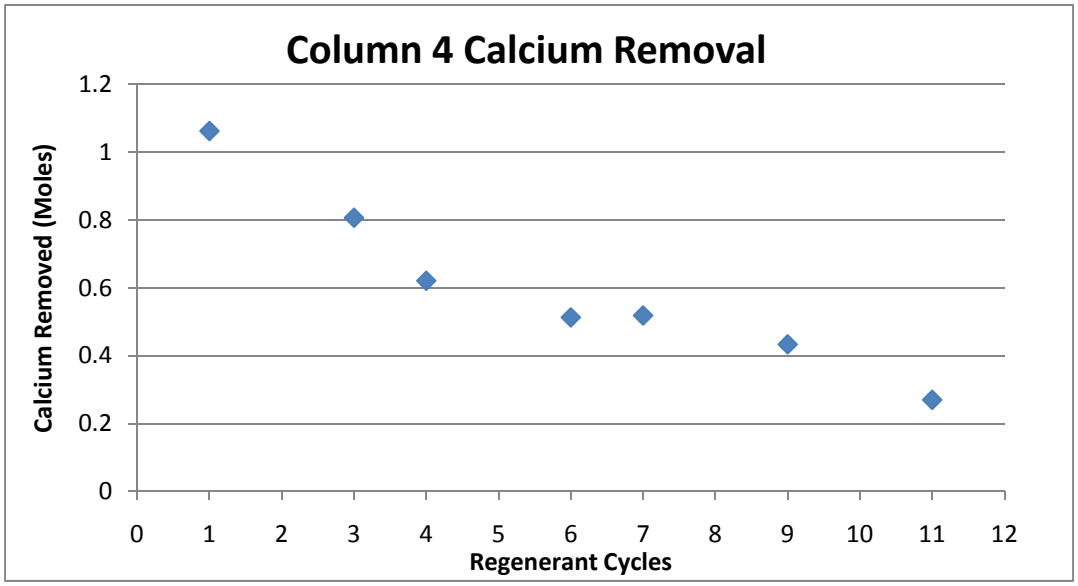


## A.2 Column 1, Cycle 1 Experiments

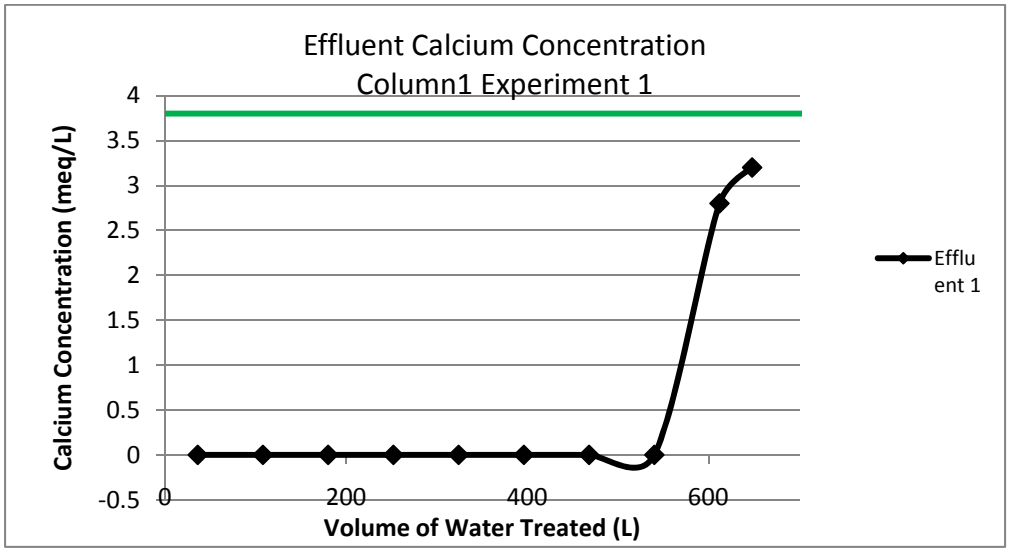


Column 1 Experiment 1: 1.081 moles of Calcium removed

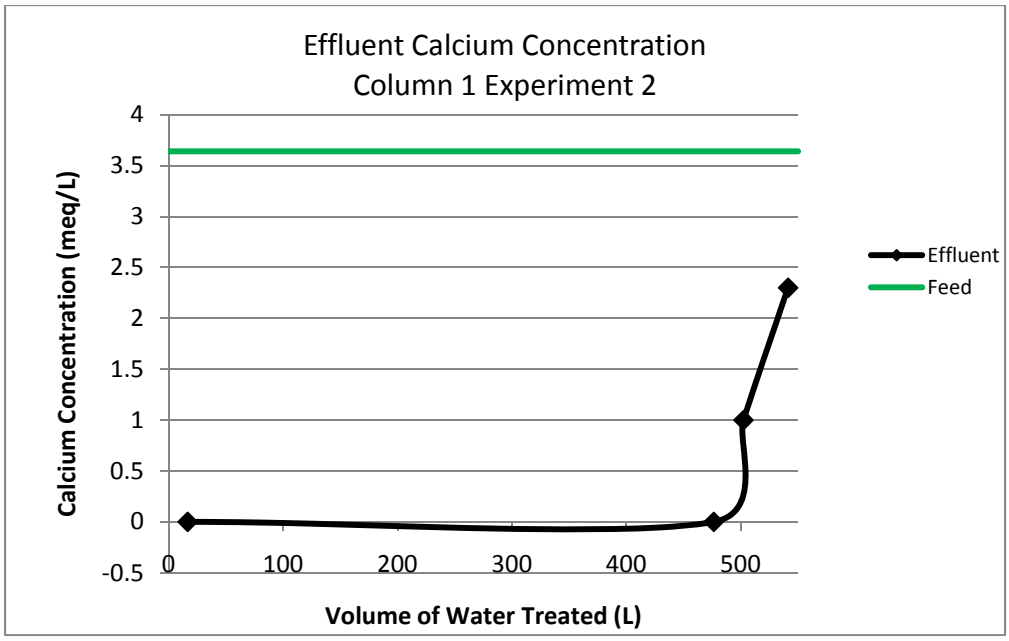
Effluent Calcium Concentration
Column 1 Experiment 2
Calcium Concentration (meq/L)
4
3.5
3
2.5
2
1.5
1
0.5
0
-0.5
0
100
200
300
400
500
Volume of Water Treated (L)
Effluent
Feed

Column Experiment 2: 0.98462 moles of Calcium removed

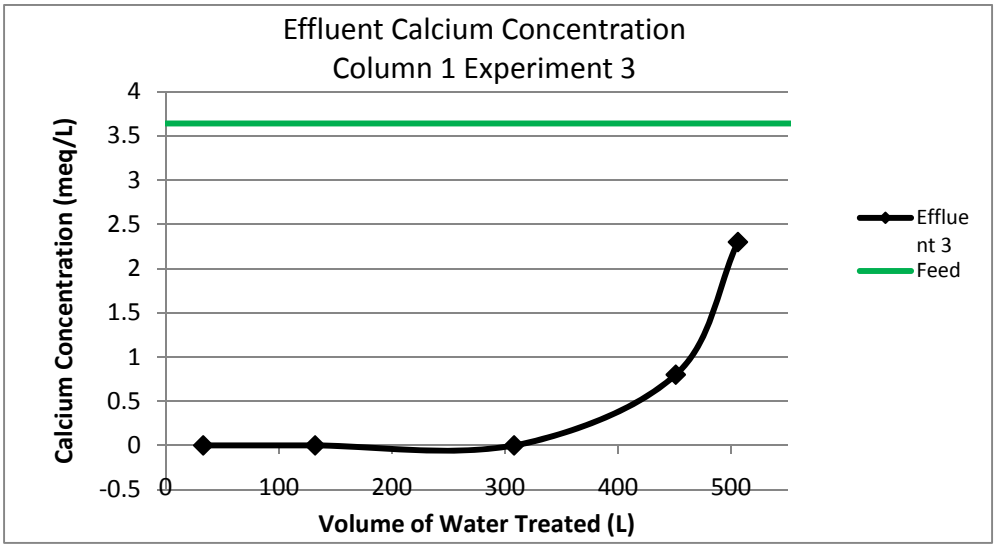


Column 1 Experiment 3: 1.021 moles of Calcium removed

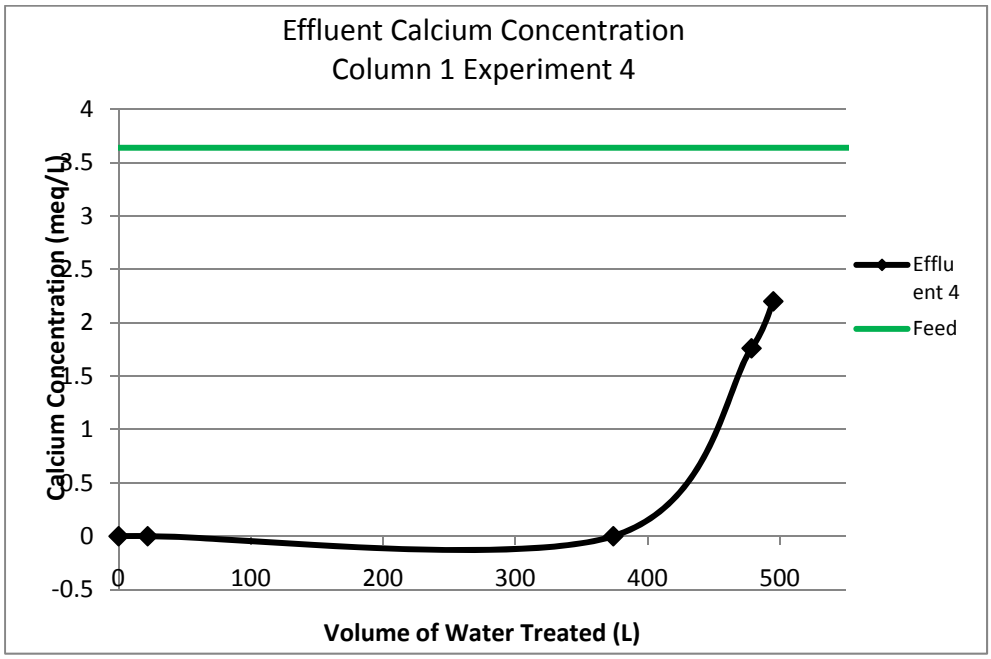


Column 4 Experimet 4: 0.871 moles of Calcium removed

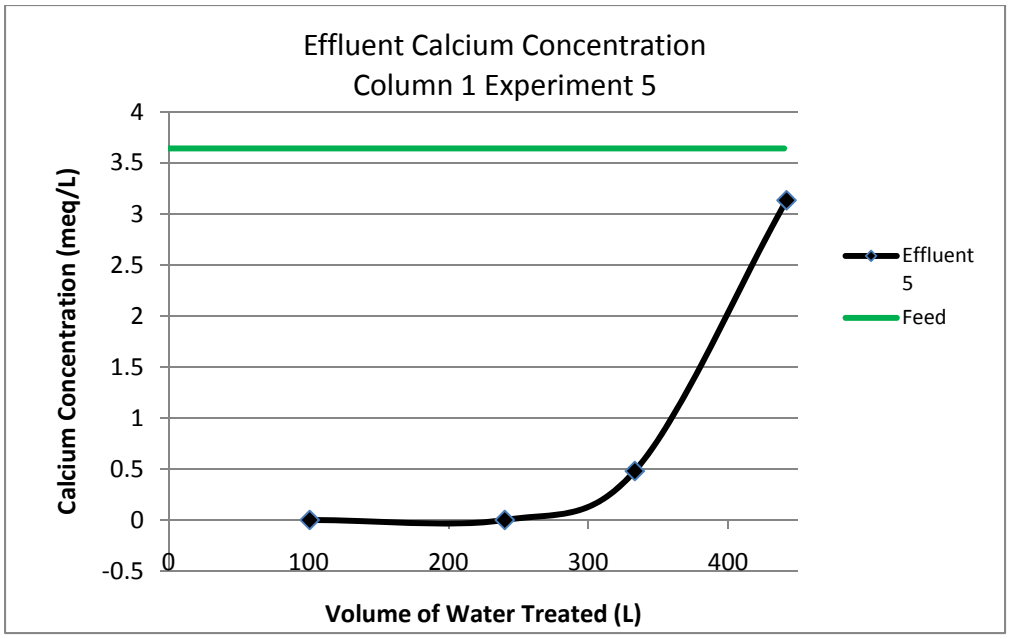


Column 1 Experiment 5: 0.621 moles of calcium removed

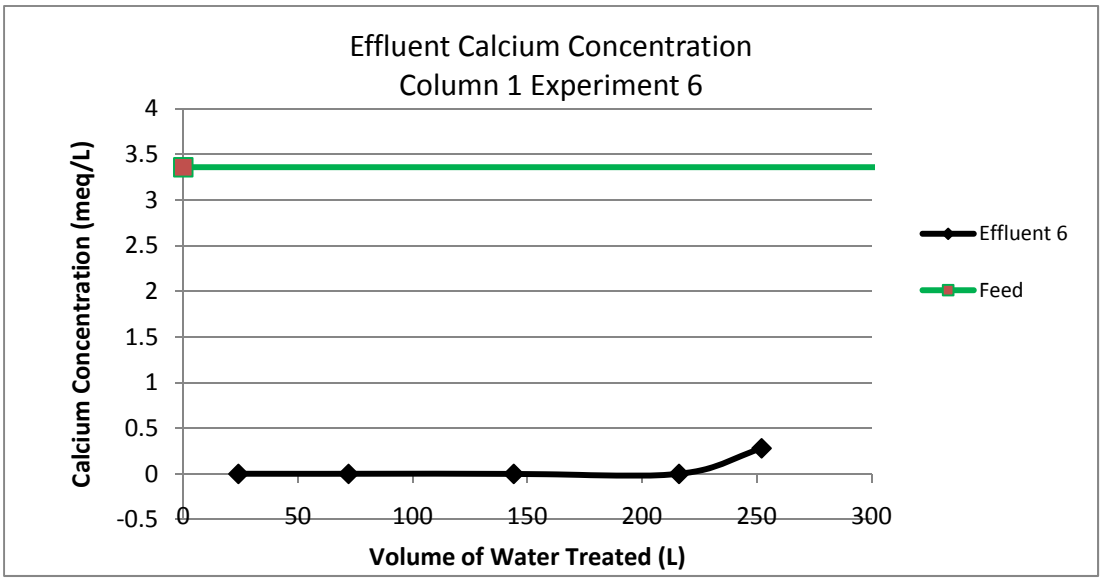


Column Experiment 6: 0.426 moles of calcium removed

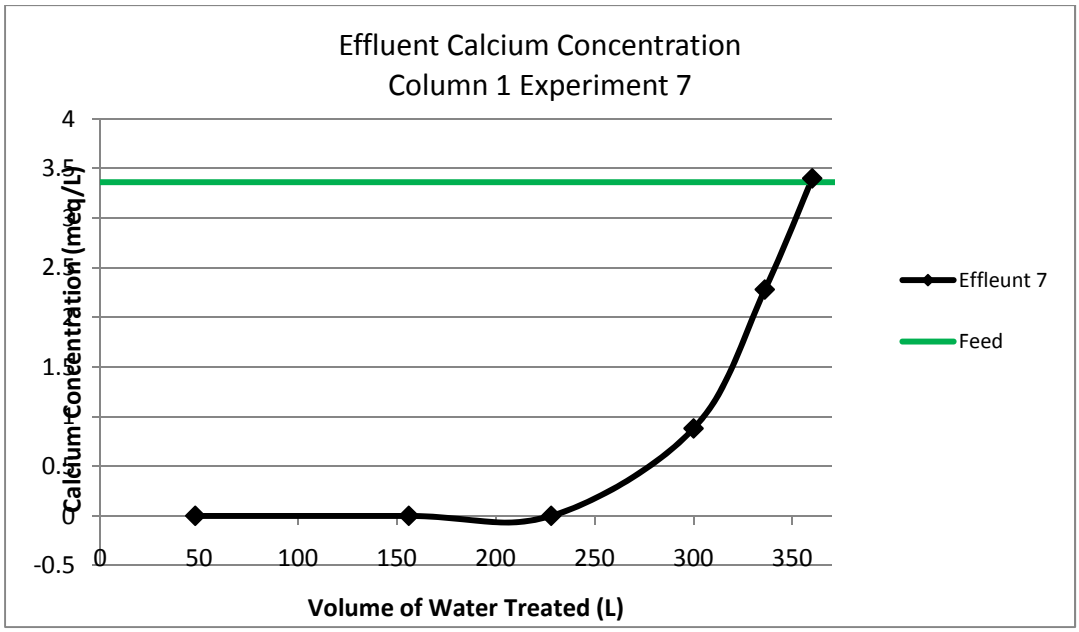


Column 1 Experiment 7: 0.535 moles of calcium removed

Displays Calcium removed from Column as function of Regenerant Uses

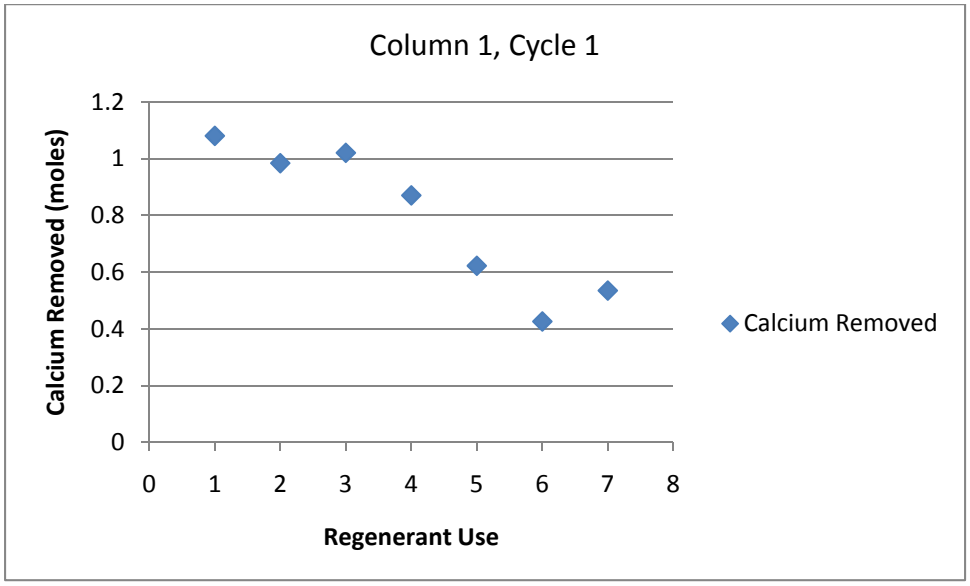


**A.3 Column 1 Cycle 2 Experiments**

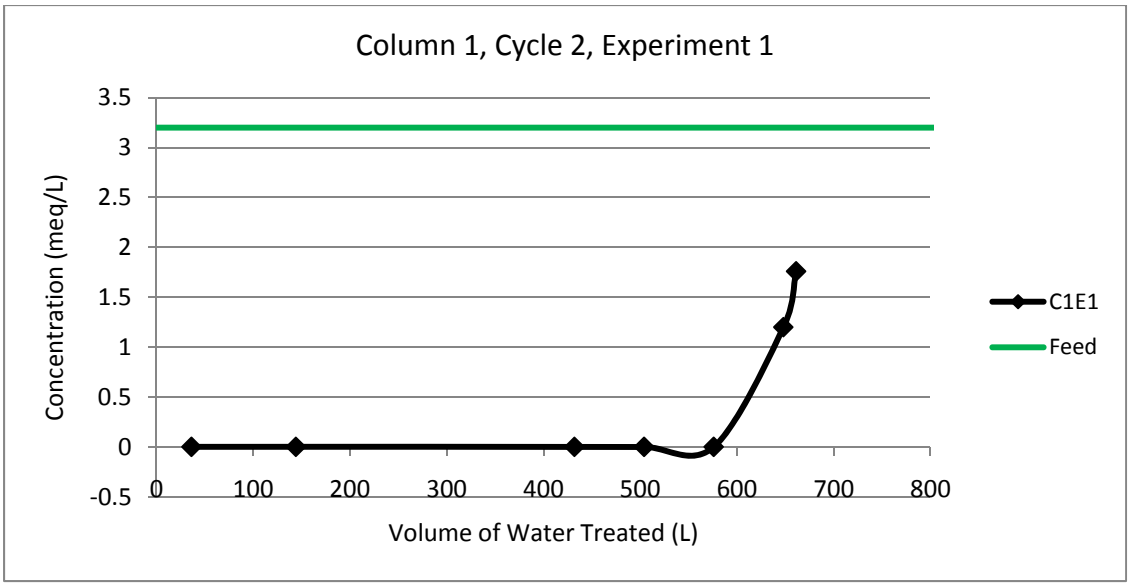


Column 1, Cycle 2, Experiment 1: 1.058 moles of calcium removed

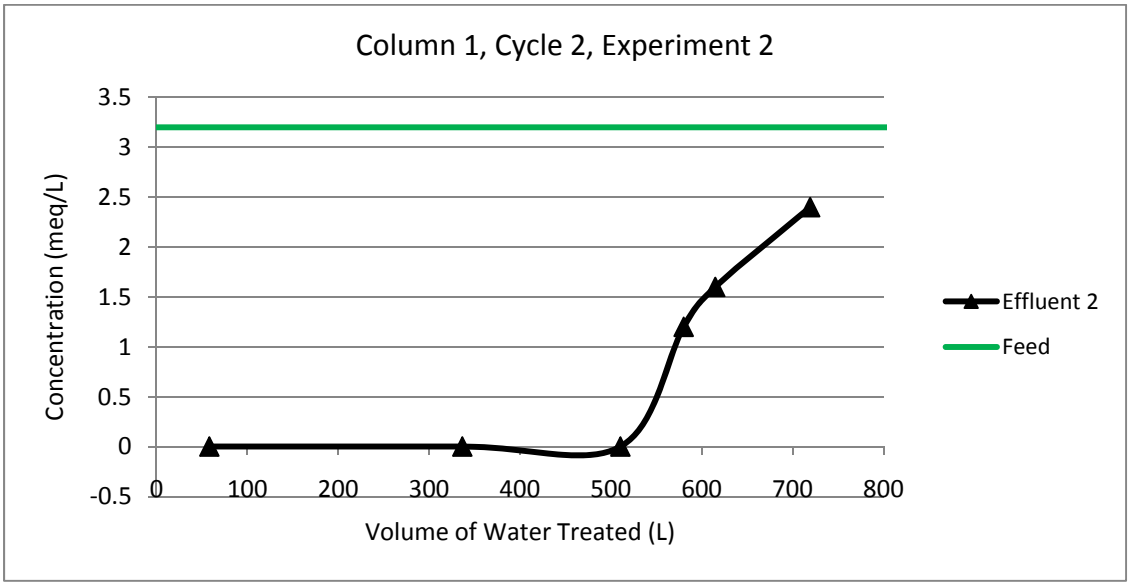


Column 1, Cycle 2, Experiment2: 1.064 moles of calcium removed

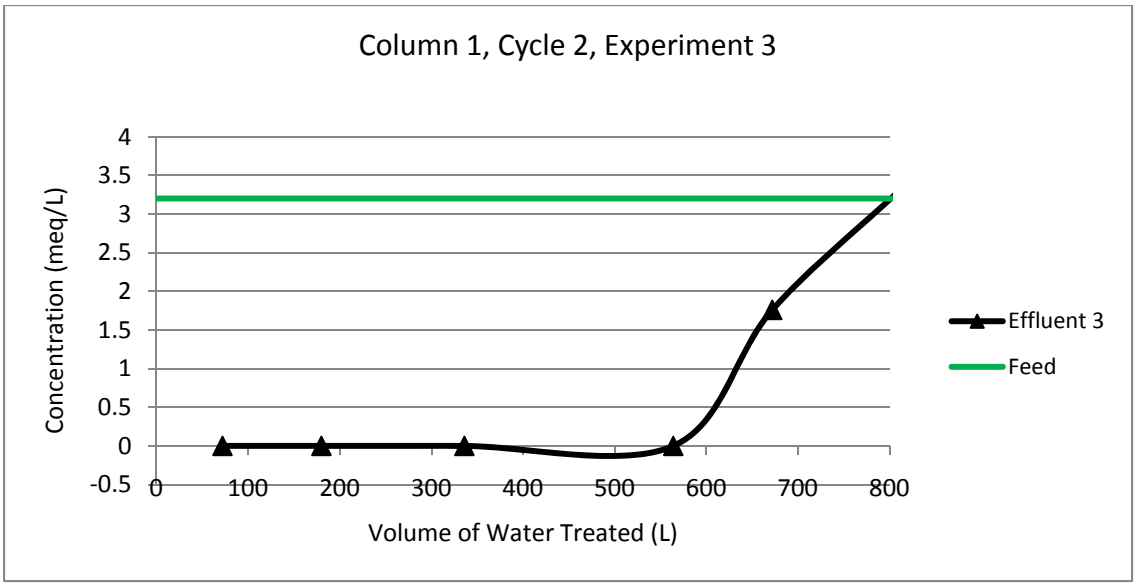


Column 1, Cycle 2, Experiment 3: 1.075 moles of Calcium removed

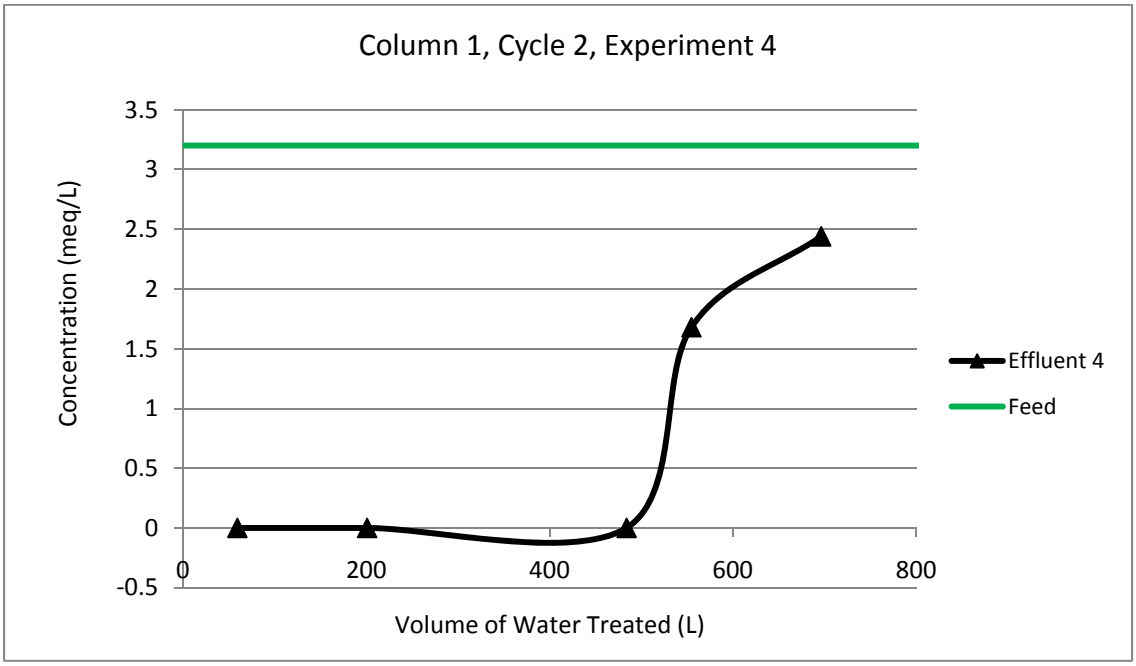


Column 1, Cycle 2, Experiment 4: 0.944 moles of calcium removed

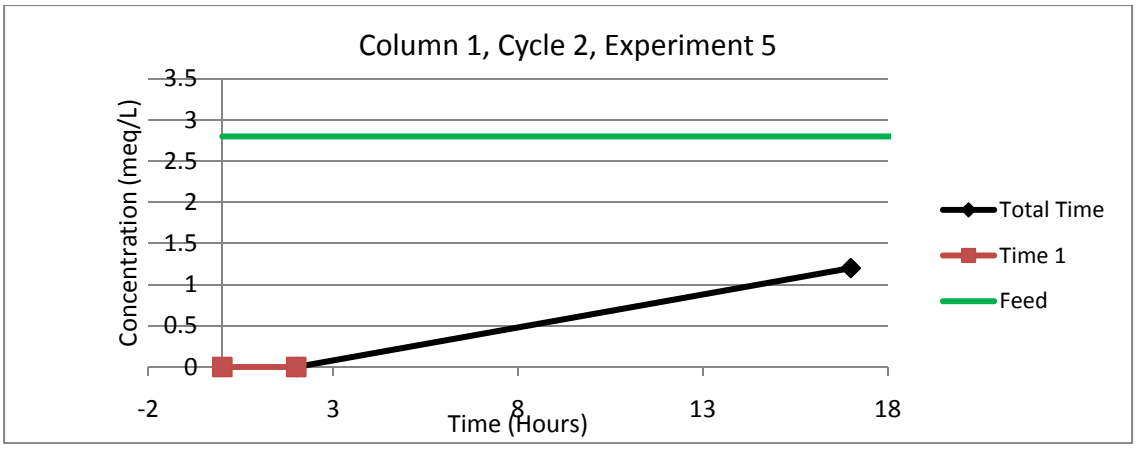


Sample Calculation

$$Total\ Ca_{out} = \left(t_1 0 + t_2 C_{avg}\right)Q$$

$$Total\ Ca_{in} = (t_1 + t_2)C_{inf}Q$$

$$Total\ Ca_{removed} = Total\ Ca_{in} - Total\ Ca_{out}$$

$$Total\ Ca_{out} = (15hr) \times 2.8\frac{meq}{L} \times \frac{1\ mol\ Ca^{2+}}{2000\ meq} \times 1.16\frac{L}{min} \times 60\frac{min}{hr}$$

$$Total\ Ca_{out} = 0.6264\ mol\ Ca$$

$$Total\ Ca_{in} = (2 + 15)hrs \times 2.8\frac{meq}{L} \times \frac{1\ mol\ Ca^{2+}}{2000\ meq} \times 1.16\frac{L}{min} \times 60\frac{min}{hr}$$

$$Total\ Ca_{in} = 1.65648\ mol\ Ca^{2+}$$

$$Total\ Ca_{removed} = 1.65648\ mol\ Ca^{2+} - 0.6264\ mol\ Ca^{2+}$$

$$Total\ Ca_{removed} = 1.03\ mol\ Ca^{2+}$$

Experiment 5: 1.03 moles of calcium removed

Calcium removal for the following figures was calculated in similar fashion.

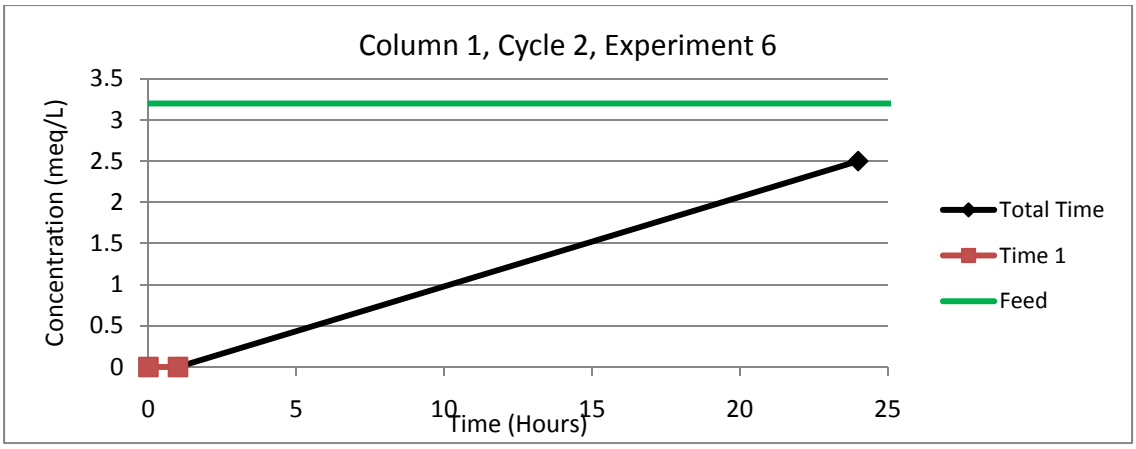


Column 1, Cycle 2, Experiment 6: 0.694 moles of calcium removed

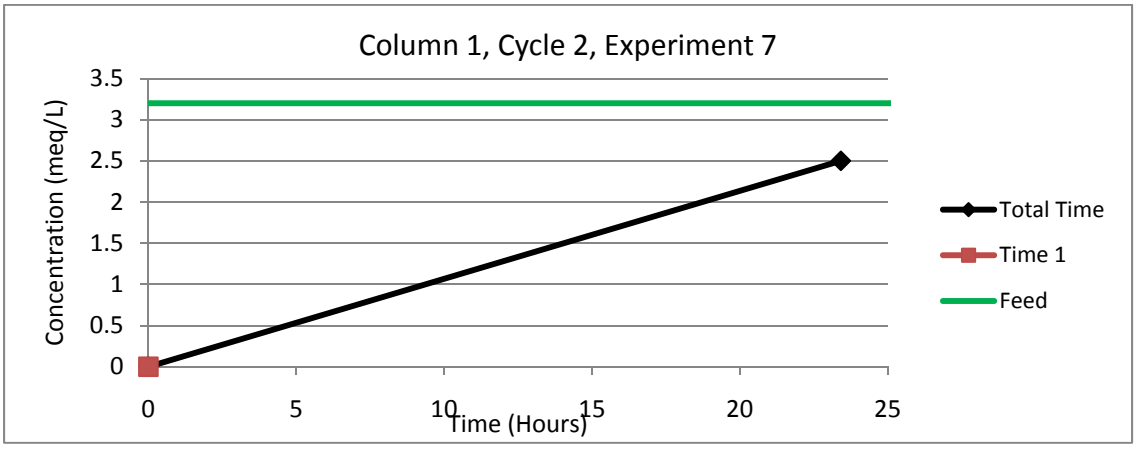


Experiment 7: 0.772 moles of Calcium removed

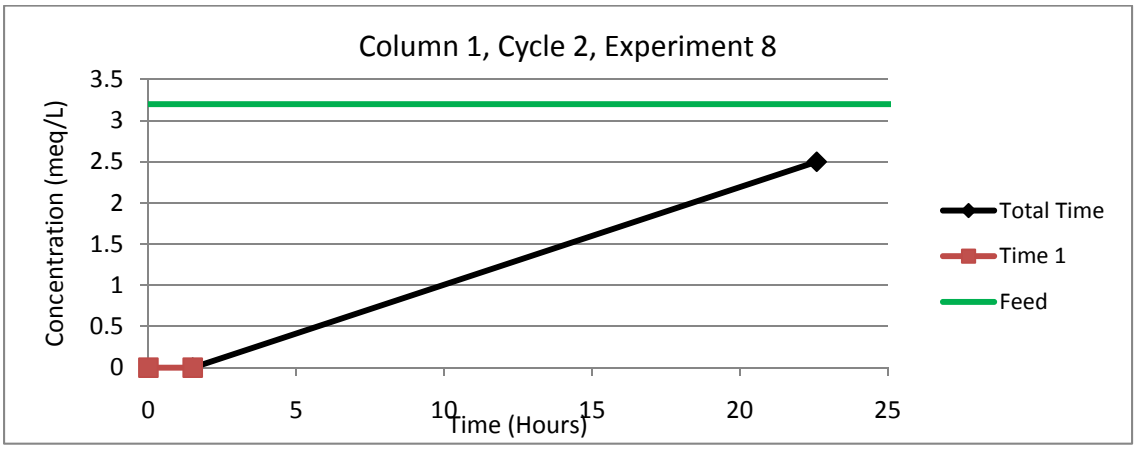


Column 1, Cycle 2, Experiment 8 0.661 moles of calcium removed

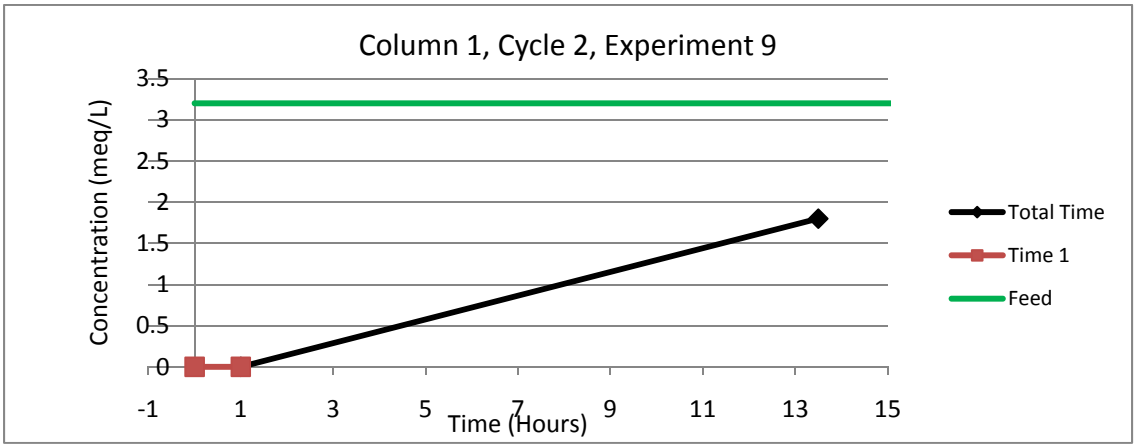


Column 1, Cycle 2, Experiment 9: 0.7452 moles of calcium removed

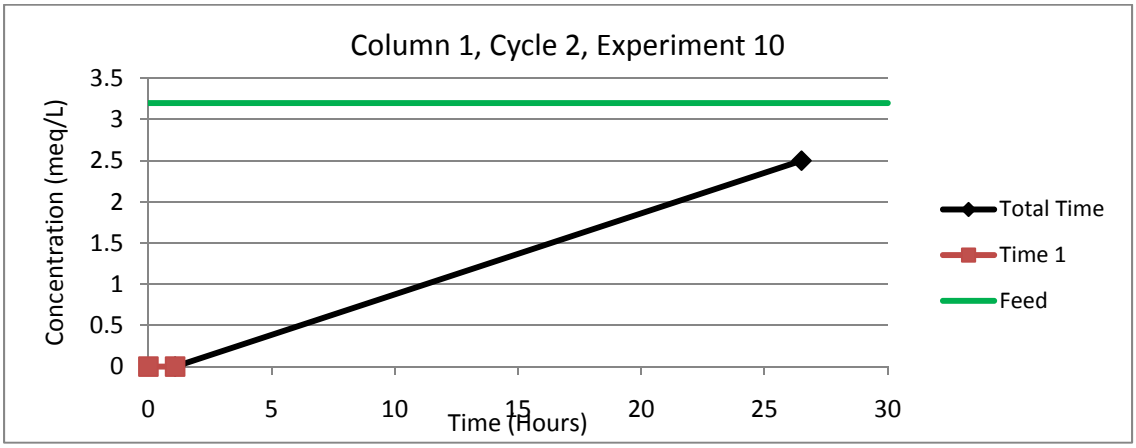


Column 1, Cycle 2, Experiment 10: 0.815 moles of calcium removed

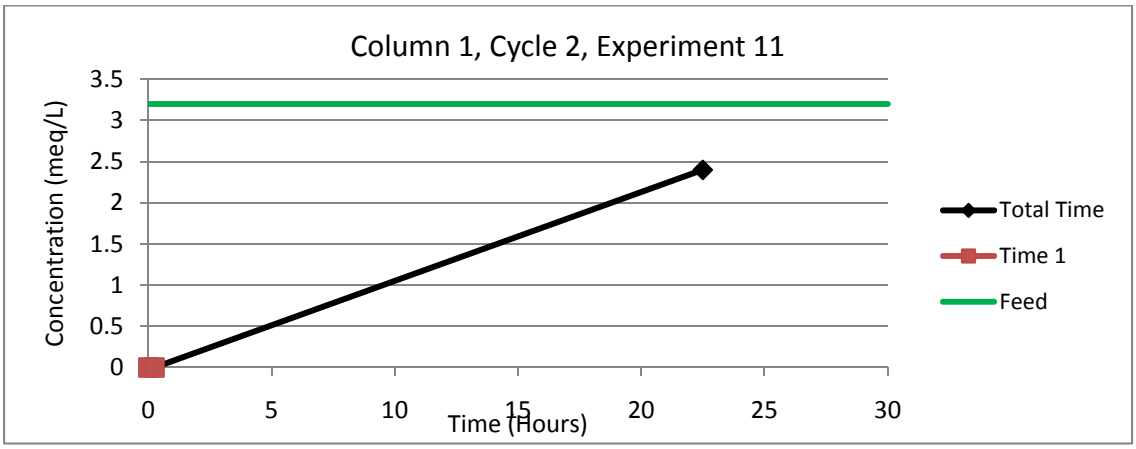

Column 1, Cycle 2, Experiment 11: 0.6388 moles of Calcium removed

Illustrates calcium removal as function of regenerant uses

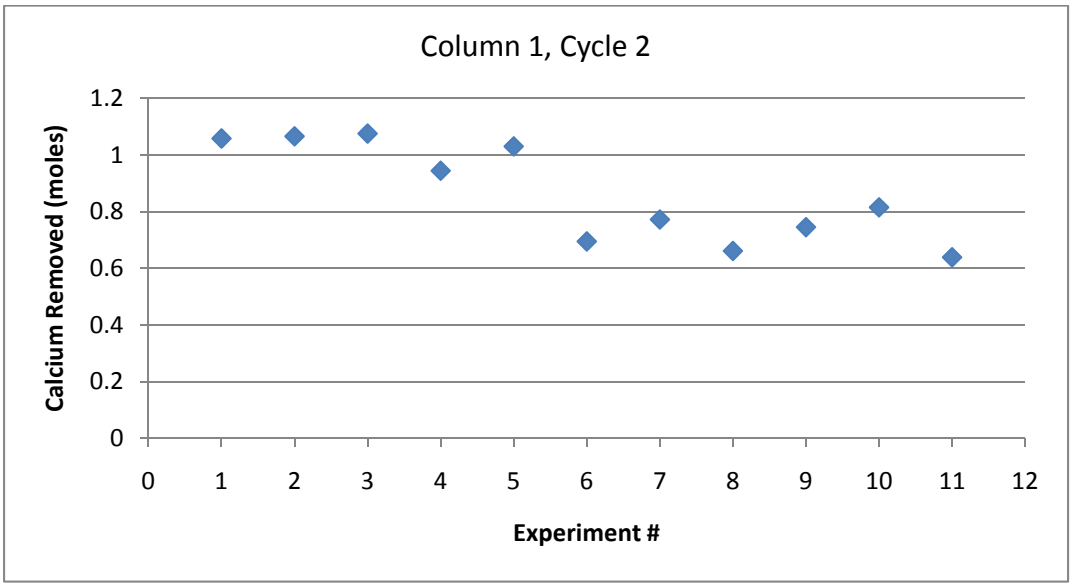


After regeneration, samples of the regenerant solution were titrated for calcium determination. Following figure displays resin capacity as function of calcium accumulated in regenerant

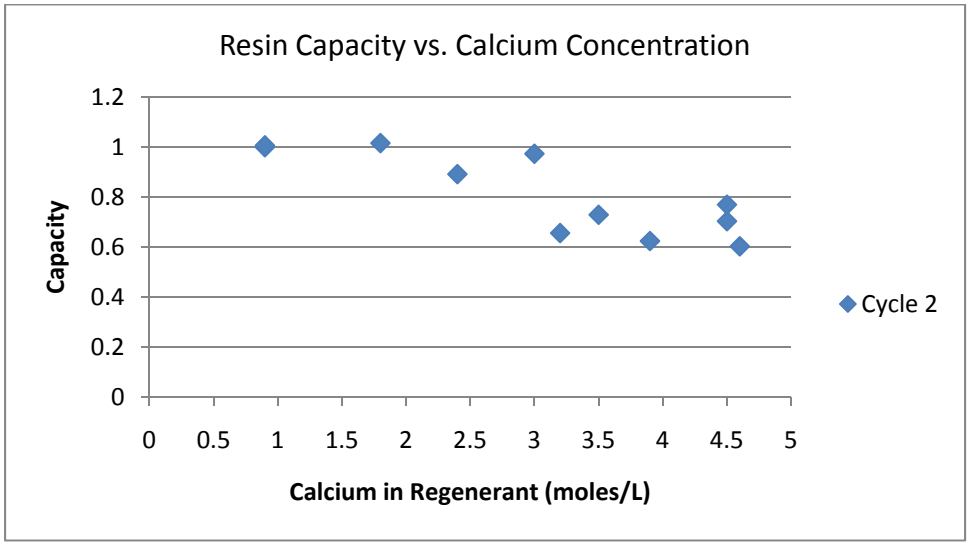


Following figure displays resin capacity with each regenerations.

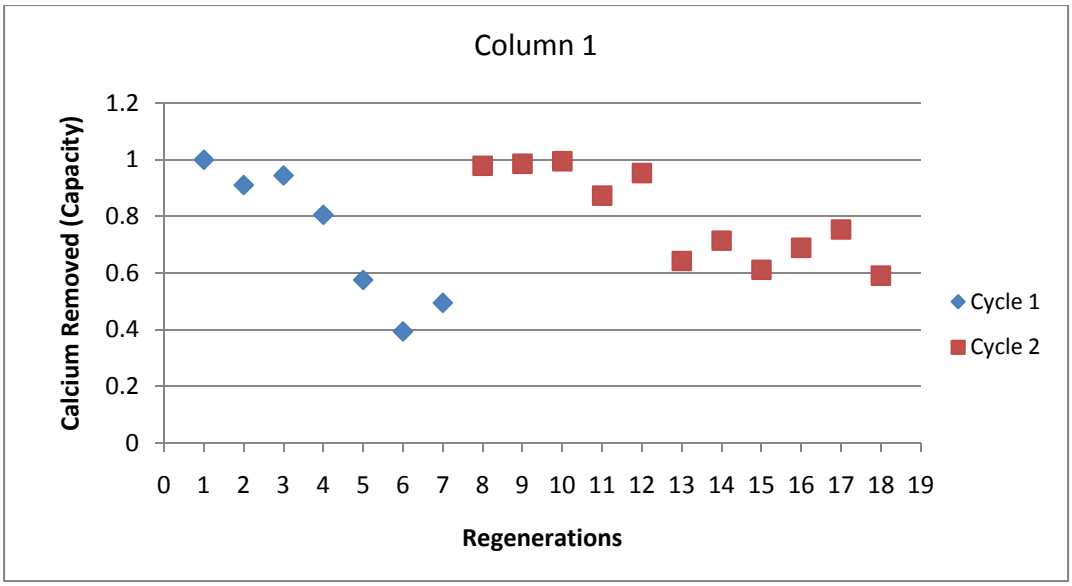


Comparison of Cycle 1 and Cycle 2. Cycle 1 had no sodium addition after regenerant. During Cycle 2, sodium was added to replenish sodium lost during previous regenerations.

# Appendix B. Raw Data for VSEP Experiments

The following Table displays measurements for the 24 hour VSEP treatment of pre-softened CAP water. VSEP operate with Recovery rate of 98% Monitored pressure, temperature, permeate flowrate and concentrate flowrate.

**Membrane**
**Test Sample. Fluid**
**Sample Vol** 12:15 **Gal**

| TIME | Time Int. | Time int. | In Pres | Out Pres | Temp | Perm Flow | Conc Flow |
|---|---|---|---|---|---|---|---|
| 12:15 PM | 0 | 0 | | 508 | 33 | 4099 | 93 |
| 1:00 PM | 45 | 1 | | 496 | 34 | 3920 | 90 |
| 2:00 PM | 105 | 2 | | 500 | 35 | 3990 | 91 |
| 3:00 PM | 165 | 3 | | 498 | 38 | 4123 | 91 |
| 4:00 PM | 225 | 4 | | 492 | 39 | 4187 | 93 |
| 5:00 PM | 285 | 5 | | 498 | 41 | 4224 | 92 |
| 6:00 PM | 345 | 6 | | 498 | 42 | 4237 | 96 |
| 7:00 PM | 405 | 7 | | 494 | 43 | 4221 | 93 |
| 8:00 PM | 465 | 8 | | 494 | 43 | 4260 | 95 |
| 9:00 PM | 525 | 9 | | 496 | 44 | 4182 | 94 |
| 10:00 PM | 585 | 10 | | 492 | 44 | 4124 | 93 |
| 11:00 PM | 645 | 11 | | 498 | 45 | 4198 | 94 |
| 12:00 AM | 705 | 12 | | 500 | 45 | 4177 | 94 |
| 1:00 AM | 765 | 13 | | 498 | 45 | 4093 | 94 |
| 2:00 AM | 825 | 14 | | 500 | 45 | 4128 | 95 |
| 3:00 AM | 885 | 15 | | 500 | 46 | 4057 | 94 |
| 4:00 AM | 945 | 16 | | 496 | 46 | 4027 | 94 |
| 5:00 AM | 1005 | 17 | | 502 | 46 | 4021 | 84 |
| 6:00 AM | 1065 | 18 | | 508 | 46 | 3865 | 88 |
| 7:00 AM | 1125 | 19 | | 504 | 47 | 3787 | 83 |
| 8:00 AM | 1185 | 20 | | 500 | 47 | 3844 | 82 |
| 9:00 AM | 1245 | 21 | | 496 | 47 | 3673 | 82 |
| 10:00 AM | 1305 | 22 | | 494 | 47 | 3636 | 81 |
| 11:00 AM | 1365 | 23 | | 498 | 47 | 3685 | 81 |

Following Table displays values calculated from figure above, such a water recovery, permeate flux, and Temperature corrected flux.

| | | | | | 20 | | |
|---|---|---|---|---|---|---|---|
| TIME | Rec | Ave Rec | Vib | Perm GFD | Temp Cor: | Vis. Fac. | Ave Flux |
| 12:15 PM | 97.8% | 97.8% | 3/4" | 92.3 | 68.6 | 0.743953 | 68.6 |
| 1:00 PM | 97.7% | 97.7% | 3/4" | 88.2 | 64.3 | 0.728725 | 64.3 |
| 2:00 PM | 97.8% | 97.8% | 3/4" | 89.8 | 64.1 | 0.714021 | 64.1 |
| 3:00 PM | 97.8% | 97.8% | 3/4" | 92.8 | 62.4 | 0.672844 | 62.4 |

| | | | | | | | |
|---|---|---|---|---|---|---|---|
| 4:00 PM | 97.8% | 97.8% | 3/4" | 94.2 | 62.2 | 0.660031 | 62.2 |
| 5:00 PM | 97.9% | 97.9% | 3/4" | 95.1 | 60.4 | 0.635662 | 60.4 |
| 6:00 PM | 97.8% | 97.8% | 3/4" | 95.4 | 59.5 | 0.624069 | 59.5 |
| 7:00 PM | 97.8% | 97.8% | 3/4" | 95.0 | 58.2 | 0.612848 | 58.2 |
| 8:00 PM | 97.8% | 97.8% | 3/4" | 95.9 | 58.8 | 0.612848 | 58.8 |
| 9:00 PM | 97.8% | 97.8% | 3/4" | 94.1 | 56.7 | 0.601982 | 56.7 |
| 10:00 PM | 97.8% | 97.8% | 3/4" | 92.8 | 55.9 | 0.601982 | 55.9 |
| 11:00 PM | 97.8% | 97.8% | 3/4" | 94.5 | 55.9 | 0.591454 | 55.9 |
| 12:00 AM | 97.8% | 97.8% | 3/4" | 94.0 | 55.6 | 0.591454 | 55.6 |
| 1:00 AM | 97.8% | 97.8% | 3/4" | 92.1 | 54.5 | 0.591454 | 54.5 |
| 2:00 AM | 97.8% | 97.8% | 3/4" | 92.9 | 55.0 | 0.591454 | 55.0 |
| 3:00 AM | 97.7% | 97.7% | 3/4" | 91.3 | 53.1 | 0.581249 | 53.1 |
| 4:00 AM | 97.7% | 97.7% | 3/4" | 90.6 | 52.7 | 0.581249 | 52.7 |
| 5:00 AM | 97.9% | 97.9% | 3/4" | 90.5 | 52.6 | 0.581249 | 52.6 |
| 6:00 AM | 97.8% | 97.8% | 3/4" | 87.0 | 50.6 | 0.581249 | 50.6 |
| 7:00 AM | 97.9% | 97.9% | 3/4" | 85.2 | 48.7 | 0.571352 | 48.7 |
| 8:00 AM | 97.9% | 97.9% | 3/4" | 86.5 | 49.4 | 0.571352 | 49.4 |
| 9:00 AM | 97.8% | 97.8% | 3/4" | 82.7 | 47.2 | 0.571352 | 47.2 |
| 10:00 AM | 97.8% | 97.8% | 3/4" | 81.8 | 46.8 | 0.571352 | 46.8 |
| 11:00 AM | 97.8% | 97.8% | 3/4" | 82.9 | 47.4 | 0.57135 | 47.4 |

Following Table displays raw data from VSEP treatment of RO brine. VSEP operated at 89% recovery giving an overall recovery of 98%

| Sample Vol | | | 16:00 | | | Gal | Net |
|---|---|---|---|---|---|---|---|
| TIME | Time Int. | Time Int. | In Pres | Out Pres | Temp | Perm Flow | Conc Flow |
| 4:15 PM | 15 | 0 | 0 | 536 | 12 | 2152 | 231 |
| 4:30 PM | 30 | 1 | 1 | 502 | 12 | 2116 | 235 |
| 5:15 PM | 75 | 1 | 1 | 496 | 13 | 2042 | 255 |
| 6:00 PM | 120 | 2 | 2 | 494 | 14 | 2039 | 255 |
| 7:15 PM | 195 | 3 | 3 | 494 | 14 | 2000 | 228 |
| 8:05 PM | 245 | 4 | 4 | 494 | 15 | 1973 | 228 |
| 9:00 PM | 300 | 5 | 5 | 494 | 15 | 1929 | 227 |
| 10:10 PM | 370 | 6 | 6 | 494 | 15 | 1898 | 229 |
| 11:00 PM | 420 | 7 | 7 | 492 | 15 | 1902 | 228 |
| 12:00 AM | 480 | 8 | 8 | 492 | 15 | 1836 | 228 |
| 1:00 AM | 540 | 9 | 9 | 492 | 15 | 1888 | 228 |
| 2:00 AM | 600 | 10 | 10 | 494 | 15 | 1836 | 227 |
| 3:00 AM | 660 | 11 | 11 | 494 | 15 | 1815 | 226 |
| 4:00 AM | 720 | 12 | 12 | 494 | 15 | 1728 | 227 |
| 5:00 AM | 780 | 13 | 13 | 494 | 15 | 1689 | 195 |
| 6:00 AM | 840 | 14 | 14 | 494 | 15 | 1659 | 192 |
| 7:00 AM | 900 | 15 | 15 | 494 | 15 | 1648 | 192 |
| 8:00 AM | 960 | 16 | 16 | 494 | 15 | 1559 | 192 |
| 9:00 AM | 1020 | 17 | 17 | 494 | 16 | 1548 | 192 |
| 10:00 AM | 1080 | 18 | 18 | 492 | 16 | 1543 | 192 |
| 11:15 AM | 1155 | 19 | 19 | 490 | 17 | 1531 | 192 |
| 1:05 PM | 1265 | 21 | 21 | 488 | 18 | 1527 | 193 |
| 2:00 PM | 1320 | 22 | 22 | 488 | 19 | 1513 | 192 |
| 3:00 PM | 1380 | 23 | 23 | 488 | 20 | 1506 | 193 |

Following Table displays values calculated from figure above, such a water recovery, permeate flux, and Temperature corrected flux.

| | | | | | 20 | | |
|---|---|---|---|---|---|---|---|
| Rec | O. Rec | Ave Rec | Vib | Perm GFD | Temp Cor: | Vis. Fac. | Ave Flux |
| 90.3% | 98.1% | 90.3% | 3/4" | 48.4 | 59.5 | 1.227105 | 59.5 |
| 90.0% | 98.0% | 90.2% | 3/4" | 47.6 | 58.4 | 1.22710 | 59.2 |
| 88.9% | 97.8% | 89.8% | 3/4" | 46.0 | 54.9 | 1.19515 | 57.7 |
| 88.9% | 97.8% | 89.4% | 3/4" | 45.9 | 53.4 | 1.16428 | 56.4 |
| 89.8% | 98.0% | 89.4% | 3/4" | 45.0 | 52.4 | 1.164281 | 55.0 |
| 89.6% | 97.9% | 89.5% | 3/4" | 44.4 | 50.4 | 1.134458 | 54.3 |
| 89.5% | 97.9% | 89.5% | 3/4" | 43.4 | 49.3 | 1.134458 | 53.5 |
| 89.2% | 97.8% | 89.5% | 3/4" | 42.7 | 48.5 | 1.134458 | 52.6 |
| 89.3% | 97.9% | 89.4% | 3/4" | 42.8 | 48.6 | 1.134458 | 52.1 |
| 89.0% | 97.8% | 89.4% | 3/4" | 41.3 | 46.9 | 1.13446 | 51.6 |
| 89.2% | 97.8% | 89.4% | 3/4" | 42.5 | 48.2 | 1.13446 | 51.1 |
| 89.0% | 97.8% | 89.3% | 3/4" | 41.3 | 46.9 | 1.13446 | 50.8 |
| 88.9% | 97.8% | 89.3% | 3/4" | 40.9 | 46.3 | 1.13446 | 50.4 |
| 88.4% | 97.7% | 89.2% | 3/4" | 38.9 | 44.1 | 1.13446 | 50.0 |
| 89.7% | 97.9% | 89.2% | 3/4" | 38.0 | 43.1 | 1.13446 | 49.5 |
| 89.6% | 97.9% | 89.3% | 3/4" | 37.4 | 42.4 | 1.13446 | 49.0 |
| 89.6% | 97.9% | 89.3% | 3/4" | 37.1 | 42.1 | 1.13446 | 48.5 |
| 89.0% | 97.8% | 89.3% | 3/4" | 35.1 | 39.8 | 1.13446 | 48.1 |
| 89.0% | 97.8% | 89.3% | 3/4" | 34.8 | 38.5 | 1.10565 | 47.5 |
| 88.9% | 97.8% | 89.2% | 3/4" | 34.7 | 38.4 | 1.10565 | 47.0 |
| 88.9% | 97.8% | 89.2% | 3/4" | 34.5 | 37.1 | 1.07783 | 46.4 |
| 88.8% | 97.8% | 89.2% | 3/4" | 34.4 | 36.1 | 1.05097 | 45.6 |
| 88.7% | 97.7% | 89.2% | 3/4" | 34.1 | 34.9 | 1.02504 | 45.2 |
| 88.7% | 97.7% | 89.2% | 3/4" | 33.9 | 33.9 | 1.00000 | 44.7 |

Flux was calculated using permeate flowrates and temperatures

Flux Comparison of RO Brine and Softened CAP Water

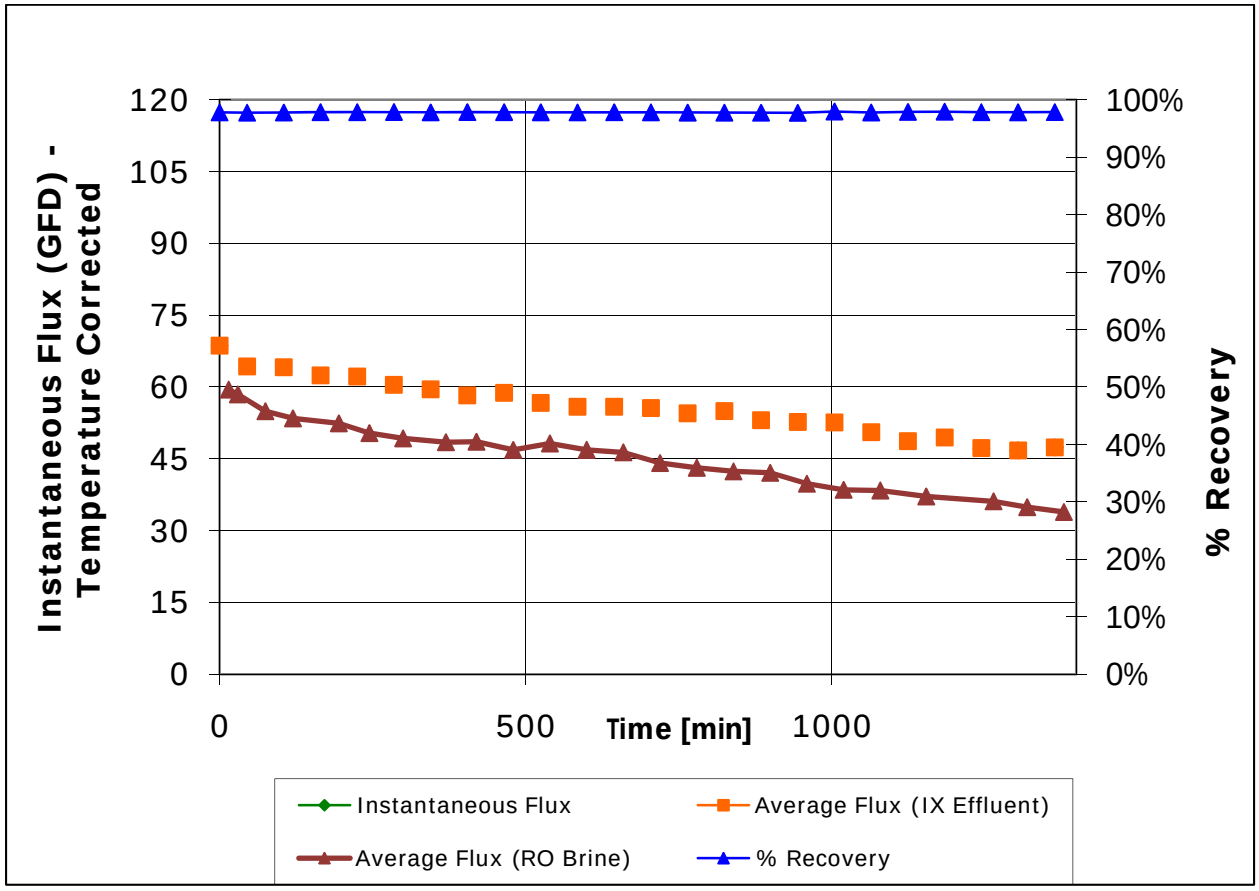

# Appendix C. XRD analysis

The following figure shows XRD analysis of 98% concentrated IX treated CAP water. CPS is plotted as function of angle of light path in degrees. The bottom chart is XRD analysis of a known Halite index. The major peaks from the sample correspond to peaks for the Halite index. This indicates that the sample contains Halite.

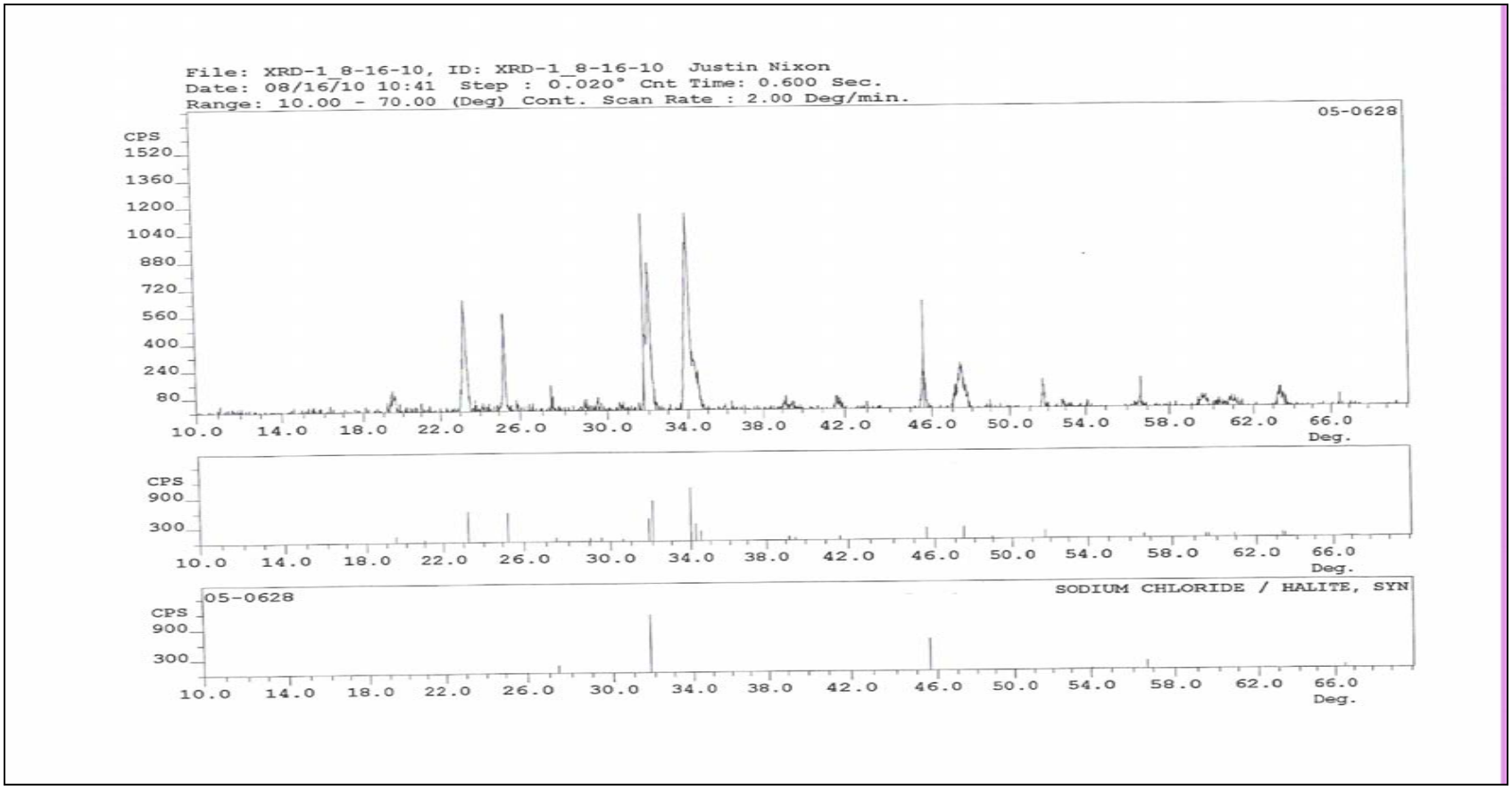

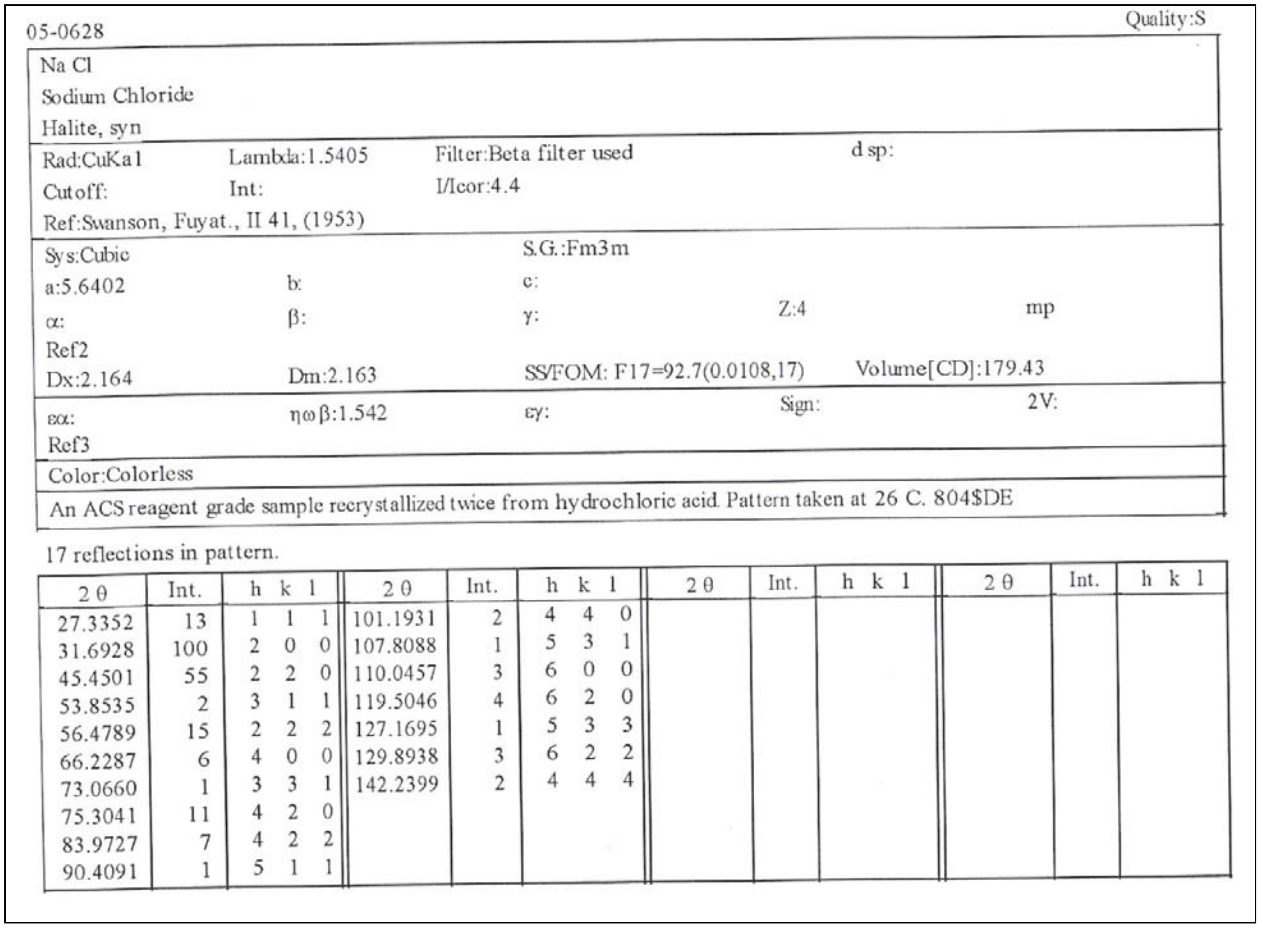

05-0628 Quality:S

Na Cl
Sodium Chloride
Halite, syn

Rad:CuKa1 Lambda:1.5405 Filter:Beta filter used d sp:
Cutoff: Int: I/Icor:4.4
Ref:Swanson, Fuyat., II 41, (1953)

Sys:Cubic S.G.:Fm3m
a:5.6402 b: c:
α: β: γ: Z:4 mp
Ref2
Dx:2.164 Dm:2.163 SS/FOM: F17=92.7(0.0108,17) Volume[CD]:179.43

εα: ηωβ:1.542 εγ: Sign: 2V:
Ref3

Color:Colorless

An ACS reagent grade sample recrystallized twice from hydrochloric acid. Pattern taken at 26 C. 804$DE

17 reflections in pattern.

| 2θ | Int. | h k l | 2θ | Int. | h k l | 2θ | Int. | h k l | 2θ | Int. | h k l |
|---|---|---|---|---|---|---|---|---|---|---|---|
| 27.3352 | 13 | 1 1 1 | 101.1931 | 2 | 4 4 0 | | | | | | |
| 31.6928 | 100 | 2 0 0 | 107.8088 | 1 | 5 3 1 | | | | | | |
| 45.4501 | 55 | 2 2 0 | 110.0457 | 3 | 6 0 0 | | | | | | |
| 53.8535 | 2 | 3 1 1 | 119.5046 | 4 | 6 2 0 | | | | | | |
| 56.4789 | 15 | 2 2 2 | 127.1695 | 1 | 5 3 3 | | | | | | |
| 66.2287 | 6 | 4 0 0 | 129.8938 | 3 | 6 2 2 | | | | | | |
| 73.0660 | 1 | 3 3 1 | 142.2399 | 2 | 4 4 4 | | | | | | |
| 75.3041 | 11 | 4 2 0 | | | | | | | | | |
| 83.9727 | 7 | 4 2 2 | | | | | | | | | |
| 90.4091 | 1 | 5 1 1 | | | | | | | | | |

Figure Displays Results for XRD analysis of 98.3 concentration of IX treated CAP water

The following figure shows XRD analysis of 98% concentrated IX treated CAP water. CPS is plotted as function of angle of light path in degrees. The bottom chart is XRD analysis of a known Halite index. The major peaks from the sample correspond to peaks for the Sodium Carbonate Sulfate index. This indicates that the sample contains Sodium Carbonate Sulfate.

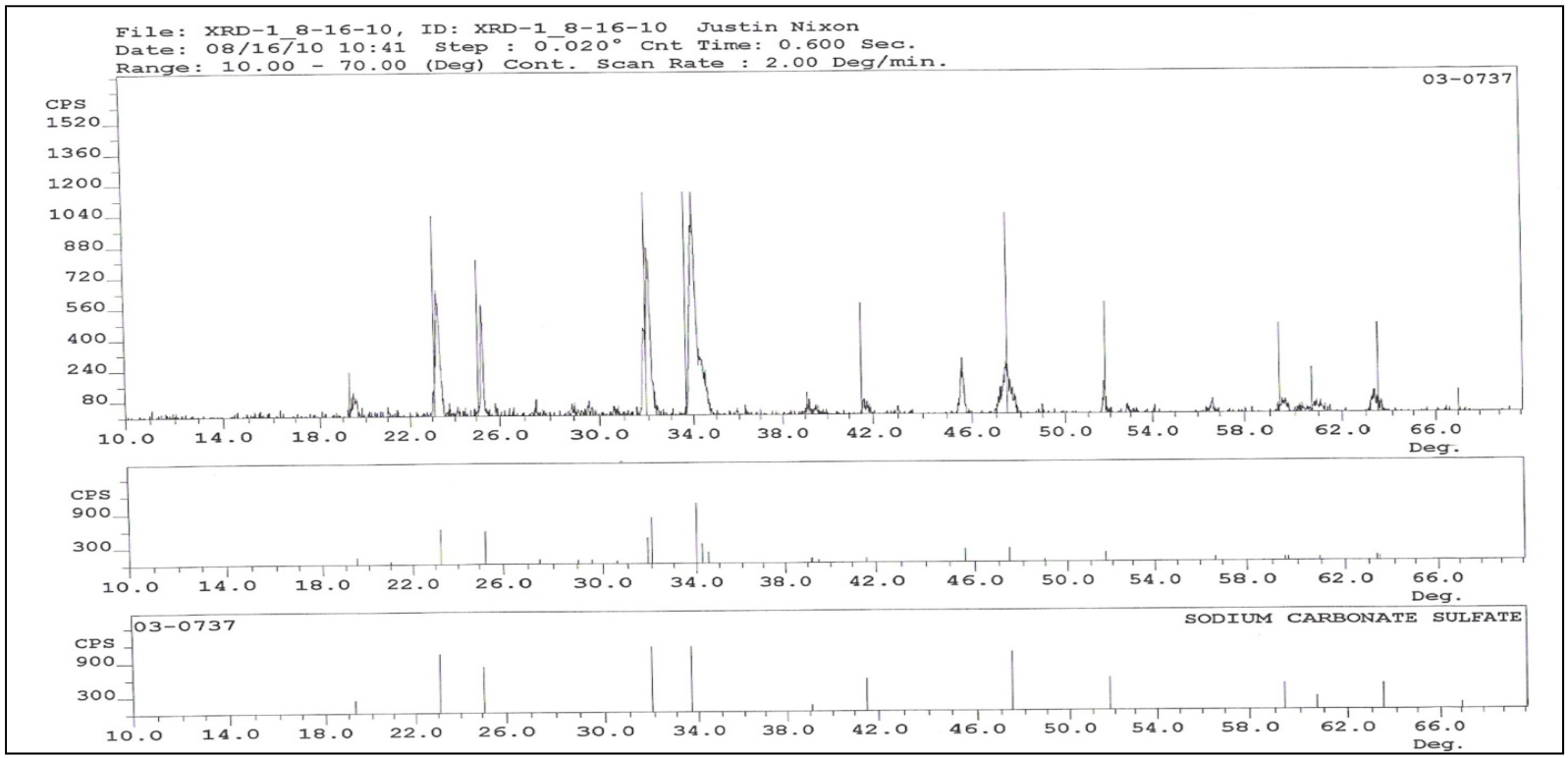

03-0737 Quality:B

3 Na2 O ! C O2 !2 S O3
Sodium Carbonate Sulfate

| | | | |
|---|---|---|---|
| Rad:MoKa | Lambda:0.709 | Filter: | d sp: |
| Cutoff: | Int: | I/Icor: | |

Ref:Lewis, S., 24 113, (1939)

| | | | | |
|---|---|---|---|---|
| Sys: | | S.G.: | | |
| a: | b: | c: | | |
| α: | β: | γ: | Z: | mp |

Ref2

| | | | |
|---|---|---|---|
| Dx: | Dm: | SS/FOM: | Volume[CD]:0 |

| | | | | |
|---|---|---|---|---|
| εα:1.463 | ηωβ:1.469 | εγ:1.480 | Sign:+ | 2V:40(15)$DE |

Ref3

Color:Colorless

Delete: Berry parcel February 5, 1959.

17 reflections in pattern.

| 2 θ | Int. | h k l | 2 θ | Int. | h k l | 2 θ | Int. | h k l | 2 θ | Int. | h k l |
|---|---|---|---|---|---|---|---|---|---|---|---|
| 19.2377 | 20 | | 60.4589 | 20 | | | | | | | |
| 23.0224 | 90 | | 63.2037 | 40 | | | | | | | |
| 24.9926 | 70 | | 66.7634 | 10 | | | | | | | |
| 31.8201 | 100 | | 70.7848 | 30 | | | | | | | |
| 33.5366 | 100 | | 76.0842 | 10 | | | | | | | |
| 38.9582 | 10 | | 79.8698 | 20 | | | | | | | |
| 41.3845 | 50 | | 82.3523 | 10 | | | | | | | |
| 47.3062 | 90 | | | | | | | | | | |
| 51.5958 | 50 | | | | | | | | | | |
| 59.1789 | 40 | | | | | | | | | | |

# Works Cited


Anderson, P. (2010, August 18). X-Ray Diffraction . (J. Nixon, Interviewer) Tucson, AZ.

Dionex Corporation.

Kaakinen, J. W., & Laverty, P. E. (1983). *Cation Exchange Pretreatment Studies for High Recovery - Yuma Plant.* Yuma: U.S. Department of the Interior - Bureau of Reclamation.

Lykins, J. (2009). *Ion Exchange Pre-treatment of Reverse Osmosis.* Master's Report, University of Arizona, Tucson.

Malcolm Pirnie Inc., and Separation Processes Inc. (2008). *Sustainable Water Deliveries from the Colorado River in a Changing Climate.*

Masters, G. M., & Ela, W. P. (2008). *Introduction to Environmental Engineering and Science.* Upper Saddle River: Prentice Hall.

McCabe, W., Smith, J., & Harriott, P. (2005). *Unit Operations of Chemical Engineering, 7th Edition.* New York: McGraw Hill.

Montemayor, K. (2010). Ion Exchange. (J. Nixon, Interviewer)

Moody, C., Garret, G., & Holler, E. (2002). *Pilot Investigation of Slow Sand Filtrationa and Reverse Osmosis Treatment of Central Arizona Project Water.* U.S. Department of the Interior, Bureau of Reclamation, Science and Technology Program Advanced Water Treatment Research Report No. 90.

Parkhurst, D. L., & Appelo, C. (1999). *User's Guide to PHREEQC (Version 2)- A Computer Program for Speciation, Batch-Reaction, One-Dimensional Transport, and Inverse Geochemical Calculations.* Denver: U.S. Department of the Interior.

Pearson, R. e. (1999). *Third Managment Plan for Tucson Active Managment 2000-2010.* Arizona Department of Water Resources.

Shroads, A. (n.d.). PHREEQC Modeling. (J. Nixon, Interviewer)

Xu, S. (2010). Induction Tests. (J. Nixon, Interviewer)

Yenal, U. (2009). *Maximizing Water Recovery During Reverse Osmosis (RO) Treatment of Central Arizona Project (CAP) Water.* Dissertation, University of Arizona, Tucson.

Yenal, U., Corral, A. F., Nixon, J., Arnold, R. G., & Ela, W. P. (2010). *Ion Exchange vs. Vibratory Shear Enhance Processiong (VSEP) For Optimized Salt Management in Lower Colorado River Water.* Tucson: University of Arizona.

# Appendix 11:

Ion Exchange vs. Vibratory Shear Enhanced Processing (VSEP®) for Optimized Salt Management in Lower Colorado River Water

# Ion Exchange vs. Vibratory Shear Enhanced Processing (VSEP®) for Optimized Salt Management in Lower Colorado River Water

*Umur Yenal[1], Andrea F. Corral[1], Justin Nixon[1], Wendell P. Ela[1], Robert G. Arnold[1]*
*[1]Department of Chemical and Environmental Engineering, The University of Arizona, Tucson, AZ*

## ABSTRACT

Water balances in central and southern Arizona depend on full utilization of the regional allotment of Central Arizona Project (CAP) water. The total dissolved solids (TDS) concentration at the terminus of the CAP canal in Tucson, AZ (~750 mg/L) is almost three times that of native groundwater in the Tucson area, and CAP water brings 200,000 tons of salt into the Tucson region each year. Essentially none of it leaves, making salt accumulation a major long-term issue. Reverse osmosis (RO) was evaluated for salt management. Pilot-scale studies indicated that scaling limits water recovery to 80% during conventional RO desalination of CAP water. To increase recovery (i) ion exchange (IX) pretreatment of the RO influent and (ii) post treatment of RO brine using vibratory shear enhanced processing (VSEP®) were evaluated.

When scale-forming cations—barium and calcium—are removed via IX treatment prior to RO, the expected maximum water recovery is >>80%. Alternatively, the water lost as brine can be reduced from 20% to 2-4% via post-RO VSEP treatment (this pilot-scale study). Estimated costs for these pre- and post-RO treatment options were compared to those of conventional RO treatment in which disposal of the entire RO brine flow was required. The cost of post-RO VSEP treatment to reduce brine volume adds a little more than $400 per acre foot of water delivered (~$1.25 per 1000 gal) for a hypothetical 15 MGD flow of CAP water (3 MGD brine flow rate). Use of VSEP results in a savings of more than $5M/year relative to RO treatment alone. The total annualized cost of VSEP operation was insensitive to the operational variables analyzed (VSEP recovery and time between VSEP membrane cleaning steps) in the vicinity of the optimal operating point.

The maximum long-term recovery using a combination of IX/RO treatments was not established experimentally due to the scale of available IX equipment. The IX/RO economics were nonetheless evaluated assuming that essentially any recovery is feasible during RO after removing the scale-forming cations via IX. This assumption remains to be tested. A recovery of 99% via IX/RO was optimal, resulting in ~$2M/yr savings to the RO/VSEP option and ~$7M/yr relative to RO treatment alone.

## INTRODUCTION

Arizona law mandates achievement of a balance between groundwater withdrawal and replenishment rates by year 2025 in “active management areas” around major population centers [1]. In the Tucson Active Management Area (TAMA), an area of 3,866 square miles that is roughly centered on Tucson in southern Arizona, projected compliance is based on full utilization of regional rights to Central Arizona Project (CAP) water and a degree of reclamation/reuse of municipal wastewater effluent. Uncertainty regarding the long-term availability of Colorado River water to the CAP, however, is a major impediment to water resources planning [2,3]. Water users in the TAMA have rights to ~250,000 AFY of CAP water, subject to availability constraints. The current water demand in the TAMA is about 400,000

AFY. The difference can be made up through a combination of groundwater withdrawals (up to 60,000 AFY, the estimated rate of natural groundwater renewal in the TAMA), and greater reliance on reuse of treated wastewater (Figure 1).

Reliance on CAP water to satisfy a major fraction of the regional water demand has consequences for the quality of delivered water (Table 1). Full use of the area's entitlement to CAP water will bring ~200,000 metric tons of salt into the TAMA each year. Without active steps to manage salt, the average salt content of the regional aquifer will increase by 5 mg/L-yr, doubling the salt content of the regional aquifer over the next 50 years [5]. CAP water is introduced into Tucson's regional water supply by temporary underground storage, mixing with native ground water and recovery, thus ensuring that salinity levels in delivered water do not rise abruptly to that of CAP water. Nevertheless, delivered water in portions of the city has TDS concentrations of ~600 mg/L and will continue to increase.

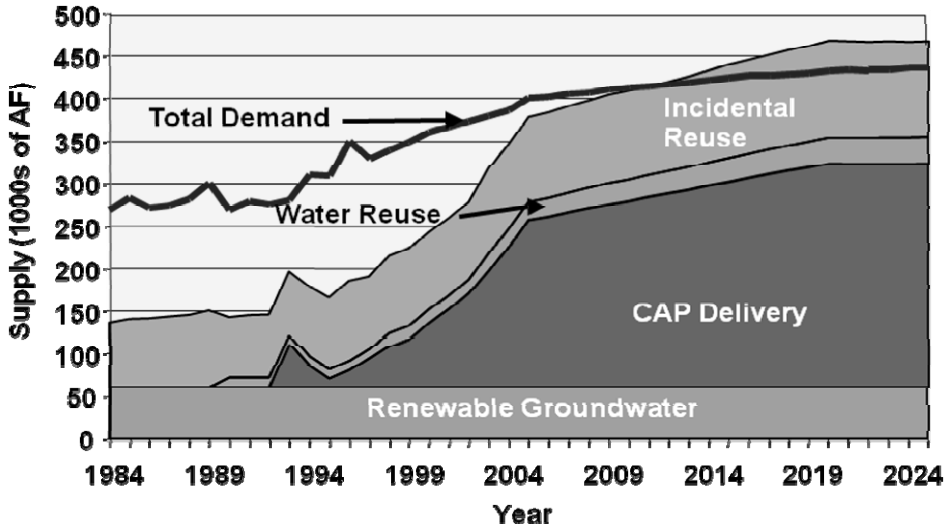


**Figure 1. Water demand/supply projections in the TAMA [4]. Water reuse consists of planned reuse of reclaimed water for landscape irrigation. Incidental reuse occurs as a consequence of inadvertent infiltration of water or effluent to the regional aquifer.**

**Table 1. Water quality comparison - Tucson ground water and CAP water at the canal terminus**

| Water Quality Constituent (mg/L) | Tucson Water Production Wells | CAP Water |
|---|---|---|
| Total Dissolved Solids | 259 | ~750 |
| Hardness (as $CaCO_3$) | 119 | 270 |
| Sodium | 40 | 112 |
| Chloride | 17 | 104 |
| Calcium | 39 | 56 |
| Magnesium | 5 | 31 |
| Sulfate | 45 | 280 |
| Alkalinity (as $CaCO_3$) | 126 | 98 |
| TOC | <1 | 3.5 |

While essential to salt management, RO treatment consumes energy and produces brine. It has been estimated that recovery during RO treatment of CAP water is limited to 75-80% to avoid membrane scaling [6], so that the value of water lost as brine contributes to the overall motivation for brine minimization should RO treatment of CAP water be deployed. The solubilities of calcium sulfate, calcium carbonate and barium sulfate, for example, are exceeded in brines derived from RO treatment of CAP water (Table 2). CAP water arrives in Tucson oversaturated with respect to barium sulfate, and it has been suggested that $BaSO_4$ precipitation limits recovery during RO treatment [ref].

If even a third of the regional CAP allotment is RO treated without additional efforts to increase recovery, the value of water lost as brine will be ~ \$20 $M \cdot yr^{-1}$ (based on a unit value of \$1000 per acre foot). The analysis does not include the cost of brine disposal, which is particularly relevant among inland communities like Phoenix and Tucson. Methods for increasing water recovery during salt removal include (i) pretreatment of CAP water to remove components of hardness (here $Ca^{2+}$ and $Ba^{2+}$) or (ii) post-treatment of CAP brines to separate additional water using Vibratory Shear Enhanced Processing (VSEP).

**Table 2. Concentration/solubility data for CAP ion pairs that may contribute to membrane scaling**

| ***Precipitate*** | ***Ion Concentration*** | ***log (ion product)*** | ***log $K_{S0}$*** | ***Degree of Saturation*** [(b)] |
|---|---|---|---|---|
| $BaSO_4(s)$ | $[Ba^{+2}] = 1.17 \times 10^{-6}$ M<br>$[SO_4^{-2}] = 2.81 \times 10^{-3}$ M | -8.48 | -10.0 | 827.83 |
| $CaSO_4(s)$ | $[Ca^{+2}] = 2.0 \times 10^{-3}$ M | -5.25 | -4.85 | 9.95 |
| $CaCO_3(s)$ | $[CO_3^{-2}] = 1.0 \times 10^{-5}$ M [(a)] | -7.7 | -8.48 | 150.64 |

[(a)] based on 120 mg/L carbonate alkalinity as $HCO_3^-$ and pH = 8.0.

[(b)] calculated as $25 \times Q_{SO}/K_{SO}$ with the assumption of RO running at 80% recovery. The value represents the approximate degree of oversaturation in the RO brine produced from CAP water.

## MATERIALS AND METHODS

A pilot-scale research facility (Figure 2a) was constructed 20 miles northwest of Tucson by the U.S. Bureau of Reclamation (USBR), the City of Tucson and a consortium of utilities in northwest Pima County—the Northwest Water Providers (NWWP). The project was designed to (i) establish the long-term (inter-seasonal) performance of RO for salt separation from CAP water at 80% recovery, (ii) compare slow sand filtration and microfiltration as pretreatment options for RO, and (iii) provide operational data with which to determine the economic feasibility of VSEP as a post-treatment of RO brine. Only the RO and VSEP units are described here. IX performance was not tested in the field but, nevertheless, a sequential treatment consisting of IX/RO was analyzed, leading to economic comparison with RO treatment (alone) and RO/VSEP salt management alternatives.

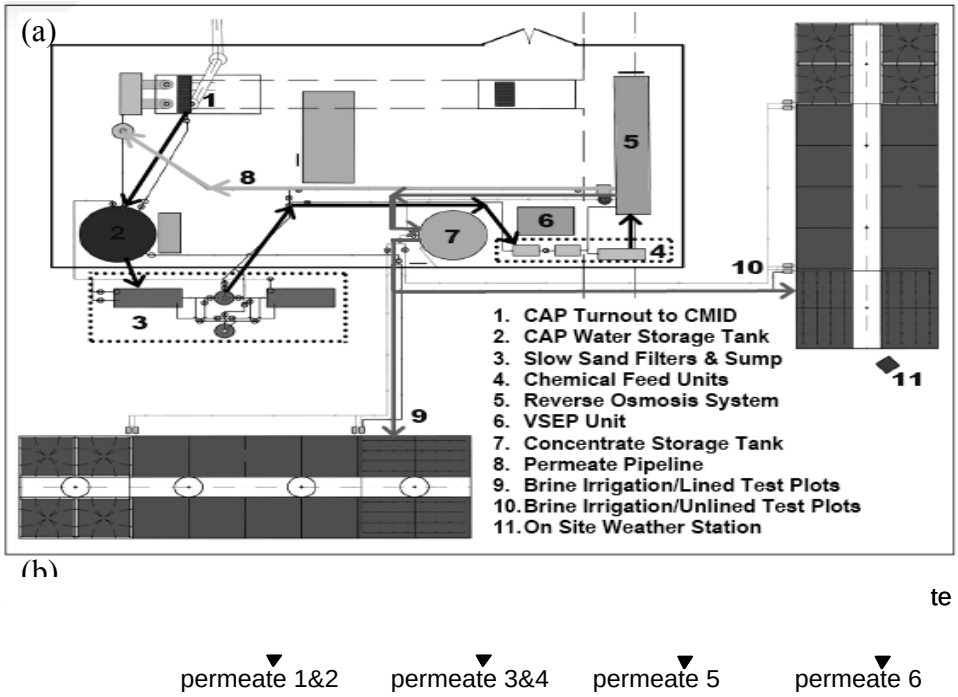


**Figure 2. (a) Site plan and water flow diagram for the Tangerine Road Field Site. Brines generated at the field site are ultimately used to irrigate salt tolerant vegetation. (b) RO consists of a 2-stage array (2:2:1:1) with each pressure vessels containing three 2.5-in spiral wound membranes. The RO processes 5 gpm of CAP water.**

***Reverse Osmosis.*** The pilot-scale RO unit consists of 6 pressure vessels containing a total of 18 elements in a two-stage, 2:2:1:1 configuration (Figure 2.b). Membrane elements were 2.5-inch x 40-inch polyamide thin film composite (PTFC) membranes (ESPA-2540). RO pressure requirements depend on the salinity of the feed water, water temperature, the membrane water transport coefficient (A, defined below), the design membrane flux (gallons of permeate per square foot of membrane per day [gfd]), and the target water recovery. Recovery is the percentage of influent that is recovered as permeate. Calculation of osmotic pressure follows the Morse equation [7]:

$$\pi = \Sigma N\ R\ T$$

where, $\pi$ is the osmotic pressure [psi]
$\Sigma N$ is the sum of concentrations of all solutes [M]
R is the ideal gas constant [0.08206 L.atm/ mol.K]
T is the absolute temperature [K]

The water transport coefficient is defined as follows:

$$A = \frac{Q_p / S}{P_f - P_p - (\pi_f - \pi_p)} \times TCF \left[ \frac{m/s}{Pa} \right]$$

where, $Q_p$ is the permeate flow rate ($m^3/s$)
S is the nominal membrane interfacial area ($m^2$)
Osmotic pressures are calculated based on feed and permeate compositions (Pa)
TCF is the temperature correction factor $[1.033^{(25-T)}]$ [ref]
$P_f$, $P_p$ are pressures on the feed and permeate sides of the membrane (Pa)
$\pi_f$ and $\pi_p$ are osmotic pressures on the feed and permeate sides of the membrane (Pa).

CAP water was pretreated via slow sand filtration and fed to the RO unit at an average flow rate of 17.9 L/min. The feed pressure was ~80 psi. The flow of reject water (brine) was maintained at 3.5 L/min to provide an adequate crossflow velocity in the final pressure vessel. The permeate flux from each element was adjusted to the design water flux, 10.9 gfd [8]. Each element nominally contained 28 $ft^2$ of membrane surface for a permeate flow of 0.8 L/min. The six pressure vessels together produced a permeate flow of 14.4 L/min. RO design and operational data are summarized in Table 3.

**Table 3. Reverse osmosis design and operational data**.

| | |
|---|---|
| Number of stages (-) | 2 |
| Number of vessels (3 elements per vessel) | 6 |
| Membrane area ($ft^2$ per element) | 28 |
| Membrane type (Hydranautics) | ESPA1 & ESPA3 |
| Water flux (gfd) | 10.9 |
| Influent flow rate (gpm) | 4.73 (17.9 L/min) |
| Feed salinity ($\mu S.cm^{-1}$) | 1000-1100 |
| Feed pressure (psi) | 80 |
| Recovery rate (%) | 80.5 |

***Vibratory Shear Enhanced Processing (VSEP®).*** VSEP (New Logic, Inc.) is a membrane separation system in which high-pressure RO or nanofiltration is used to extract additional water from highly saline solutions (Figure 3).

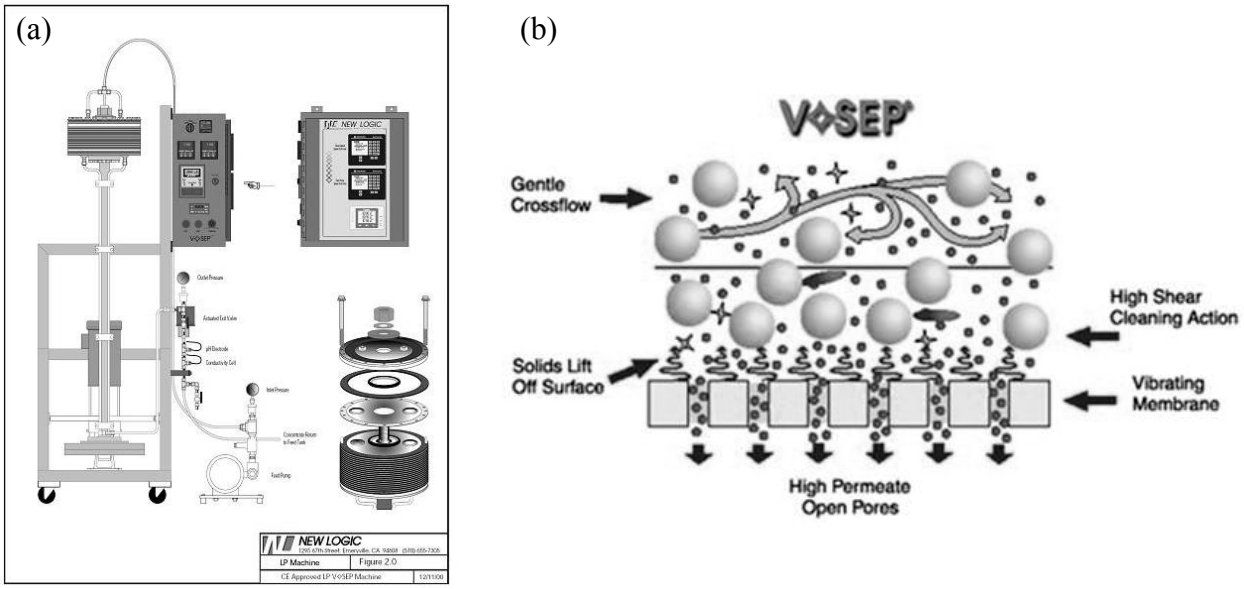


**Figure 3. (a) VSEP LP Machine shown in pilot-scale (P) mode (b) Principle of VSEP operation—mechanical vibration at the membrane surface produces a shear wave that prevents solids formation on membrane surfaces while forcing additional water from brines via high pressure RO.**

The VSEP reactor was a pilot scale, LP Series unit containing 16.44 $ft^2$ of ESPA1 membrane (Hydranautics). The feed flow (RO brine) was provided at 500 psi based on preliminary testing to select an operating pressure. The unit was operated by automatically cycling the brine retention valve between its closed and open positions. With the valve closed, fluid left the reactor only as permeate. In the open-valve position, brine was briefly flushed from the unit and completely replaced with reactor influent (RO brine). During each cycle, the valve was opened (flush position) for six seconds. The length of the closed valve period was adjusted to yield target permeate recoveries. In general, the average permeate flow rate during an open-valve period was inversely related to VSEP recovery and elapsed time of operation following membrane cleaning. Design and operational parameters for the VSEP in P-mode (pilot mode) are presented in Table 4.

**Table 4. Vibratory shear enhanced processing operational parameters**

| | |
|---|---|
| Membrane type | ESPA1 |
| Membrane surface area (sqft) | 16.44 (P-mode) |
| Conductivity of influent brine ($\mu S.cm^{-1}$) | 3000 – 5000 |
| Operating pressure (psi) | 500 |
| Vibration frequency (Hz) | 52.0 – 52.5 |
| Flow rate (gpm) | ~1.0 |
| Recovery rate (%) | 75 – 90 |
| Open valve period (min) | 0.1 |
| Closed valve period (min) | 0.9 – 6.9 |

Cleaning of the VSEP involves five steps. The first is a 15-minutes fresh water flush. Cold water is passed through the VSEP unit in a single-pass routine at 50 psi. The second step is the low-pH cleaning with 3% NLR 404 solution, a citric acid based solution formulated to remove metallic-based foulants and scaling components. The best result is obtained between pH 2.0 and 3.0 [38]. The third step of the cleaning process is another 15-minute cold fresh water flush, and the fourth is the high-pH cleaning with 3% NLR 505 solution, a blend of surfactants and chelating agents in a caustic liquid. Best results are obtained between pH 11.0 and 11.5. The temperature of the cleaning solutions in steps 2 and 4 is maintained at 50°C during the 45-minute recycling period. The last step of the cleaning process is another 15-minute cold fresh water flush. Throughout the process, the VSEP filter pack is vibrated at 3/4" amplitude (~52 Hz). At the end of each fresh water flush, the pressure is increased to 300 psi while the vibration frequency and amplitude are maintained. The permeate flow rate is measured by weighing the total amount of water collected in one minute. Cleaning adequacy is evaluated on the basis of post-cleaning permeate flow rate.

***Ion Exchange.*** In theory, removing hardness cations from CAP water prior to RO treatment will make it possible to drive reverse osmosis well past 80 percent recovery without precipitating $BaSO_4(s)$ or $CaSO_4(s)$. Ion exchange itself produces brine for disposal, however, and in communities that practice both salt management and wastewater reclamation/reuse the disposal of brines in municipal sewers is counter-productive. Nevertheless, ion exchange was proposed as a pretreatment for CAP water, to increase water recovery during RO and minimize RO brine volume. Bench-scale IX experiments designed to confirm the feasibility of presoftening CAP water via IX involved a strong acid cation (SAC) synthetic polymeric resin [resin identifier] (USA Resin) to remove hardness ions.

The bench-scale the ion-exchange reactor was too small for experiments necessary to establish the long-term feasibility of enhanced recovery during IX/RO treatment of CAP water, so that the economic analysis provided subsequently necessarily assumed that post-IX recoveries during RO would not be limited by membrane scaling. That assumption remains to be tested experimentally, however.

The city of Tucson loaned a bench-scale ion exchange reactor system (Tomar Water Systems, Inc.) to the project. The system consists of 4 columns of S40 clear PVC pipe, each with a 2-in diameter and a 32-in length. Resin capacity per vessel was 0.061 $ft^3$. Optimal flow for each column was 0.25 gpm and used in each experiment, for an overflow rate of ~11.5 $gpm/ft^2$. This is well within the norms for field-scale operation of ion exchange processes. The resin bed volume was approximately 2 L, and the regenerant solution consisted of water amended with 200 g/L NaCl. Regeneration was conducted by applying 7 empty bed volumes of the regenerant solution during a one-hour period.

A Dionex DX500 ion chromatograph was used with CD20 conductivity detector for anion and cation analyses. A 30 mM MSA solution buffered the mobile phase. Flows were regulated using an IP25 Isocratic gradient pump system. A dual head pump transports the mobile phase solution from the proportioning valve, where buffers are combined in the injection valve ahead of the ion exchange column (Model CS16). Primary cation concentrations in CAP water and CAP water following IX treatment suggest that downstream RO recoveries on the order of

99% should be possible without mineral precipitation and membrane scaling. That is, a 100-fold increase in IX-treated CAP water would yield a free calcium ion concentration of ~$10^{-4}$M and a free sulfate ion concentration of 0.2M. Thus the ion product for the calcium sulfate ion product would be similar to its solubility product, and precipitation should be avoidable via antiscalant addition.

**Table 5. Concentrations of primary cations in CAP water and CAP water following IX treatment using the project's bench-scale reactor.**

| Source | Sodium (mM) | Magnesium (mM) | Calcium (mM) |
|---|---|---|---|
| CAP Feed Water | 3.79 | 1.01 | 1.27 |
| IX Effluent | 6.68 | ND[1] | ND[1] |

[1]ND = non detect. Quantity was below the method detection limit, which was << 10 μM.

## RESULTS

***RO Performance.*** The extended record of RO performance for desalination of CAP water (Figure 5) suggests that membrane scaling or fouling was observed on a time scale of months. Impaired hydraulic performance was first observed in vessels 5 and 6, where ion concentrations were highest. Membrane cleaning in March 2008 temporarily restored membrane permeability, but downstream (stage 2) recovery again declined precipitously after a short period of steady operation. When the stage 2 recovery fell to 25% (from an initial 55%), the membranes were replaced and the system was operated to achieve a slightly higher overall recovery (80-85%) for four months. Near the end of that period, there was again preferential loss of permeability in the downstream RO vessels. At that point, the membranes were again replaced, the unit was thoroughly cleaned and operation at an overall recovery of ~75% led to reasonably stable performance for the next 8 months. In summary, the record of performance suggests that long-term, satisfactory RO performance is possible at recoveries approaching 80% without pretreatment to remove hardness cations. Higher recovery without water softening ahead of RO is inadvisable.

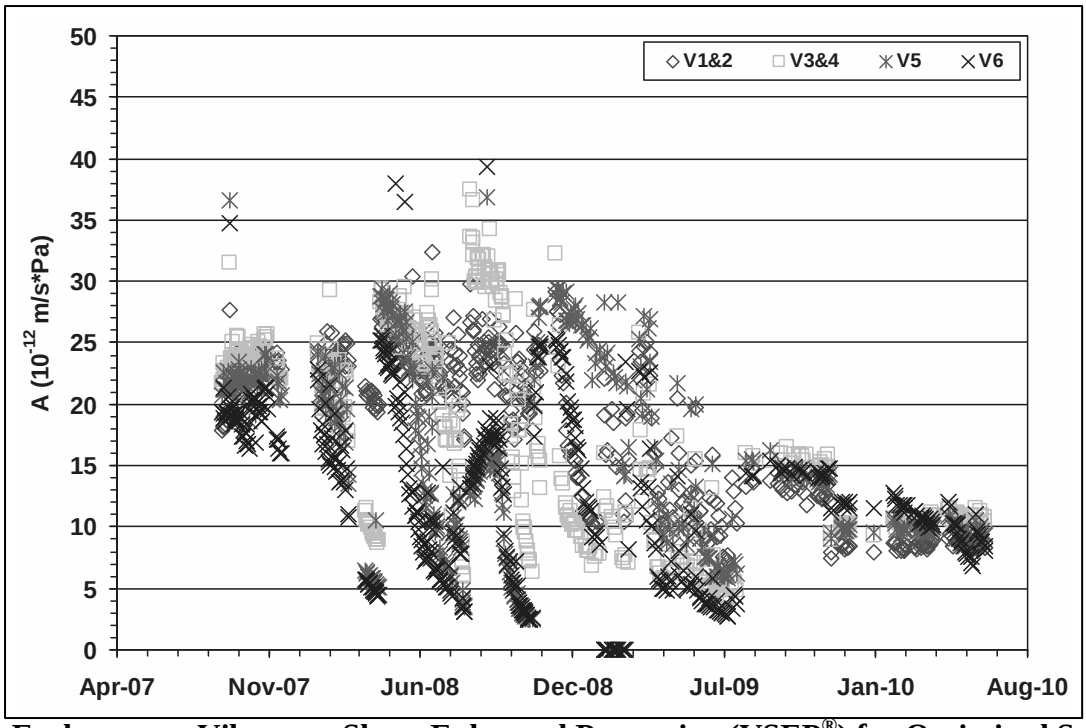

**Figure 5. Water transport coefficient (A) profile for RO operation (for gfd/psi, multiply y – scale by 0.0146). All values are adjusted to 25°C.**

***VSEP Performance—Post Treatment of RO Brine.*** VSEP recovery and the time between reactor cleanings were decision variables for VSEP operation. It was postulated that some combination of these variables leads to economically optimal VSEP performance. Increased VSEP recovery produces additional potable water and decreases the cost of brine disposal but also lowers the average permeate flux so that more reactors are necessary to treat the same brine flow. Similarly, less frequent reactor cleaning saves on cleaning costs but, again, lowers the average VSEP permeate flux leading to purchase and operation of additional reactors. VSEP recoveries of 89.2%, 85.7 % and 82.4 % were selected for this phase of study (overall recoveries of 98%, 97% and 96.5%), and 24-hour pilot experiments were run to establish the time-dependent permeate flux at each recovery level (Figure 6). Based on these results, linear relationships were established between the temperature-corrected water flux and the time of operation between membrane cleanings. Simple linear regression results are summarized (Figure 6).

In the 89.2% recovery experiment, for example, the length of the closed-valve period necessary to maintain recovery increased from 4.7 minutes to 6.9 minutes over 23 hours of continuous operation. The temperature-corrected water flux dropped from 59.5 gfd to 33.9 gfd over the same period. Other VSEP operating conditions were as follows: ¾-inch amplitude of torsional vibration, 500 psi operating pressure (during the closed-valve period), and 0.1 minute open-valve time. The influent TDS concentration was about 2300 mg/L, and the product water had an average TDS of 46.5 mg/L. The TDS of the concentrate was ~20,000 mg/L. A salt balance, defined below, around the reactor produced a positive MBD ≤+5%. The temperature of the water varied between 12°C and 20°C during the day-long study, averaging 15.3 °C. The results of day-long experiments at the other recoveries were similar.

$$\text{Salt Mass Balance Deviation } (\text{MBD}_S) = \frac{\left[Salt(in) - \sum Salt(out)\right]}{Salt(in)} \times 100[\%]$$

where, Salt(in) is the salt mass flux entering the RO unit (mg/min)
Salt(out) is the sum of salt mass fluxes leaving the reactor in permeate and brine streams (mg/min)

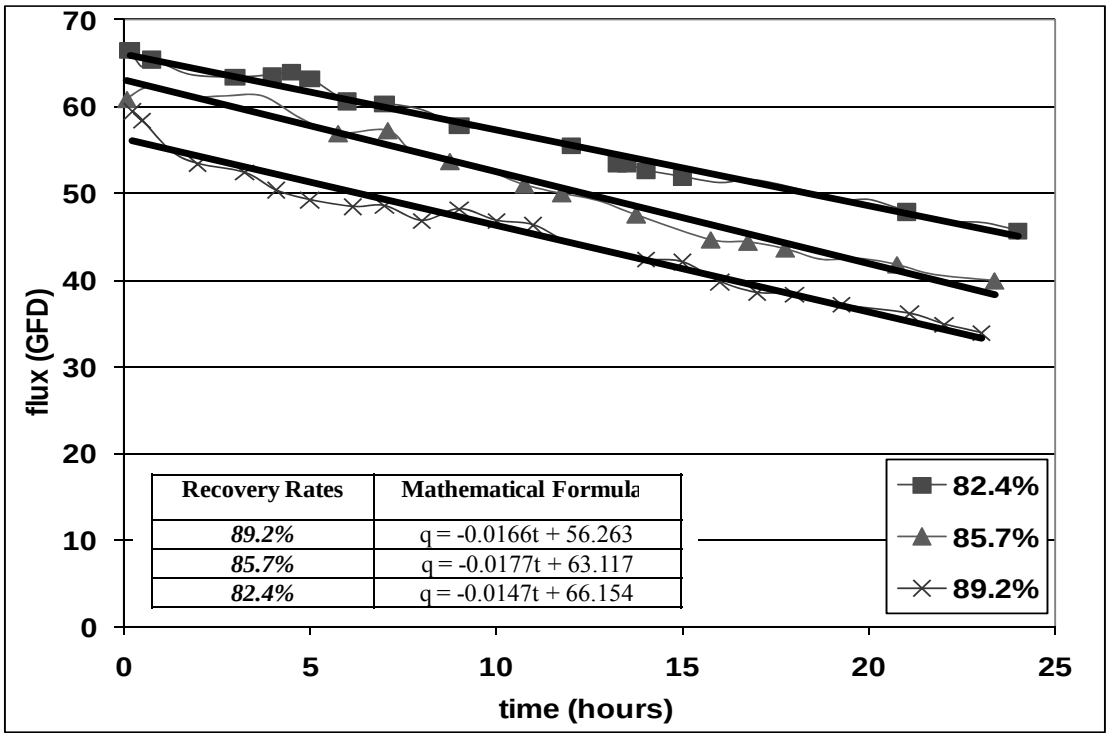


**Figure 6. The temperature-corrected permeate flux as a function of overall VSEP recovery and time of continuous operation following membrane cleaning. Regression lines of best fit are shown.**

***Economic Analysis.*** Three cases were selected for economic comparison—(i) RO alone, with brine disposal via enhanced evaporation, (ii) IX before RO to achieve higher recoveries without scaling during RO, and (iii) RO followed by VSEP to minimize the volume of brine for evaporative disposal. Economic and performance data for VSEP operation were derived from experiments or provided by New Logic, Inc. It is reemphasized that the long-term feasibility of recoveries >>80% via combined IX softening/RO has not yet been demonstrated, and only a theoretical treatment of RO performance and corresponding cost development is possible without addition pilot work.

For cost comparison, the total flow to be treated was assumed to be 15 mgd. The period of the economic analysis was 30 years (the assumed service life of the RO vessels), and the discount operator was 0.06 $yr^{-1}$. All costs are in January 2010 dollars. The unit value of the water is assumed as $1000/AF considering the average value that the farmers pay in Arizona by 2010 **[need to reference that]**.

***RO Treatment/Brine Disposal.*** The extended record of performance suggests that long-term, satisfactory RO performance is possible at recoveries approaching 80% without pretreatment to remove hardness cations. Therefore, the entire 15 MGD flow was to be treated by RO running at 80% recovery as the first case selected for economic comparison. The rest 20% of the flow was to become brine to be disposed of. Enhanced evaporation as one of the major strategies for brine disposal at inland desalination plants [Ahmed et. al.] is chosen as the strategy. Microfiltration was to be used as the pre-treatment for the RO operation. The filtered water

quality is assumed to be matched with the water quality suggested by the RO membrane manufacturers, i.e. SDI<5. The recovery rate for the microfiltration is assumed as 100% since the backwash water was to be mixed with the 15 MGD influent flow and the amount can be neglected. The costs for the chemicals used in water chemistry adjustments and the chemical cleanings for both MF and RO operations are included in the O&M costs as well as the disposal cost for spent solution after cleaning processes.

The cost for the microfiltration as pretreatment and the cost for the RO running at 80% recovery is taken as the basic cost for all the options and the details for those costs are not going to be discussed in this paper. Furthermore, the constituents of the cost for this option includes (i) the capital cost for enhanced evaporation ponds, (ii) the O&M cost for enhanced evaporation ponds, (iii) the cost of the water not treated by RO, and (iv) the cost of the personnel. The cost estimate and alternatives review performed by Carollo Engineers for the Northwest Water Providers is used while estimating the cost for evaporation ponds. The overall cost, $11.9 M/yr, is well distributed between the constituents presented above, where the capital cost for EP, the O&M cost for EP, the cost of the untreated water, and the personnel cost is 36%, 33%, 28% and 3% of overall cost.

***Ion Exchange/RO.*** Incremental costs attributable to the IX/RO alternative include capital and/or operational costs arising from (i) IX pretreatment, (ii) addition of a third RO stage, necessary to satisfy crossflow requirements at postulated recoveries, (iii) energy required to overcome osmotic pressure in the third RO stage and (iv) disposal of the residual RO brine volume and spent IX regenerant by enhanced evaporation. The entire 15 mgd flow was to be treated by IX. Osmotic pressure was calculated based on the recovery dependent ion composition of the brine. Components of IX reactor costs are summarized in Table 6, and the recovery-dependent incremental costs are shown in Figure 7.

**Table 6. Capital cost components for pressure IX (x is process capacity in mgd).**

| Cost Category | Cost Equation | Cost (×$1000) |
|---|---|---|
| Manufactured Equipment[1] | 154K**x** + 439K | 2,800 |
| Excavation and Sitework | 208**x** + 2K | 5 |
| Concrete | 623**x** + 7K | 17 |
| Steel | 974**x** + 12K | 26 |
| Labor | 24K**x** + 12K | 378 |
| Pipe and Valves | 34K**x** + 60K | 575 |
| Electrical and Instrumentation | 44K**x** + 4K | 659 |
| Housing | 18K**x** + 90K | 363 |
| Miscellaneous and Contingency | 38K**x** + 29K | 599 |
| **TOTAL** | **314Kx + 655K** | **5,422** |

[1] Manufactured equipment cost curve is obtained from Malcolm Pirnie Inc.

Design of the IX reactor was based on an assumed resin bed depth of 8 ft. The reactor diameter was assumed to be 12 ft, so that 12 IX units were required to treat 15 mgd at an overflow rate of 7.7 gpm/ft$^2$ (selected as design criterion based on typical water application rates for IX treatment). The calculated bed capacity for specific ions and volume to breakthrough were then determined based on an assumed resin capacity of 2.0 equivalents per liter and the composition of CAP water (Table 1). Results suggest that about 225 bed regenerations would be necessary per year for each IX reactor. At 10 bed volumes per regeneration [?? MWH], the IX process will generate about 0.5 million gallons of brine in the regeneration of all 12 reactors. This volume was added to the RO brine in order to estimate the cost of enhanced evaporation for the IX/RO alternative. It was assumed that chlorine disinfection would be unnecessary ahead of IX treatment. Resin costs, IX brine production volumes and other cost factors were as summarized in Table 7.

**Table 7. Cost parameters, regenerant volume for IX pretreatment [9]**

| **IX brine disposal (gal/day)** | 499K |
|---|---|
| Resin Price ($/m3) | $4,240 |
| Resin Lifetime (yrs) | 5 |
| IX Design Life (yrs) | 30 |
| Total Resin Volume (m3) | 307 |
| Total Resin Cost per Replacement | $1.30M |
| **Total Resin Cost (present worth)** | $4.26M |

Cost functions used to calculate the total annualized (incremental) cost attributable to IX/RO brine are summarized in Table 8. Each cost component is a function of a single independent variable—the anticipated recovery during RO treatment of the pre-softened water. A plot of annualized cost versus recovery (Figure 7) indicates that economies are achieved by increasing RO recovery up to 99%, much less brine is generated for disposal and less water is lost in the process. Beyond that point, however, the energy necessary to overcome osmotic pressure in the final stage of RO dominates the calculation, leading to much rapidly increasing total cost. The feasibility of 99% recovery following IX pre-softening remains to be established. IX ahead of RO treatment was predicted to increase power costs for operation of the first two stages of RO by <1%. Nevertheless, that increase is included in the analysis. The capital costs for IX, RO and augmented evaporation are the primary sources (50%) of the overall cost for the IX pre-softening alternative.

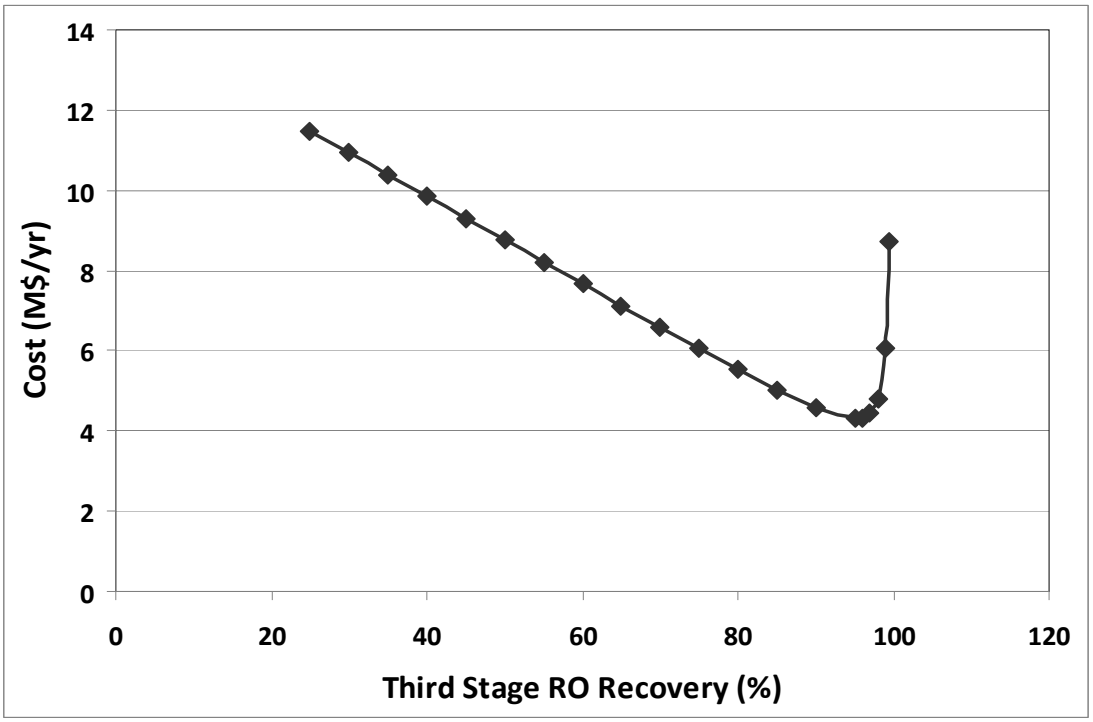


**Figure 7. The overall incremental cost for IX, RO and augmented evaporation as a function of recovery during reverse osmosis.**

**Table 8.** IX and third stage RO cost summary

| Item | Basis of Calculation | Assumptions | Contribution to Annualized Cost |
|---|---|---|---|
| **Capital costs:** | | | |
| IX units construction cost | $(314{,}215.7Q_{TP} + 655{,}103.9) \times F_{30}$ | 30-year service life. | 3%-8% |
| Disposal of brine cost (augmented evaporation ponds) | $59M\$ \times (Q_{VSEP,total}/3MGD) \times F_{30}$ | There is a linear relation between the capital cost of evaporation ponds and the flow rate of the brine to be disposed (Malcom Pirnie and Separation Processes, 2008). | 19%-33% |
| Third stage RO cost | $2.1M\$ \times Q_{RO3} \times (R_{RO3}/100) \times F_{30}$ | Linear relation between the water treated in MGD and the capital cost of RO | 1%-11% |
| **Energy costs:** | | | |
| Pumping cost (addition to the first two stages of RO) | $Q_{TP} \times \Delta\Pi_{RO1\&2} \times$ 0.12\$/kWh / 3,6M Nm/kWh × 24hrs/d × 365 days/yr | Increase in the concentration of divalent cations due to the operation of IX | 0.04%-0.1% |
| Pumping cost (third stage RO) | $Q_{RO3} \times [(J_W / A) + (M_{ions\ in\ reject} \times R \times T \times 14.7\ psi/atm)] \times 6894.8$ $((N/m^2)/psi)$ / 3,6M Nm/kWh × 0.12\$/kWh × 24hrs/d × 365 days/yr | It is required to overcome the osmotic pressure at the last element. | 0.8%-12% |
| **O&M Costs:** | | | |
| Resin cost | $4{,}240\$/m^3 \times V_{bed} \times n$ | It is required to buy the resin 6 times during the 30-years service life. | 3%-7% |
| Membrane replacement cost | $[(QTP / A) / A_{mem.element}] \times 594.99\$/element$ | A single set of membranes lasts for 3 years. 10 sets of membranes neded. | 1%-2% |
| O&M cost for evaporation ponds | $3.9M\$ \times (Q_{RO\ reject} + Q_{IX\ brine}) / 3MGD)$ | There is a linear relation between the O&M cost and the flow rate of the brine to be disposed. | 17%-30% |
| Personnel cost | 400K\$/yr | There are 4 personnel with 8 hours shifts around the clock at the facility. | 3%-8% |
| **Miscellaneous Costs:** | | | |
| Brine cost (due to loss of water) | $(C_{w,unit} / 0.33\ Mgal/AF) \times (Q_{RO\ reject} + Q_{IX\ brine}) \times 365days/yr$ | Unit value of water ($C_{w,unit}$) is 1000\$/AF. | 15%-26% |

***RO/VSEP.*** Incremental costs attributable to the RO/VSEP option include the capital plus operation and maintenance costs for (i) VSEP treatment for brine minimization, (ii) augmented evaporation of residual (post-VSEP) brine and (iii) water lost as brine. A near-optimum period of VSEP operation (between membrane cleanings) was determined as a function of VSEP recovery as follows: Fitted curves (Figure 6) were used to represent permeate flow rate as a function of time of continuous operation at each recovery. The total volume of permeate produced between cleaning operations, divided by the operational period plus cleaning time (Table 9), yields the average permeate production rate for a single VSEP device. That is,

$$Q_i = \frac{(a_i \times T + 2b_i) \times A \times T}{2(T + T_C)}$$

where, $Q_i$ is average permeate flow rate for a single VSEP unit at VSEP recovery rate i [gpd]

T is the VSEP run time between cleanings [days]
$T_C$ is time required for membrane cleaning [days]
$a_i$ is the slope of the fitted relationship between flux and run time [gfd/day]
$b_i$ is the intercept (vertical axis) of the same fitted relationship [gfd]
A is the membrane area for a single VSEP unit [$ft^2$].

The number of VSEP units required ($N_i$) at VSEP recovery $R_i$ is then given by :

$$N_i = Q_{ROB} \times R_i / Q_i$$

where, $Q_{ROB}$ is the total rate of brine flow from the RO process [gpd]

Table 9 provides unit costs and manufacturer's data for the full-scale VSEP reactors. Operational costs that were considered include (i) VSEP power costs—500 psi feed pressure and generation of torsional vibration (manufacturer's data), (ii) membrane cleaning and replacement costs and (iii) personnel costs. The value of water lost as VSEP brine was again taken as a system cost, estimated at $1000 per acre foot of unrecovered brine. The service life for VSEP reactors was assumed to be 10 years. For evaporation ponds and related equipment, service life was assumed to be 30 years. The largest VSEP unit manufactured by New Logic, Inc., the I-84, was used for the economic analysis. The membrane area of the I-84 unit is 1500 $ft^2$, and the cost is $250,000 per unit.

At each recovery rate for which there were pilot data ($R_i$), the annualized cost for treating 3 mgd of RO brine was calculated as a function of the period of VSEP operation between membrane cleanings (Figure 8). The global optimum was found at the combination of recovery and cleaning frequency that provided the lowest total annualized cost. Results suggest that there is a broad operational region in which VSEP operation is near optimal—that total annualized cost is fairly insensitive to recovery in the range 80-90 percent and period between cleanings in the range of 25-40 hrs. In those ranges, the total annualized cost for the VSEP system was significantly lower ($6.6 M/yr versus $11.9 M/yr) than the cost of the no-VSEP option (Table 9). In the RO/VSEP system, only 2-4% of the CAP water treated would be lost as brine. The

incremental cost of VSEP treatment is about $400 per acre foot of water treated (as influent to the RO unit). The cost per unit of water recovered from RO brine is about $2400 per acre foot.

**Table 9. Summary of VSEP related cost functions and contribution to annual cost**

| Item | Basis of Calculation | Assumptions | Contribution to Annualized Cost |
|---|---|---|---|
| **Capital costs:** | | | |
| VSEP units | $(d \times n) + \frac{d \times n}{(1+r)^{10}} + \frac{d \times n}{(1+r)^{20}}$ | 10-year service life. | 18%-21% |
| Disposal of brine cost (augmented evaporation ponds) | 59M$ × ($Q_{VSEP,total}$/3MGD) × $F_{30}$ | There is a linear relation between the capital cost of evaporation ponds and the flow rate of the brine to be disposed (Malcom Pirnie and Separation Processes, 2008). | 6%-12% |
| **Energy costs:** | | | |
| Pumping cost | $\left[\left(\frac{Q_{VSEP,total} \times g \times \rho \times h}{3.6 \times 10^{12}}\right)/\eta_p\right] \times 0.12\$/kWh \times 24hrs/d \times 365days/yr$ | The shaft efficiency of the pump is 80%. | 8%-9% |
| Vibration cost | $P_{vibration}$ × n × 0.12$/kWh × 24hrs/d × 365 days/yr | Power requirement for vibrating each VSEP unit is 12 hp | 5%-6% |
| **Cleaning costs:** | | | |
| Chemical cost | $C_{chem}$ × [24hrs/d × 365days / ($\check{T}$+$T_C$)] × n | | 12%-21% |
| Water cost | $C_{w,cleaning}$ × [24hrs/d × 365days / ($\check{T}$+$T_C$)] × n × ($C_{w,unit}$ / 3.3×10$^5$ gal/AF) | Unit value of water ($C_{w,unit}$) is 1000$/AF. | 0.4%-0.8% |
| **O&M Costs:** | | | |
| Membrane replacement cost | ($C_{memb.set}$ / 2 yrs) × n | A single set of membranes lasts for 2 years. | 18%-22% |
| O&M cost for evaporation ponds | 3.9M$ × ($Q_{VSEP,total}$/3MGD) | There is a linear relation between the O&M cost and the flow rate of the brine to be disposed. | 5%-11% |
| Personnel cost | 400K$/yr | There are 4 personnel with 8 hours shifts around the clock at the facility. | 5%-6% |
| **Miscellaneous Costs:** | | | |
| Brine cost (due to loss of water) | ($C_{w,unit}$ / 0.33 Mgal/AF) × [$Q_{VSEP,total}$ × (1 – $R_{VSEP}$)] × 365days/yr | Unit value of water ($C_{w,unit}$) is 1000$/AF. | 5%-9% |

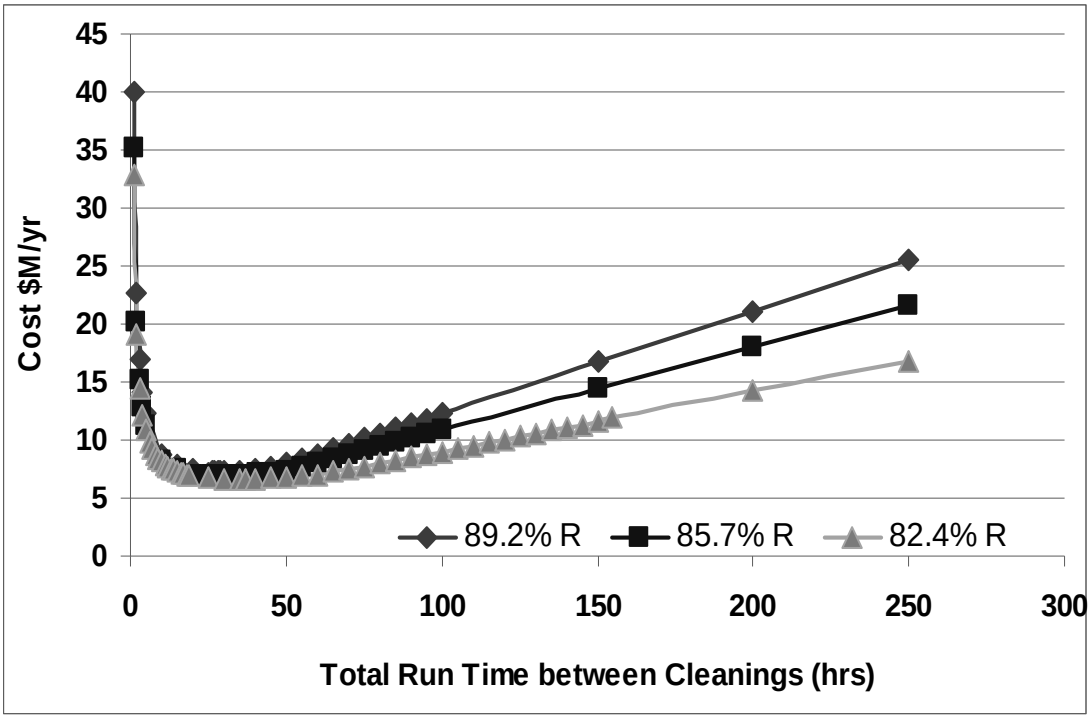


**Figure 8. Annualized VSEP capital/O&M costs as a function of VSEP recovery and time between cleanings**

## Conclusion

RO brine was further desalinated using the vibratory shear-enhanced processing (VSEP®; New Logic, Inc.). Water loss during desalination was reduced from 20% to 2-4% via post-RO VSEP treatment. Under optimal conditions, VSEP treatment achieved >80% recovery of brine. The total annualized cost of brine treatment was fairly insensitive to VSEP recovery in the range 80-90% and the period between cleanings in the range 25-40 hrs. These values define a fairly broad window for near optimal VSEP operation under the conditions of the study. The cost of VSEP treatment to decrease overall brine loss to 3.5% (82.5% VSEP recovery) was estimated at $394 per acre foot ($1.21 per 1000 gal) assuming 15 MGD CAP water is treated by the treatment plant. For a hypothetical 3 MGD RO brine flow, the use of VSEP to recover water and reduce the volume of brine for disposal results in a savings of more than $5M/year compared to the no-VSEP brine disposal alternative.

**Table 10. Economic summary of treatment options – percentages represent overall recoveries**

| RO Treatment | VSEP as Post-treatment of RO | | | IX as Pre-treatment of RO | | |
|---|---|---|---|---|---|---|
| | 96.5% | 97.1% | 97.8% | 96.5% | 97.1% | 97.8% |
| $11.9M ($2.18/1Kgal) | $6.62M ($1.21/1Kgal) | $6.85M ($1.25/1Kgal) | $7.23M ($1.32/1Kgal) | $5.84M ($1.07/1Kgal) | $5.55M ($1.01/1Kgal) | $5.22M ($0.95/1Kgal) |

IX pretreatment is predicted to do slightly better than RO/VSEP, but there are no field data to confirm the feasibility of the assumed IX/RO recoveries. Overall recoveries >>80% might be achievable if IX removes essentially all the divalent cations and no other precipitation reactions occur during RO treatment. IX used as pretreatment of RO is predicted to save ~$1-2 M/yr more than VSEP post-treatment of RO brine. These values should not be accepted, however, without experimental support for the assumed IX/RO recovery.

## References


1. Pearson, R., et. at., 1999, Third Management Plan for Tucson Active Management Area 2000-2010, Arizona Department of Water Resources.

2. Barnett, T. P. and Pierce, D. W. (2008). Sustainable water deliveries from the Colorado River in a changing climate.

3. Malcom Pirnie Inc., and Separation Processes Inc. (2008). Evaluation for Water Treatment Options for TDS Control, Draft Technical Memorandum

4. Osmotic Pressure. (2009). URL http://en.wikipedia.org/wiki/Osmotic_pressure

5. Moody, C., Garret B., and Holler E. (2002). Pilot Investigation of Slow Sand Filtration and Reverse Osmosis Treatment of Central Arizona Project Water. U.S. Department of the Interior, Bureau of Reclamation, Science and Technology Program Advanced Water Treatment Research Program Report No. 90.

6. Gumerman, Robert C., Russell L. Gulp, and Sigurd P. Hansen. (1979) *Estimating Water Treatment Costs: Cost Curves Applicable to 1 to 200 mgd Treatment Plants*. Vol. 2. Cincinaati: U.S. Environmental Protection Agency

7. Seider, Warren D. (2004) Product and process design principles synthesis, analysis, and evaluation. New York: Wiley

8. Crittenden, John C., R. R. Trussell, David W. Hand, Kerry J. Howe, and George Tchobanoglous. (2005) Water treatment principles and design. Hoboken, N.J: John Wiley

9. Ion Exchange Chemistry and Operation; Ion Exchange Systems and Equipment; REMCO Engineering Water Systems and Controls (2009). URL http://www.remco.com/ix.htm